Molecular genetic regulation of *de novo* assembly of shoot meristem in *Arabidopsis*

A thesis

Submitted in partial fulfillment of the requirements of the degree of

Doctor of Philosophy

By

Vijina V P
PhD20213133

Indian Institute of Science Education and Research Pune-411008, India
May 2023

“A seed is a life, a home, and the soul.

It smells the soil,

experiences the flow of water

and smiles at the wind”

Dedicated to

Amma, Achan, Ettan and my soul

Declaration

I declare that this written submission represents my ideas in my own words and where others' ideas have been included, I have adequately cited and referenced the original sources. I also declare that I have adhered to all principles of academic honesty and integrity and have not misrepresented or fabricated or falsified any idea/data/fact/source in my submission. I understand that violation of the above will be cause for disciplinary action by the Institute and can also evoke penal action from the sources which have thus not been properly cited or from whom proper permission has not been taken when needed.

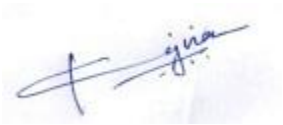

Place: IISER Pune Vijina VP

Date: 25th May 2023

Certificate

Certified that the work incorporated in the thesis entitled ***"Molecular genetic regulation of de novo assembly of shoot meristem in Arabidopsis"*** submitted by **Vijina V P** was carried out by the candidate under my supervision. The work presented here or any part of it has not been included in any other thesis submitted previously for the award of any degree or diploma from any other University or institution.

Place: IISER Pune

Dr. Kalika Prasad

Date: 25th May 2023

(Thesis supervisor)

Publications arising out of Ph.D. Thesis work

Research articles

1. **Varapparambath, V.**, Mathew, M. M., Shanmukhan, A. P., Radhakrishnan, D., Kareem, A., Verma, S., ... & Prasad, K. (2022). Mechanical conflict caused by a cell-wall-loosening enzyme activates de novo shoot regeneration. ***Developmental Cell***, *57*(17), 2063-2080. (*Featured Article, Featured on Cover Page, highlighted in Preview: Shoot meristem progenitors emerge from mechanical heterogeneities* https://doi.org/ 10.1016/j.devcel .2022.08.004 *(Hamant, 2022), highlighted in Faculty Opinions:* https://facultyopinions .com/article/74229178)
2. Garg, T., Singh, Z., Chennakesavulu, K., Mushahary, K. K. K., Dwivedi, A. K., **Varapparambathu, V.**, ... & Yadav, S. R. (2022). Species-specific function of conserved regulators in orchestrating rice root architecture. ***Development***, *149*(9), dev200381.

3. Shanmukhan, A. P., Mathew, M. M., Aiyaz, M., **Varaparambathu, V.**, Kareem, A., Radhakrishnan, D., & Prasad, K. (2021). Regulation of touch-stimulated de novo root regeneration from Arabidopsis leaves. ***Plant Physiology***, *187*(1), 52-58.

4. Radhakrishnan, D., Shanmukhan, A. P., Kareem, A., Aiyaz, M., **Varapparambathu, V.**, Toms, A., ... & Prasad, K. (2020). A coherent feed-forward loop drives vascular regeneration in damaged aerial organs of plants growing in a normal developmental context. ***Development***, *147*(6), dev185710. *[Featured on the cover of the journal, Editor's pick for the summary and highlight of the journal issue, selected by Company of Biologists as one of the most cherished cover images of 2020, selected for highlight by Plantae.org (American Society of Plant Biologists), highlighted in the blog by Theory of Living Matter Group, Cambridge, UK].*

Protocols

1. Mathew, M. M., Shanmukhan, A. P., **Varapparambath, V**., & Prasad, K. (2023). Protocol for real-time imaging, polar protein quantification, and targeted laser ablation of regenerating shoot progenitors in Arabidopsis. ***STAR protocols***, 4(2), 102184. *(Equal contribution).*

2. Radhakrishnan, D., Shanmukhan, A. P., Kareem, A., Mathew, M. M., **Varaparambathu, V.**, Aiyaz, M., ... & Prasad, K. (2021). Age, Wound Size and Position of Injury–Dependent Vascular Regeneration Assay in Growing Leaves. ***Bio-protocol***, *11*(9), e4010-e4010.

Acknowledgements

"I haven't failed. I have just found 10,000 ways that won't work."

—Thomas Alva Edison

'Each day I learned something new to build my thoughts'.

First of all, I would like to acknowledge my gratitude for giving me the opportunity to pursue a doctoral degree. I would like to begin by expressing my deepest appreciation to Ettan, Amma, and Achan for their constant support during my PhD period, to whom this thesis is dedicated. In particular, my Ettan implanted in me the perseverance to achieve this far.

I gathered a keen interest to know about the complex biological mechanisms when I joined Dr. Kalika Prasad's lab in Trivandrum, where the best minds in the country confluence in their love for research; my horizons expanded and gave me a flavor of research that drives the science of today. I want to start by thanking Dr. Kalika Prasad, my project supervisor, who has supported me throughout my PhD. Kalika gave special attention to my professional life to mould me. He shed new light on my career and helped me to stand in front of the crowd the way I am now. As the years passed, his unique way of mentoring and the discussions helped me to learn many things. I extend my heartiest gratitude and respect to Kalika because, without him, nothing would have been possible for me. I am grateful for giving me a chance to work with him, and I appreciate his patience with me. Thank you, Kalika!

Dr. Dhanya Radhakrishnan, my PhD senior, I am grateful to her. She helped me like an elder sister in my difficulties without any hesitation and poured a lot of confidence into me in my career. She is a good teacher, advisor, motivator, and whole of our lab. I am lucky to work with such a great polite person. I can't thank you enough!

I want to thank Anju, Dr. Mohammed Aiyaz, and Mabel for being a part of PhD time and feeling like another family, 'our MGPB'. We five created a good vibe in the lab, and the

‘tea sessions’ we had in Trivandrum were awesome. They provide constant support and help in the past and present to tackle the problems in my work. They have stood by me, heard me, appreciated me, and inspired me to be better. Especially, Anju, we both started our journey together in Kalika's lab. She was a good companion, and I learned multiple deals from her. The foundation of this thesis work was laid by Dr. Kareem, a former PhD student in our lab. Thank you, Kareemetta, for providing the exciting leads which led to the work in this thesis.

I extend my thanks to Dr. Jishy Varghese and Dr. Ravi Maruthachalam from IISER Trivandrum, members of the Doctoral Committee, for providing valuable input during the PhD time in Trivandrum. Also, I would like to express my gratitude towards Dr. Gayathri Pananghat and Dr Nishad Matange as research advisory committee members in IISER Pune, with whom I had discussions for my project and provided a couple of useful insights.

I want to express my gratitude towards my collaborator, Dr. Shri Ram Yadav. He gave me a chance to collaborate with him and be a part of his research. Also, I would like to acknowledge my other collaborator, Prof. Ari Pekka Mähönen, Dr. Marcus Heisler, and Prof. Dolf Weijers, for their valuable input on my project.

It is also important to mention and appreciate the people who worked with me, Bejoy, Archana, Raji, Neha, Anchal, Ashna, and Khaganshu, to help me to work along with me tirelessly. I would like to mention people from IISER Trivandrum, Sarika, Sandhya, Jijith, Naveen, Anil, Beena, and Hariharakrishan, for all the administrative support and help during my tenure and their determined work made the difficulties easier for us. I acknowledge Saket, Yadhu, Akansha, Srijan, Ankita, Shubham and other lab members in IISER Pune.

Special mention goes to Navaneeth, Anu, Anusha, Allipra, and all my other friends in Trivandrum, who made colourful days in TVM. Anu and Navaneeth became dear brothers with whom I have shared my secrets. Allipra, taught me the basics of molecular biology and showed me the beauty of the IISER-TVM, ‘such a beautiful place it is’. Renjithettan from Tapas Manna lab taught me protein-related work in my initial time when I joined and described it well for a beginner. Thanks, Renjithetta. I acknowledge the Department of Biology and administrative staff for giving me the opportunity to get exposure to another institute during my PhD period. They made the way easier to reach here.

I also would like to mention ‘Mallu-group’ in IISER Pune, especially 5th year BS-MS students (2018 batch). They gave moral support on the campus when I shifted from Trivandrum to Pune. They helped me to acclimatize to a new condition. A special thanks to you all.

I am grateful to Dr. Vineeth Sabastian and Dr. Anpin Raj from Nirmalagiri College, where I completed my BSc Degree, and Prof. Joseph Job and Ast.Prof. Tom Joseph from SB College from Changanassery, where I pursued my MSc; for making the choice of becoming a research student.

I would be happy to thank CSIR for providing me with the funding for my research. I would like to acknowledge IISER Trivandrum and IISER Pune for providing the infrastructure.

As I conclude my PhD journey, I realized that the journey was not smooth for me. Indeed, it was adventurous. I am grateful to Kuttu for providing mental support in my hardest time. He helped me to relax and shaped me in multiple aspects. We had a lot of fun moments together and provided strength to face the difficulties. Thank you for helping me to jump out of the problems. Lots of respect!

Vijina VP

Synopsis

Introduction

Various organisms on the planet have the ability to grow. Animals develop their entire body plan during embryogenesis and grow extensively to maintain their adult form. However, plants only develop a limited body-plan during embryogenesis and contain miniature precursors like cotyledon, plumule, and radicle inside a seed. All plant organs, such as leaves, shoots, flowers, or roots, develop post-embryonically during growth. The cells responsible for this growth are located at the apex in a shoot apical meristem (SAM) and at the opposite end in a root apical meristem (RAM).

Every organism encounters various injuries as they grow, and they have the remarkable ability to repair their losses. Unlike animals, where this ability is limited to specific lineages, plants possess remarkable developmental plasticity to repair their injuries across all tissues. Plants can not only repair wounds and regain their lost tissue, but also regenerate the entire plant system from a few cells of somatic tissue, which is termed as totipotency (Durgaprasad et al., 2019; Efroni & Birnbaum, 2016; Plant Regeneration: Cellular Origins and Molecular Mechanisms, 2016; Iwase et al., 2011; Kareem et al., 2015a; Kuchen et al., 2012; Mathew & Prasad, 2021; Mazur et al., 2016; Reinhardt et al., 2003; Shanmukhan et al., 2021). Interestingly, plants cannot recruit specialized cells to the wounded site because of the lack of cell migration; the key mechanism in animals is absent in plants because they are encased in a cell wall. However, plants can reprogram the cells in the vicinity of the wound to regenerate the lost tissue or heal the wound, or create a new individual organism (Durgaprasad et al., 2019; Efroni et al., 2016; Iwase et al., 2011; Kuchen et al., 2012; Mazur et al., 2016; Radhakrishnan et al., 2020; Reinhardt et al., 2003).

Objective and scope

My first objective was to investigate the fundamental molecular mechanism underlying the process of self-organizing a few cells into a functional shoot meristem during tissue-culture-induced regeneration. Additionally, I sought to explore the extent of gene function conservation in controlling regeneration across various plant species.

My study provides a novel insight into *de novo* shoot organogenesis, which occurs through

tissue culture and involves self-organized morphogenesis in the absence of pre-patterning cues. Through my investigation, I discovered that a regulatory axis is necessary to guide a few cells in the callus toward a complete shoot meristem fate, which is essential for *de novo* shoot morphogenesis.

By examining the conservation of gene function in the context of regeneration across divergent plant species that evolved 60 million years ago, my second study has provided a fresh perspective on conservation biology. Furthermore, this research lays the groundwork for further studies on the conservation of regeneration and the development of a regeneration circuit among monocotyledonous and dicotyledonous plant classes.

Contents of thesis

Chapter 1

Plants show exceptional cell plasticity in response to biotic or abiotic environmental stresses. This remarkable ability of plants to robustly adapt external stress conditions is due to their stationary nature. Nevertheless, they are sessile; the system has been widely studied for decades to understand the cellular and molecular mechanisms regulating their cellular plasticity. Plants display a variety of regenerative responses in response to injury or external inductive cues (Plant Regeneration: Cellular Origins and Molecular Mechanisms, 2016; Mathew & Prasad, 2021), and the researchers mimic these situations in the laboratory setup to study the repair mechanism adopted by the plants (Iwase et al., 2011; Radhakrishnan et al., 2020; Sabatini et al., 1999). Based on these studies, regenerative responses can be classified as firstly, mechanical-injury-induced regeneration, where the lost or damaged tissue is precisely restored, such as root tip regeneration, leaf vascular regeneration, *de novo* root organogenesis or restoration of ablated QC cells (J. Liu et al., 2014; Mathew & Prasad, 2021; Radhakrishnan et al., 2020; Sena et al., 2009; van den Berg et al., 1997). Second response is tissue-culture-induced regeneration, where a new plantlet can be created upon hormonal supplements in an artificial culture condition such as *de novo* shoot/root regeneration or somatic embryogenesis (Gordon et al., 2007; Huang & Yeoman, 1995; Kareem et al., 2015b; Skoog & Miller, 1957). In this chapter, I would like to introduce different types of regenerative responses in aerial and below-ground organs of plants and the underlying mechanism studied so far in *Arabidopsis thaliana*.

Chapter 2

The second chapter opens the subject of *de novo* shoot regeneration in *Arabidopsis* and details the necessity of PIN1 during organogenesis. Tissue-culture-mediated shoot regeneration is a widely used practice to propagate plants artificially using external hormone supplements. Any plant organ such as root, leaf, or cotyledon termed as 'explant' incubates in a high auxin-rich callus induction medium, it generates a pluripotent callus. If exposed to a cytokinin-rich shoot induction medium, this pluripotent callus will make new shoots. Unlike embryonic shoot apical meristem, *de novo* shoots have emerged in the absence of embryonic positional cues. The initiation and the progression of a group of cells called 'shoot progenitor' were followed using PIN1, which is one of the earliest known markers. We observed two distinct shoot progenitors; one where PIN1 is polarly localized in polygonal and compactly packed cells that become a functional shoot, whereas the other category of progenitor displays aberrant PIN1 localization with loosely adhered large cells which fails to make a shoot meristem. I studied deeper about the PIN1 localization pattern during *de novo* shoot regeneration. I showed the relevance of PIN1 polarization in the progenitor by modulating the expression of PIN1 or its polarity regulators or by various genetic approaches. These evidences state that the localization of polarity protein can predict the fate of regenerating foci.

Chapter 3

Chapter 3 explains the physiological significance of the PIN1 polarization pattern in the shoot progenitor during the foci initiation. Regenerating foci requires a critical low auxin concentration in the PIN1-marked progenitor cells compared to surrounding cells to successfully develop a shoot meristem *de novo*. While the regenerating foci does not maintain a differential auxin level between the progenitor cells and cells surrounding the progenitor does not progress into a shoot meristem. This indicates that the role of polarized pattern of PIN1 is to drain the auxin out of the progenitor to create a relatively low auxin environment for the successful development of regenerating foci. Alteration in the auxin levels also affects the *de novo* shoot regeneration.

Chapter 4

The fourth chapter of my thesis is titled '*Cell wall loosening enzyme XTH9 promotes PIN1 localization pattern to confer the productive fate'*. Differential Spatial distribution of PIN1 and auxin infer the fate of regenerating foci. This chapter talks about what promotes their spatial distribution to self-organize the initials (shoot progenitor) to a shoot fate. Comparative transcriptome analysis of different genetic backgrounds involved in *de novo* shoot regeneration led to the identification of a cell wall loosening enzyme XTH9. XTH9-expressing cells form a shell surrounding the PIN1-marked progenitor, and such shoot progenitor progresses into a complete shoot system. If the progenitor fails to restrict the domain of XTH9 spatially, i.e., expanded expression of XTH9 in the progenitor cells halts its development and eventually aborts the reprogramming into a shoot. Thus, XTH9 in non-progenitor cells promotes progenitor growth, and it is necessary to be excluded from the PIN1 domain. I analyzed the activity of XTH9 in the surrounding non-progenitor cells by using three independent approaches - loss-of-function mutant, inducible downregulation, or inducible knock-out of *XTH9* to modulate the XTH9 expression during the onset of progenitor formation and showed that shoot regeneration is highly impaired by the miss-expression of XTH9. Also, I showed that the tight spatio-temporal activity of XTH9 is critical for regulating the PIN1 localization pattern during shoot meristem formation *de novo*.

Chapter 5

The final chapter about *de novo* shoot regeneration is titled *'CUC2 activates the expression of XTH9 to promote shoot meristem formation de novo'*. The influence of auxin-PIN1 interplay and the encapsulation of XTH9 shell confer the productive fate to a shoot progenitor. A previous study has shown that 'a two-step mechanism of *de novo* shoot regeneration', there are three transcription factors coded by a large gene family *PLETHORA* such as *PLT3, PLT5*, or *PLT7* redundantly activate root stem cell regulators *PLT1/PLT2* to make a pluripotent callus and they activate shoot promoting factor *CUC2* to form shoot system from this pluripotent callus (Kareem et al., 2015). However, how *CUC2* promotes the self-organization of cells to generate a shoot system is unknown. I monitored CUC2 expression in the shoot progenitors and found that CUC2 is completely excluded from the

progenitor of a productive one. Surprisingly, it is expressed in the non-progenitor cells like XTH9 and not expressed in the progenitor. On the other hand, in the pseudo-progenitor, CUC2 is expressed in both progenitor and in the non-progenitor cells, very much like XTTH9. ChIP-Seq analysis revealed that CUC2 directly binds to *XTH9* and activates its expression in the surrounding non-progenitor cells. Here, we discovered CUC2-XTH9 regulatory axis acts non-cell autonomously for coordinated self-organogenesis. Genetic experiments and altered expression of CUC2 highlight its necessity in the surrounding non-progenitor cells to promote the emergence of a shoot meristem.

Based on the presence or absence of CUC2-driven XTH9, the cell wall modification in the surrounding non-progenitor cells and cell polarity in the progenitor act in a regulatory feedback loop to make the dome-shaped shoot meristem *de novo*. Examining the PIN1 localization in the *cuc2* or *xth9* mutants reveals an aberrant localization of PIN1 that negate progenitor formation. On the other hand, the loss of spatial-specific expression of *CUC2* and *XTH9* in PIN1 or its polarity regulator mutants (*pin1*, *pidwag1wag2* or *pin1,pin3,pin4,pin7*) results in early progenitor termination. My experiments cumulatively suggest that a tight regulatory feedback loop controls the programming of a progenitor, to its morphogenesis into a complete shoot.

Chapter 6

The sixth chapter of this thesis discusses the *'Conserved function of Rice PLT proteins in controlling developmental process and regeneration in Arabidopsis'*. Though we are addressing fundamental questions using *Arabidopsis* as a model to apply the universality of particular regulatory logic, we must test if it holds true in other species. As mentioned earlier, I wanted to examine the genes that participate in regenerative responses and whether they are conserved across the species. *PLETHORA* transcription factors such as *PLT3*, *PLT5*, and *PLT7* are known as the master regulator of regeneration, and also, they are involved in controlling a variety of normal development (Kareem et al., 2015b; Pinon et al., 2013; Prasad et al., 2011). Comparative analysis of *PLETHORA* genes in *Arabidopsis* and distantly related monocotyledon *Oryza sativa (Rice)* at the protein level shows the homology between *Arabidopsis* PLETHORAs with *Rice* PLETHORAs, i.e., OsPLT1 and OsPLT2. This chapter describes the functional rescue of regeneration in

Arabidopsis PLETHORA mutant by expressing *OsPLT* gene under *Arabidopsis* promoter. This study suggests the conserved function of *Rice* PLT proteins in *Arabidopsis*.

Chapter 7

This chapter titled '*Conclusion*' provides a capsulization of underlying molecular mechanisms and the existence of a regulatory feedback loop involved in tissue-culture mediated *de novo* shoot organogenesis (based on Chapter 2-Chapter 5) and functional conservation of molecular factors in controlling multiple regenerative responses across plant species (based on Chapter 6). My primary study unfolds the biochemical patterning created by molecular factors such as *CUC2* and *XTH9* in the process of *de novo* shoot regeneration. The PIN1 polarization on the membrane of the progenitor is crucial for the differential distribution of auxin and leads to the generation of relatively low auxin level in the progenitor. PIN1 helps to up-the-gradient of auxin (Jönsson et al., 2006; Smith, Guyomarc'h, et al., 2006) in the cells surrounding the progenitor during the development of shoot meristem from a callus rich in auxin. *CUC2*, a shoot-promoting factor, activates XTH9 in the cells surrounding the progenitors. This further facilitates PIN1-recruitment on the progenitor membrane, critical for *de novo* shoot meristem formation. Any variation in this local biochemical environment by the perturbation of the PIN1-CUC2- XTH9 module discontinues the progression of a progenitor. Therefore, this study provides a model for self-organized morphogenesis in the absence of embryonic positional cues.

Additionally, this chapter discusses how plant regenerative responses are controlled by a conserved transcription factor found in diverse plant species.

Chapters 8 and 9

Chapter 8 includes the materials, methods, tools, and the techniques used to accomplish my thesis work. Chapter 9 contains the literature details that are referred to throughout my study.

Conclusion and future perspective

Callus-mediated regeneration helps rebuild an entire organism from any tissue of the plant body; however, how the self-organization is reprogrammed from a heterogenous callus

tissue remains unclear. This intrigued me to delve deeper into investigating how this self-organization initiates the formation of a shoot using *Arabidopsis* as a model. This is the first study to look at how cell-wall mechanics interact to determine cell fate during plant regeneration, an important developmental decision to make a complete shoot from a few cells in the callus (Varapparambath et al., 2022). Cellular heterogeneity generated by the activity of CUC2-XTH9 promotes cell polarity, which leads to the regeneration of a complete organism in the absence of embryonic tissue patterning cues. These questions have remained unrevealed by the scientific field for decades due to the fragile nature of the callus. This study opened up a new direction in the field of regeneration to learn about the cell mechanics and stochasticity for the selection and initiation of the progenitor from a chaotic mass of callus tissue. The long-term objective will be to find solutions to address some fundamental questions, such as stochastic initiation of regenerative progenitor, cellular heterogeneity of callus, and the relationship between cell polarity and cell division during *de novo* organogenesis.

Additionally, The PLETHORA family of proteins in plants has been found to maintain functional conservation across species, controlling developmental processes and regenerative responses. Future studies should determine the function of *Arabidopsis* PLETHORA protein in *Rice*. Further research is needed to determine if these transcription factors have conserved cis-regulatory elements for responses to injury or regenerative responses across plant species.

Bibliography

Durgaprasad, K., Roy, M. V., Venugopal M., A., Kareem, A., Raj, K., Willemsen, V., Mähönen, A. P., Scheres, B., & Prasad, K. (2019). Gradient Expression of Transcription Factor Imposes a Boundary on Organ Regeneration Potential in Plants. *Cell Reports*, *29*(1), 162. https://doi.org/10.1016/j.celrep.2019.08.099

Efroni, I., & Birnbaum, K. D. (2016). The potential of single-cell profiling in plants. *Genome Biology*, *17*(1), 1–8. https://doi.org/10.1186/s13059-016-0931-2

Efroni, I., Mello, A., Nawy, T., Ip, P.-L. L., Rahni, R., Delrose, N., Powers, A., Satija, R., & Birnbaum, K. D. (2016). Root Regeneration Triggers an Embryo-like Sequence Guided by Hormonal Interactions. *Cell*, *165*(7), 1721–1733.

https://doi.org/10.1016/j.cell.2016.04.046

Gordon, S. P., Heisler, M. G., Reddy, G. V, Ohno, C., Das, P., & Meyerowitz, E. M. (2007). Pattern formation during de novo assembly of the Arabidopsis shoot meristem. *Development*, *134*(19), 3539–3548. https://doi.org/10.1242/dev.010298

Haberlandt, G. (1902). Experiments on the culture of isolated plant cells. *The Botanical Review*, *35*(1), 68–88. https://doi.org/10.1007/BF02859889

Huang, B., & Yeoman, M. M. (1995). Somatic embryogenesis in Arabidopsis thaliana L. *Somatic Embryogenesis and Synthetic Seed II*, 371–384.

Plant regeneration: Cellular origins and molecular mechanisms, 143 Development (Cambridge) 1442 (2016). https://doi.org/10.1242/dev.134668

Iwase, A., Mitsuda, N., Koyama, T., Hiratsu, K., Kojima, M., Arai, T., Inoue, Y., Seki, M., Sakakibara, H., Sugimoto, K., & Ohme-Takagi, M. (2011). The AP2/ERF transcription factor WIND1 controls cell dedifferentiation in arabidopsis. *Current Biology*, *21*(6), 508–514. https://doi.org/10.1016/j.cub.2011.02.020

Jönsson, H., Heisler, M. G., Shapiro, B. E., Meyerowitz, E. M., & Mjolsness, E. (2006). An auxin-driven polarized transport model for phyllotaxis. *Proceedings of the National Academy of Sciences*, *103*(5), 1633–1638. https://doi.org/10.1073/pnas.0509839103

Kareem, A., Durgaprasad, K., Sugimoto, K., Du, Y., Pulianmackal, A. J., Trivedi, Z. B., Abhayadev, P. V., Pinon, V., Meyerowitz, E. M., Scheres, B., & Prasad, K. (2015a). PLETHORA Genes Control Regeneration by a Two-Step Mechanism. *Current Biology*, *25*(8), 1017–1030. https://doi.org/10.1016/j.cub.2015.02.022

Kuchen, E. E., Fox, S., De Reuille, P. B., Kennaway, R., Bensmihen, S., Avondo, J., Calder, G. M., Southam, P., Bangham, A., & Coen, E. (2012). Generation of leaf shape through early patterns of growth and tissue polarity. *Science*. https://doi.org/10.1126/science.1214678

Liu, J., Sheng, L., Xu, Y., Li, J., Yang, Z., Huang, H., & Xu, L. (2014). *WOX11* and *12* Are Involved in the First-Step Cell Fate Transition during de Novo Root Organogenesis in *Arabidopsis*. *The Plant Cell*, *26*(3), 1081–1093. https://doi.org/10.1105/tpc.114.122887

Mathew, M. M., & Prasad, K. (2021). Model systems for regeneration: Arabidopsis. *Development (Cambridge)*, *148*(6). https://doi.org/10.1242/dev.195347

Mazur, E., Benková, E., & Friml, J. (2016). Vascular cambium regeneration and vessel formation in wounded inflorescence stems of Arabidopsis. *Scientific Reports*, *6*(1), 33754. https://doi.org/10.1038/srep33754

Pinon, V., Prasad, K., Grigg, S. P., Sanchez-Perez, G. F., & Scheres, B. (2013). Local auxin biosynthesis regulation by PLETHORA transcription factors controls phyllotaxis in Arabidopsis. *Proceedings of the National Academy of Sciences of the United States of America*, *110*(3), 1107–1112. https://doi.org/10.1073/pnas.1213497110

Prasad, K., Grigg, S. P., Barkoulas, M., Yadav, R. K., Sanchez-Perez, G. F., Pinon, V., Blilou, I., Hofhuis, H., Dhonukshe, P., Galinha, C., Mähönen, A. P., Muller, W. H., Raman, S., Verkleij, A. J., Snel, B., Reddy, G. V., Tsiantis, M., & Scheres, B. (2011). Arabidopsis PLETHORA transcription factors control phyllotaxis. *Current Biology*, *21*(13), 1123–1128. https://doi.org/10.1016/j.cub.2011.05.009

Radhakrishnan, D., Shanmukhan, A. P., Kareem, A., Aiyaz, M., Varapparambathu, V., Toms, A., Kerstens, M., Valsakumar, D., Landge, A. N., Shaji, A., Mathew, M. K., Sawchuk, M. G., Scarpella, E., Krizek, B. A., Efroni, I., Mähönen, A. P., Willemsen, V., Scheres, B., & Prasad, K. (2020). A coherent feed-forward loop drives vascular regeneration in damaged aerial organs of plants growing in a normal developmental context. *Development (Cambridge, England)*, *147*(6), 1–10. https://doi.org/10.1242/dev.185710

Reinhardt, D., Pesce, E.-R., Stieger, P., Mandel, T., Baltensperger, K., Bennett, M., Traas, J., Friml, J., & Kuhlemeier, C. (2003). Regulation of phyllotaxis by polar auxin transport. *Nature*, *426*(6964), 255–260. https://doi.org/10.1038/nature02081

Sabatini, S., Beis, D., Wolkenfelt, H., Murfett, J., Guilfoyle, T., Malamy, J., Benfey, P., Leyser, O., Bechtold, N., Weisbeek, P., & Scheres, B. (1999). An Auxin-Dependent Distal Organizer of Pattern and Polarity in the Arabidopsis Root. *Cell*, *99*(5), 463–472. https://doi.org/10.1016/S0092-8674(00)81535-4

Sena, G., Wang, X., Liu, H.-Y., Hofhuis, H., & Birnbaum, K. D. (2009). Organ regeneration does not require a functional stem cell niche in plants. *Nature*, *457*(7233), 1150–1153. https://doi.org/10.1038/nature07597

Shanmukhan, A. P., Mathew, M. M., Aiyaz, M., Varaparambathu, V., Kareem, A., Radhakrishnan, D., & Prasad, K. (2021). Regulation of touch-stimulated de novo root

regeneration from Arabidopsis leaves. *Plant Physiology*, *187*(1), 52–58. https://doi.org/10.1093/plphys/kiab286

Skoog, F., & Miller, C. O. (1957). Chemical regulation of growth and organ formation in plant tissues cultured in vitro. *Symposia of the Society for Experimental Biology*, *11*, 118–130.

Smith, R. S., Guyomarc'h, S., Mandel, T., Reinhardt, D., Kuhlemeier, C., & Prusinkiewicz, P. (2006). A plausible model of phyllotaxis. *Proceedings of the National Academy of Sciences*, *103*(5), 1301 LP – 1306. https://doi.org/10.1073/pnas.0510457103

van den Berg, C., Willemsen, V., Hendriks, G., Weisbeek, P., & Scheres, B. (1997). Short-range control of cell differentiation in the Arabidopsis root meristem. *Nature*, *390*(6657), 287–289. https://doi.org/10.1038/36856

Varapparambath, V., Mathew, M. M., Shanmukhan, A. P., Radhakrishnan, D., Kareem, A., Verma, S., Ramalho, J. J., Manoj, B., Vellandath, A. R., Aiyaz, M., Radha, R. K., Landge, A. N., Mähönen, A. P., Heisler, M. G., Weijers, D., & Prasad, K. (2022). Mechanical conflict caused by a cell-wall-loosening enzyme activates de novo shoot regeneration. *Developmental Cell*, *57*(17), 2063-2080.e10. https://doi.org/10.1016/j.devcel.2022.07.017

Abbreviations

0 Hr- 0 Hour
24 Hr- 24 Hour
4 Hr- 4 Hour
48 Hr- 48 Hour
8 Hr- 8 Hour
AM- Axillary Meristem
AP2- APETELLA2
At- *Arabidopsis thaliana*
AXR3- Auxin-response Locus
ChIP- Chromatin Immuno-precipitation
CFP- Cyan Fluorescent Protein
CRISPR- Clustered Regularly Interspaced Short Palindromic Repeats
CUC- CUP-SHAPED COTYLEDON
DEG- Differentially expressed genes
DEX- Dexamethasone
dsRNAi- double-strandedRNA interference
dpi- day post incision
DR- Double reconstitution
DUG- Differentially upregulated genes
D-Day
FM- Floral meristem
GFP- Green Fluorescent Protein
GR- Glucocorticoid Receptor
IGE- Inducible Genome Editing
IM- Inflorescence Meristem
LEC1- Leafy cotyledon 1
mm- Millimeter
MS- Murashige and Skoog Medium
OS- *Oryza sativa*
PID- PINOID
PIN- PINFORMED
PIN1- PINFORMED 1
PI- Propidium Iodide
PLT- PLETHORA
RAM- Root Apical Meristem
ROI- Region of Interest
R2D2- Ratiometric version of 2 D2's
SAM- Shoot Apical Meristem
SEM- Standard Error of Mean
SIM- Shoot Induction Medium
SR- Single reconstitution
TZ- Trans-Zeatin
UI- Uninduced
UTR- Untranslated region
vYFP- venus Yellow Fluorescent Protein
WT- Wildtype
WUS- WUSCHEL
XTH- Xyloglucan Endotransglucosylase/Hydrolase
YUC- YUCCA
µM- Micrometer

Table of contents

List of Figures

List of Tables

Abstract

Totipotency is a hallmark of plants, where entire shoots/roots can be formed *de novo* from undifferentiated callus in response to external inductive cues. Interestingly, during *de novo* shoot organogenesis, only a few initial cells known as 'progenitor' can develop into an entire shoot system. How these initials are selected and what governs their subsequent progression to a patterned organ system remain unresolved. My work led to the discovery of a new regulatory axis where shoot-promoting factor *CUC2* activates the expression of cell wall loosening enzyme XTH9 in the cells surrounding the progenitors. Encapsulation of progenitors by a shell of cells expressing cell wall loosening enzyme serves as a mechanism for selecting productive progenitors in undifferentiated callus. *CUC2-XTH9* activates cell polarity non-cell autonomously to confer the productive fate to regenerating progenitors. Interestingly, cell wall modification in surrounding non-progenitor cells and cell polarity in the progenitors act in a regulatory feedback loop to make the dome-shaped shoot meristem *de novo*. Together, my studies provide a simple model accountable for self-organized morphogenesis in the absence of pre-pattern cues.

CUC2 expression is activated by plant-specific transcription factor *PLETHORA*. *PLETHORA* proteins control a variety of developmental and regenerative processes in *Arabidopsis*. I have examined the role of monocot, *Rice PLETHORA* genes in dicot plants, *Arabidopsis*. My studies reveal the conserved function of *Rice PLETHORA* proteins in controlling both developmental processes, such as lateral root outgrowth, and regenerative responses, such as regeneration of damaged tissues or complete shoot system in evolutionary diverged dicot plant species.

Chapter 1

Introduction

1.1 Introduction

All living organisms have an inherent ability to grow, survive and produce off-springs in their growing territory. They promptly respond to injury or damage they encounter during their growth. The inability to repair this wound or lost tissue will diminish their growth and development followed by elimination from their population. Animals and plants have developed the ability to respond to injury by repairing and reprograming the tissue/organ subjected to injury. Especially plants, due to their sessile nature, are adapted more to fight against various environmental (biotic and abiotic) circumstances for their survival. They display a remarkable capacity to repair, regain and sustain the stress experience during their life cycle. Unlike animals, plants have shown enormous cell plasticity and high regeneration in order to maintain growth and survival through different responses, such as wound-induced regeneration or *de novo* organogenesis. Irrespective of evolutionary origin, both plants and animals share regeneration potency, and the underlying reprogramming mechanism is likely to adopt similar strategies (Meyerowitz, 2002). Unlike plants that can repair and regenerate tissues throughout the body parts, this ability is restricted to specific lineages in the animal kingdom (Birnbaum & Alvarado, 2008; Pulianmackal et al., 2014; Sugimoto et al., 2011). Regeneration has been widely studied in both kingdoms in the past few decades to unravel the underlying processes and the molecular mechanism to draw a parallel between them (Atta et al., 2009; Efroni & Birnbaum, 2016; Plant Regeneration: Cellular Origins and Molecular Mechanisms, 2016; Kareem et al., 2015b; Sánchez Alvarado & Yamanaka, 2014; Sena et al., 2009; Sugimoto et al., 2010; Takahashi & Yamanaka, 2006; J. Xu et al., 2006).

All living organisms are made up of cells and they originate from pre-existing cells (Virchow, 1859). Unlike most animals, regeneration is restricted to a few cell lineage; plants can create new life from a single cell irrespective of origin due to their extraordinary plasticity. Totipotency of plant cells was discovered by Haberlandt in 1902 and was the turning point for the experimentation with plants in laboratory conditions that mimic natural regeneration, which opened up a new field of investigation (Haberlandt, 1902) to science. The hormonal combinations of Miller and Skoog have been widely exploited in plant species for the past 60 years and have been shown to facilitate the formation of plants or

organs, serving as a simple method (Skoog & Miller, 1957). The ability of regeneration has been investigated across the plant kingdom such as algae, bryophytes, and flowering plants in the last decades, though the underlying molecular regulators are yet to be fully explored (Birnbaum & Alvarado, 2008; Duclercq et al., 2011; Plant Regeneration: Cellular Origins and Molecular Mechanisms, 2016; Pulianmackal et al., 2014). Regeneration in plants can be broadly classified into two categories; one is mechanical-injury-induced regeneration, and another is *de novo* organogenesis (Mathew & Prasad, 2021). Here I provide a brief overview of two types of regenerative responses studied using the model plant species *Arabidopsis thaliana.*

1.2 Mechanical-injury-induced regeneration

Despite the restricted movements (mainly nastic movements), plants acquired the ability to repair or regenerate the lost tissue or organ with high regeneration efficiency compared to animals (Efroni et al., 2016; J. Liu et al., 2014; Mathew & Prasad, 2021; Radhakrishnan et al., 2020). Due to their immobile nature, regeneration is the inevitable process in their life cycle for survival. Plants experience a vast variety of biotic stresses such as herbivore attacks, insect bites, nematode attacks, or human interruptions as well as abiotic stresses such as wind, snowfall, heavy rain, or lesions through friction. Mechanical damages are caused by these circumstances; plants respond to these injuries either by wound healing or by cell proliferation, or by re-growing the lost organ completely. These types of responses are similar in the injured tissue, whether it is attached to the parental plant or in the detached body part (Durgaprasad et al., 2019; Feldman, 1976; Plant Regeneration: Cellular Origins and Molecular Mechanisms, 2016; Mathew & Prasad, 2021; Radhakrishnan et al., 2020; Reinhardt et al., 2003; Schiavone & Racusen, 1991; Shanmukhan et al., 2021; van den Berg et al., 1995). However, the injured tissue attached to the parental plant shows a prominent regenerative response compared to the detached one. As an initial trigger of the wound response, the surrounding differentiated tissue enters into the cell cycle leading to wound healing or local cell proliferation (Zhou et al., 2019). According to the depth of the injury, the cells reinstate the lost tissue or organ or just simply cell proliferates to protect the exposed tissue from further infection (Radhakrishnan et al., 2020). This mechanical-injury-

induced regeneration has been extensively investigated and documented in *Arabidopsis thaliana* for the past several decades. Recent studies have mimicked natural mechanical wounding by biotic or abiotic means in the laboratory platform to study the responses and elucidate the underlying molecular mechanisms.

1.2.1 Regeneration of vascular tissues in aerial parts of plants

Plants exhibit mechanical-injury-induced regenerative responses throughout the body, such as aerial organs as well as underground tissue. Both body parts exhibit differences in the regeneration efficiency along the shoot-root axis and are exploited widely to understand the regenerative responses. Regeneration in lateral aerial organs such as leaves is a recently explored area in the field where mechanically injured mid-vein get repaired and regenerate new vascular tissues (Radhakrishnan et al., 2020). These regenerative responses mimic the injury inflicted by the proboscis of the insect, caterpillar bite, or herbivores attack to grab the minerals and nutrients passing through the main transporting area, that is mid-vein, to the other plant body. Or the damage due to the wind or snowfall on the mid-vein could be another reason. Restoration of vascular tissue in a disconnected mid-vein of a growing leaf and the underlying molecular mechanism was reported recently. The new vascular tissues are formed in a D-loop to reunite the disconnected upper and lower pre-existing vasculature through a coherent feed-forward action of *PLT3, PLT5, PLT7-CUC2* module by regulating the auxin expression in the injured site (Figure 1.1A and 1.1D). Notably, the reconnection of the midvein bypasses the wounded site and creates a vasculature with the nearest pre-existing vasculature, either with the midvein or lateral vein. Re-specification of the tissue into new vascular cells leads to the restoration of the transport in the growing leaves (Radhakrishnan et al., 2020). Local abrasion by friction or the breakage in the vascular strand on the stem is also used as a model for regeneration study. New vascular cell formation was observed in the partially disconnected vein in the *Arabidopsis* inflorescence stem, showing the initial cell proliferation followed by new vascular tissues to re-establish the connection (Figure 1.1B). Depending on the depth or size of the wound, the local cell proliferation increases and it ceases to make a vascular connection between them and leaves a cell mass, called callus, in the wounded area (Radhakrishnan et al., 2020). The healing of the local abrasion on the inflorescence stem experiences a similar phenomenon. The cell proliferation occurs in the injured part to seal the wound to protect the tissue from bacterial

or fungal infection (Figure 1.1C) (Radhakrishnan et al., 2020).

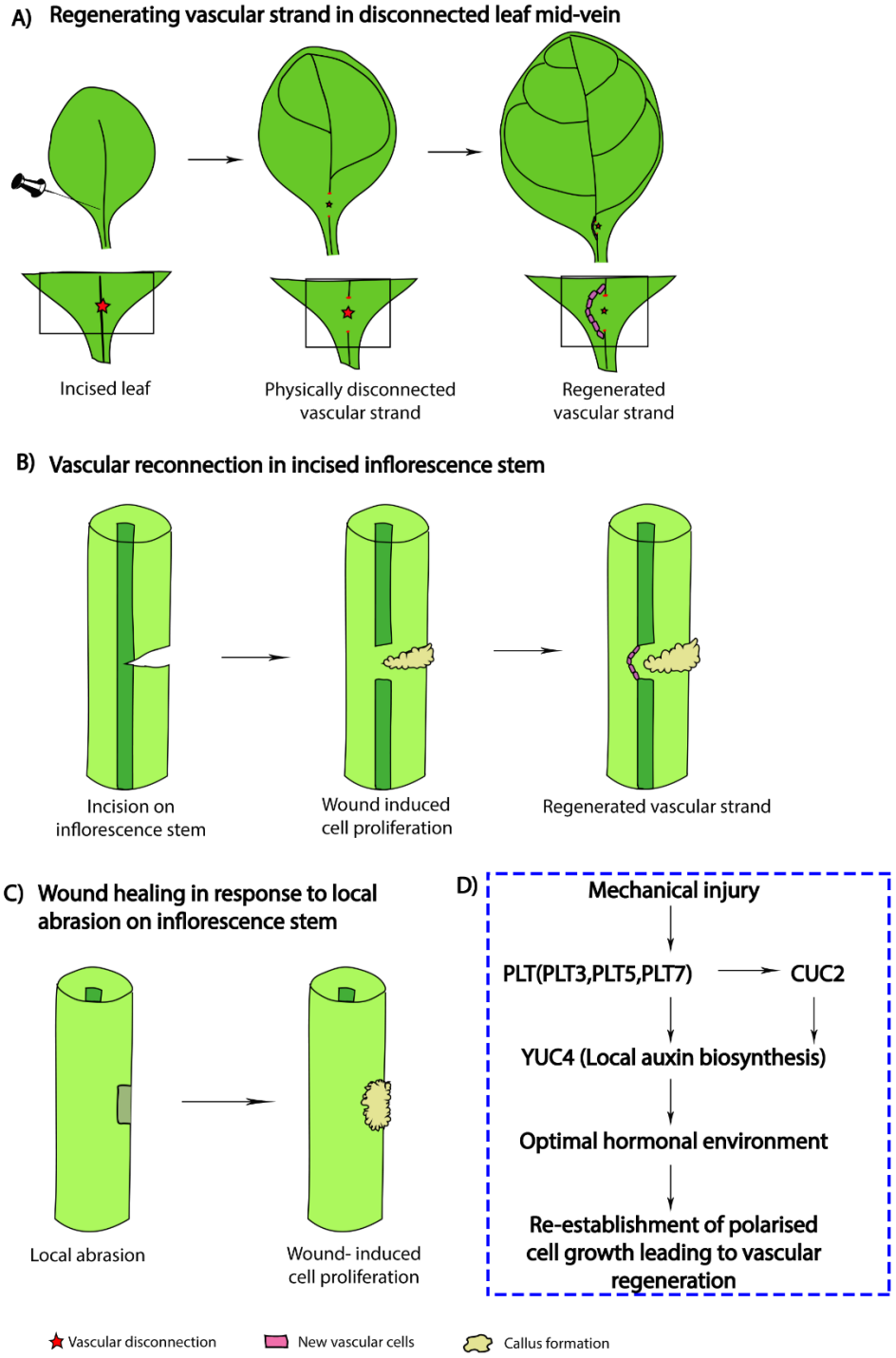

Figure 1.1: Types of mechanical-injury-induced regeneration in *Arabidopsis thaliana*.

(A) Schematic representation of vascular regeneration in leaf. Physically separated veins (red asterisks) regenerate in response to injury and join the top and bottom of the existing vascular strand by forming a D-loop shaped new strand (magenta) in a developing leaf. **(B)** Schematic depiction of a partially disconnected vascular strand of *Arabidopsis* inflorescence stem in response to injury by

local cell proliferation (cream) and restore the disconnected vein by reprograming new vascular cells (magenta) from surrounding. **(C)** Schematic showing the wound healing by local cell proliferation (cream) in response to local abrasion on the inflorescence stem. **(D)** Flow chart representing PLTs-CUC2 regulatory module involved in the regeneration response upon mechanical injury.

1.2.2 Regeneration of specific cell types or tissues in root

Restoration of damaged cells or the root tip studies have been started long ago, and still, biologists are addressing mind-twisting questions in this field. As mentioned earlier, an attack of nematode, bacterial infection, or mechanical injury leads to the damage of the cells or even loss of root tip. These natural injuries were recreated *in vitro* by ablating the different types of cells in the layers or by resecting the root tip (Fulcher & Sablowski, 2009; Grieneisen et al., 2007; Hong et al., 2017; Scheres et al., 1997; Sena et al., 2009; van den Berg et al., 1995; Y. Zhang et al., 2016). Ablation of quiescent center (QC), the root organizer, disrupts the flow of auxin, and 1-2 cell layers above the abated QC experience the accumulation of auxin. It leads to the re-specification of stellar cells into new QC. The surrounding cells near the new QC acquire the root stem cell property by the non-autonomous influence of QC, whereas the cells between the ablated and new QC would turn into columella (Figure1.2A) (van den Berg et al., 1995; J. Xu et al., 2006). Ablation of the root stem cell or any cell in the root layers initiates the periclinal division of the adjacent cell, and it reinstates the lost cell by re-specifying the fate in that position (Figure1.2A) (Marhava et al., 2019; van den Berg et al., 1995). It is still unclear why only the cells inside of damaged ones can divide and respecify. Growing roots experience intrinsic axial and radial growth pressure, which is known to affect them differently in their inner and outer cell files (Clark et al., 2003). Unlike the damaged cell replacement after ablation, the entire root tip is regenerated upon the root tip resection (Figure1.2B). The plant responds to this kind of injury immediately and replaces the lost part as fast as possible because the root of a plant is a vital organ meant for the absorption of water, minerals, and nutrients from the surrounding for growth. The loss of the distal end of the root (tip portion) triggers the positional cues in the wounded site, and the auxin and jasmonic acid (JA) get accumulated at the site of injury. A high amount of auxin and JA experienced in the injured part recognizes the damage and activates the stem cell regulators like *RETINOBLSTOMA-RELATED- SHORT-ROOT -SCARECROW* (*RBR-SHR-SCR)* through *ETHYLENE RESPONSE FACTOR09 (ERF09)*, *ERF115*, and *CYCLIND6;1* (Figure1.2C) (Zhou et al.,

2019).

As a response, the differentiated vascular tissue would reprogram and switch its fate to QC, followed by stem cell niche formation enabling the restoration of root tip through cell local proliferation followed by cell fate determination at the distal end. Restoration of the root tip is dependent on the area where the root is injured. The competence zone for the regeneration is attributed to the gradient expression of root stem cell regulator *PLETHORA2* (*PLT2*), whose auto-activation guides the regeneration. *PLT2* expression is high in the competence zone, and it decreases from the distal (competence zone) to the proximal end (non-competence zone) of the root (Durgaprasad et al., 2019). Root organ regeneration would cease when the dosage-dependent *PLT2* expression goes beyond the threshold rather than a long root meristem (Figure1.2D) (Durgaprasad et al., 2019). Interestingly the detached organ behaves entirely differently from the injured organ attached to the growing plant. It responds in such a way that it establishes a new organ or plant from the cut end (Amano et al., 2019, 2020; Chen et al., 2014; Shanmukhan et al., 2021). Single-cell RNA Sequencing, lineage analysis, and live imaging reveal that the wounded site follows the embryonic pathway for the replacement of the root tip after resection (Efroni et al., 2016). An interesting fact is that these molecular regulators involved in the various regenerative responses play a vital role in normal growth and development. It explains the complex multifunctional action of these factors during regeneration as well as in normal development (Cruz-Ramírez et al., 2012, 2013; Durgaprasad et al., 2019; Efroni et al., 2016; Galinha et al., 2007; Hardtke & Berleth, 1998; Mähönen et al., 2014; Zhou et al., 2019).

Auxin is also involved in root regeneration after abiotic stress, such as exposure to cold temperatures. Stem cell niche (SCN) cells, including QC cells, are protected here by sacrificing columella stem cell daughters (CSCDs). Similarly, the ablated QC cells block auxin transport, resulting in the regeneration of new QC. Dead CSCD cells block auxin transport, resulting in elevated auxin levels in the QC, which in turn prolongs the existing QC rather than regenerates a new one (Hong et al., 2017). Other than auxin, jasmonic acid and ethylene are also responsible for regenerative responses. Both the phytohormones are activated immediately as defense mechanisms and contribute their effect to promoting the regeneration of organs (Zhou et al., 2019).

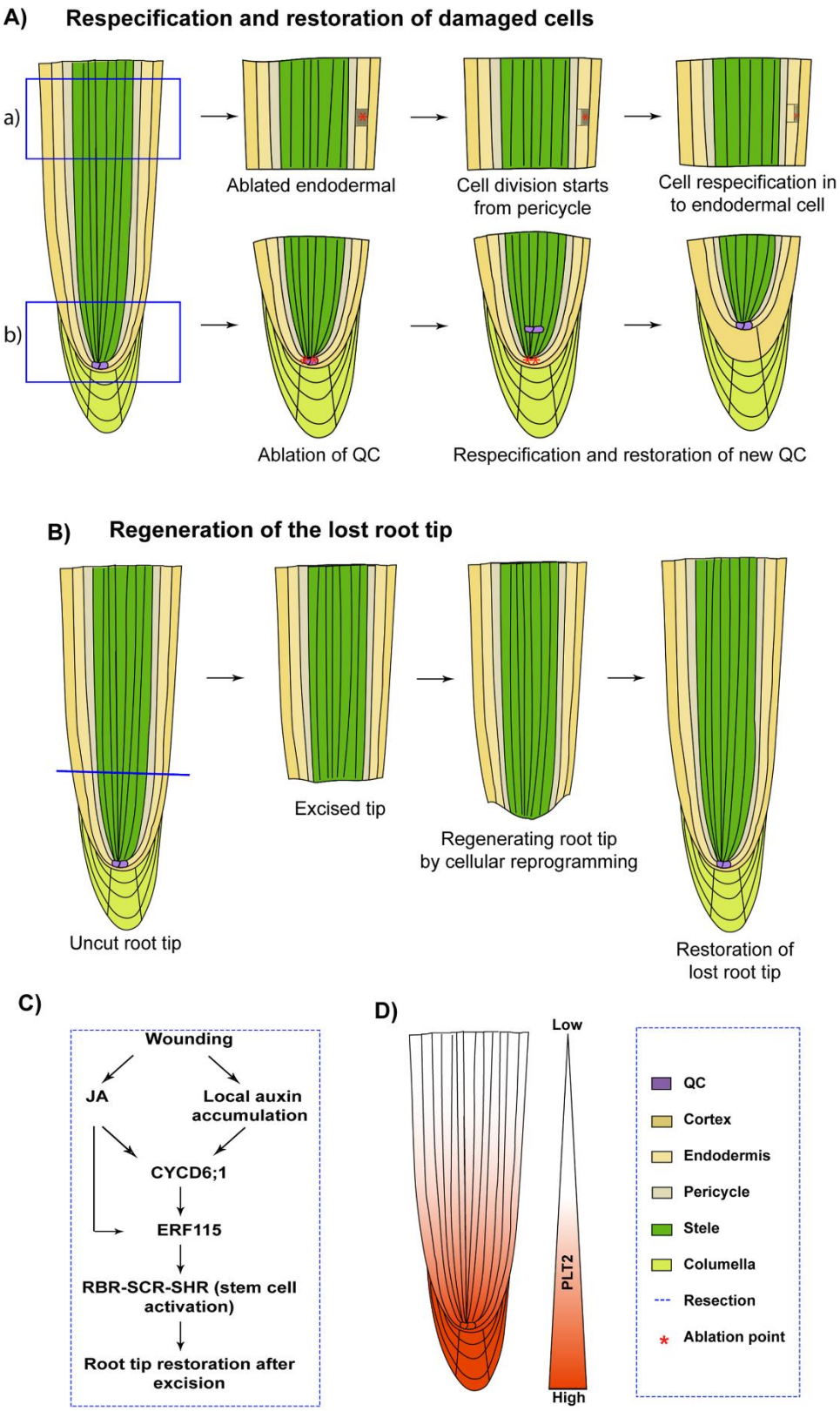
A) Respecification and restoration of damaged cells
a)
b)
Ablated endodermal
Cell division starts from pericycle
Cell respecification in to endodermal cell
Ablation of QC
Respecification and restoration of new QC
B) Regeneration of the lost root tip
Uncut root tip
Excised tip
Regenerating root tip by cellular reprogramming
Restoration of lost root tip
C)
Wounding
JA
Local auxin accumulation
CYCD6;1
ERF115
RBR-SCR-SHR (stem cell activation)
Root tip restoration after excision
D)
Low
PLT2
High
QC
Cortex
Endodermis
Pericycle
Stele
Columella
Resection
Ablation point

Figure 1.2: Restoration of damaged tissue or lost organ of root.

(A) a) Ablation of endodermal cell initiate neighboring pericycle cell to divide periclinally, the daughter cell eventually reprogramed to endodermal fate to replace the lost endodermal cell, b) ablation of QC cells activate stellar cells to re-specify into new QC leads to the re-establishment of the root tip.
(B) In root tip resection, cells at the vicinity of excision undergo division and activate embryonic patterning to re-establish the excised root tip. **(C)** Flowchart representing wound-induced signaling pathway to re-establish damaged cells or lost organ in the root. (D) Schematic depiction of gradient distribution of *PLT2* in the root shows PLT2 protein expression decreases from distal and to the proximal end of the root.

1.2.3 Injury-induced *de novo* root regeneration (DNRR) from detached leaf

The wound is the first trigger to initiate various types of responses such as regeneration. *De novo* root organogenesis (DNRR) from a detached leaf using a simple method without hormone supplementation is a suitable example to study such responses (Chen & Engert, 2014; J. Liu et al., 2014). Mechanical-injury-induced root formation from the cut end of the petiole has been studied previously, though the molecular basis of wound signaling and corresponding responses have been studied recently (Bustillo-Avendaño et al., 2017; Chen & Engert, 2014; Plant Regeneration: Cellular Origins and Molecular Mechanisms, 2016; J. Liu et al., 2014; G. Zhang et al., 2019). The auxin accumulation at the cut end of the detached *Arabidopsis* leaves triggers the homeobox transcription factors, WUSCHEL RELATED HOMEOBOX11 (WOX1) and WOX12. Direct response of WOX1 leads to the activation of LATERAL ORGAN BOUNDARIES-DOMAIN 16 (LBD16) and LBD29, and subsequently WOX5 through its redundant gene WOX12. WOXs and LBDs expression result in the transition of leaf procambium cells to root founder cells (Figure 1.3A) (J. Liu et al., 2014). Programing of procambial cells in the petiole into root primordia follows distinct developmental stages consisting of 1) vasculature proliferation and endogenous callus formation by the action of *ABERRANT LATERAL ROOT FORMATION 4* (*ALF4*) and *KIP-RELATED PROTEIN2* (*KRP2*), 2) endogenous micro-callus precedes root founder cell specification, 3) root primordia initiation and patterning through the activity of *PL1*, *PLT2* , and *SHR*, and 4) root meristem activation and emergence (Bustillo-Avendaño et al., 2017) to specify the postembryonic root formation (Figure 1.3A). The initial signal in response to the wound from the cut of the petiole is JA gets activated within 2hrs that leads to the *ETHYLENE RESPONSE FACTOR109 (ERF109)* mediated upregulation of *ANTHRANILATE SYNTHASE α1* (*ASA1*). The activity of ERF109 has been

inhibited after 2hr by direct interaction of JA to prevent hypersensitivity to wound signaling showing the feedback regulation by JA initial signal during DNRR (G. Zhang et al., 2019). Another interesting finding that has been observed recently in this field is the regulation of contact dependent *de novo* root formation from the cut end of the petiole. The cut of the petiole experiences an elevated auxin-maxima; it directs the different regenerative responses in response to the wound. Here the root fate is determined by the physical contact of the injured cut end to any media such as agar, soil, or water favor to direct root formation, whereas it makes a proliferated mass of callus from the wounded site in the absence of any contact (Figure 1.3B) (Shanmukhan et al., 2021). The expression of PLT7 also appears within 24 hr and upregulated at the cut end of the petiole with contact activating the root-specific *PLT* such as *PLT1*, showing that *PLT3*, *PLT5*, *PLT7* is necessary and sufficient for contact-mediated DNRR (Figure 1.3A) (Shanmukhan et al., 2021). Based on these evidences, the initiation and the emergence of the adventitious root show a similar regulatory mechanism with that of the callus whereas after initiation of the adventitious root, shares a common developmental pathway as like lateral root (Bustillo-Avendaño et al., 2017; J. Liu et al., 2014; Shanmukhan et al., 2021).

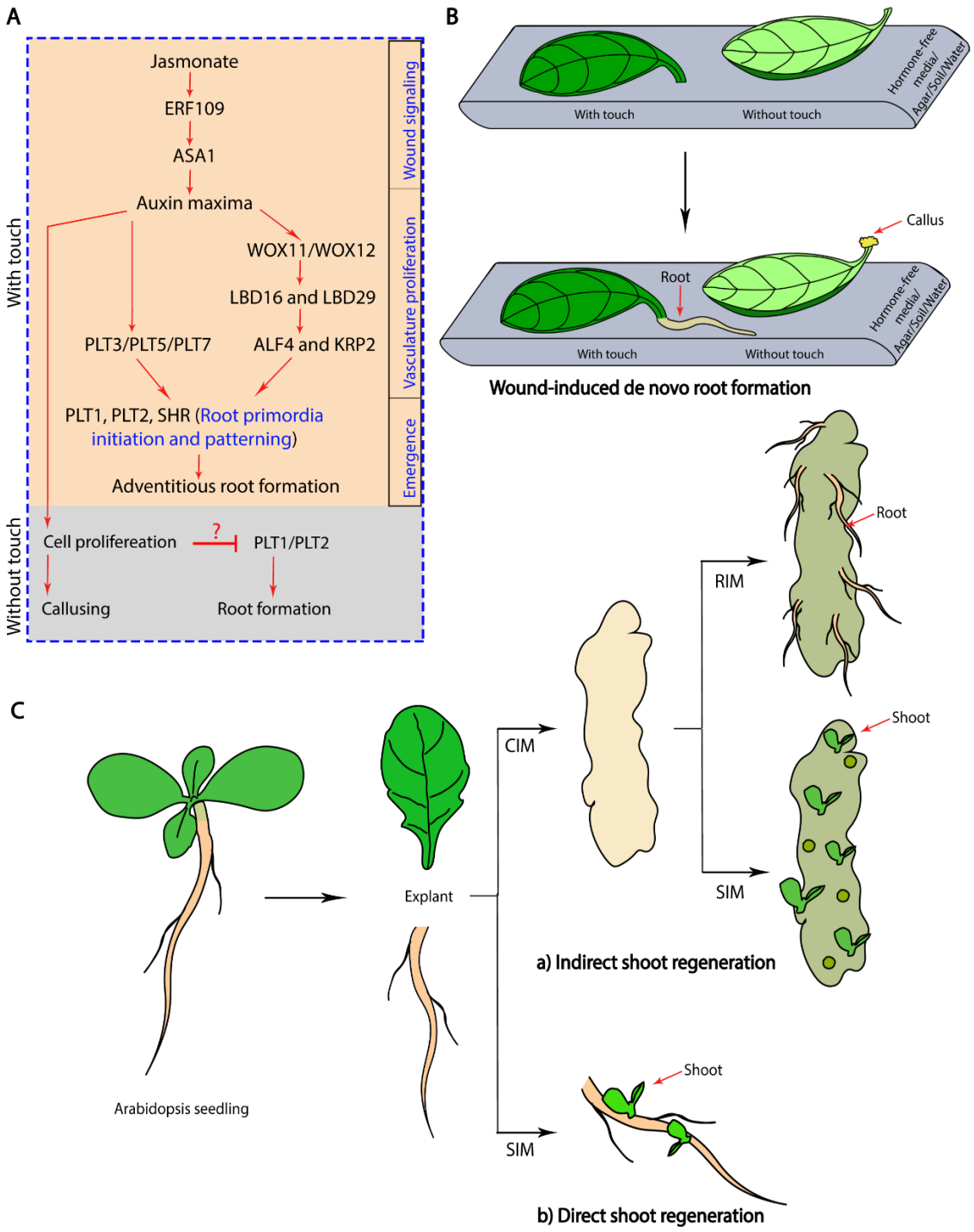

Figure 1.3: Regenerative responses with and without external hormonal inductive cues

(A) Flow-chart representing the signaling module involved in wound-induced *de novo* root regeneration. **(B)** Schematic representation of touch dependent *de novo* root regeneration from cut end of a detached petiole. **(C)** An outline of tissue culture mediated *de novo* organogenesis. a) Indirect shoot or root regeneration, and b) direct shoot regeneration from any explant.

1.3 Tissue culture-induced regeneration

Nevertheless, from unicellular to multicellular organisms, life starts from a single cell, that is, the zygote. Unlike animals which develop an entire body plan during embryogenesis, plants build their body structure post-embryonically during the course of development. It retains the body plan in a miniature form and is located at opposite poles of the embryo called plumule (contains the shoot apical meristem-SAM) and radicle (root apical meristem-RAM). Plants are exceptional, have an extraordinary ability termed totipotency to make an organ or entire organism from any tissue from a different developmental origin. The cell or tissues are treated with various phytohormones in vitro and are able to create a new organism from a small piece of somatic cells called an explant (Figure 1.3C). There are two methods to create a new organism from the explant with the help of external inductive cues: 1) somatic embryogenesis (Huang & Yeoman, 1995; Pulianmackal et al., 2014; Zimmerman, 1993) in vitro *de novo* organogenesis (Che et al., 2006; Valvekens et al., 1988) directed only by external inductive cues.

1.3.1 Regeneration via somatic embryogenesis

Somatic embryogenesis is the practice of generating embryos from a single somatic explant. Differentiated somatic cells go back to the embryonic state with the treatment of a high concentration of auxin, 2,4-D during the process of somatic embryogenesis (Ikeda-Iwai, 2002; Su et al., 2009). Interestingly somatic embryos pre-specify the pole as in the zygotic embryo (Thorpe & Stasolla, 2001) and do not retain the vascular connection with the explant (Nowak & Gaj, 2016).

1.3.2 *De novo* organogenesis

In tissue culture-mediated *de novo* organogenesis, the cells to be committed completely bypass the

embryonic positional cues to create an organism. As mentioned in somatic embryogenesis, the *de novo* organogenesis is completely modulated by external hormonal cues. Contrarily, positional information during *de novo* organogenesis is primarily derived from the reconstitution of stem cells and the building of spatiotemporally regulated regulatory connections. Tissue culture-mediated regeneration can be achieved by either direct reprogramming into organs or indirect regeneration (Figure 1.3C). In direct regeneration,

the shoot or root arises from the explant without an intermediate cell stage like callus based on the incubation with hormonal inductive cues. The cells undergo trans-differentiation of differentiated tissue and acquire new fates such as shoot or root (Figure 1.3C.a) (Chatfield et al., 2013; Kareem et al., 2016; J. Liu et al., 2014). The adventitious shoots are developed by synchronous initiation of lateral root primordia/meristem (LRP/LRM) by the treatment of auxin. It is followed by subsequent incubation with cytokinin leads to the conversion of LRP to shoot meristem. Here the cytokinin-induced expression of *WUS* in the LRP re-specify the tissue and converts it to functional SAM (Chatfield et al., 2013). However, the indirect mode of regeneration has been studied extensively compared to direct reprogramming (Atta et al., 2009; Che et al., 2007; Gordon et al., 2007; Kareem et al., 2015b; Rosspopoff et al., 2017; Sugimoto & Meyerowitz, 2013; Valvekens et al., 1988; T.-Q. Zhang et al., 2015). Callus-mediated regeneration of organs involved a sequence of incubation of explant upon auxin-rich callus induction medium followed by cytokinin-rich shoot/auxin-rich root induction medium (Atta et al., 2009; Che et al., 2007; Gordon et al., 2007; Kareem et al., 2015a; Sugimoto & Meyerowitz, 2013). The regeneration potency in indirect organogenesis relies on the developmental time window (Sugimoto & Meyerowitz, 2013; T.-Q. Zhang et al., 2015) and the origin (Akama et al., 1992; Valvekens et al., 1988) of the explant, whereas in direct regeneration dependent upon the suitable explant which responds to suitable hormonal inductive cues (Figure 1.3C.b) (Atta et al., 2009; Chatfield et al., 2013; Kareem et al., 2015a, 2016; Rosspopoff et al., 2017). Moreover, the critical role of plant hormones, especially auxin and cytokinin, regulates the reprogramming of the somatic cells by modulating their plasticity to gain pluripotent meristematic activity that leads to acquiring a new fate during the *de novo* regeneration (Atta et al., 2009; Sugimoto et al., 2010).

1.3.2.1 Recruitment of lateral root developmental pathways to establish the pluripotency during *de novo* organogenesis

Auxin and cytokinin have the varied potential for organogenesis. Auxin mediates the activation of cell division of the xylem pole pericycle. In contradiction to that, phloem pole pericycle cells undergo division when the explant incubates with cytokinin-rich media (Atta et al., 2009). It is well known that the initiation of LRP (Lavenus et al., 2013) and the involvement of acquiring pluripotency followed by the callus formation are regulated by

auxin (Figure 1.4A) (Ikeuchi et al., 2013). Root trait determinants are down-regulated in the cytokinin-rich medium, showing its inability to make a cell competent and establish pluripotency (Atta et al., 2009; Sugimoto et al., 2010). This suggests that cytokinin alone is not sufficient to drive cell division and acquire pluripotency to respond to regeneration. However, the cytokinin-rich medium is sufficient to generate plantlets in the presence of auxin-induced LRP during direct regeneration (Figure 1.3C.b) (Atta et al., 2009; Chatfield et al., 2013; Kareem et al., 2015a; Radhakrishnan et al., 2018; Rosspopoff et al., 2017). During the incubation of CIM, a pool of adult stem cells that are partially differentiated, such as the xylem pole pericycle in the root or pericycle-like cells in the aerial organ, undergo cell division when it experiences high auxin. It modulates the cells to attain competency and helps to acquire pluripotency for the further molecular framework (Figure 1.4B) (Atta et al., 2009; Che et al., 2007; Gordon et al., 2007; Kareem et al., 2015b; Sugimoto et al., 2010, 2011). *J0121*, a marker of pericycle cells, expression starts to disappear from the cells which respond to the high concentration of auxin. The complete disappearance of *J0121* can be correlated with a high chance for the formation of the callus as in the case of the callus formation related 1(*cfr1*) mutant (Shang et al., 2016). Note that the wildtype callus shows a moderate amount of *J0121* expression, and it persists in the solitary-root (*slr/iaa14*) mutants (Fukaki, 2002). However, it does not mean that the disappearance of the *J0121* is directly correlating to acquiring competency, but it ensures the transition of pericycle cells to the callus tissue (Che et al., 2007; Shang et al., 2016; Sugimoto et al., 2010). Interestingly, the gene expression profile and cellular organization of the root and callus are similar. Root-specific genes such as *WUSCHEL RELATED HOMEOBOX5* (*WOX5*), *SCARECROW* (*SCR*), *SHORT-ROOT* (*SHR*), QC marker *QC25*, *PINFORMED1*(*PIN1*), *PLETHORA1* (*PLT1*), *PLT2*, *GLABRA2* (*GL2*), *ROOT-CLAVATA HOMOLOG1* (*RCH1*) are also expressed in the callus regardless of which plant tissue used an explant (Atta et al., 2009; Kareem et al., 2015b; Radhakrishnan et al., 2018; Sugimoto et al., 2010). Interestingly, defective *ALF4* (aberrant lateral root formation 4) expression in the *alf4* mutant compromise or altogether abolish the callus formation (Sugimoto et al., 2010) as well as the lateral root formation (Celenza et al., 1995). And the crucial role of *LATERAL ORGAN BOUNDARIES DOMAIN* (*LBD*) in the lateral root development and the callus formation emphasize the genetic and morphological

relation of root and callus (Fan et al., 2012; Lee et al., 2009; Okushima et al., 2007).

1.3.2.2 The necessity of PLT-CUC2 module in *de novo* organogenesis

Lateral root development and callus formation are interconnected with each other by their genetic and molecular composition dealing with. The regenerative potency of the callus, irrespective of its origin, has been unraveled recently using *plt3,plt5-2,plt7* mutant. The PLETHORA/AINTEGUMENTA-LIKE (PLT/AIL) proteins belong to the double APETALA2/ETHYLENE RESPONSE FACTOR domain family (Aida, Beis, Heidstra, Willemsen, Blilou, Galinha, Nussaume, Noh, Amasino, Scheres, et al., 2004; Galinha et al., 2007; Horstman et al., 2014; Mähönen et al., 2014; Nole-Wilson et al., 2005). *plt3,plt5-2,plt7* mutant, defective in the lateral root primordial outgrowth, show defective in regeneration. The callus tissue fails to activate root stem cell regulators such as *PLT1* or *PL2* and is unable to make the callus competent for external inductive cues and unable to regenerate (Kareem et al., 2015). *PLT3*, *PLT5*, and *PLT7* mediate regeneration by regulating the expression of *PLT1* or *PLT2* (root stem cell regulators) to acquire the pluripotency in an auxin-rich pool (Figure 1.4A.a) and overexpressing a shoot promoting factor *CUP-SHAPED COTELYDON 2* (*CUC2*) in a cytokinin-rich medium by helping the shoot progenitor outgrowth (Figure 1.4A.b). The two-step mechanism of *de novo* shoot regeneration mediated by PLT3, PLT5, or PL7 transcription factors is conserved all over the plant body part (Figure 1.4A) (Kareem et al., 2015). Root-specific stem cell regulator expression in the callus during incubation on callus induction media (CIM- auxin-rich) starts downregulating, and shoot forming factors get activated when the callus is exposed to cytokinin-rich media (shoot induction media- SIM) (Figure 1.4B). Unlike indirect shoot regeneration, direct regeneration possesses a developmental time window of LRP neither early nor too late stage to convert into the shoot (Kareem et al., 2016; Rosspopoff et al., 2017). Cells in the LRP would be in a transient fate by the rapid gene expression of *WOX5* followed by shoot-specific *WUS*, *STM*, or *CLV3* when the LRP incubated with a cytokinin-enriched media stimulate the pluripotency for the conversion of LRP to shoot during the direct shoot regeneration (Rosspopoff et al., 2017).

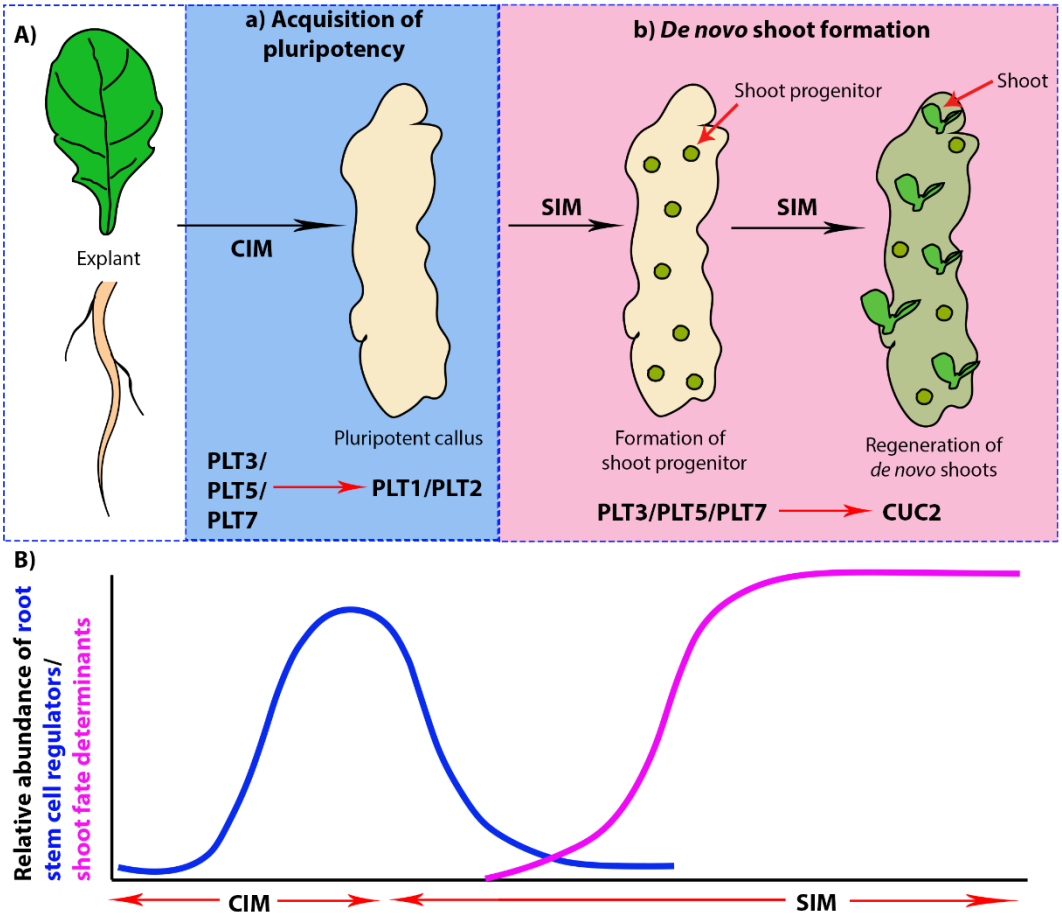

Figure 1.4: PLETHORA activates root stem cell regulators and shoot determinants through two steps during indirect shoot regeneration.

(A) An overview of the two-step mechanism involved during shoot regeneration mediated by tissue culture. *PLT3/PLT5/PLT7* induce pluripotent callus is first formed from any explant (irrespective of origin) upon auxin-rich callus induction medium (CIM) by activating root-specific genes such as *PLT1* or *PLT2* to acquire competency to the cells (a). Upon cytokinin-rich short induction media (SIM), they undergo self-organization and develop into shoot progenitor cells, eventually resulting in the growth of a shoot outgrowth controlled by the *PLT-CUC2* module (b). **(B)** Graphical representation of the appearance of stem cell regulators in CIM and shoot fate-determining factors upon SIM induction during *de novo* shoot formation.

1.3.2.3 Wound-induced shoot regeneration

Another signaling pathway for organ regeneration is mediated by *WOUND INDUCED DEDEIFFERENTIATION1* (*WIND1*). *WIND1* is rapidly upregulated at the wound site, and initiates cell division, followed by the formation of cell proliferation from the epidermal cells of the explant such as cotyledon, root, or hypocotyl (Iwase et al., 2011). It activates the cytokinin signaling pathway by regulating B-type Arabidopsis response regulator

(ARR), leads to cell de-differentiation, and produces callus. This wounding-induced signaling mediated by *WIND1* directly activates *ENHANCER OF SHOOT REGENERATION 1* (*ESR1*) to promote *CUP SHAPED COTYLEDON 1* (*CUC1*) during the *de novo* organogenesis (Iwase, 2016). Moreover, overexpression of *WIND1* can bypass the external application of auxin in the media, suggesting the sufficiency of *WIND1* during the shoot organogenesis (Iwase et al., 2011). Interestingly, the root stem regulators do not display a prominent upregulation by *WIND1* as compared to the *PLT*- mediated regeneration, where the root trait determinants play an essential role in acquiring the competency for the callus (Iwase et al., 2011; Kareem et al., 2015b; Radhakrishnan et al., 2018). However, the formation of pluripotent callus in the *WIND1* pathway is needed to gain deeper insights.

1.3.2.4 Self-organization of shoot foci in heterogenous callus

De novo shoot formation is a programmed self-organization from a chaotic mass of callus cells. Spatio-temporal expression of factors is tightly modulated for recreation of shoot from a group of cells in the absence of embryonic positional cues. Despite the root trait determinants making the calli pluripotent with a high concentration of auxin in the media, all the cells do not respond to the cytokinin signaling for self-organization. The calli behave as a heterogeneous mass, and the initiation of shoot fate-determining cells called regenerating foci stochastically. The existence of heterogeneity in the pluripotent callus is due to the difference in the expression patterns of key shoot regulatory genes in the callus (Atta et al., 2009; Gordon et al., 2007; Kareem et al., 2015b; Radhakrishnan et al., 2018). The heterogeneity increases over time in the culture (Landrein et al., 2015). Random initiation of regenerating foci from a heterogeneous mass of calli express PIN1, a known marker of early shoot progenitor, but it does not indicate the formation of functional shoot outgrowth. Some of the regenerating shoot foci attain the shoot structure, whereas some others lose their ability to reach the final form. This is an interesting fact that the stochastically initiated regenerating foci are again screened at the level of the shoot formation stage. The decision of a regenerating shoot progenitor to a complete shoot could be influenced by irregular callus topology that could impose growth-driven mechanical tension (Landrein et al., 2015; Radhakrishnan et al., 2018). The level of gene of expression

and the difference in the epigenetic regulators due to multiple cell division or the hormonal treatment could be another influencer of the heterogeneous behavior of the callus (Shemer et al., 2015). Epigenetic regulation of *WUS* (W. Li et al., 2011; G. Zhang et al., 2019) acts to maintain the shoot stem cell niche during normal (K. F. . Mayer et al., 1998; Schoof et al., 2000) or *de novo* shoot formation (Gallois et al., 2004; Gordon et al., 2007; Rosspopoff et al., 2017; T.-Q. Zhang et al., 2017) provides an insight of cellular heterogeneity in the callus. De-regulation of epigenetic modification in the *WUS* locus can change cellular heterogeneity or expression competence. The higher number of organizing centers in the *met1* (*methyltransferase 1*), DNA hypomethylated mutant, could be a result of ectopic relaxation of repressive epigenetic control at the *WUS* locus (W. Li et al., 2011). Moreover, other molecular modifiers like epigenetic regulators also contribute to the change degree of cellular heterogeneity in the callus (Z. Liu et al., 2016).

Arabidopsis is used as a model to study fundamental concerns in the field of regeneration that focus on the plant's ability to regenerate its shoot or root. The regeneration studies in the root have explored largely and shown that the lost cell respecified from the surrounding cells and resected root goes back to the embryonic state to reprogram the lost system (Efroni et al., 2016; Fulcher & Sablowski, 2009; Grieneisen et al., 2007; Hong et al., 2017; Sena et al., 2009; van den Berg et al., 1995, 1997; Y. Zhang et al., 2016). However, the *de novo* shoot organogenesis and the patterning from a heterogenous callus have not yet been fully understood in how the shoot determinants orchestrate shooting. Here, we investigate how shoot-determining elements involved to designate a single or group of cells, leads to the shoot fate, in the absence of cell mobility, the primary mechanism in the animal kingdom. And, we explain how the shoot progenitor, a pre-state that gives rise to the shoot, is fabricated by the effort of a group of molecular factors that govern a shoot outgrowth from a heterogeneous callus.

Chapter 2

Localization pattern of PIN1 confers the productive fate to regenerating shoot progenitors

2.1 INTRODUCTION

Cell polarity is a fundamental process that coordinates a wide range of cell behavior in all organisms. It is an essential programming component for their growth and development. The polarity of a cell is determined by the asymmetric partitioning of its cytoskeleton, protein molecules, signaling factors, and organelles. Establishing cell polarity requires three sequential sets of processes: (1) marking a site and decoding cues via receptors or signal transduction network, (2) reiterating the cues via actin and septin assembly, and (3) spreading the cues via cytoskeleton and secretary apparatus rearrangement or protein sorting (Drubin & Nelson, 1996). A proper polarity organization in the cell is maintained by feedback between these stages.

Cell polarity forms *de novo* and is maintained through cell division, cell shape, dynamic cell behavior, and cell fate. Polarity signaling networks in egg of Caenorhabditis elegans and early embryo of Drosophila melanogaster are well-known (Nance & Zallen, 2011; St Johnston & Ahringer, 2010; B. J. Thompson, 2013; Wodarz, 2002). Knockouts of polarity genes in mice are embryonic lethal (Campanale et al., 2017; Murdoch, 2003). Plant cells exhibit anatomically and physiologically polar axes (Lin et al., 1996; Molendijk, 2001). Algal cells have a stable polar axis (Bünning, 1952; Quatrano, 1978; Schechter, 1935). Griffithsia and Cladophora can regenerate shoot or rhizoid cells from an isolated cells (Miehe, 1905; Quatrano, 1978; Schechter, 1935; Waaland, 1975; Waaland & Cleland, 1972).

Cell polarity in plants regulates growth via systemic hormone distribution. It involves polarizing membrane-associated proteins and is crucial for each stage of the life cycle, from zygote division to organ initiation and morphogenesis (Benková et al., 2003; Friml et al., 2003; Grieneisen et al., 2007; Muroyama & Bergmann, 2019; Petrášek & Friml, 2009; Reinhardt et al., 2003; Sabatini et al., 1999; Z. Yang, 2008). The polarization of factors for auxin flow and distribution regulates plant tissue patterning (Grieneisen et al., 2007; Wiśniewska et al., 2006; Z. Yang, 2008). It is fundamental for organ and tissue formation, including embryo axis specification, root development, fruit growth, and organ generation (Benková et al., 2003; Friml et al., 2003; Sabatini et al., 1999; Sorefan et al., 2009; Z. Yang, 2008). Auxin's dynamic activity is regulated by PINFORMED (PIN) and AUX1 carriers on

the plasma membrane (Kleine-Vehn & Friml, 2008; Z. Yang, 2008). *Arabidopsis* has eight PIN auxin transporters —PIN1, PIN2, PIN3, PIN4, PIN5, PIN6, PIN7, and PIN8, with distinct polar localization within the cell, changing polarity during development (Friml et al., 2003; O. Leyser, 2005). AUX1 plays a secondary role in the polar distribution of auxin. The dynamic activity of these polar efflux proteins tightly regulates the gradient distribution and concentration of auxin throughout the plant. Therefore, it is evident that the polar localization of PIN proteins is tied to the polar distribution of auxin. The question is, however, how are these proteins localizing on the plasma membrane distinctively? A well-regulated signaling mechanism is required for the specific localization pattern of PINs. PINOID serine/threonine AGC3 protein kinases, PROTEIN PHOSPHATASE 2A (PP2A), and D6 PROTEIN KINASE (D6PK) determine to localize particular domains by partially localizing with PIN1 in the plasma membrane (Benjamins et al., 2001; Christensen et al., 2000; Friml et al., 2004; Michniewicz et al., 2007; Muroyama & Bergmann, 2019; Z. Yang, 2008). Mis-expression of these PIN regulators leads to the change in the polarity domain rather than the perturbation of PINs on the membrane, stating that the critical spatial control of these regulators on PINs (Benjamins et al., 2001; Christensen et al., 2000; Friml et al., 2004).

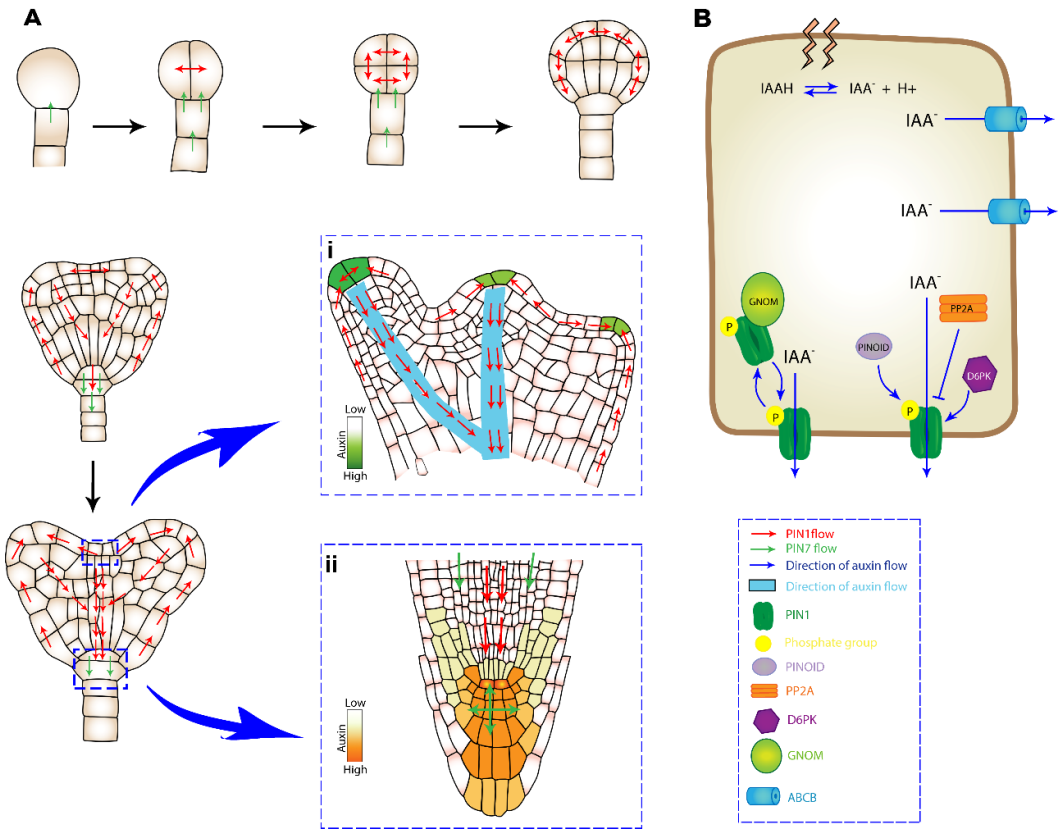

Figure 2.1: Steep auxin gradient distribution, regulated by auxin pumps, is essential for tissue patterning.

(A) Schematic representation of PIN polarity protein (red arrow PIN1 and green arrow PIN7) to direct and distribute the auxin in the meristematic tissue during the embryogenesis (from globular to torpedo stage) and in the normal development (blue boxes enlarged: Upper box depicts the PIN1 distribution (red arrow) and direct of auxin flow (blue) in the shoot apical meristem. The auxin gradient is represented as green to white range (Ai). The lower box depicts the PIN1(red arrow) and PIN7 (green arrow) distribution in the root apical meristem. Gradient distribution of auxin is represented in orange to the white range) (Aii). **(B)** Illustration of auxin flow from one cell to the neighbouring cell undertaken by a group of regulators to ship the auxin, facilitated by basally localized PIN1 and laterally located by ABCB protein.

The flexibility of auxin can be associated with normal development as well as in response to wounding or organ regeneration (Asahina et al., 2011; Durgaprasad et al., 2019; Heyman et al., 2016; Iwase et al., 2011; Mathew & Prasad, 2021; Matosevich et al., 2019; Mitchison GJ & Brenner S, 1980; Radhakrishnan et al., 2020; T. Sachs, 1968, 1969, 1991; Santuari et al., 2016; Sena et al., 2009; Shanmukhan et al., 2020, 2021; Valvekens et al., 1988; J. Xu et al., 2006; G. Zhang et al., 2019). Several studies have been conducted to investigate the distribution and dynamics of auxin. The re-establishment of new QC after ablation, wound-induced *de novo* root formation, and vascular reconnection in a disconnected vein

demonstrate the importance of auxin in cellular reprogramming (Radhakrishnan et al., 2020; T. Sachs, 1968, 1969, 1981, 1991; Shanmukhan et al., 2021). It plays an important role in inducing pluripotency in the callus during tissue culture-mediated regeneration (Atta et al., 2009; Gordon et al., 2007; Malamy & Benfey, 1997; Skoog & Miller, 1957; Sugimoto et al., 2010). The 'all-rounder' activity of auxin is mediated by their incredible partner, PIN transporters. Here we will discuss how the PIN proteins, particularly PIN1, express and localize during *de novo* shoot organogenesis.

As was previously mentioned, PIN1 expression can be seen in two cells staged embryo during embryogenesis (Friml et al., 2003; Heisler et al., 2005) and the primordium initiation (Gordon et al., 2007). Furthermore, it is a known marker to identify the shoot progenitor and localizes in the shoot progenitor of regenerating shoots very early in the process of *de novo* shoot formation (Gordon et al., 2007). However, what impact does the PIN1 polarization regime affect the shoot progenitors that are regenerating into a complete shoot system? What is the physiological relevance of PIN1 polarization? During normal development, the embryonic SAM and axillary meristem grow in the context of lateral organs that help to maintain an auxin minimum which is required for the proper development of the shoot meristem (Benková et al., 2003; De Smet et al., 2010; Moller & Weijers, 2009; Q. Wang et al., 2014; Y. Wang et al., 2014). It is currently not known how low auxin pockets are generated in undifferentiated callus to facilitate *de novo* shoot meristem formation. In this chapter, we will describe PIN1 localization patterns in regenerating shoot progenitors and will provide genetic evidence for its necessity in controlling *de novo* shoot meristem formation. The chapter explains the impact of PIN1 and its polarity regulators on *de novo* shoot morphogenesis demonstrates that polarity protein localization can predict the outcome of regenerating foci.

2.2 RESULTS

2.2.1 *De novo* shoot organogenesis occurs in the absence of embryonic positional cues.

The limb regeneration in Axolotl follows the embryonic state to restore the amputated part by transcriptional activation of embryo-specific genes in the blastema (Alvarado & Tsonis, 2006; Gerber et al., 2018). Similarly, mechanical injury on an organ triggers to re-establish

the lost part by reprogramming and re-patterning of surrounding cells mediated through embryonic signals in *Arabidopsis* root tip regeneration (Durgaprasad et al., 2019; Efroni et al., 2016; Sugimoto et al., 2011). We examined the possibility of embryonic pathways in *de novo* shoot formation from an island of amorphous callus tissue where the regeneration in the animal kingdom is initiated from callus-like blastema cells (Alvarado & Tsonis, 2006). We analyzed the presence of *LEAFY COTYLEDON1* (*LEC1*), an embryonic gene required to specify the cotyledon identity (Harada, 2001; West et al., 1994). We could barely detect the expression of LEC1 in the epidermal cells of the callus (Figure 2.2A, 2.2B) and could not detect it during the regenerating shoot progenitor (Figure 2.2D-2.2L). The expression analysis of the embryonic genes enlightens the repatterning of the entire organism *de novo* is independent of the embryonic pathway, unlike root tip regeneration in *Arabidopsis* (Figure 2.2M-2.2R).

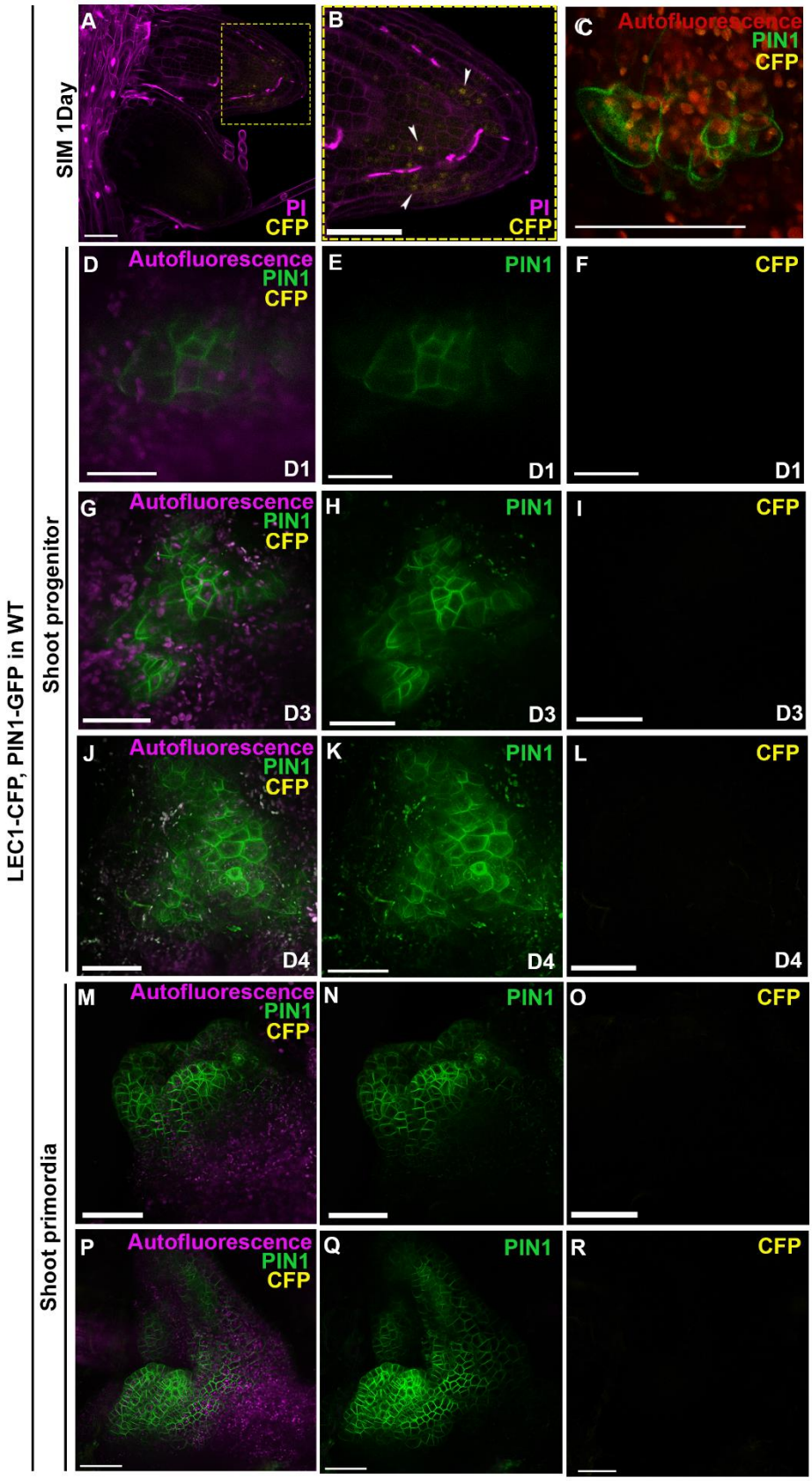
LEC1-CFP, PIN1-GFP in WT
SIM 1Day
Shoot progenitor
Shoot primordia
A
PI
CFP
B
PI
CFP
C
Autofluorescence
PIN1
CFP
D
Autofluorescence
PIN1
CFP
D1
E
PIN1
D1
F
CFP
D1
G
Autofluorescence
PIN1
CFP
D3
H
PIN1
D3
I
CFP
D3
J
Autofluorescence
PIN1
CFP
D4
K
PIN1
D4
L
CFP
D4
M
Autofluorescence
PIN1
CFP
N
PIN1
O
CFP
P
Autofluorescence
PIN1
CFP
Q
PIN1
R
CFP

Figure 2.2: Embryonic marker LEC1 is not expressed in the regenerating shoot progenitors.

(A-B) Callus incubated on SIM for 1 day showed weak, sporadic expression of *LEC1* in the epidermal layers of the callus, stained with propidium iodide (PI). (B) Magnified image of the area is enclosed in a dotted box in Figure2.2A. Arrows indicate cells weakly expressing LEC1-CFP in the epidermal cells of the callus. **(C)** Pseudo-progenitor with non-polar PIN1 expressing cells shows the lack of LEC1-CFP expression. **(D-L)** The Time-lapse of a regenerating shoot progenitor marked with PIN1 does not show LEC1-expression as it develops (F,I,L). **(M-R)** Promeristem (M-O) and *de novo* shoot (P-R) do not express LEC1-CFP representative CFP channel showing no LEC1 expression in the PIN1 marked structures (O, R). CFP is represented by the pseudo-colour yellow to distinguish it from green easily. Scale bars represent 50µm. Magenta colour represents propidium iodide (PI) staining in A and B while it represents chlorophyll autofluorescence in (D,G,J,M,P) Red colour represents autofluorescence in C.

2.2.2 PIN1 localization pattern correlates with the *de novo* shoot meristem formation

While it is known that the shoot meristem arises from the middle layer of the callus in response to shoot inductive cues (Zhai & Xu, 2021). Only a subpopulation of cells from this middle layer, called shoot progenitors, progresses into a meristem (Figure 2.3A-2.3H). Shoot inductive cues (high cytokinin) trigger the expression of the shoot stem cell regulator, WUS, and polar auxin transporter PINFORMED1 (PIN1) in the callus. The Spatio-temporal expression pattern of shoot-specific genes was already well documented but limited to late progenitors and promeristem (dome-shaped stage during meristem formation just prior to primordia emergence, Figure 1A) (Gordon et al., 2007; Kareem et al., 2015b), with no insights into their initial stages. To investigate how the progenitors even begin to self-organize into a meristem (Figure 2.3A), we tracked them in real time by confocal-based live imaging. Towards this, we used PIN1-GFP (*pPIN1::PIN1-GFP*), the earliest known marker of progenitor identity (Gordon et al., 2007; Kareem et al., 2015b). In the initial 2-10 celled stages, the progenitors were located a few cell layers beneath the callus surface (n=34) (Figure 2.3B, 2.3C). This, in addition to the highly irregular topology of the callus made progenitor detection and their real-time tracking challenging (see Chapter 7). Nevertheless, we followed hundreds of these PIN1-

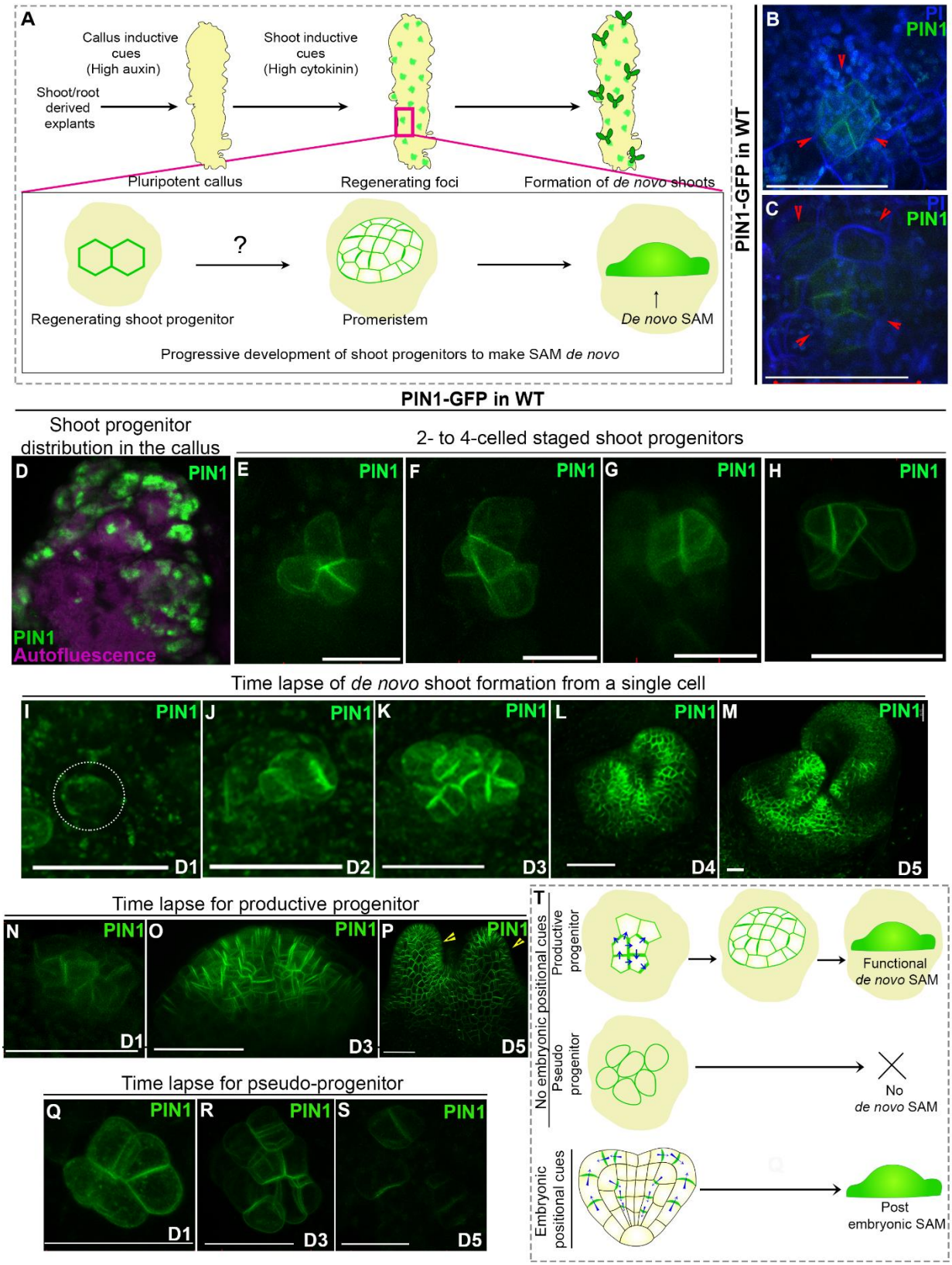

Figure 2.3: Localization pattern of polarity proteins governs the shoot meristem formation

(A) Schematic representation of the progressive development of PIN1-GFP (green) marked progenitor into promeristem, then into shoot meristem which gives rise to a complete shoot system *de novo*. We define promeristem as a dome-shaped structure just before the emergence of leaf primordia. Note that not all the regenerating foci (green dots) make a shoot meristem. **(B-C)** Representative images of 2-4 celled PIN1-GFP marked progenitor(B) and 8-10 celled PIN1-GFP marked progenitor buried under a layer of callus cells (n=34). Red arrowheads indicate the PIN1-GFP. **(D)** Live image of callus taken at 10X magnification where several progenitors of various stages marked with PIN1-GFP (green) can be seen. **(E-H)** Representative Live images of 2-4 celled progenitors marked with PIN1-GFP (green)(n=24). **(I-M)** Representative real-time live imaging showing the progression of a single progenitor cell to shoot meristem(n=4). The White dotted circle indicates the PIN1-GFP (green) marked single-celled progenitor (I), which in response to shoot inductive cues, progressed into a functional shoot meristem by day5 (D5) of progenitor spotting (n=211) (M). **(N-P)** Representative time-lapse images showing PIN1-GFP expression in a productive progenitor on day 1 (N), day 3 (O), and day 5 (F)(n=211). Note that by day 5, the shoot meristem produced leaf primordia (indicated by yellow arrowheads) (P). **(Q-S)** Representative time-lapse images showing a pseudo-progenitor on day 1 (Q), day 3 (R), and day 5 (S)(n=76). Note that the cells are enlarged and bubble-shaped with the progressive disappearance of PIN1-GFP (S). **(T)** Schematic representation of PIN1-GFP polarization in the absence or presence of embryonic positional cues. All the confocal images are z-stack of 5 µm intervals except B and C (1 µm). GFP channel (D-S), GFP/PI stain channel merge (B and C). Scale bars: 50µm, n: sample number.

GFP-marked progenitors. We started to detect PIN1-GFP localization at the cell membrane from the 2-4 celled stage(n=29) (Figure 2.3E-2.3H) but rarely from the 1-celled stage(n=4) (Figure 2.3I-2.3M). Interestingly, not all progenitors with cell membrane-localized PIN1-GFP progressed into shoot meristems (Figures 2.3A, 2.3D). Accordingly, we classified them into two types based on their fate. (i) PIN1-GFP marked cells that developed into a functional meristem were termed “Productive progenitors” (n, number of PIN1 marked foci=211/287) (Figure 2.3N-2.3P, 2.3T), (ii) PIN1-GFP marked cells that abort mid-way were termed “Pseudo-progenitors” (n=76/287) (Figure 2.3Q-2.3T). The productive progenitors could be distinguished as small, often polygonal, compactly arranged cells with intense PIN1-GFP sharply localized to the cell membrane (Figure 2.3N, 2.3T). We quantified the PIN1-GFP signal (Figures 2.4A, 2.4B) from multiple productive progenitors (n=10) and found a pattern of PIN1 localization wherein each progenitor cell has abundant PIN1 localized either away from the progenitor or towards its neighbour on the side (Figures 2.4A, 2.4C). This pattern remained invariant across the productive progenitors, though the number of cells with PIN1 localization sideward or outward varied. In contrast, pseudo-progenitors typically consisted of large, bubble-shaped, loosely packed cells (Figures 2.3Q-2.3T). As opposed to the productive progenitors, the PIN1-GFP in pseudo-progenitors (n=10) was reduced in expression, weakly localized onto the cell membrane, and did not

show any PIN1 localization pattern (Figures 2.4C). It is important to note that the pseudo-progenitors undergo abortion marked by the loss of PIN1-GFP (Figure 2.3S) before reaching the 15-20 celled stage (Figures 2.3Q-2.3S). In contrast, the productive progenitors continue to grow, and at the 100-120 celled stage, it forms a dome-shaped structure called pro-meristem (Figure 2.3O), which is made prior to the fully developed shoot meristem with leaf primordia (Figure 2.3P). Quantification of PIN1-GFP along the cell membrane further supports our observation that the abundance of cell membrane-localized PIN1-GFP in the productive progenitors was significantly higher than that of pseudo-progenitors (Figure 2.4B, 2.4C). Since the localization pattern of PIN1-GFP did not distinguish 2-4 celled productive progenitor from pseudo-progenitor of the same stage, we further examined the 6-15 celled stage, which was found to be the earliest stage that the two kinds of progenitors can be distinguished based on PIN1-GFP for quantification (Figures. 2.3N, 1H, 2.4B,2.4C). From here on, all the live-imaging data acquired for comparing the two kinds of progenitors begin from the 6-15 celled stage for this reason. Since spotting the progenitors pose a challenging task, we do not rule out the possibility of other kinds of progenitors that do not fit into the aforementioned binary classification.

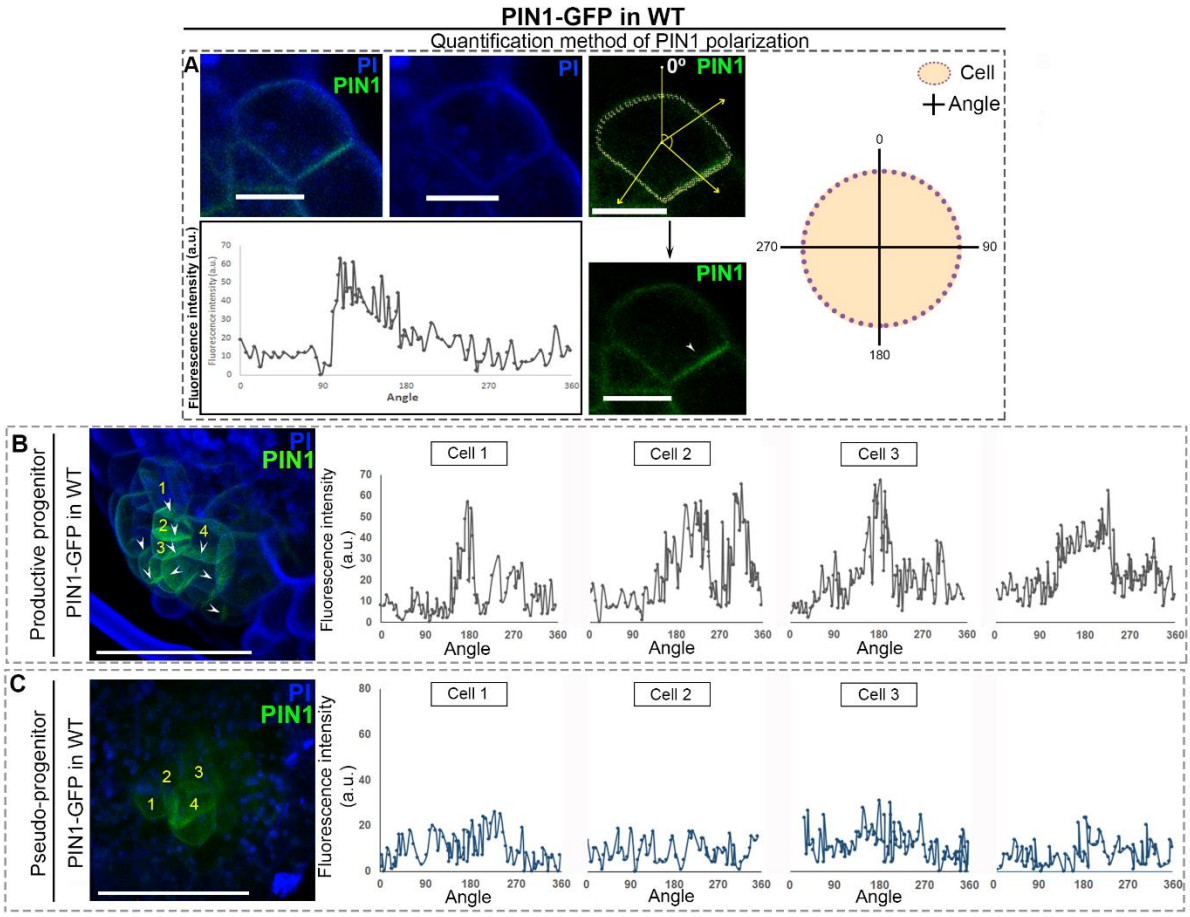

Figure 2.4: Abundance of PIN1 and its specific polar localization correlates with *de novo* shoot meristem formation.

(A) Representative method to check fluorescence intensity of PIN1-GFP on the cell membrane and directionality of PIN1 polarization. **(B and C)** Representative images of productive progenitor and pseudo-progenitor with PI-stained cell walls. White arrowheads: direction of PIN1-GFP polarization (left). Graph depicts the fluorescence intensity of PIN1-GFP along the membrane of the cells annotated (1, 2, 3, and 4) (ns, p = 0.1163, Kruskal-Wallis test PP cells) (x = 94 cells), (ns, p = 0.1764, Kruskal-Wallis test PSP cells) (x = 73 cells) (***p = 0.000, Kruskal-Wallis test followed by post-hoc Dunn's test between PP and PSP cells). The peak denotes the wall with maximum PIN1-GFP fluorescence (right).

2.2.3 Genetic evidence for the necessity of PIN1 polarity during *de novo* shoot regeneration

While PIN1 shows expression throughout the callus during its formation (Kareem et al., 2015a), we observed the confinement of PIN1 to specific domains during the onset of progenitor formation in shoot induction media (SIM) (Figure 2.3A, 2.3D). We, therefore, investigated the genetic basis of the PIN1 expression profile specific to the progenitor initiation stage. One approach widely used to silence the expression of a gene is RNA

interference, which is a molecular tool used to degrade the mRNA after transcription (Borghi et al., 2010; Guo et al., 2014; Siligato et al., 2016). Inducible downregulation of *PIN1* using *pG1090:XVE::PIN1-dsRNAi* in WT throughout SIM (n=104, 0.59 ± 0.31), or even for 24 h (8^{th} day on SIM) (n=123, 2.41 ± 0.24) during the onset of progenitor, nearly abolished shoot regeneration compared to uninduced (n=77, 4.52 ± 0.89) (Figures 2.5A–2.5D). Treating WT calli with estradiol did not cause any change in shoot regeneration, thereby serving as a mock and nullifying the effect of external steroid treatment (Figures 2.5E, 2.5F). This finding corroborated with the abolishment of regeneration in the calli of loss of function mutant combinations of *pin1*. The regeneration efficiency of the hypocotyl explant of the *pin1-1* mutant shows high reduction in shoot formation (n=62, 0.42± 0.188) compared to wildtype (4.167± 1.50) (Figure 2.5G-2.5I). We have also checked the regeneration ability of the root explant. Similarly, like hypocotyl *de novo* shoot formation is compromised in the root explant (n=62, 0.221± 0.089) with respect to wildtype (n=65, 3.771± 0.628) (Figure 2.5J, 2.5L). We also examined the regeneration potential of *PIN* redundant family using *pin1, pin3, pin4, pin7* quadruple mutant, which shows a functional embryonic shoot with short root (Figure 2.5Q) (Verna et al., 2019). The shoot regeneration is drastically reduced in the quadruple mutant (n = 88, 0.0825 ± 0.0497) (Figure 2.5J, 2.5M). Next, we addressed the effect of *PIN* polarity regulators' role in shoot regeneration. We analyzed *pid,wag1,wag2* triple mutant (Dhonukshe et al., 2015) shows no-cotyledon phenotype with functional shoot apical meristem (Figure 2.5R). We found severe regeneration defects in the triple mutant (n = 60, 0.02 ± 0.02) and seldom produced progenitors compared to wildtype (n = 60, 4.134 ± 0.346) (Figure 2.5J, 2.5N). These evidences suggest that alteration of PIN1 *(pin1-1,* and *pin1,pin3,pin4,pin7*) or its polarization regulators (*pid,wag1,wag2*) completely obstruct *de novo* shoot regeneration (Figure 2.5G-2.5N). The *pid,wag1,wag2* callus seldom produced progenitors, all of which had aberrant PIN1 localization (n=21)(Figure 2.6O). Interestingly, the specification of the embryonic SAM (Shoot Apical Meristem) as well as leaf emergence remain unaffected in *pin1-1*, *pin1,pin3,pin4,pin7*, and *pid,wag1,wag2* (Figure 2.5O-2.5V), implying that PIN1 polarization is dispensable for the generation of the shoot meristem during development but indispensable for its regeneration *de novo*.

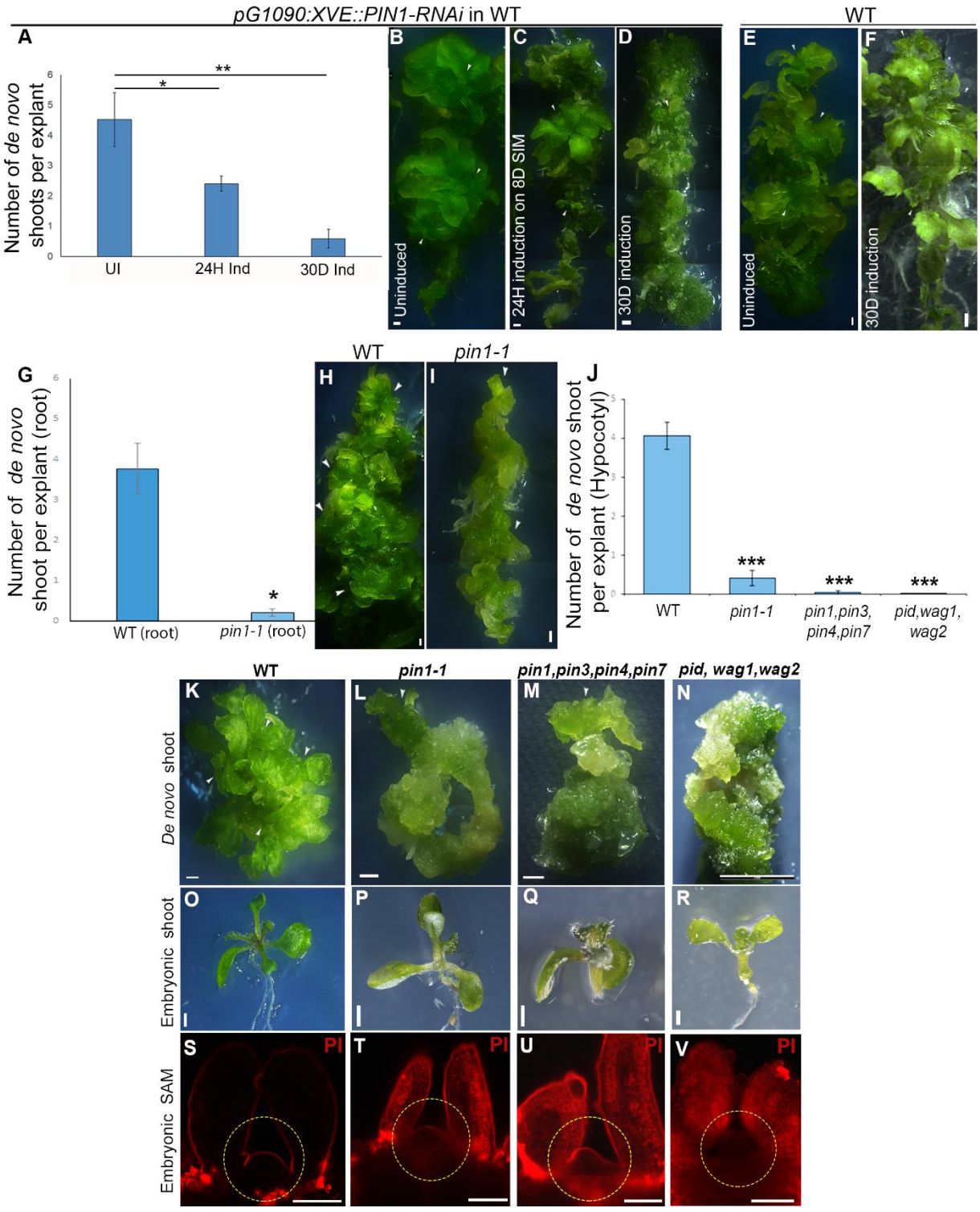

Figure 2.5: PIN1 and its specific polar localization instructs *de novo* shoot meristem formation.

(A-D) Downregulation of PIN1 in *pG1090:XVE::PIN1:dsRNAi* in WT reduces shoot regeneration. Graph depicting the reduction in shoot regeneration upon PIN1 downregulation in an estradiol inducible fashion for 24hr (8th Day SIM) and upon continuous induction for 30 days on SIM compared to uninduced explants (A). Shoot regeneration is unperturbed in uninduced callus

(B)(n=52) but severely reduced upon 24hr (C)(n=72, ***P*=0.009629, Welch Two Sample t-test) and 30days induction on SIM (D)(n=41, **P*=0.04115, Welch Two Sample t-test). **(E-F)** Uninduced WT callus (E) and induced for 30 days on SIM with estradiol (F), used as mock. **(G-I)** Shoot regeneration from root explant of *pin1-1* mutant shows a considerable decrease (n=60,****P=0.0001358*, Welch Two Sample t-test) compared to Wildtype(WT)(n=90). **(J)** Shoot regeneration from hypocotyl explant shows a severe reduction in *pin1-1* (n=62,****P=0.0001358*, Welch Two Sample t-test) and *pin1,pin3,pin4,pin7*(n=88,****P=0.0002533*, Welch Two Sample t-test) mutant compared to Wildtype(WT)(n=96), but gets abolished in pid,wag1,wag2 mutant,(n=60,****P=0.0002823*, Welch Two Sample t-test). **(K-N)** Shoot regeneration is perturbed in mutant combinations of PIN1 and regulators of PIN1. Wildtype callus that is not defective in shoot regeneration (Q)(n=96). *pin1-1* mutant callus with reduced shoot regeneration (R)(n=62). *pin1,pin3,pin4,pin7* mutant callus with reduced shoot regeneration(S)(n=88). Loss of shoot regeneration in *pid,wag1,wag2*(T)(n=60). **(O-V)** Embryonic shoot apical meristem (SAM) of wildtype (O,S); *pin1-1* single mutant (P,T); *pin1,pin3,pin4,pin7* quadruple mutant (Q,U); and *pid,wag1,wag2* triple mutant (R,V). White arrowheads indicated regenerated shoots. Scale bars:1mm (B-F,H,I,K-R), 50µm (S-V). n=sample number. Error bars represent s.e.m.

2.2.4 *De novo* shoot meristem initiation is hypersensitive to genetic modulations of PIN1 polarity

PINOID (*PID*), which encodes a protein-serin/threonine kinase and helps to polarize the PIN1 in the shootward side of the plasma membrane (Benjamins et al., 2001; Friml et al., 2004; Michniewicz et al., 2007). We next examined if perturbation of PIN1 localization by modulating PID expression affects *de novo* shoot regeneration. Continuous or transient (24h induction on the 8th day of SIM) overexpression of *PID* in the wildtype reduces the shoot regeneration which is sufficient to obstruct shoot formation (Figure 2.6A-2.6J). Moreover, transient perturbation of PIN1 localization by inducible overexpression of *PID*, by using *pG1090:XVE::PID-vYFP* in the WT, aborted the progenitor (Figures 2.6E-2.6N). A short, 20-min pulse (see Chapter 7) of transient *PID* overexpression already disrupted the PIN1-GFP localization pattern in 4- to 6-celled (n = 14) (Figure 2.6E) or 15-celled progenitors (n = 25) (Figure 2.6G), which was conspicuous 24 h after the removal of steroid induction (Figures 2.6F, 2.6H, 2.6I). These experiments demonstrated the temporal necessity of PIN1 and its localization pattern. Similarly, like PID, WAG1 and WAG2 are AGC3 kinases collectively command to recruit PIN1 on the apical recycling pathway. We next examined the PINI localization in the *pid,wag1,wag2* (Dhonukshe et al., 2015), all of which had aberrant PIN1 localization (n = 21) (Figure 2.6 O). These evidences suggest that *de novo* shoot regeneration is hypersensitive by modulating the PIN1 polarity by altering its polarity regulators.

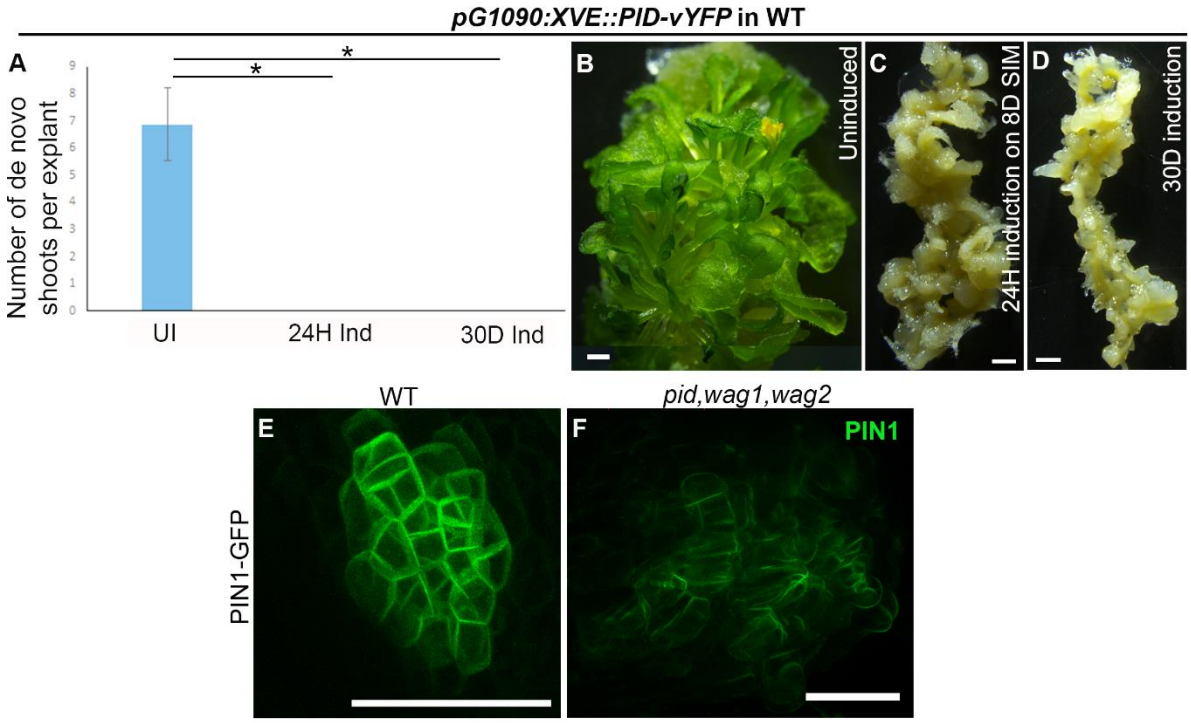

Figure 2.6: Abundance of PIN1 and its specific polar localization correlates with *de novo* shoot meristem formation.

(A-D) PINOID overexpression using *pG1090: XVE::PID-vYFP* in WT abolishes shoot regeneration. Graph depicting the complete loss of shoot regeneration upon PINIOD overexpression in an estradiol inducible fashion for 24hr (8th D SIM) and upon continuous induction for 30 days on SIM compared to uninduced explants (A). Shoot regeneration is unperturbed in uninduced callus(n=39) (B) but aborted upon 24hr(n=36,*P=0.03932, Welch Two Sample t-test) (C) and 30days induction on SIM (n=44,*P=0.03932, Welch Two Sample t-test) (D). **(E-F)** Representative image showing that polarly localized PIN1 on the membrane of progenitor in the wildtype(n=55) (E) and *pid,wag1,wag2* suffers from the disorganized pattern of PIN1-GFP localization pattern(n=21) (F). All the confocal images are z-stack of 5 µm intervals except B-E, which are of 1 µm intervals for clarity of PIN1 polarity. Error bar represents s.e.m. Scale bars: 1mm (B-D), 50µm (E-O).

2.3 DISCUSSION

Living systems are characterized by the emergence of orderly arranged patterns from chaotic ones. One such instance is the stochastic initiation of regenerating foci from an island of amorphous callus that develops into a new shoot. Numerous studies emphasized the significance of cell wall modification and cell polarity in plant development, but all in the presence of embryonic positional cues. What gives these foci their positional

information and how progenitor cells can self-organize to give rise to shoots are yet unknown.

The choice of cells, termed as progenitor, in which few of them attain shoot fate, and others fail to develop from a mass. It indicates the heterogeneity among the callus cells in responding to hormonal induction cues. We addressed how these progenitors are developed stochastically from a heterogenous callus and the underlying mechanism of self-organization.

Root tip regeneration in *Arabidopsis* and limb regeneration in Salamander follows an embryonic pathway to reset the lost organ tip (Alvarado & Tsonis, 2006; Efroni et al., 2016; Gerber et al., 2018). Here we find that self-organization during *de novo* shoot regeneration occurs in the absence of embryonic positional cues (Figure 2.2A-2.2R). Tissue patterning and plant body development, such as early embryogenesis and post-embryonic SAM formation, are marked by auxin maxima (Benková et al., 2003; Friml et al., 2003; Grieneisen et al., 2007; Petrášek & Friml, 2009; Reinhardt et al., 2003; Sabatini et al., 1999). Here the auxin minima for the patterning is created by a polarly localized PIN1 to suck up the auxin from the meristem and transported to the lateral organ or to the cotyledon (Benková et al., 2003; Reinhardt et al., 2003). Unlike normal development, shoot meristem *de novo* establishes in the absence of such lateral organ from the callus by creating an auxin minima in the center by pushing out the auxin from inward to outward direction by PIN1 on the plasma membrane. In contrast to root development, where the gradient distribution of auxin guides the root growth and the tip serves as an ‘auxin capacitor’ (Laskowski et al., 2008; Sabatini et al., 1999), *de novo* shoot meristem establishment requires auxin minima. Quantification of auxin in the progenitor by using DII-Venus mDII-ntdtomato (R2D2) confirmed the generation of auxin minima in the regenerating foci (done by Anju PS, Varapparambath et.al, 2022) shows that maintenance of low auxin in the shoot progenitor essential for their development.

Our study shows that the distinct localization of polar auxin transporter and cell polarity regulators correlates with the compact cell adhesion in the productive progenitors (Figure 2.4B,2.4C). The cell wall degradation approach has shown that cell wall mechanics can influence the polar localization of PIN1 (Feraru et al., 2011). We find a direct correlation of cell polarity with cell wall mechanics by distinguishing productive progenitor and pseudo-

progenitor by elucidating their cell polarity and cell arrangement comparison (Figure 2.3N-2.3T,2.4B,2.4C). Loss-of-function mutants of *pin* (*pin1-1* and *pin1,pin3, pin4,pin7*) or its polarity regulators and aberrant PIN1 localization in *pid,wag1,wag2* dictates self-organization from chaos initiated through a cell-to-cell communication which is crucial for such differential expression of PIN1 that directs to the *de novo* formation of the shoot. During the selection process of progenitor cells, the PIN1polarity and cell-to-cell communication play a significant role. Understanding how PIN1-marked cells differ from the surrounding cells and the factors regulating this process requires further investigation. Additionally, wall mechanics and cell division plane are crucial for a unique arrangement of regenerating foci. These components, including cell division, cell wall mechanics, and cell-to-cell communication, collectively contribute to recruiting PIN1 to the membrane of a group of cells that define a shoot progenitor. This implies that changes in PIN polarity have a significant impact on *de novo* shoot regeneration. Although the maintenance of low auxin levels in progenitor cells is explained by our study, is maintaining low auxin levels necessary in the progenitor? What will be the outcome when the auxin is eliminated from the progenitor cells? Manipulation of auxin level in the progenitor and the in the callus cells, how does it impact the fate of shoot progenitor? These questions still need to be explored.

Chapter 3

Physiological relevance of localization pattern of polarity protein

3.1 INTRODUCTION

Tissue culture-induced regeneration is a well-known phenomenon that utilizes the advantages of plant's regenerative abilities. In the previous chapters (Chapter 1 and Chapter 2), we discussed the regenerative responses in plants, especially how the shoot meristem precursor, i.e., shoot progenitor, begins its journey stochastically to a shoot. The fate of the final shoot is not shared by all of the shoot progenitors, as was previously mentioned (Chapter 2) (Figure 2.3A). We observed that difference in the PIN1 protein localization on the progenitor cell membrane and classified the shoot progenitors into two types—productive progenitors and pseudo-progenitors (Figure 2.3N-2.3O). We discovered that PIN1 is polarized on the productive progenitor, whereas it is uniformly distributed in the pseudo-progenitor, and this difference in the PIN1 localization pattern can predict the fate of a progenitor (Figure 2.4B,2.4C). PIN1 is an auxin efflux carrier. Several molecular factors could control the recruitment of PIN1 on the membrane; one of the pronounced ones could be the auxin. Previous studies have explored the auxin-PIN1 regulation in normal development (Hazak et al., 2010; O. Leyser, 2018). However, the relation between auxin and PIN1 in *de novo* organogenesis needs to be investigated. Since PIN1 was covered in chapter 1, we will focus on its regulator, auxin, in this section.

Auxin is one of the phytohormones reported in the plant system many decades ago and the term is originated from the Greek word auxein", that means "to grow". The most abundantly occurring auxin in plants is Indole-3-acetic acid (IAA), a weak acid (p*K*a = 4.75), and it is maintained in conjugated forms with amino acids or sugars (Bandurski et al., 1995; Bartel, 1997). Mainly, auxin is synthesized in young leaves and cotyledons and transported to root tips (Blakeslee et al., 2005; Ljung et al., 2002). There are other hormones, such as cytokinin, ethylene, gibberellic acid, and abscisic acid, present in plants; however, auxin is considered to be a 'cellular currency' for plant life (O. Leyser, 2018; Stewart & Nemhauser, 2010). Because it orchestrates almost all aspects of plant growth and development (Bartel & Fink, 1995; Benková & Hejátko, 2009; Fukaki & Tasaka, 2009; Heisler et al., 2005; King, 1988; Overvoorde et al., 2010; Reinhardt et al., 2003; Vanneste & Friml, 2009; Woodward, 2005). In land plants, the embryonic and post-embryonic patterning and body axis establishment are controlled by auxin (Benková et al., 2003; Bowman & Floyd, 2008;

Cooke et al., 2002, 2004; Finet & Jaillais, 2012; Friml et al., 2003). It mediates gravitropism (Feldman, 1985) and promotes stem elongation (T. Yang et al., 1993) but inhibits root elongation (Evans, 1984; Galinha et al., 2007). It controls axillary meristem growth (Tamas 1988), cotyledon development during embryogenesis (Stone et al., 2008), and stem cell and quiescent centre (QC) maintenance in the root meristem (Aida, Beis, Heidstra, Willemsen, Blilou, Galinha, Nussaume, Noh, Amasino, Scheres, et al., 2004). Cellular responses such as cell elongation (Gee et al., 1991) by acidifying the apoplastic space of the cell (Heisler et al., 2010; Rayle & Cleland, 1992), cell specification (Blilou et al., 2005; Friml et al., 2002; Grieneisen et al., 2007; Sabatini et al., 1999) secondary xylem (Uggla et al., 1996) and patterning of embryo sac (Pagnussat et al., 2009) are regulated by auxin. Therefore, auxin is believed as a dominant regulator of plant architecture. Auxin was subsequently classified by scientists as both a hormone and a morphogen. However, due to the auxin's pleiotropic action in the plant system, neither of these terms will apply to it (Paque & Weijers, 2016).

How is it possible for a molecule to participate in an enormous number of molecular, cellular, and physiological processes going on in the system? The action of auxin at a specific time or in specialized tissue or organ is armed by a complex regulatory system that includes auxin biosynthesis, polar auxin transport, conjugation, and auxin signaling mediated by a class of molecules. As previously stated, auxin (IAA) synthesis takes place in the younger tissues. It is synthesized from tryptophan and can be produced by both tryptophan-dependent and -independent pathways. Polarized membrane transporters, particularly PIN proteins, control auxin distribution and direction. Auxin efflux carriers like PIN1 are crucial for the formation of specific organs during development. Auxin influx is facilitated by proteins like AUX1 and LAX. Furthermore, auxin must be released and degraded in a timely manner in order for homeostasis to be maintained. Various conjugates associated with auxin have been reported. These conjugates such as IAA–Ala, IAA–Leu may be used for storage or conjugates such as IAA–Phe or IAA–Asp or IAA–Glu leads to the auxin degradation (Gallavotti, 2013; Ludwig-Müller, 2011; Ruiz Rosquete et al., 2012). Another important auxin regulation is through its complex TIR1/AFB, Aux/IAA and auxin response factors (ARFs) signaling pathway (Bargmann & Estelle, 2014; T. J. Guilfoyle, 2015; Paque & Weijers, 2016).

As a necessary component of plant life, auxin is dealt with by a diverse regulatory system.

As I discussed above, auxin is the key hormone that establishes tissue patterning of aerial or ground organs (Aida, Beis, Heidstra, Willemsen, Blilou, Galinha, Nussaume, Noh, Amasino, & Scheres, 2004; Blilou et al., 2005; Galinha et al., 2007; Heisler et al., 2005; Reinhardt et al., 2003). There are various types of apical meristem above ground—shoot apical meristem (SAM), axillary meristem (AM), inflorescence meristem (IM), floral meristem (FM), and adventitious shoot meristem (*de novo* shoot meristem). All others, except shoot apical meristem, develop post-embryonically. Despite the fact they are structurally similar, their programming and early initiation are different from embryonic SAM (Schmitz & Theres, 2005; Serrano-Mislata et al., 2016; Q. Wang et al., 2014, 2016; Y. Wang et al., 2014; Y. Wang & Jiao, 2018; M. Yang & Jiao, 2016). Once it makes a meristem, they follow the same growth trajectory as SAM. This distinction is brought about by the hormone auxin. The establishment of SAM in the vegetative phase or FM in the reproductive phase requires a local auxin maximum to guide the primordial initiation (Reinhardt et al., 2000; Sassi et al., 2014; Y. Wang & Jiao, 2018). The formation of AM, however, necessitates a low auxin environment (Q. Wang et al., 2014; Y. Wang et al., 2014). Adventitious shoot meristem is unique in that it can develop from root or leaves or any part of the plant either it can form naturally from the cut end or artificially by using a low auxin/cytokinin ratio (Moo-Young, 2019; Skoog & Miller, 1957). The artificial tissue culture method follows low auxin/cytokinin ratio for shoot development, while high auxin/cytokinin ratio for root development. An intermediate concentration creates a pluripotent cell mass known as a callus (Skoog & Miller, 1957). Despite this, the level of auxin during the adventitious (*de novo)* formation of shoot meristem is poorly understood, possibly due to the use of a low auxin/cytokinin ratio in the process of the artificial culturing process. we will discuss the necessity of auxin and reveal how it plays a crucial role in the formation of *de novo* shoot meristem.

3.2 RESULTS

3.2.1 The necessity of low auxin level in the regenerating foci facilitates shoot meristem formation

We examined the physiological relevance of the PIN1 localization pattern during shoot regeneration. Our data suggest that the localization pattern of PIN1 (Figure 2.4B and 2.4C) could transport excess auxin away from the progenitor cells. This is likely to generate differential auxin accumulation between the progenitor and surrounding cells. Using the auxin-sensitive marker DII-Venus mDII-ntdtomato (R2D2) (Liao et al., 2015), we quantified the auxin level within the progenitor cells and the outer, juxtaposed non-progenitor cells (done by Anju PS, Varapparambath et al., 2022- data not shown). In support of the proposal, she found that the productive progenitors marked by the characteristic PIN1 localization pattern had a low auxin level relative to their neighboring cells (Figure 3.1A). Contrarily, the pseudo-progenitors with weak membrane localization of PIN1 had auxin levels similar to their neighboring cells (Figure 3.1B). This suggests that the PIN1 polarization pattern facilitates draining of excess auxin away from the progenitor cells to create differential auxin level within the progenitor and surrounding cells for the successful development of *de novo* shoot meristem.

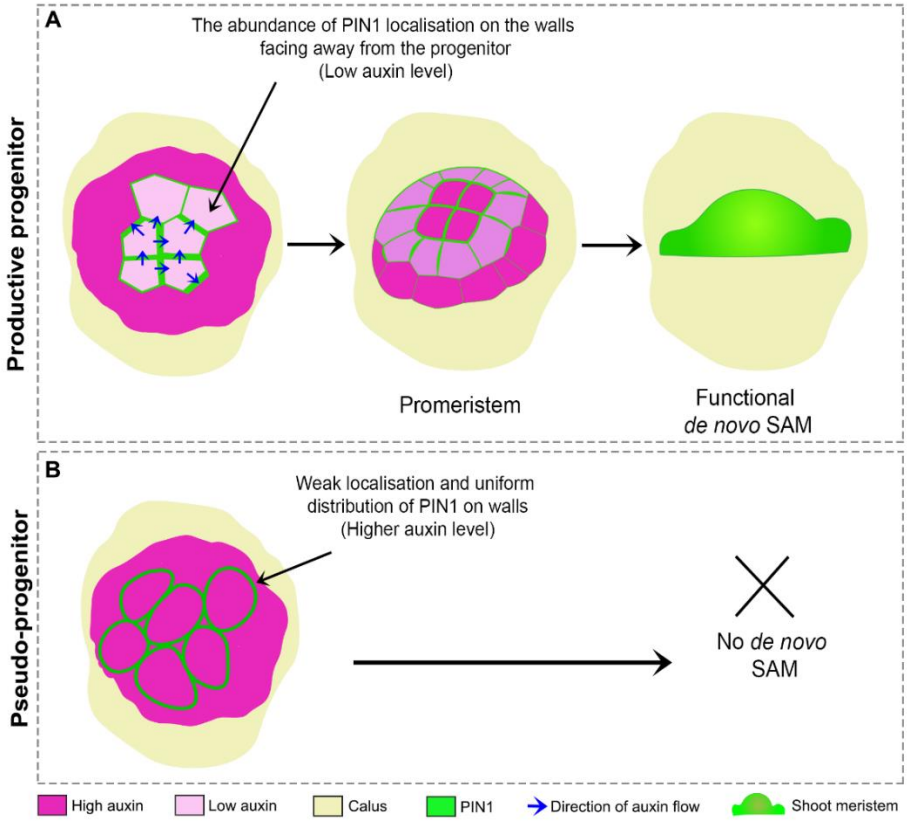

Figure 3.1: The PIN1 localization pattern generates a region of relatively low auxin which is necessary to facilitate shoot meristem formation

(A) Illustration of PIN1 localization pattern onto the cell membrane generates a region of low auxin in the progenitor to facilitate shoot meristem formation *de novo*. **(B)** Auxin accumulates in the pseudo-progenitors where PIN1 localization is deregulated, and such progenitors fail to make shoot meristem.

Therefore, we wanted to reduce auxin level from the callus to investigate the involvement of auxin hormone during shoot formation. We used *pG1090:XVE::axr3-1-RFP* (*pG1090:XVE>>axr3-1-RFP* in WT) to alter auxin response (Siligato et al., 2016). *AXR3*, also known as IAA17, belongs to Aux/IAA protein family (Ouellet et al., 2001). axr3-*1*, is a semi-dominant mutation in the second domain of AXR3, which is hypersensitive to auxin and acts as a dominant negative regulator of auxin signaling (H. M. O. Leyser et al., 1996). Even a transient 5-minute pulse with 5 µM steroid or 30 minutes pulse with a low concentration of steroid (1 µM) during the onset of progenitor formation (8thday on SIM) severely impaired the shoot regeneration (Figure 3.2A- 3.2E). Moreover, 24hr sustained induction of *axr3-1* onto SIM incubation completely abolished the shoot formation (Figure

3.2F-3.2O). This indicates that the activity of auxin signaling is crucial at each stage of *de novo* organogenesis, and the lack of auxin, even in the presence of a sufficient amount of cytokinin in the supplementary media fails to support *de novo* shoot regeneration.

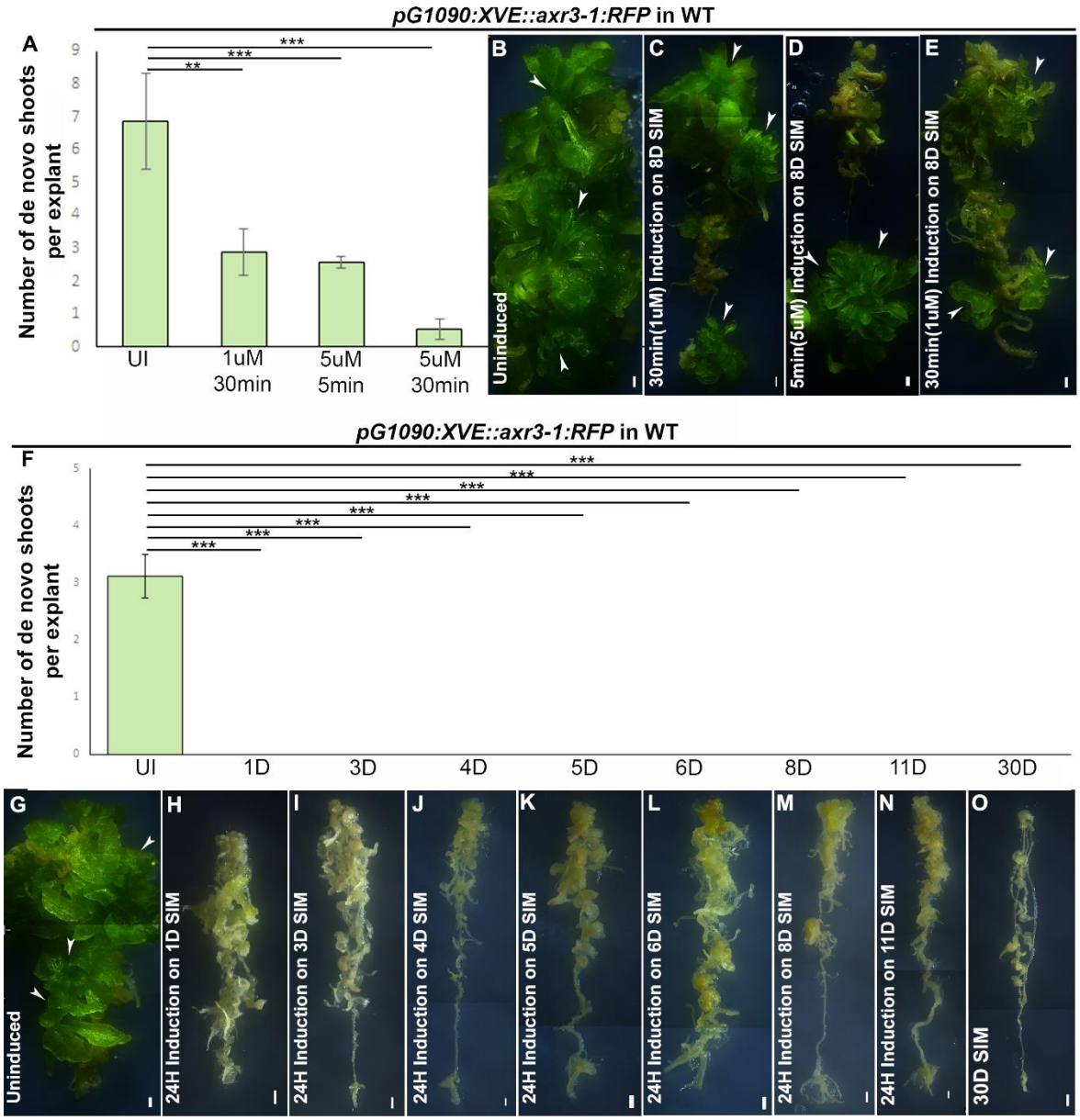

Figure 3.2: Auxin activity is essential during *de novo* shoot organogenesis.

(A) graph depicting the number of *de novo* shoots per explant by inducing *axr3-1* to modulate auxin level in different pulses during the onset of progenitor formation (Uninduced,n=50, 6.882±1.46; 30min(1µM),n=65, 2.88±0.707; 5min(5µM),n=68, 2.586±0.169; 30min(5µM),n=36, 0.52±0.310; Uninduced *Vs.* 30min(1µM) ***P=0.0093;* Uninduced *Vs.* 5min(5µM) ****P=0.0009;* Uninduced *Vs.* 30min(5µM) *****P=0.0005*) (Unpaired t-test). **(B-E)** Representative stereo-image of 30 minutes incubation of samples on 8th day SIM using 1µM estradiol (C), 5 minutes incubation of samples on 8th day SIM using 5µM estradiol (D), and 30 minutes incubation of samples on 8th day SIM using

5µM estradiol (E) showing reduced shoot formation compared to Uninduced (B). **(F-O)** Graph showing shoot regeneration is completely abolished by 24hr induction of *axr3-1* in day1 (1D) (n=45, 0±0, ****P=0.0001*), day3 (3D) (n=71, 0±0, ****P=0.0001*), day4 (4D) (n=56, 0±0, ****P=0.0001*), day5 (5D) (n=48, 0±0, ****P=0.0001*), day6 (6D) (n=59, 0±0, ****P=0.0001*), day8 (8D) (n=78, 0±0, ****P=0.0001*), day11 (11D) (n=63, 0±0, ****P=0.0001*) and throughout SIM (30D) (n=55, 0±0, ****P=0.0001*) compared to uninduced (n=52) (Unpaired t-test) (F). *axr3-1* overexpression using *pG1090: XVE::axr3-1-RFP* in WT abolishes shoot regeneration (H-O) compared to WT (G). Error bars represent s.e.m. Scale bars: 1mm(B-E,G-O), n: sample number and Mean±SEM.

3.2.2 Local auxin over production in the progenitor cells impairs shoot regeneration

Next, we wanted to examine the effects of high auxin within the regenerating progenitors where auxin is relatively lower than the cells surrounding the progenitors. Towards this, we expressed *YUCCA4(YUC4),* a local auxin biosynthesis gene, under 5.7Kb *WUS* promoter, which specifically express in early progenitors and in shoot stem cell organizer. *pWUS::YUC4:tWUS* in WT showed normal vegetative growth. Strikingly, *pWUS::YUC4:tWUS*; WT formed a pin-formed inflorescence which resembled the *pin1* mutant (Figure 3.3A,3.3B) (Friml et al., 2004; Gälweiler et al., 1998; R. Li et al., 2014; Okada et al., 1991; Petrášek & Friml, 2009). *YUCCA* genes overexpression leads to the elevation of free auxin and displays auxin overproduction phenotypes (Finet & Jaillais, 2012; Stepanova et al., 2011; Won et al., 2011; Zhao et al., 2001). We also noted low number of flowers, and which eventually die off (Figure 3.3A,3.3B). To rule out the indirect effects of phenotypic changes in transgenic shoots we considered a weak line which shows normal vegetative and reproductive development to examine the shoot regeneration efficiency in *pWUS::YUC4:tWUS*;WT (Figure 3.3C,3.3D). Forced over expression of *YUC4* under *WUS* promoter lead to significant reduction in shoot regeneration (Figure 3.3E-3.3G). This suggests that the level of auxin in the progenitor should be relatively low as compared to the cells surrounding the progenitors for the successful initiation of shoot formation *de novo*, and the loss of differential distribution of auxin in the regenerating foci abrogates the entire process.

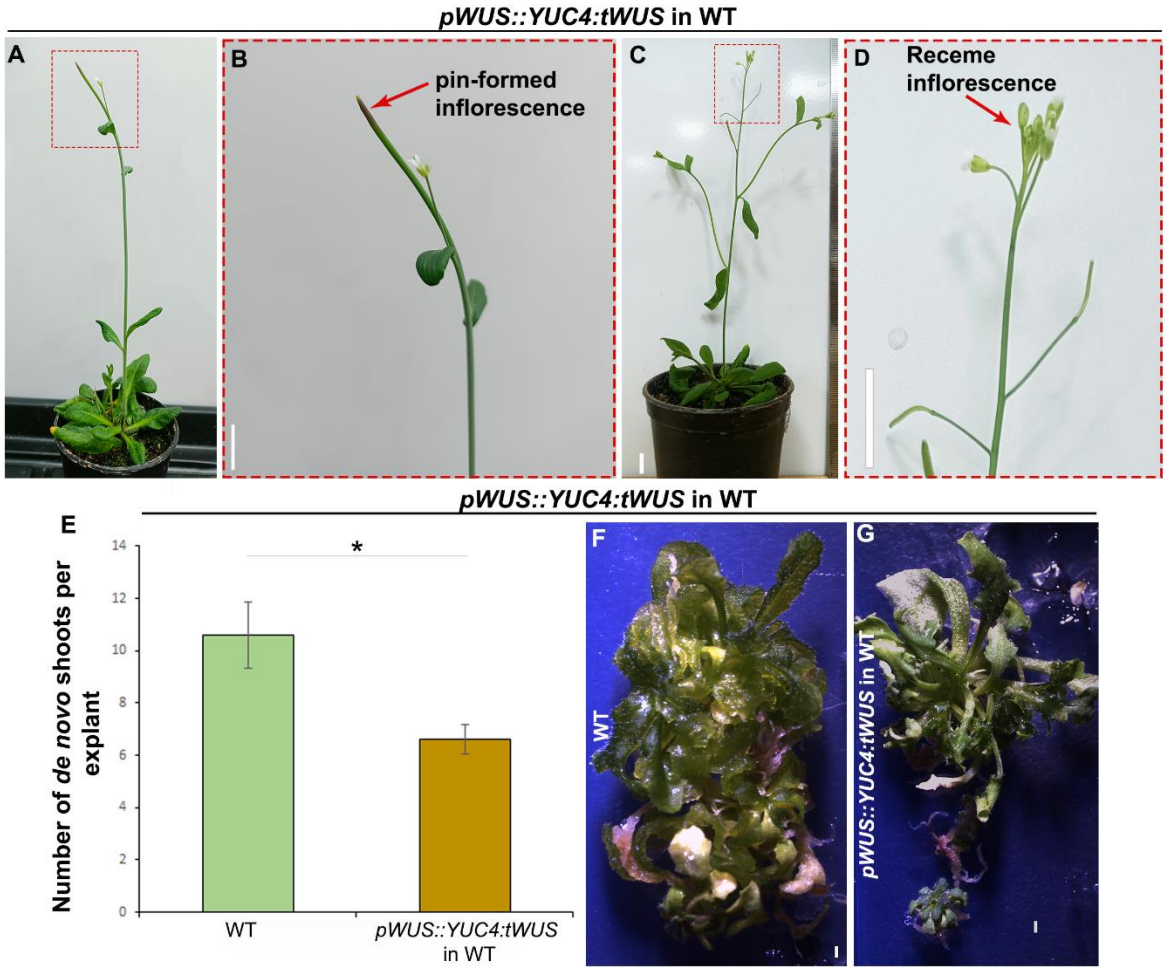

Figure 3.3: increasing the concentration of auxin in the progenitor affects the shoot regeneration.

(A-B) Representative image of a strong line with pin-formed inflorescence phenotype by the insertion of *pWUS::YUC4:tWUS* in WT (n=3/35). **(C-D)** Representative image of a weak line by the insertion of *pWUS::YUC4:tWUS* in WT(n=32/35) (Red dotted rectangles represent the type of inflorescence which is enlarged as B and D panels). **(E-G)** The graph represents that shoot regeneration (using a weak line) is reduced by increasing the auxin biosynthesis in the progenitor cells (n=151, 10.6±1.28) compared to WT (n=123, 6.616±0.584) (**P*=0.0309, Unpaired t-test). Error bar represents s.e.m. Scale bars: 1cm (A-D),1mm(F,G), n: sample number and Mean±SEM.

3.3 DISCUSSION

Auxin can be considered as a key coordinator of plant growth and development. Here we examined the necessity of auxin in conferring the productive fate of progenitors during *de novo* shoot regeneration.

According to "Turing's pattern", a low level of a substrate can trigger its activity (Turing & Brooker, 1952). Here, in our model system (*de novo* shoot regeneration), a low level of auxin patches on the callus seems to triggers its own activity to maintain the membrane localization of PIN1 on the regenerating foci to create a differential auxin level between progenitor and the surrounding cells for successful formation of functional shoot meristem. Here, the cells with low auxin sense the surrounding high auxin level and direct the PIN1 to the neighboring cells against the gradient, and it mimics the 'up-the-gradient' (concentration-based) movement of auxin (Jönsson et al., 2006; Smith, Guyomarc'h, et al., 2006). The necessity of relatively low auxin in the progenitor makes them distinct from pseudo progenitor which is eventually exiting from the playground by the lack of differential auxin gradient distribution. Thus, the establishment of *de novo* shoot meristem demands critical low auxin compared to the surrounding callus cells that are pivotal for shoot regeneration *de novo*. Progression of shoot progenitors to the meristem appears to be highly sensitive to any alteration in auxin levels. It breaks the concentration-based movement of auxin, thereby limiting the low auxin pocket formation in the callus. To facilitate this movement of auxin, PIN1 plays a major role. What triggers the activation of PIN1? One possible mechanism is uneven diffusion can lead to relatively higher level of auxin in callus cells which can turn on active transport stochastically. Subsequently PIN1 marked cells can self-organize to form multicellular progenitors where PIN1 get asymmetrically distributed and transport the auxin our of growing progenitors.

In this chapter, we discussed the indispensability of auxin hormone in the shoot meristem formation artificially. However, the role of other phytohormones during *de novo* shoot regeneration is poorly understood, and what promotes the PIN1 localization for the self-organization of a few cells to a shoot meristem needs to be addressed.

Chapter 4

Cell wall loosening enzyme XTH9 promotes PIN1 localization pattern to confer the productive fate

4.1 INTRODUCTION

Previously (Chapter 2), we classified the regenerating foci into two distinct categories with their unique characteristics. Cells are polygonal and compactly arranged in productive progenitor, which converts into a shoot meristem. Whereas pseudo-progenitor is composed of loosely packed cells. Here, we observed that cell adhesion and wall integrity correlate with the fate of a shoot progenitor.

Plant cells are composed of a protoplast surrounded by a wall of multi-unit polysaccharides. This dynamic structure provides mechanical support to a plant cell during its growth. The cell wall composition changes in response to abiotic or biotic factors in order to maintain the turgor pressure of the cell, which is a fundamental force that a plant cell applies to its wall. This dynamic action in response to different environments is termed as 'cell wall plasticity' (Vaahtera et al., 2019). The plasticity of the wall enables the plant to adapt quickly to changes in its surroundings. There are two distinct walls that make up the plant cell wall: the primary and the secondary cell wall. Both are made up of cellulose, hemicellulose, lignin, and structural proteins such as hydroxyproline-rich glycoproteins (N. Carpita et al., 2001; N. C. Carpita & Gibeaut, 1993; Hyodo et al., 2003; Meents et al., 2018). Each cell is cemented to the other by a pectin molecule, a heteropolysaccharide that makes the middle lamellae of a plant cell (Figure 4.1) (Bidhendi et al., 2020; Braidwood et al., 2014). The primary structural component of the plant cell wall is cellulose, which is made up of (1,4)-linked β-D-glucan paracrystalline ribbon, also known as microfibril and are arranged parallel to the plasma membrane (N. C. Carpita & Gibeaut, 1993; Cosgrove & Jarvis, 2012; Crowell et al., 2010; Feraru et al., 2011). Hemicellulose, also known as xyloglucans, is a heteropolymer composed of β-1,4- linked D-glucose with xylose, galactose, and fucose as a side chain (Fry, 1989; Hayashi, 1989; Hyodo et al., 2003; McNeil et al., 1984). There are two different models proposed for cellulose/ hemicellulose network to describe wall architecture, 1) cellulose microfibrils surface is coated with hemicellulose, which directly links the cellulose backbone of the wall, and 2) cellulose microfibrils are indirectly linked through an additional layer of hemicellulose matrix (Figure4.1) (Brett & Waldron, 1996; N. C. Carpita & Gibeaut, 1993; Cosgrove, 1999; Cosgrove & Jarvis, 2012; Passioura & Fry, 1992). Xyloglucans are considered a load-bearing component in the wall

due to the slippage action of microfibrils on hemicellulose in response to growth or stress relaxation (Brett & Waldron, 1996; N. C. Carpita & Gibeaut, 1993; Cosgrove, 1999; Fry, 1995; Hyodo et al., 2003; Nishitani, 1995, 1997; Passioura & Fry, 1992; Whitney et al., 1999). Additionally, hydroxyproline-rich glycoproteins, named as 'extensin', which are involved in cell-to-cell communication and have an impact on extensibility or reinforcement of the wall (Cooper et al., 1987; Deepak et al., 2010; Lamport, 1963; Ringli, 2010).

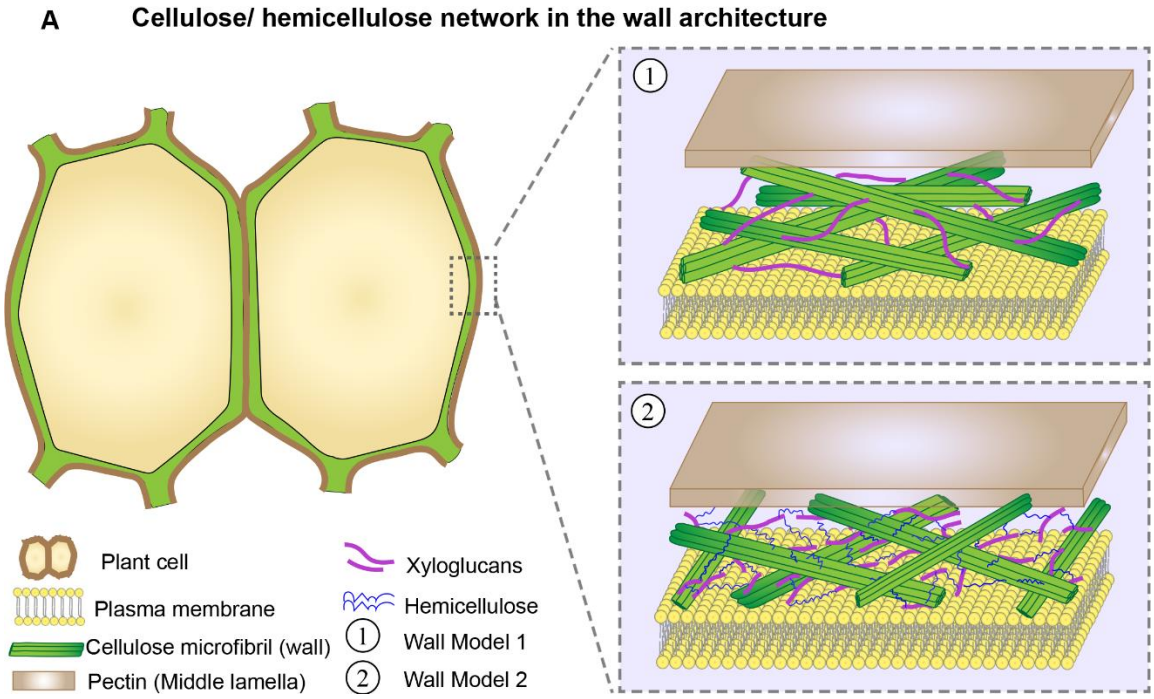

Figure 4.1: Two distinct models of plant cell wall topology showing the cellulose/hemicellulose/pectin network

(A) The illustration demonstrates the architecture of the cell wall of the plant. Two different experimentally proven models of cellulose/ hemicellulose network are used to describe wall architecture, Model 1) cellulose microfibrils (Green) surface is coated with hemicellulose (Magenta), which directly links the cellulose backbone of the wall, and Model 2) links the cellulose microfibrils indirectly by adding another layer of hemicellulose matrix (Blue).

Cell wall integrity can adapt in response to stress, turgor pressure changes, and developmental growth, driven by plasticity and extensibility (Cosgrove, 2016; Peaucelle et al., 2011). Controlled movement of cellulose microfibrils with the extracellular matrix is regulated by proteins and enzymes like CELLULOSE SYNTHASE A (CESA), XYLOGLUCAN ENDO TRANSGLUCOTRANSFERASE/HYDROLASE (XTHs),

EXPANSIN, and pectinolytic enzymes (Feraru et al., 2011; Hyodo et al., 2003; Nishitani & Vissenberg, 2006). CESA extends microfibrils, XTHs restructure xyloglucans and act as "molecular grafters", EXPANSIN, mediates ‘an acid growth’, facilitates cell expansion, and pectinolytic enzymes catalyze pectin rearrangement (Cosgrove, 2005; Gainvors et al., 1994; Rose et al., 2002; J. E. Thompson & Fry, 2001). These processes enable the cell wall to adjust its structure and properties but may also lead to wall thinning and loss of integrity (Hyodo et al., 2003; Yokoyama & Nishitani, 2001).

Various proteins with diverse biochemical, biophysical, and physiological functions adapt the cell wall to a changing environment, leading to remodeling and changes in wall integrity. This dynamic structural remodeling is unavoidable in the cellular process, such as cell division, cell differentiation, cell specification, cell elongation or expansion, and cell morphogenesis (Cosgrove, 1999; Vaahtera et al., 2019). Changing in the physical force between the wall and plasma membrane changes the concomitant cell shape, cell-to-cell communication, adhesion with neighboring cells, or cell polarity (Cosgrove, 1999; Dong et al., 2009; Feraru et al., 2011; Shao & Dong, 2016; Vaahtera et al., 2019; Y. Zhang & Dong, 2018). Proper cell adhesion is required to establish cell polarity that can control cell division or cell dynamics in response to hormone pH or stress response (Feraru et al., 2011; Meents et al., 2018; Muroyama & Bergmann, 2019; Vaahtera et al., 2019). The PIN polarity state can be altered by the pharmacological inhibition (treatment with isoxaben) of cellulose biosynthesis (Feraru et al., 2011). This study found that wall integrity correlates with cell polarity and that manipulation of the cell wall changes the polarity domain of polar proteins. Combining these arguments suggests that cell polarity and cell wall mechanics are strongly correlated in order to promote growth and development. However, it is unknown how the cell wall integrity controls the asymmetric distribution of polar protein or vice versa to guide the cellular processes for the normal functioning of the plant tissue. Polar localization of PIN protein, considered to be a molecular landmark, to directs the flow of auxin is a crucial mechanism in plant tissue patterning during *In vivo- In vitro* organogenesis (Benková et al., 2003; Friml et al., 2003; Gordon et al., 2007; Grieneisen et al., 2007; Kareem et al., 2015a; Petrášek & Friml, 2009; Reinhardt et al., 2003). PIN1 depolarization during protoplasting and altered localization in the cellulose synthase mutant suggest mechanical force perturbation on cell wall impinges cell polarity and tissue patterning.

(Asnacios & Hamant, 2012; Boutté et al., 2006; Feraru et al., 2011). As I have mentioned in previous chapters (chapter 2 and chapter 3), the localization pattern of PIN1 directs the shoot progenitor to develop into a shoot by creating an auxin-minima at the PIN1 marked cells compared to the surrounding cells and must be maintained in order for the shoot to emerge successfully. Notably, the maintaining an optimal cell adhesion during the process is also a crucial for shoot emergence. Here we hypothesize that disrupted PIN1 polarization is caused by the altered cell-to-cell adhesion and inability to maintain the compact arrangement, in order to create differential auxin distribution followed by fate specification in the shoot progenitors. In this chapter, we will discuss how cell adhesion and wall mechanics influence PIN1 localization and cell fate determination during the *de novo* shoot regeneration process.

4.2 RESULTS

4.2.1 Enrichment of Xyloglucan Endotransglucosylase/Hydrolase 9 (XTH9) during progressive development of regenerating shoot progenitors.

We aimed to identify the regulators that promote the PIN1 localization pattern observed in the regenerating progenitors. Towards this, we performed a comparative transcriptome analysis on calli representing multiple genetic backgrounds engineered to be either capable or incapable of progressing from progenitor to shoot meristem. These include *pPLT7::cPLT1-vYFP in plt3,plt5-2,plt7 (plt3,5,7/PLT1-vYFP)* (single reconstitution-SR) calli that generates progenitors which cannot progress into shoot meristem, *pPLT7:cPLT1-vYFP,p35S::CUC2-3AT* in *plt3,plt5-2,plt7* (plt3,5,7/PLT1-vYFP, 35S::CUC2) (double reconstitution-DR) which makes progenitors that can progress to functional shoot meristem, and *p35S::CUC2:GR* in WT that yields an increased number of progenitors capable of making meristem upon dexamethasone treatment (Kareem et al., 2015a). Note that *plt3,plt5,plt7* triple mutant is defective in lateral root outgrowth and never regenerates (Kareem et al., 2015a). Calli incubated on SIM for 8 days were taken for the analysis ((Figure4.2A). 636 genes were upregulated in DR compared to SR, and 2592 genes were upregulated in DEX-treated *p35S::CUC2:GR in WT* compared to mock treatment (Figure4.2B-4.2C). Upon comparing the upregulated genes in DR with those upregulated in

DEX-treated *p35S::CUC2:GR in WT,* we found an overlap of 218 genes (Figure 4.2D). A Gene Ontology (GO) analysis of the 218 genes from the transcript profiling revealed their enrichment in Metabolite Interconversion enzymes, which was further enriched in Hydrolases (Figure 4.2E,4.2F). Since cell wall modulation correlates with PIN1 polarity during the shoot and root development (Feraru et al., 2011; Peaucelle et al., 2011; Wachsman et al., 2020), we chose Hydrolases for further study. We found enrichment in *XTH7, XTH9, XTH24,* and *XTH32* of the *XYLOGLUCAN ENDOTRANSGLUCOSYLASE/HYDROLASE* (XTH) gene family. It was shown that XTH genes cause cell wall loosening and cell wall modulation (Fry et al., 1992; Van Sandt et al., 2007). Among *XTH7, XTH9, XTH24,* and *XTH23,* the shoot-promoting factor CUC2, which is an important gene involved in the shoot regeneration (Kareem 2015), bound only to XTH9 as revealed by the ChIP-Seq analysis (see chapter 5). From this comparative transcriptome profiling, we found that enrichment of XTH9 levels correlated with an increase in shoot regeneration (Figure4.2A 4.2D)(Kareem et al., 2015a) and was validated using qPCR (Figure4.2G, 4.2H). This was intriguing since XTH9 causes expansion and loosening of the cells, a process expected to favour the formation of a pseudo-progenitor (Figure 2.3Q-2.3S, Figure 2.4C). To explain this apparent contradiction, we decided to monitor the Spatio-temporal expression of XTH9.

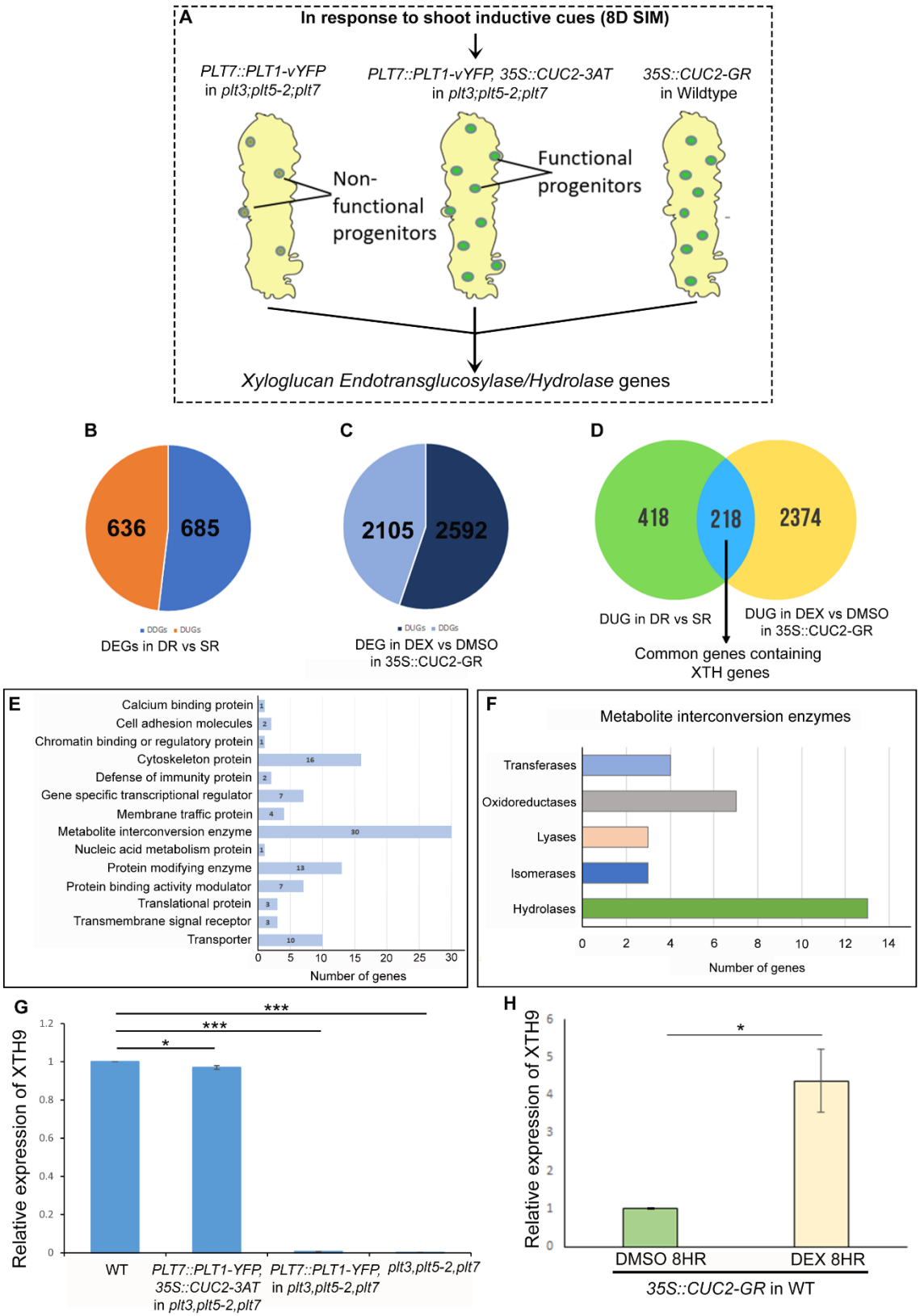

Figure 4.2: Cell wall loosening enzyme XTH9 is required for *de novo* shoot regeneration.

(A) Comparative transcriptome analysis on calli representing multiple genetic backgrounds engineered to be either capable or incapable of progressing from progenitor to shoot meristem revealed that a cell wall loosening enzyme XTH9 was imperative to propel the self-organization of these progenitor cells. The calli taken for the analysis included *pPLT7::cPLT1-vYFP* in *plt3,plt5-2,plt7 (plt3,5,7/PLT1-vYFP)* (single reconstitution-SR) calli that generate progenitors which cannot progress into shoot meristem, *pPLT7:cPLT1-vYFP,35S::CUC2-3AT* in *plt3,plt5-2,plt7* (*plt3,5,7/PLT1-vYFP, 35S::CUC2*) (double reconstitution-DR) which makes progenitors that can progress to functional shoot meristem, and *35S::CUC2:GR* in WT that yields an increased number of progenitors capable of making meristem upon Dexamethasone (DEX) induction. **(B)** 636 genes were upregulated in DR compared to SR. **(C)** 2592 genes were upregulated in DEX-treated *35S::CUC2:GR* in WT compared to mock (DMSO)treatment. **(D)** Upon comparing the upregulated genes in DR with those upregulated in DEX-treated *35S::CUC2:GR* in WT, we found an overlap of 218 genes. **(E)** Using PANTHER Gene Ontology (GO), the 218 genes were categorized into 14 protein classes, out of which the class of metabolite interconversion enzymes was enriched. **(F)** The genes enriched in metabolite interconversion enzymes were further classified into different 5 different enzyme categories, out of which hydrolases were enriched. **(G)** Graph depicting the downregulation of *XTH9* in the *plt3,5,7/PLT1-vYFP,35S::CUC2-3AT*(**P*=0.0351,Welch Two Sample t-test), *plt3,5,7/PLT1-vYFP*(****P*=0.0003188,Welch Two Sample t-test) and *plt3,plt5-2,plt7* in comparison to wildtype(****P*=0.0009612, Welch Two Sample t-test). **(H)** The regulation of XTH9 by CUC2-GR after 8hr induction using Dexamethasone was validated by qPCR(**P*=0.01097, Welch Two Sample t-test). Error bar in G,H represents s.e.m. from three independent biological replicates. n=sample number.

4.2.2 XTH9 directs *de novo* shoot organogenesis by promoting the polarization of PIN1 cells non-cell autonomously

Previous studies documented the distribution of cell wall-modifying enzymes by immunohistochemistry (Haas et al., 2021; Rivai et al., 2021). However, the fragile nature of the callus limits the usage of such techniques. We, therefore, used confocal-based live imaging to monitor the distribution pattern of XTH9 using the translational fusion, *pXTH9::XTH9-vYFP* (XTH9-YFP), which complements the defects in the lateral root (Figure4.3A-4.3C) (Xu and Cai, 2019) and shoot regeneration of the *xth9 3'UTR* mutant (see below for shoot regeneration

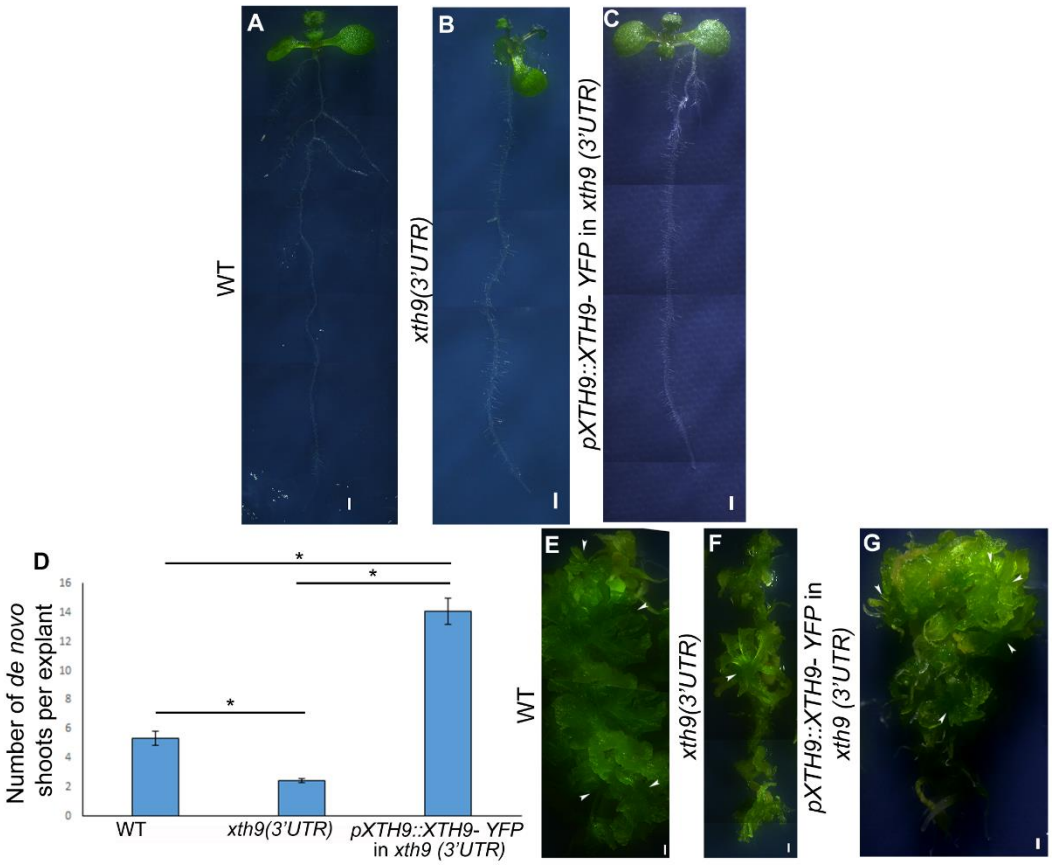

Figure 4.3: XTH9 is necessary for *de novo* shoot regeneration.

(A) 7-dpg WT seedling with normal lateral root development(n=10), **(B)** 7-dpg *xth9(3'UTR)* seedlings with defective later root development (delayed lateral root outgrowth) (n=12), **(C)** 7-dpg XTH9-YFP in *xth9(3'UTR)* rescued the defect in lateral root development defect(n=17). **(D)** Graph depicting the rescue of shoot regeneration in XTH9-YFP in *xth9(3'UTR)*(WT vs. *xth9(3'UTR)*:n=65,**P*=0.04857; WT Vs. XTH9-YFP in *xth9(3'UTR)*:n=53,**P*=0.04021; XTH9-YFP in *xth9(3'UTR) Vs xth9(3'UTR)*:n=55,**P*=0.04536, Welch Two Sample t-test). **(E-G)** Shoot regeneration in *xth9(3'UTR)*(n=53) (F) is reduced compared to WT(n=65) (G), but is rescued in *xth9(3'UTR)* reconstituted with XTH9-YFP(n=55) (G). Scale bar 1mm. Error bar represents s.e.m. from three independent biological
replicates. n=sample number.

defects) (Figure 4.3D-4.3 G). XTH9-YFP had an interesting spatial expression, where XTH9-YFP was undetectable in the PIN1 marked cells of a productive progenitor but detected robustly in a shell of non-progenitor cells that encapsulates the progenitor (Figure4.4A-4.4I). This expression pattern was particularly evident during the initial stages of progenitor (5-10 celled stages), where a layer of XTH9-YFP expressing cells overlaid the progenitor surface (Figure 4.4A-4.4C, 4.4G-4.4H) Deeper optical sections revealed that XTH9 is expressed in a ring-like fashion around the PIN1-GFP marked progenitor cells

(Figure 4.4G(iv-v), 4.4H(iv-v), 4.4I(iv-v)). With the progression of the progenitor, PIN1-GFP marked progenitor cells emerged through the overlaying cells (15-70 celled stages), and XTH9-YFP became confined around the immediate vicinity of the progenitor in a ring-like fashion (Figure 4.4A, 4.4D, 4.4E). Upon making a mature shoot, XTH9-YFP was seen along the meristem periphery and the base of emerging leaf primordia but remained undetectable in the meristem centre (Figure 4.4F). Unlike the productive progenitors, XTH9 and PIN1 did not have mutually exclusive domains in the pseudo-progenitors. Instead, we found abundant expression of XTH9 in the spatial domain of PIN1-GFP marked cells (10-12 celled stage) (n=20) (Figure 4.5A-4.5D). These progenitors soon got aborted, as supported by the disappearance of PIN1-GFP (Figure.4.5C).

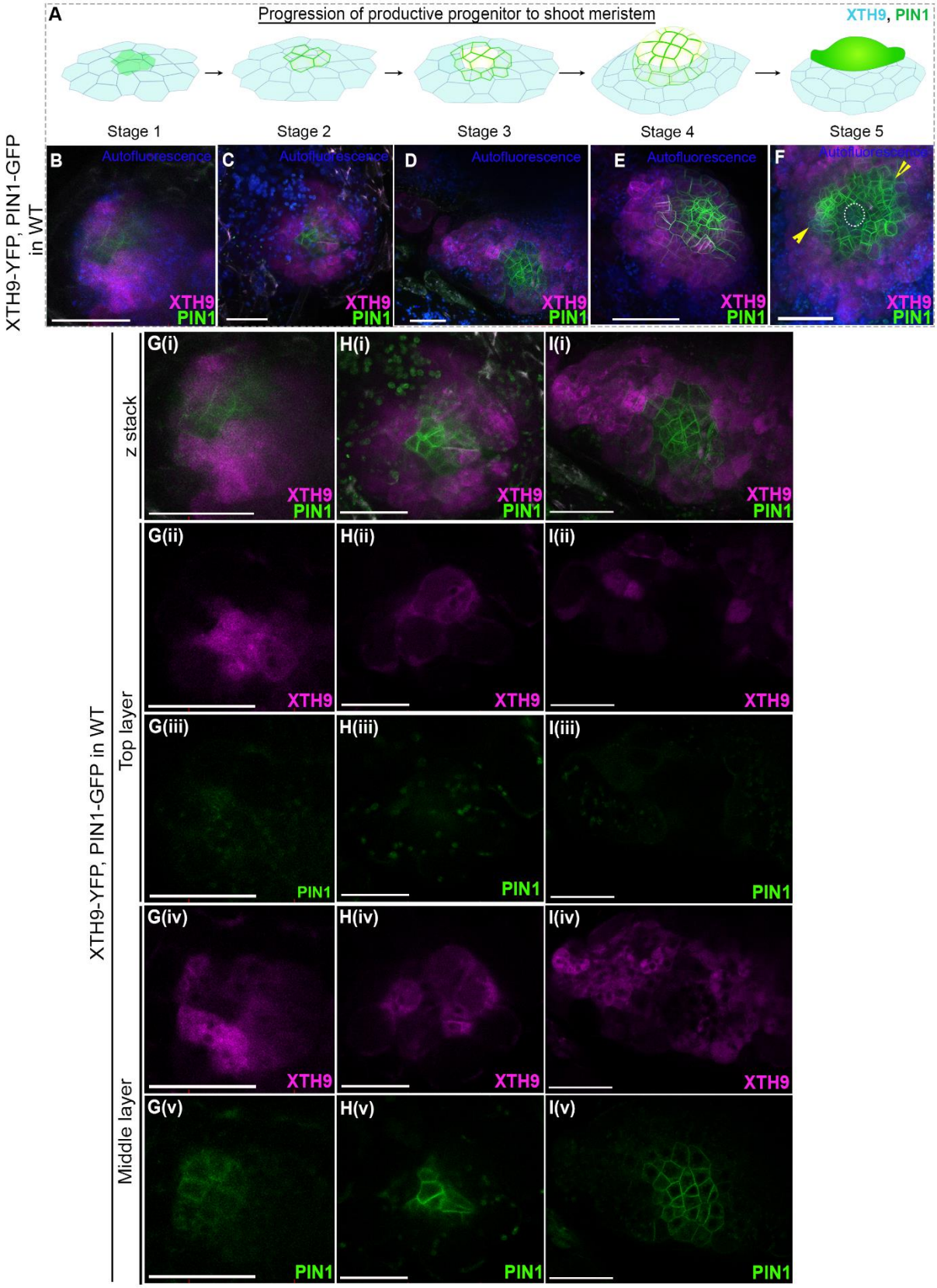
A
Progression of productive progenitor to shoot meristem
XTH9, PIN1
Stage 1
Stage 2
Stage 3
Stage 4
Stage 5
XTH9-YFP, PIN1-GFP in WT
B Autofluorescence
C Autofluorescence
D Autofluorescence
E Autofluorescence
F Autofluorescence
XTH9
PIN1
XTH9-YFP, PIN1-GFP in WT
z stack
Top layer
Middle layer
G(i)
H(i)
I(i)
G(ii)
H(ii)
I(ii)
G(iii)
H(iii)
I(iii)
G(iv)
H(iv)
I(iv)
G(v)
H(v)
I(v)

Figure 4.4: XTH9, a cell wall loosening enzyme promotes the self-organization of progenitor cells non-cell autonomously.

(A) Schematic depicting the spatial specific expression of XTH9 (blue) during progenitor progression to shoot meristem. XTH9 marked shell of non-progenitor cells encapsulates the progenitor (green bordered), even before membrane localization of PIN1-GFP (stage1). By promeristem (stage 4), the PIN1 marked cells begin to protrude through the overlaying XTH9 layer and attain a dome shape. **(B-F)** Representative live-images showing the Spatio-temporal expression of XTH9-YFP (magenta) at different time points of productive progenitor progression. B, C, D, E, and F corresponds to stages 1, 2, 3, 4, and 5 respectively. Till stage 2 (8-10 celled stage, C) XTH9-YFP is confined to the shell of non-progenitor cells and excluded from the PIN1-GFP (green) marked progenitor cells enclosed within the shell (B, C). At stage 4 (15-20 celled stage, D), XTH9-YFP is not detectable at the top of the PIN1- marked cells. At stage 4, which is the promeristem stage (60-70 celled stage, E), the PIN1 marked cells are seen emerging as a dome-shaped stricture through the overlaying XTH9 layer of cells. By stage 5 (shoot meristem, F), XTH9-YFP is detected at the peripheral cells of mature meristem and the base of the emerging leaf primordia (F). Yellow arrowheads indicate the emerging leaf primordia, and white dotted circles indicate the meristem centre. (n=18(stage 1), 18(stage 2), 14(stage 3), 30(stage 4), 24(stage 5). **(G-I)** Representative live images showing the mutually exclusive domains of PIN1-GFP and XTH9-YFP in the first three stages of developing progenitor, G(i)-G(v) corresponds to B, H(i)-H(v) corresponds to C, I(i)-I(v) corresponds to D. Complete z-stack of XTH9-YFP, PIN1-GFP (in GFP/YFP merged channel G(i), H(i), I(i)). Top layer of z-stack of XTH9-vYFP, PIN1-GFP in YFP channel (G(ii), H(ii), I(ii)). Top layer of z-stack of XTH9-vYFP, PIN1-GFP in GFP channel (G(iii), H(iii), I(iii)). Note that here PIN1-GFP was not detected. The middle layer of z-stack of XTH9-YFP, PIN1-GFP in YFP channel (G(iv), H(iv), I(iv)). The middle layer of z-stack of XTH9-YFP, PIN1-GFP in GFP channel (G(v), H(v), I(v)). Note that the expression domain of XTH9-YFP is observed to be encircling the expression domain of PIN1-GFP (G(iv)-G(v), H(iv)-H(v), I(iv)-I(v)). Scale bars: 50µm, n: sample number.

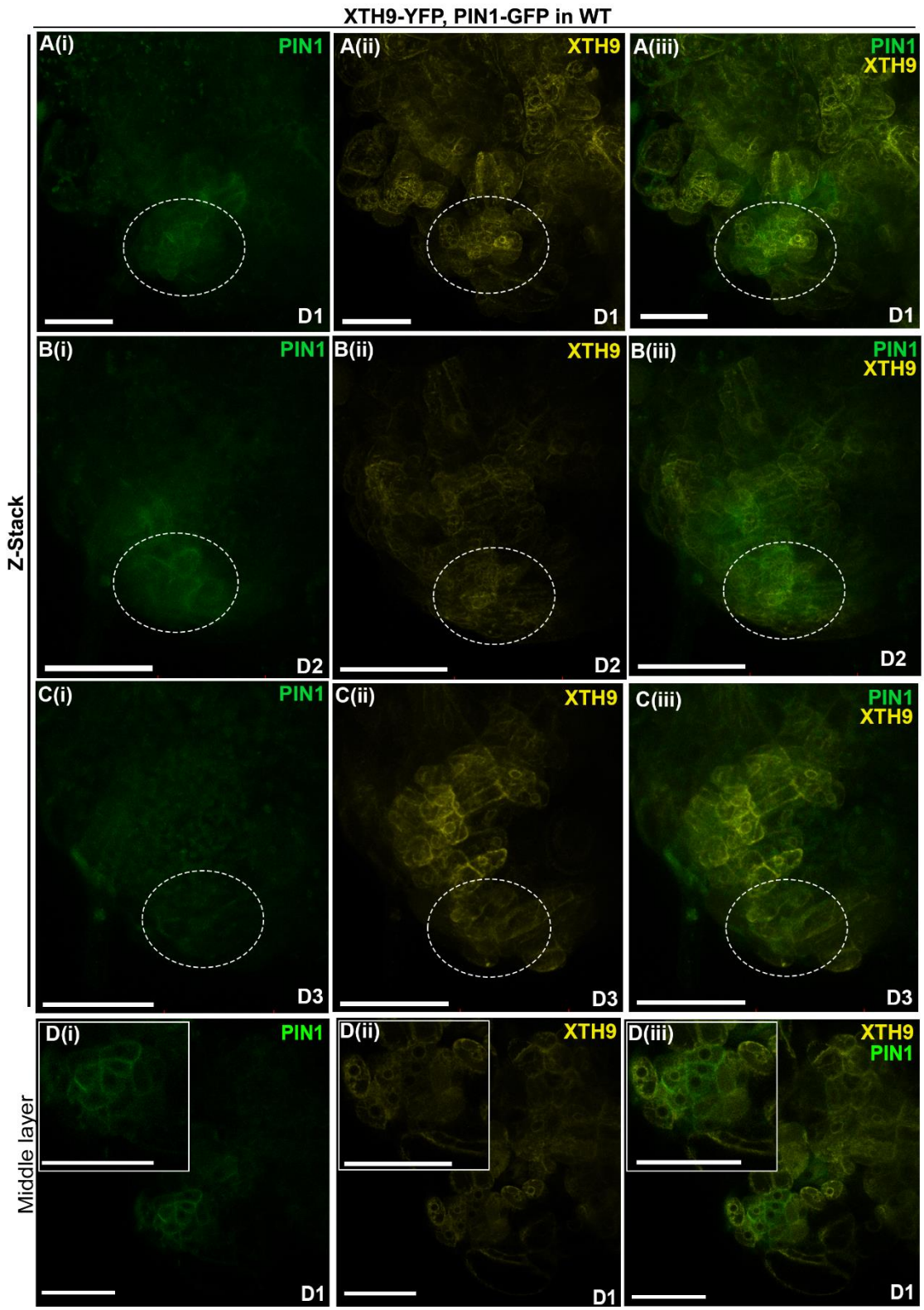

Figure 4.5: Altered spatial expression of XTH9 in the progenitor perturbs the shoot formation *de novo.*

(A-C) Representative time-lapse images of pseudo-progenitor showing XTH9-YFP(n=20) (progenitor is marked by white-dotted circle). **(D)** Middle layer of the pseudo-progenitor (insets show the enlarged portion of the progenitor). GFP channel (A(i), B(i), C(i), D(i)), YFP channel ((A(ii), B(ii), C(ii),D(ii)), merged image (A(iii), B(iii), C(iii),D(iii)) of the pseudo-progenitors with XTH9-YFP, PIN1-GFP in WT. Scale bars: 50µm (A-D).

4.2.3 Functional characterization of the role of cell wall modulating enzyme XTH9 in *de novo* shoot regeneration

These observations raise the question, what is the physiological relevance of the distinct expression pattern of XTH9? The spatial expression of XTH9 around a productive progenitor suggests a difference in mechanical properties between the juxtaposed progenitor and non-progenitor cells leading to a "mechanical conflict" (Hervieux et al., 2017) between the two cell types. We asked if disruption of this mechanical conflict either by removing XTH9 function from non-progenitor cells or its forced expression within the progenitor cells impinges on the progenitor progression to meristem. Indeed, the *xth9 3'UTR* mutant callus had dramatically reduced shoot regeneration (n = 105, 1.602 ± 0.259) compared with WT (n = 77, 13.463 ± 1.160) (Figure 4.6A–4.6C). Notably, the *xth9 3'UTR* mutant seedlings grew and developed robust shoot and shoot-derived organs similar to WT (Figure 4.3B). In corroboration with results from *xth9 3'UTR* loss of function mutant in callus, inducible downregulation of XTH9 using *pG1090:XVE::XTH9-dsRNAi* throughout the SIM incubation period (n = 121, 0.40 ± 0.234) or even for 24Hr during the onset of progenitor formation (8th day SIM) (n = 94, 1.353 ± 0.233) reduced shoot regeneration dramatically (Figure 4.6D-4.6G). Further, the inducible genome editing (IGE)-based knockout (X. Wang et al., 2020) of XTH9 (*pG1090:XVE::Cas9p-tagRFP-XTH9 in pXTH9::XTH9-vYFP/WT*) throughout the SIM incubation period (n = 67, 0.97 ± 0.2778) or for 48Hr (n = 66, 1.21 ± 0.079) during the onset of progenitor formation also led to a severe reduction in shoot regeneration (Figure 4.6H-4.6W). Mock induction of dCas9 either transient (n = 56, 4.95 ± 0.2858) or continuous on SIM (n = 45, 7.73 ± 0.0677), the shoot formation remains comparable with uninduced control (n = 82, 7.56 ± 0.0.841) (Figure 4.6Q, 4.6U-4.6W). Notably, neither the formation nor the phenotype of the callus in these backgrounds was compromised, indicating that reduced shoot regeneration was not due to a defective callus (Figures 4.6C, 4.6E-4.6G, 4.6R-4.6W). Interestingly, even a brief downregulation of XTH9 by 20 minutes of steroid induction of ~6 celled (Figure 4.7A) or ~15celled progenitor

(Figure 4.7D) of *pG1090:XVE::XTH9-dsRNAi* callus abolished their progression (n=26) (Figure 4.7A-4.6C, 4.7D-G). In support, PIN1-GFP was not detectable even after 4-days post removal of the 6 celled progenitor from the steroid pulse (Figure 4.7C). Nevertheless, ~25 celled progenitor made shoot meristem after the 20min brief downregulation of XTH9 (Figure 4.7H-4.7J). These observations demonstrated the temporal specificity of XTH9, particularly during progenitor initiation and early stages of progenitor development.

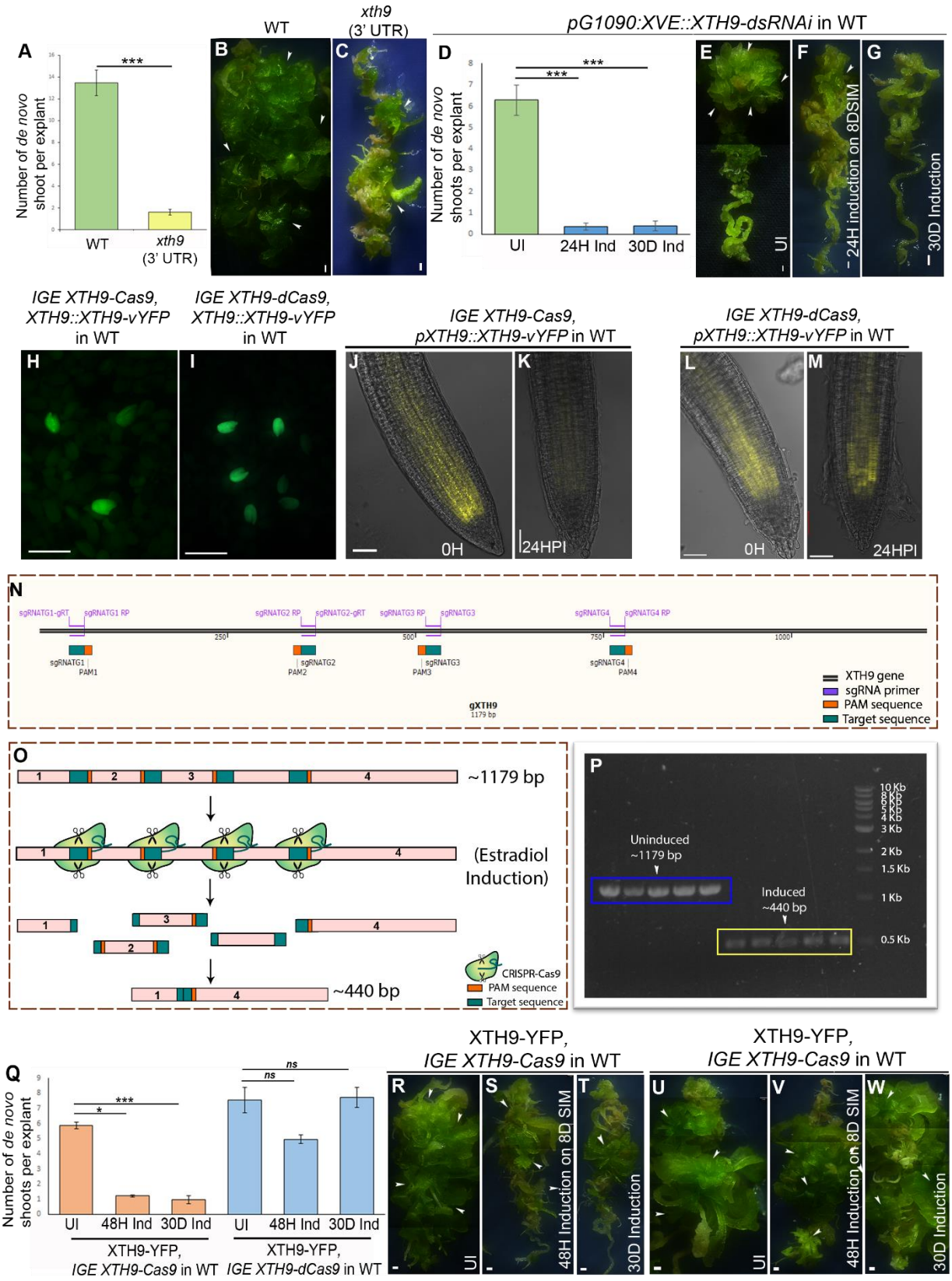
A
Number of de novo shoot per explant
***
WT
xth9 (3' UTR)
WT
xth9 (3' UTR)
B
C
pG1090:XVE::XTH9-dsRNAi in WT
D
Number of de novo shoots per explant
***
***
UI
24H Ind
30D Ind
E
F
G
UI
24H induction on 8DSIM
30D Induction
IGE XTH9-Cas9, XTH9::XTH9-vYFP in WT
IGE XTH9-dCas9, XTH9::XTH9-vYFP in WT
IGE XTH9-Cas9, pXTH9::XTH9-vYFP in WT
IGE XTH9-dCas9, pXTH9::XTH9-vYFP in WT
H
I
J
K
L
M
0H
24HPI
0H
24HPI
N
sgRNATG1-gRT
sgRNATG1 RP
sgRNATG2 RP
sgRNATG2-gRT
sgRNATG3 RP
sgRNATG3
sgRNATG4
sgRNATG4 RP
250
500
750
1000
sgRNATG1 PAM1
sgRNATG2 PAM2
sgRNATG3 PAM3
sgRNATG4 PAM4
gXTH9 1179 bp
XTH9 gene
sgRNA primer
PAM sequence
Target sequence
O
~1179 bp
(Estradiol Induction)
~440 bp
CRISPR-Cas9
PAM sequence
Target sequence
P
Uninduced ~1179 bp
Induced ~440 bp
10 Kb
8 Kb
6 Kb
5 Kb
4 Kb
3 Kb
2 Kb
1.5 Kb
1 Kb
0.5 Kb
Q
Number of de novo shoots per explant
***
*
ns
ns
UI
48H Ind
30D Ind
UI
48H Ind
30D Ind
XTH9-YFP, IGE XTH9-Cas9 in WT
XTH9-YFP, IGE XTH9-dCas9 in WT
XTH9-YFP, IGE XTH9-Cas9 in WT
XTH9-YFP, IGE XTH9-Cas9 in WT
R
S
T
U
V
W
UI
48H Induction on 8D SIM
30D Induction
UI
48H Induction on 8D SIM
30D Induction

Figure 4.6: XTH9 activity shows temporal specificity during shoot meristem regeneration *de novo*.

(A-C) The shoot regeneration is severely reduced in the *xth9 (3'UTR)* mutant (n=130, ***P=0.0007686, Welch Two Sample t-test) compared to WT(n=134)(A). Stereo-image showing shoot regeneration in a WT callus (B) and *xth9 (3'UTR)* callus (C). **(D-G)** Transient downregulation of XTH9 in *pG1090:XVE::XTH9-dsRNAi* in WT for 24Hr (8th Day SIM)(n=24) *(***P=0.0009285*, Welch Two Sample t-test) or sustained downregulation throughout the SIM incubation period (0-30 days SIM)(n=121)(***P=0.0004166, Welch Two Sample t-test) in an estradiol inducible fashion severely reduced shoot regeneration in comparison to uninduced (D).Stereo-image showing shoot regeneration in uninduced *pG1090:XVE::XTH9-dsRNAi* in WT callus (E), upon downregulation of XTH9 for 24Hr on 8th Day SIM (F), upon sustained downregulation of XTH9 throughout SIM incubation (0-30 days SIM) (G). **(H-I)** Non-destructive fluorescent tagged transformed seeds containing pFG7m34GW destination vector with gOLE-GFP in *pG1090(I)::Cas9-XTH9 sgRNA* cassettes (IGE XTH9-Cas9) in *pXTH9::XTH9:vYFP* in WT (H) and IGE-XTH9-dCAS9 in *pXTH9::XTH9:YFP* in WT (I) were generated for this study. **(J-K)** Confocal image showing expression of XTH9-YFP in the root tip of *pG1090(I)::Cas9-XTH9 sgRNA* cassettes in *pXTH9::XTH9:YFP* in WT at 0hr induction (J). 24hr Cas9 induction using 5µM estradiol resulted in a loss of XTH9-YFP from the root tip (K). **(L-M)** But, 24hr induction using 5µM estradiol, dCas9 did not change any expression in XTH9-YFP. **(N-P)** Schematic characterization showing the effect of induction of CRISPR-Cas9 system on the XTH9 gene. XTH9 gene body showing the selected area to target (Orange represents the PAM sequence, and the green represents the sgRNA sequence to make a double-stranded break) (N) Illustration of how gene editing worked in the system (O). Agarose gel image showing the PCR product of XTH9 gene in the uninduced plant (~1179 bp) (blue box) and induced plant (~440 bp) (yellow box) of *pG1090(XVE)::Cas9-XTH9 sgRNA* cassettes (IGE XTH9-Cas9) in *pXTH9::XTH9:vYFP* in WT (P). **(Q-W)** Inducible knockout of XTH9 in pXTH9:gXTH9::vYFP, IGE XTH9-Cas9 in WT (pG1090:XVE::Cas9TagRFP-XTH9 sgRNA cassettes in XTH9-YFP; WT) for 48Hr (8th Day SIM)(n=66), or sustained induction throughout the SIM incubation period (0-30 days SIM)(n=67) dramatically reduced shoot regeneration compared to uninduced(n=121). The shoot regeneration in pXTH9::gXTH9::vYFP, IGE XTH9-dCas9 in WT (pG1090:XVE::dCas9t35S-XTH9 sgRNA cassettes in XTH9-YFP; WT) remained comparable to uninduced (n=82), even after induction for 48Hr (8th Day SIM) (n=56), or sustained induction throughout the SIM incubation period (0-30 days SIM) (H) (n=45) (IGE XTH9-Cas9:-UI:n=121;48HI: n=66, *P=0.01543, Welch Two Sample t-test; CI: n=67 ,***P=0.0008666, Welch Two Sample t-test), IGE XTH9-dCas9:UI:n=82;48HI: n=56 , ns,P=0.2125, Welch Two Sample t-test; CI: n=45 ,ns,P=0.91,Welch Two Sample t-test). Stereo-image showing shoot regeneration in a uninduced callus of IGE-XTH9-Cas9 (R) upon induction of IGE-XTH9-Cas9 for 24Hr on 8th Day SIM (S), upon continuous induction of IGE-XTH9-Cas9 (T), uninduced callus of IGE-XTH9-dCas9 (U) upon 48hour induction of IGE-XTH9-dCas9 (V), upon sustained induction of IGE-XTH9-dCas9 throughout SIM incubation (0-30 days SIM) (W). Error bar represents s.e.m. Scale bars: 50µm(J-M), 1mm(B,C,E-I,R-W), n:sample number.

4.2.4 Activity of XTH9 expression within the progenitor cells impairs the shoot regeneration

Not only the removal of XTH9 activity from non-progenitor cells, but even its forced expression within the PIN1 marked progenitor cells can impinge on the meristem formation *de novo*. We found that sustained ectopic overexpression of XTH9 (pG1090:XVE::XTH9-

vYFP) in a steroid-inducible manner throughout SIM generated a phenotypically fragile callus incapable of meristem formation. Even a transient overexpression of XTH9 for 24 Hr during progenitor onset (8th D SIM) abolished shoot regeneration (Figure 4.7K-4.7N). However, a brief upregulation of XTH9 in the progenitors (~20 cells) by 20 minutes of local steroid induction did not abolish its progression (n=14)(data not shown). Instead, it led to a transient delocalization of PIN1, which was evident by weak PIN1-GFP localization on the cell membrane by 2 days post-removal of the steroid pulse (Figure 4.7D). These findings indicate that the tight Spatio-temporal activity of XTH9 is critical for regulating the PIN1 localization pattern during shoot meristem formation *de novo*. Next, we asked if we forcefully express XTH9 in the progenitor, what will be the fate of such regenerating foci? To address this question, we chose *WUSCHEL* promoter to drive *XTH9* because *WUSHEL* is a shoot meristem organizer (T.-Q. Zhang et al., 2017). We generated a translational fusion of *WUS::XTH9:tWUS* where we used 5.7Kb of *WUS* upstream sequences and 1.6kb of downstream sequences to deliver the XTH9 enzyme in the progenitor (T.-Q. Zhang et al., 2017). We could observe a reduction in shoot formation *de novo* when forced to express XTH9 in the progenitor under *WUSCHEL* promoter (*pWUS::XTH9;tWUS* in WT(n=112, 4.556 ± 0.557)) compared to the wildtype (n=67, 7.854 ± 1.179) (Figure 4.7O) Suggesting that the XTH9 should be excluded from the progenitor and required in the non-progenitor cells for the successful shoot emergence.

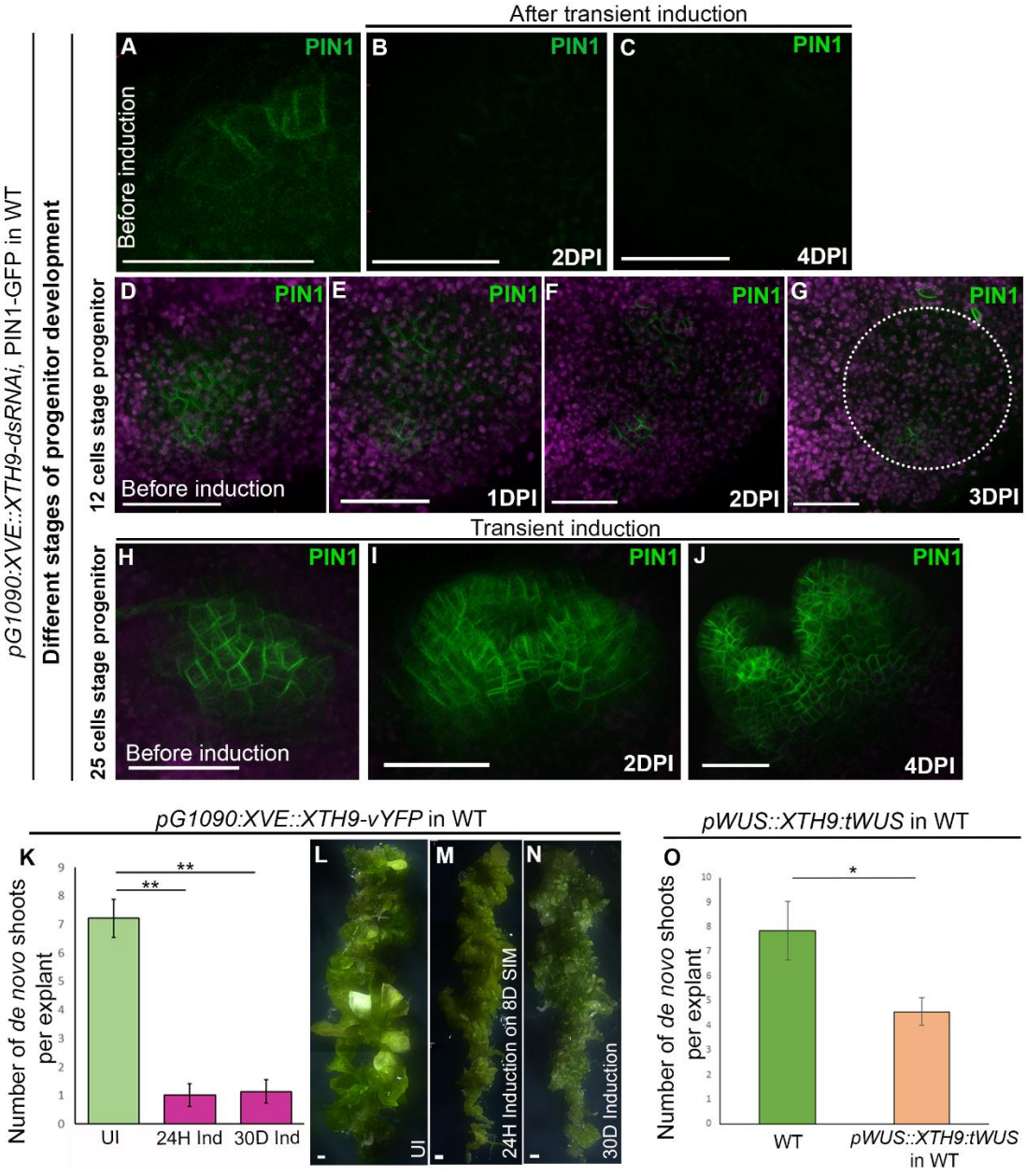

Figure 4.7: Spatio-temporal activity of XTH9 is essential for shoot meristem formation *de novo*.

(A-C) Representative time-lapse images showing PIN1-GFP in pG1090:XVE::XTH9-dsRNAi before induction (A). A brief 20 minutes induction of XTH9-dsRNAi by local application of estradiol to the progenitor (15-celled stage) led to the disappearance of PIN1-GFP and abortion of progenitor(n=26) (B, C). **(D-G)** Representative time-lapse images showing that transient downregulation of XTH9 in 12-15 celled progenitor (D) by 20 minutes induction of XTH9-dsRNAi using local application of estradiol after progenitor spotting led to abortion of progenitor by 3-days post removal from the steroid induction, as indicated by the disappearance of PIN1-GFP(G). **(H-J)** Representative time-lapse images showing that downregulation of XTH9 by 24Hr induction in a late progenitor (25-celled stage)(H), after progenitor spotting, however, did not perturb the progenitor

progression. By 2nd day of sustained induction, it progressed into promeristem (I), and by 4th day of sustained induction, it formed a functional shoot (J**). (K-N)** Overexpression of XTH9 in *pG1090:XVE::XTH9-vYFP* (XTH9-OE) in WT upon estradiol induction for 24Hr (8th Day SIM)(n=50) , or sustained induction throughout the SIM incubation period (0-30 days SIM)(n=54) (**P=0.00872, Welch Two Sample t-test) dramatically reduced shoot regeneration compared to uninduced(n=68) (K). Stereo-image showing shoot regeneration in uninduced callus of XTH9-OE (L) upon XTH9 overexpression for 24Hr(8th Day SIM) (M), upon sustained XTH9 overexpression throughout the SIM incubation period (0-30 days SIM) (N). **(O)** Forced expression of XTH9 within the progenitor under the WUS promoter using *pWUS::XTH9:tWUS* in WT(n=112) showed reduced shoot regeneration (**P*=0.0461, Welch Two Sample t-test) compared to wildtype (n=67). Error bar represents s.e.m. Scale bars: 50µm(A-L, Q-X), 1mm(N-P), n: sample number, Magenta colour depicts auto-fluorescence.

4.3 DISCUSSION

How does feedback between two types of juxtaposed cells experiencing distinct force fields instruct meristem formation? We propose a self-sustained model where a shell of non-progenitor cells expressing cell wall loosening enzyme XTH9 acts as a "constriction-shell" encapsulating the progenitor (Figure 4.4G(i),4.4H(i),4.4I(i)). Based on our results that progenitor cells are compressed into tight packing. In contrast, the non-progenitor cells of the constriction shell undergo expansion (Mabel Maria Mathew, Varapparambath et al., 2022); we formulated the following hypothesis. The prolific division and growth of progenitor cells mechanically impact the slowly dividing cells of the constriction-shell to expand circumferentially (Mabel Maria Mathew, Varapparambath et al., 2022). Consistent with the notion of feedback, we found that biochemical or genetic perturbation of the progenitor cells impairs the XTH9-marked shell of non-progenitor cells (Figures 4.6A-4.6G,4.6Q-4.6W, 4.7A-4.7G). We showed that conflict between neighbouring cells by the presence or absence of cell wall loosening enzyme resulting from this feedback instructed the localization pattern of polarity protein in the progenitor (Figure 2.4B, 4.7A-4.7G). We propelled the sculpting of a dome-shaped meristem in the absence of tissue patterning cues (Figure 2.3O,2.3P), and perturbations to the feedback disrupted the localization pattern of polarity proteins and aborted progenitor progression (Figures 4.6A-4.6G,4.6Q-4.6W, 4.7A-4.7G, 2.6O).

Our finding is that progenitor progression to meristem relies on the conflict of progenitor and non-progenitor cells by the inevitable action of XTH9. The presence of XTH9 in the

surrounding cells aids in their tangential expansion and directs these cells to form a constriction belt, leading to the outward bulging of PIN1 marked progenitor cells. In contrast, when PIN1 marked cells experience XTH9 in the pseudo-progenitor, the cells become loosely arranged and irregular in shape, causing the inability of PIN1 to polarize on the membrane. Through various molecular tools such as RNAi interference, overexpression, inducible CRISPR-Cas9 gene editing, expression modulation experiments, and quantitative real-time PCR (Figure 4.6, 4.7, see Figure 5.2) in concomitant with extensive genetic follow-up solved the hypothesis in which to emphasize the cross-talk between wall mechanics and cell polarity during *de novo* shoot regeneration.

Chapter 5

CUC2 activates the expression of XTH9 to promote shoot meristem formation *de novo*

5.1 INTRODUCTION

The shoot apical meristem (SAM) acts as a reservoir for lateral organs by retaining a small pool of pluripotent cells. It eventually creates the lateral organ by orchestrating intracellular and intercellular networks. Regardless of how the apical meristem develops—embryonically (shoot or root apical meristem) or post-embryonically (*de novo* adventitious shoot, floral meristem, or lateral root)—this essential characteristic of the shoot apical meristem is maintained throughout the lifetime of the plant. *De novo* shoot organogenesis is a systemic process not only establishes the defined system but also to begins to lay the groundwork for it. As described earlier (chapter 2 to Chapter 4), reprogramming of shoot progenitor architecture from an unorganized callus is governed by various factors, including *PIN1* and *XTH9* (Figure 2.3-2.6, 4.2-4.5). PIN1 is an essential protein present from the early developmental stage of the shoot progenitor. It releases auxin into the surrounding cells and builds a new skeleton for the shoot (Figure 2.4). The expression of a cell-wall loosening enzyme XTH9 in the surrounding non-progenitor cells allows for the proper expression and maintenance of PIN1 localization on the membrane of the shoot progenitor (Figure 4.3,4.4). The polar localization of PIN1 and the dynamic cell wall modulation activity of the XTH9 enzyme need precise guidance to execute the self-organization from heterogenous callus tissue. Evidence supports the boundary marker gene *CUP-SHAPED COTYLEDON (CUC)* being linked to PIN1 polarization and *de novo* shoot organogenesis (Bilsborough et al., 2011; Daimon et al., 2003; Gordon et al., 2007; Kareem et al., 2015a). *CUC* genes, part of the NAC domain (NAM-ATAF1-CUC) family protein, regulate boundary separation between organs, including cotyledon, shoot apical meristem, and floral organs (Aida et al., 1999; Duval et al., 2002; Gonçalves et al., 2015; Ishida et al., 2000; Takada et al., 2001; Vroemen et al., 2003). Eudicots have a distinct cotyledon separated by an asymmetric division at the upper part of the globular embryo (Aida et al., 1997, 1999; Barton & Poethig, 1993; Mansfield & Briarty, 1991; U. Mayer et al., 1991; West & Harada, 1993), which is primarily regulated by *CUC* genes (Figure 5.1A) (Aida et al., 1997, 1999).

The *CUC* subfamily includes three genes - *CUC1*, *CUC2*, and *CUC3*, with conserved NAC domain sequences and partial functional redundancy (Aida et al., 1997, 1999; Daimon et al., 2003; Duval et al., 2002; Gordon et al., 2007). *CUC1* and *CUC2* are expressed at the

boundary region of cotyledon primordia and floral organs (Aida et al., 1997; Aida & Tasaka, 2006; Ali et al., 2020; Baker et al., 2005; Laufs et al., 2004; Mallory et al., 2004; Takada et al., 2001; Vroemen et al., 2003). Mutation in either *CUC1* or *CUC2* has no effect, but the *cuc1,cuc2* double mutant exhibits a fused cotyledon without a distinct shoot apical meristem (Figure 5.1C) (Aida et al., 1997; Ali et al., 2020; Duval et al., 2002; Radhakrishnan et al., 2020; Takada et al., 2001; Vroemen et al., 2003; Weir et al., 2004). *CUC3* plays a secondary role in boundary maintenance, with strong expression in the epidermis during embryogenesis (Duval et al., 2002). The *cuc3-2* mutant occasionally shows heart-shaped or cup-shaped cotyledons, demonstrating *CUC3*'s early boundary maintenance contribution (Figure 5.1B, 5.1C) (Duval et al., 2002).

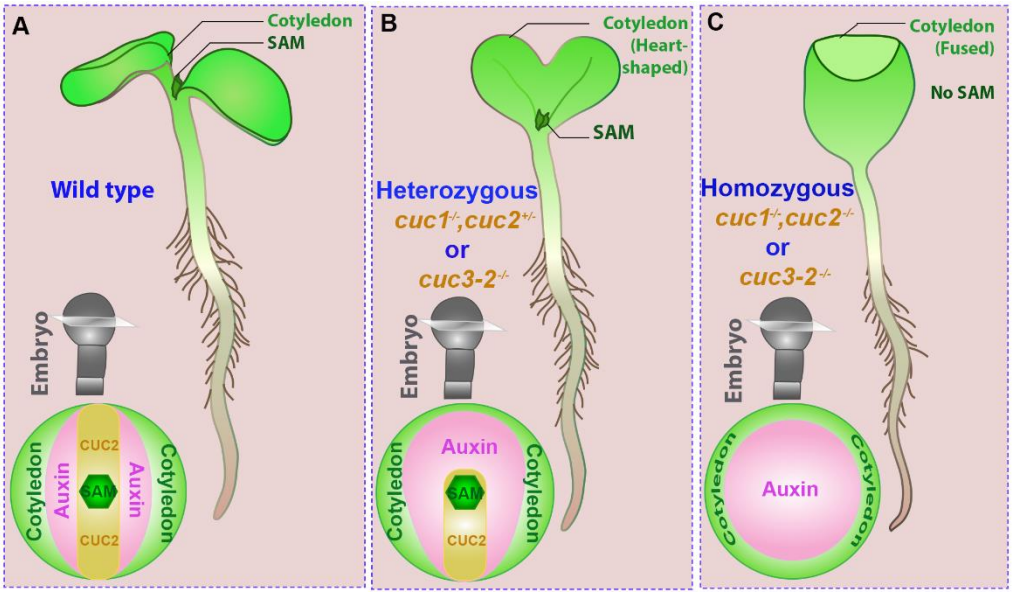

Figure 5.1: *CUC* genes are necessary to maintain the organ boundary during SAM initiation.

(A-C) Illustration of *CUC2* activity to separate the shoot apical meristem (SAM) and cotyledon during embryogenesis. (A) Represents the wild type *Arabidopsis* seedling developed from an embryo organized well by the action of the *CUC* genes boundary marker. (B) Seedling with heart-shaped cotyledon explains the spatial limitation of CUC genes that interfere with the cotyledon separation during organ boundary development during embryogenesis (prominent phenotype of *cuc1*$^{-/-}$,*cuc2*$^{+/-}$ or rare phenotype of *cuc3-2*$^{-/-}$). (C) In the absence of *CUC* genes, especially in the double mutant (*cuc1*$^{-/-}$,*cuc2*$^{-/-}$) or very rarely in the single mutant (*cuc3-2*$^{-/-}$ in very low frequency), the embryo unable to make a boundary between SAM and lateral organ that is resulting in the cup-shaped (fused) cotyledon lacking a functional meristem.

The *CUC* subfamily plays a role in both embryonic and adult plant development (Duval et al., 2002; Gonçalves et al., 2015; Hasson et al., 2011; Kawamura et al., 2010; Nikovics et al., 2006; Serra & Perrot-Rechenmann, 2020; Shuai et al., 2002; Vroemen et al., 2003). It

influences leaf serration, with *CUC2* involved in early tooth emergence, and *CUC3* maintaining tooth shape (Kawamura et al., 2010; Nikovics et al., 2006). Overexpressing *CUC1* can increase serration or induce leaflet formation (Hasson et al., 2011; Takada et al., 2001). Precise spatial coordination between cells with different growth kinetics is crucial for establishing new growth axes, defining proliferating organs like shoot apical meristem, leaf margin, or floral organs (Aida et al., 1997; Dumais & Kwiatkowska, 2002; Gonçalves et al., 2015; Hasson et al., 2011; Kwiatkowska, 2004; Serra & Perrot-Rechenmann, 2020).

Many factors influence *CUC* gene expression, such as *STM*, auxin, microRNAs, and chromatin remodeling. Auxin significantly impacts spatial *CUC* expression (Aida et al., 1999, 2002; Aida & Tasaka, 2006; Baker et al., 2005; Furutani et al., 2004b; Kwon et al., 2005; Laufs et al., 2004; Mallory et al., 2004; Treml et al., 2005; Vernoux et al., 2000). *CUC2* controls auxin by polarizing PIN1 at the leaf margin, determined by auxin downregulation of CUC2 during leaf teeth development (Bilsborough et al., 2011). *CUC2* is downregulated in *PIN1* or *MONOPTEROS* (*MP*) mutants (Aida et al., 2002; Gordon et al., 2007; Leibfried et al., 2005). Therefore *PIN1-CUC2* combination is essential for shoot apical meristem formation and organogenesis (Bilsborough et al., 2011; Furutani et al., 2004a; Vernoux et al., 2000).

The *cuc1,cuc2* double mutant, as well as the *cuc3-2* mutant (albeit at a very low frequency), exhibit a phenotype lacking an embryonic meristem (Aida et al., 1997; Duval et al., 2002). Although the mutation partially affects *de novo* shoot organogenesis, these mutants are unaffected in their capacity to form adventitious shoots originating from lateral root primordia (LRP) (Aida et al., 1997; Duval et al., 2002). Compared to the wildtype, *CUC* mutants (both single and double mutant) are defective in *de novo* shoot regeneration (Aida et al., 1997; Daimon et al., 2003; Duval et al., 2002; Hibara et al., 2003; Taoka et al., 2004). The ectopic overexpression of either *CUC1/CUC2* or chimeric NAC domain promotes adventitious shoot formation, emphasizing its transcriptional activator ability. (Daimon et al., 2003; Gordon et al., 2007; Kareem et al., 2015a; Takada et al., 2001; Taoka et al., 2004; Xie et al., 2000). The early developmental regulator *WUS* or master regulators *PLT3, PLT5,* or *PLT7,* which regulates the adventitious shoot formation *de novo,* appear to overlap with *CUC2* among all other *CUC* genes (Gordon et al., 2007; Kareem et al., 2015a). However, overexpression of *CUC2* in *plt3,plt5-2,plt7* mutant (triple mutant defective in regeneration)

couldn't rescue shoot regeneration defect. It implies that *CUC2* can function downstream for the root stem regulator (*PLETHORA1* and *PLETHORA2*), which generates a competency for exposing the tissue to establish a baseline floor for *CUC2*, for the shoot outgrowth. Once the callus tissue acquires the pluripotency, *CUC2*, which is activated by *PLT3*, *PLT5*, or *PLT7,* can set up a shoot outgrowth program from the shoot progenitor (Kareem et al., 2015a). But how does *CUC2* aid in the shoot formation from shoot progenitor cells during the *de novo* shoot regeneration? How does *CUC2* interact with *PIN1* or *XTH9* to facilitate the emergence of the shoot during *de novo* shoot organogenesis? The mechanisms by which *CUC2* helps with the formation of shoot *de novo* are not yet fully understood. However, it is believed that *CUC2* may play a crucial role, working alongside *PIN1* and *XTH9* to facilitate the emergence of shoots during *de novo* shoot organogenesis. As mentioned earlier in chapters 2, 3, and 4, the possible reason for *CUC2's* activity during *de novo* shoot formation is by defines the spatio-temporal regulation of PIN1 localization on the membrane of the shoot progenitor non-cell autonomously and regulates *XTH9* directly to create a dynamic cell wall loosening environment. And form a shell to encapsulate the PIN1-marked cells to guide the cells well to establish a tissue system organization for the successful outgrowth shoot progenitor. In this chapter, we will discuss the importance of *CUC2* during the very early stages of shoot progenitor initiation as well as the regulation of the cell wall loosening enzyme XTH9 and cross-talk between PIN1 during *de novo* shoot regeneration.

5.2 RESULTS

5.2.1 CUC2 activates XTH9 expression during *de novo* shoot regeneration

Consistent with the transcriptome analysis, XTH9 transcripts were reduced in the SIM calli of *cuc2-3* mutant and rapidly upregulated in CUC2 overexpressing line (*p35S::CUC2-GR* in WT*)* upon Dexamethasone induction (Figure 5.2A, 5.2B). Interestingly genome-wide Chromatin Immuno-Precipitation Sequencing (ChIP-Seq) using *pCUC2::CUC2:*vYFP in WT during the onset of progenitor formation revealed that the XTH9 gene has two significant CUC2 binding motifs. A weak motif in exon 1 of *XTH9* and a prominent binding motif in exon 4 of the XTH9 gene (Figure 5.2C). In corroboration with this data, we find

potential cis-regulatory binding sites for NAC domain transcription factors in exon1 and exon4 of *XTH9* (Figure 4D). This suggests the direct activation of *XTH9* transcription by CUC2 (Figure 5.2D) is the underlying cause of the unique spatial expression of XTH9 (Figure 4.3A-4.3K). There are reports of similar scenarios where transcription factors bind to coding exons in vertebrate developmental genes (Ritter et al., 2012). To further investigate the interaction between *XTH9* and CUC2, we decided to monitor the Spatio-temporal expression pattern of CUC2 in a regenerating SIM callus.

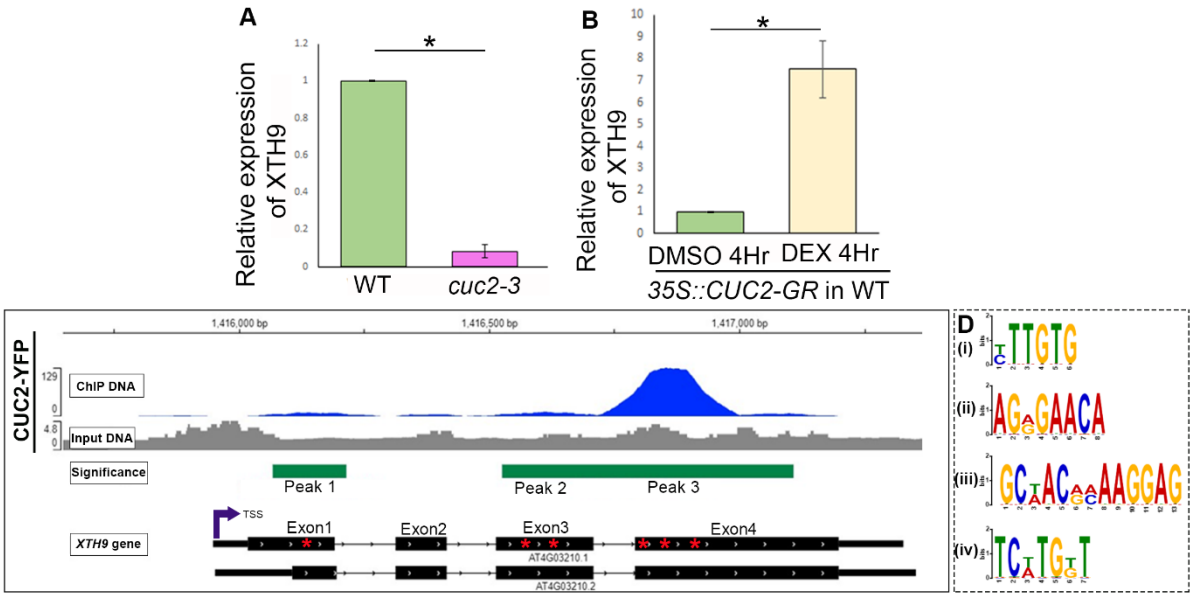

Figure 5.2: CUC2 binds on the cell wall loosening enzyme XTH9 and activates its expression during *de novo* shoot formation.

(A-B) The transcript level of *XTH9* is downregulated in *cuc2-3* mutant (A)(**P*=0.0152, Welch Two Sample t-test) and upregulated in *p35S::gCUC2:GR* upon 4hr Dexamethasone induction at the onset of progenitor formation (8th day SIM) (B)(**P*=0.0198, Welch Two Sample t-test). **(C-D)** Graphical representation of Chromatin Immuno-Precipitation Sequencing (ChIP-Seq) using CUC2-YFP (*pCUC2::gCUC2:vYFP*) shows direct interaction of CUC2 on *XTH9*. A weak motif (Peak1 (blue)) and a prominent motif (Peak2 (blue) reveals the direct regulation of CUC2 on *XTH9* in the DNA pulled-down by anti-GFP antibody (ChIP DNA) in comparison with input DNA (negative control DNA (*pCUC2::gCUC2:vYFP*) without antibody treatment) analyzed using Integrated Genome Viewer. Red asterisks in the representative *XTH9* gene body show the identified CUC2 NAC Domains (C). 4 different NAC domains of CUC2 protein were identified in the exon1, exon3, and exon4 of the *XTH9* gene using MEME and TOM-TOM analysis (D). Error bar in A,B represent s.e.m. from three independent biological replicates. Scale bars: 1mm, n: sample number.

5.2.2 Spatial expression pattern of CUC2 guides the PIN1-marked cells to a shoot meristem

Although the activity of CUC2 was previously reported, it was done using a transcriptional fusion of promoter CUC2 driving 3XVENUS *(pCUC2::3XVENUS:3AT),* which was not tested for complementation (Gordon et al., 2007; Kareem et al., 2015a). Due to this reason, CUC2 was reportedly activated throughout the PIN1-marked progenitors (Gordon et al., 2007). However, it was confounding since our current study found XTH9, which is the downstream target of CUC2, to be confined to the adjacent non-progenitor cells and not within the PIN1-marked progenitor (Figure 4.3A-4.3K). To explain this apparent contradiction, we generated a translational fusion of CUC2 where the native promoter was used to drive the *CUC2* gene with exon and intron *(pCUC2::CUC2-vYFP).* Using the *pCUC2::CUC2-vYFP* (CUC2-YFP), which complemented the *cuc2-3* mutant (WT (n=65), cuc2-3 (n=37), CUC2-YFP in cuc2-3 (n=122)) (Figure 5.3A-5.3D) (see below for shoot regeneration defect), we re-investigated the spatio-temporal expression of CUC2. Strikingly, CUC2-YFP was conspicuously expressed in the adjacent non-progenitor cells but excluded from the PIN1-GFP marked cells of early progenitors (2-celled stage, n=13) (Figure 5.3E), which turned out to be productive. Along the course of their progression, these progenitors expressed CUC2-YFP in a ring-like fashion around the peripheral PIN1-GFP marked cells (Figure 5.3F-5.3L). Upon regeneration into a shoot meristem, we observed expression of CUC2-YFP in the peripheral PIN marked cells and along the meristem boundary, but it remained undetectable in the meristem centre (Figure 5.3K).

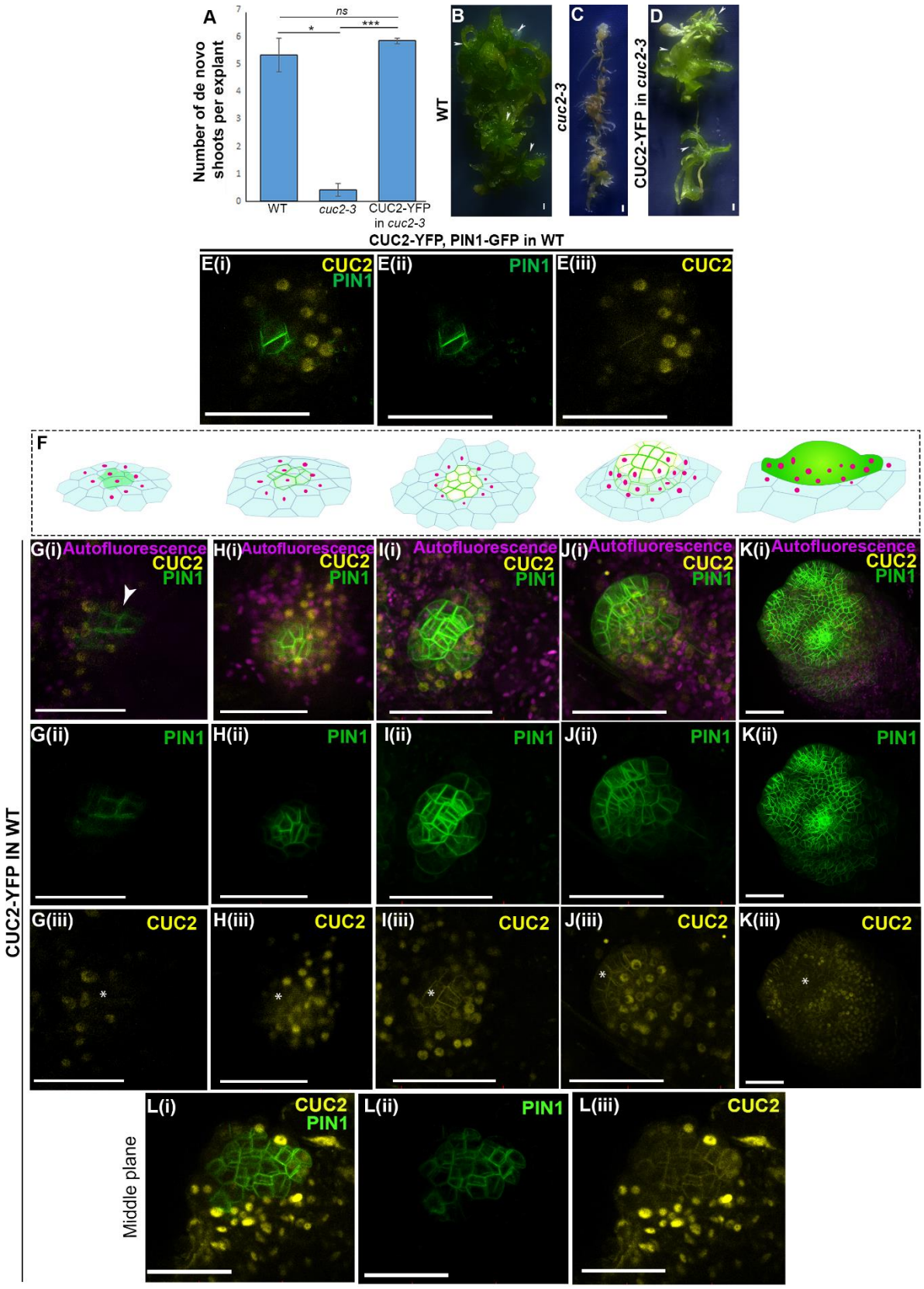
A
Number of de novo shoots per explant
ns
*
***
WT
cuc2-3
CUC2-YFP in cuc2-3
B
WT
C
cuc2-3
D
CUC2-YFP in cuc2-3
CUC2-YFP, PIN1-GFP in WT
E(i) CUC2 PIN1
E(ii) PIN1
E(iii) CUC2
F
CUC2-YFP IN WT
G(i) Autofluorescence CUC2 PIN1
H(i) Autofluorescence CUC2 PIN1
I(i) Autofluorescence CUC2 PIN1
J(i) Autofluorescence CUC2 PIN1
K(i) Autofluorescence CUC2 PIN1
G(ii) PIN1
H(ii) PIN1
I(ii) PIN1
J(ii) PIN1
K(ii) PIN1
G(iii) CUC2
H(iii) CUC2
I(iii) CUC2
J(iii) CUC2
K(iii) CUC2
Middle plane
L(i) CUC2 PIN1
L(ii) PIN1
L(iii) CUC2

Figure 5.3: Exclusion of CUC2 from the shoot progenitor and expression in the surrounding non-progenitor cells governs a functional SAM.

(A) Graph depicting the rescue of the severe shoot regeneration defect in *cuc2-3* mutant by the translational fusion *pCUC2::CUC2-vYFP*(WT vs. *cuc2-3*:**P*=0.01288, *cuc2-3 vs.* CUC2-YFP in *cuc2-3:***P*=0.0002419, WT *vs.* CUC2-YFP in *cuc2-3: *P*=0.5477, Welch Two Sample t-test). **(B-D)** Shoot regeneration was unperturbed in WT calli (n=65) (B) but severely reduced in *cuc2-3* mutant (n=74) (C) but rescued by *pCUC2::CUC2-YFP* (D). **(E)** CUC2-YFP (magenta) is excluded from the PIN1-GFP (green) marked progenitor cells at the 2-3 celled stage (E(ii)) but conspicuously expressed in the surrounding non-progenitor cells(n=14) (E(iii)). **(F)** Schematic depicting the spatial specific expression of CUC2 (magenta) during the progression of PIN1-GFP marked progenitor (green bordered) to shoot meristem. **(G(i)-K(iii))** Representative live images showing the spatio-temporal expression pattern of CUC2-vYFP at different time points of progenitor progression. At the 2-3 celled stage, CUC2 is completely excluded from the PIN1 marked progenitor cells but expressed in the surrounding cells (n=13) (G). At the 30-celled stage(I) and stages thereafter, CUC2-YFP extends to the peripheral PIN1-GFP (green)cells but remains undetectable in the central PIN1-GFP (n=57). White asterisks indicate CUC2-vYFP absence (G(iii), H(iii), I(iii), J(iii), K(iii)). CUC2-YFP (yellow) is excluded from the PIN1-GFP (green) marked progenitor cells at the 2-celled stage but conspicuously expressed in the surrounding non-progenitor cells. **(L)** Representative image showing the middle plane of a progenitor showing that CUC2-YFP is mostly excluded from the PIN1-GFP marked cells, instead form a ring around the progenitor. E(i), E(ii) and E(iii) are the GFP/YFP merge channel, GFP channel, and YFP channel respectively for CUC2-YFP, PIN1-GFP in WT. Merge channel showing both CUC2 and PIN1 (G(i), H(i),I(i), J(i), K(i)). GFP channel showing PIN1-GFP (E(ii), G(ii), H(ii), I(ii), J(ii), K(ii), L(ii)). YFP channel showing CUC2-YFP (E(iii), G(iii), H(iii), I(iii), (Jiii), K(iii), H(Liii). Scale bars: 50µm, 1mm. n: sample number.

Unlike these productive progenitors that had characteristic CUC2-YFP expression pattern, we also came across another set of progenitors that had prominent CUC2-YFP within the PIN1-GFP marked progenitor cells at the 2-celled stage (Figure 5.4A). Such progenitors continued to express CUC2-YFP within the PIN1-marked cells (n=19) and soon got aborted (Figure 5.4B-5.4D), suggesting that they were pseudo-progenitors. These expression studies revealed that, although the PIN1 expression pattern remained invariant in both productive and pseudo-progenitors at the 2-3 celled stage, the spatial expression of CUC2-YFP along with PIN1-GFP can predict the progenitor fate as early as a 2-celled stage. These observations show that both CUC2 and its downstream target XTH9 are expressed in the same spatial domain (Figure 4.3A-4.3I, 4.4D, 5.3E-5.3L, 5.4E-5.4G). Further, the results show that the exclusion of XTH9 and CUC2 expression from the PIN1 marked cells is a pronounced indication of a productive progenitor (Figure 5.4E-5.4G).

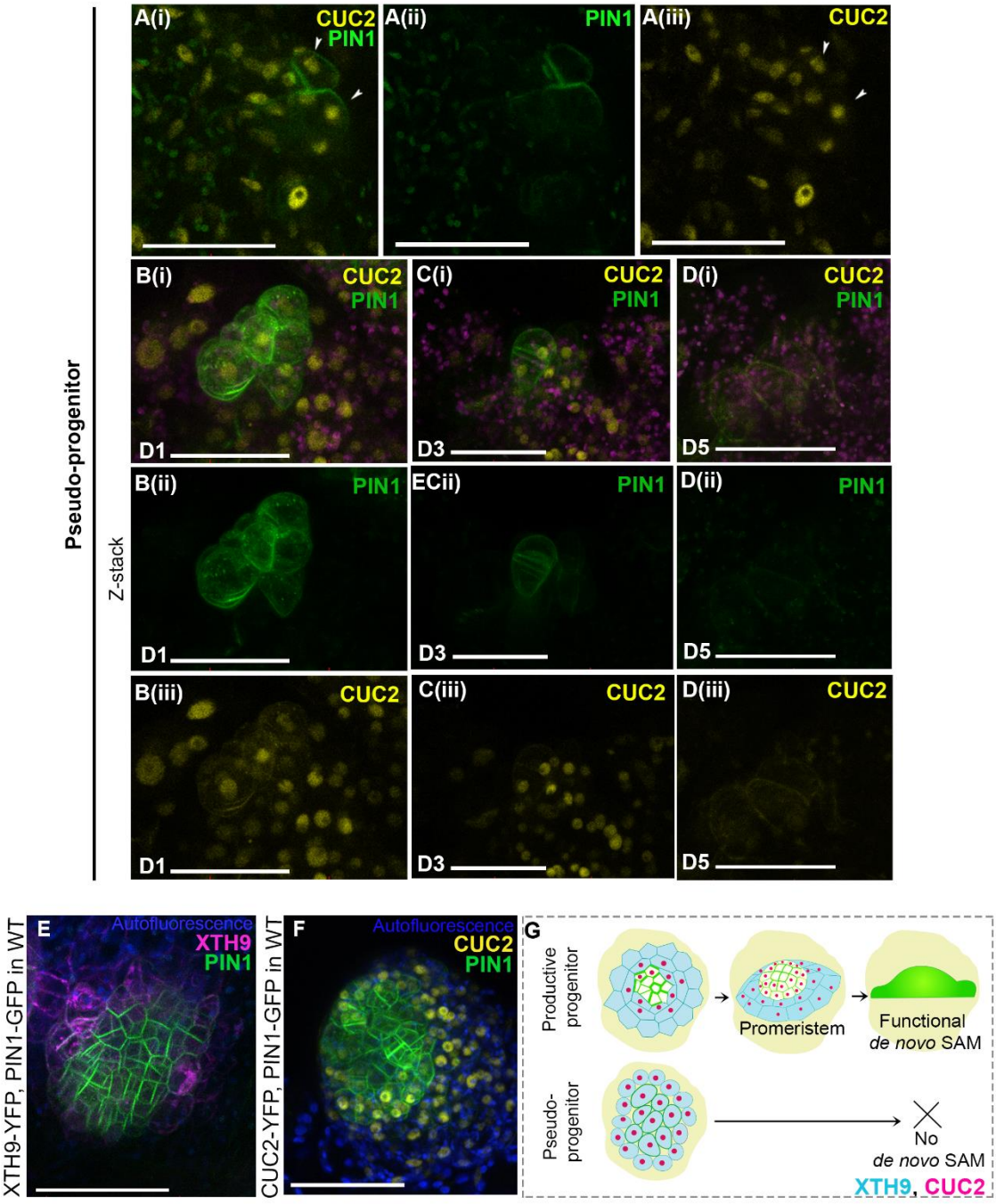

Figure 5.4: CUC2 promotes progenitor progression non-cell autonomously by activating XTH9 in non-progenitor cells.

(A) 2- celled pseudo-progenitor showing CUC2-YFP within the PIN1 marked cells as well as around them. **(B(i)-D(iii))** Representative time-lapse images revealing that pseudo-progenitor shows predominant CUC2-YFP in the PIN1-GFP marked progenitor cells (n=19). Note that the PIN1-GFP and CUC2-YFP vanish progressively, marking the progenitor abortion. **(E-F)** Representative live images showing the Expression pattern of XTH9-YFP (E) and CUC2-YFP (F) around the progenitor. **(G)** Schematic depicting the Spatio-temporal expression pattern of CUC2(red) and its

downstream target XTH9(blue) during shoot meristem formation *de novo* and embryogenesis. In the case of productive progenitors, CUC2 and XTH9 are excluded from the progenitor but robustly expressed in the neighbouring non-progenitor cells. In the pseudo-progenitor, CUC2 and XTH9 intrude into the spatial domain of progenitors. A(i), B(i), C(i), D(i), E,F show GFP/YFP merge channel, A(ii), B(ii), C(ii), D(ii) show GFP channel and A(iii), B(iii), C(iii), D(iii) show YFP channel. Scale bars: 50µm, n: sample number. Magenta represents autofluorescence.

5.2.3 *CUC2* activity is required exclusively in non-progenitor cells for the development of *de novo* SAM

Previous studies in plants and animals have shown that autoregulation of developmentally important regulatory proteins maintains their required constant levels for extended developmental periods (Crews & Pearson, 2009; Durgaprasad et al., 2019). So, we next asked whether *CUC2* maintains its threshold in the regenerating progenitors through auto-activation. To test our hypothesis, we examined the transcript level of endogenous *CUC2* upon its inducible overexpression (*35S::CUC2-GR* in WT). Our data shows that CUC2 indeed auto-activates its own expression (within 4Hr and 8Hr), and the auto-activation is reflected in the ChIP-Seq of CUC2 showing CUC2 binds on the *CUC2 gene* (Figure 5.5A-5.5C). Previous studies have reported that *CUC2* enhances *de novo* shoot regeneration (Daimon et al., 2003; Kareem et al., 2015a). We overloaded CUC2 in the callus throughout the SIM incubation (using *35S::CUC2-GR* in WT) to check the shoot formation efficiency. Surprisingly the *de novo* shoot formation is impaired when we overloaded the callus with CUC2, suggesting that it could indeed maintain its threshold level during *de novo* shoot regeneration (Figure 5.5D-5.5F).

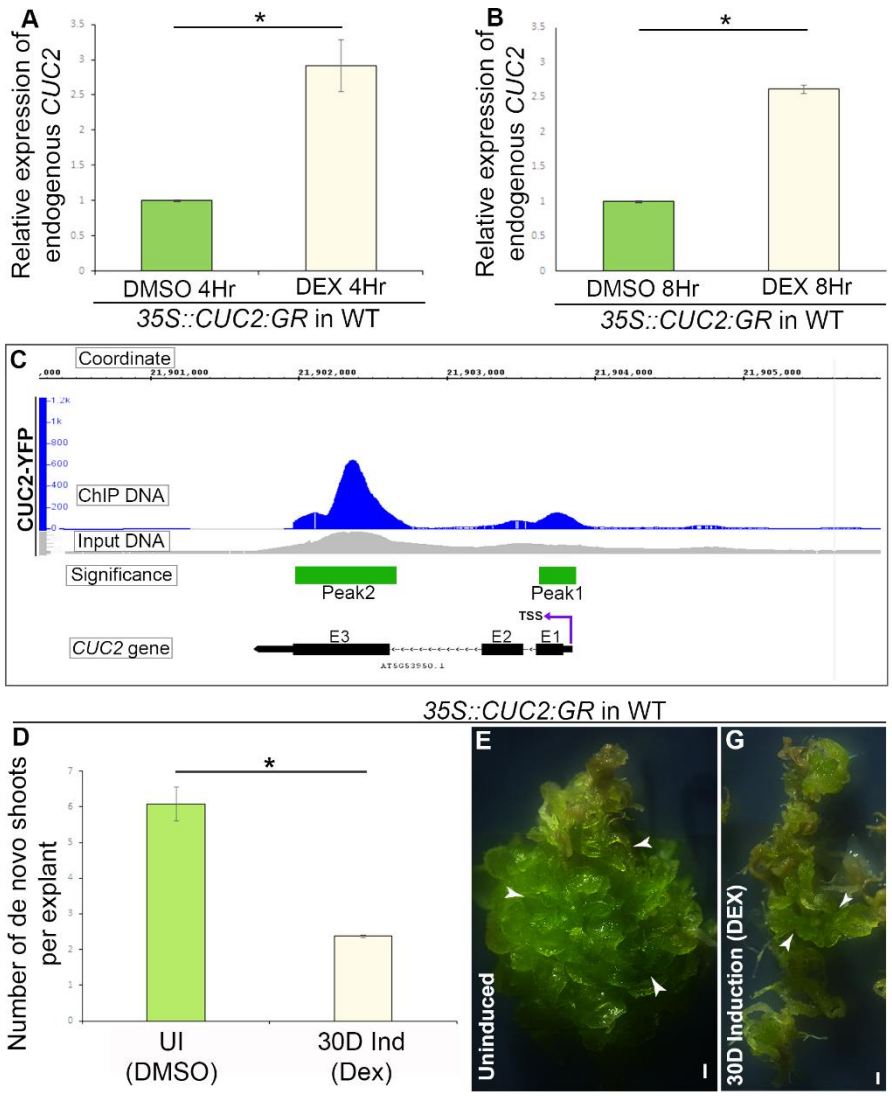

Figure 5.5: Threshold level of CUC2 should be maintained during *de novo* shoot regeneration.

(A-B) The graphs depict the increased relative transcript level of endogenous *CUC2* upon overexpression of CUC2 (*35S::CUC2-GR* in WT) for 4Hr and 8Hr using dexamethasone. Upregulation of endogenous *CUC2* transcript after 4hr (A) *(*P= 0.01226, Welch Two Sample t-test*)and 8hr induction (B) (**P=0.02371, Welch Two Sample t-test*) in comparison to mock induction (DMSO). Error bar represents s.e.m. from three independent biological replicates. **(C)** Graphical plot of ChIP-Seq showing the autoregulation of CUC2 (CUC2 Protein binds its own gene) (Blue: represents the pull-down of CUC2 (ChIP DNA) using an anti-GFP antibody against CUC2-YFP; Grey: represents the Input DNA (without antibody treatment); Green: represents the significance of the peak of ChIP DNA in comparison with Input; Black: represents the *CUC2* gene). **(D-F)** The graph shows the reduction in shoot regeneration when overloading the CUC2 in the callus compared to its mock (DMSO) *(* DMSO, n=65;30D DEX,n= 51*; *P= 0.01226, Welch Two Sample t-test*). Stereo images showing the reduced shoot formation *de novo* by inducing CUC2 (using Dex) throughout the SIM incubation (F) compared to Uninduced mock control (DMSO) (E). Error bar in A,B represent s.e.m. from three independent biological replicates. Scale bars: 1mm, n: sample number.

We next asked if shoot regeneration *de novo* necessitates *CUC2* activity exclusively outside the progenitor. Toward this, we generated a translational fusion where the *WUS* promoter drives *CUC2* (*pWUS::CUC2-vYFP:tWUS*). We used a 5.7kb long promoter of *WUS*, which limits the WUS activity to PIN1-marked cells in the mature meristem (T.-Q. Zhang et al., 2017). Misexpression of *CUC2* within the progenitor indeed reduced the shoot regeneration dramatically (*pWUS::CUC2- vYFP;tWUS* in WT(n=136), WT (n=69)) (Figure 5.6A-5.6C). This was further reflected during live imaging using *pPIN1::PIN1-GFP*, *pWUS::CUC2-vYFP:tWUS*, where the number of PIN1-marked progenitors spotted was extremely low. The progenitors spotted with CUC2-YFP within the PIN1 marked cells showed a dramatic phenotype with severely impaired PIN1-GFP localization pattern even as early as the 2-celled stage (n=5) (Figure 5.6D-5.6E) or as late as the 40-celled stage (n=13) (Figure 5.6F-5.6G). Such progenitors soon underwent an abortion, as marked by the disappearance of PIN1-GFP and CUC2-YFP (Figures 5.6E, 5.6G). Thus, both the expression and misexpression studies indicate the necessity of CUC2 activity strictly outside the progenitor, very much like XTH9 (Figure 5.4A-5.4D, 5.6A-5.6H, add figure from chapter 4).

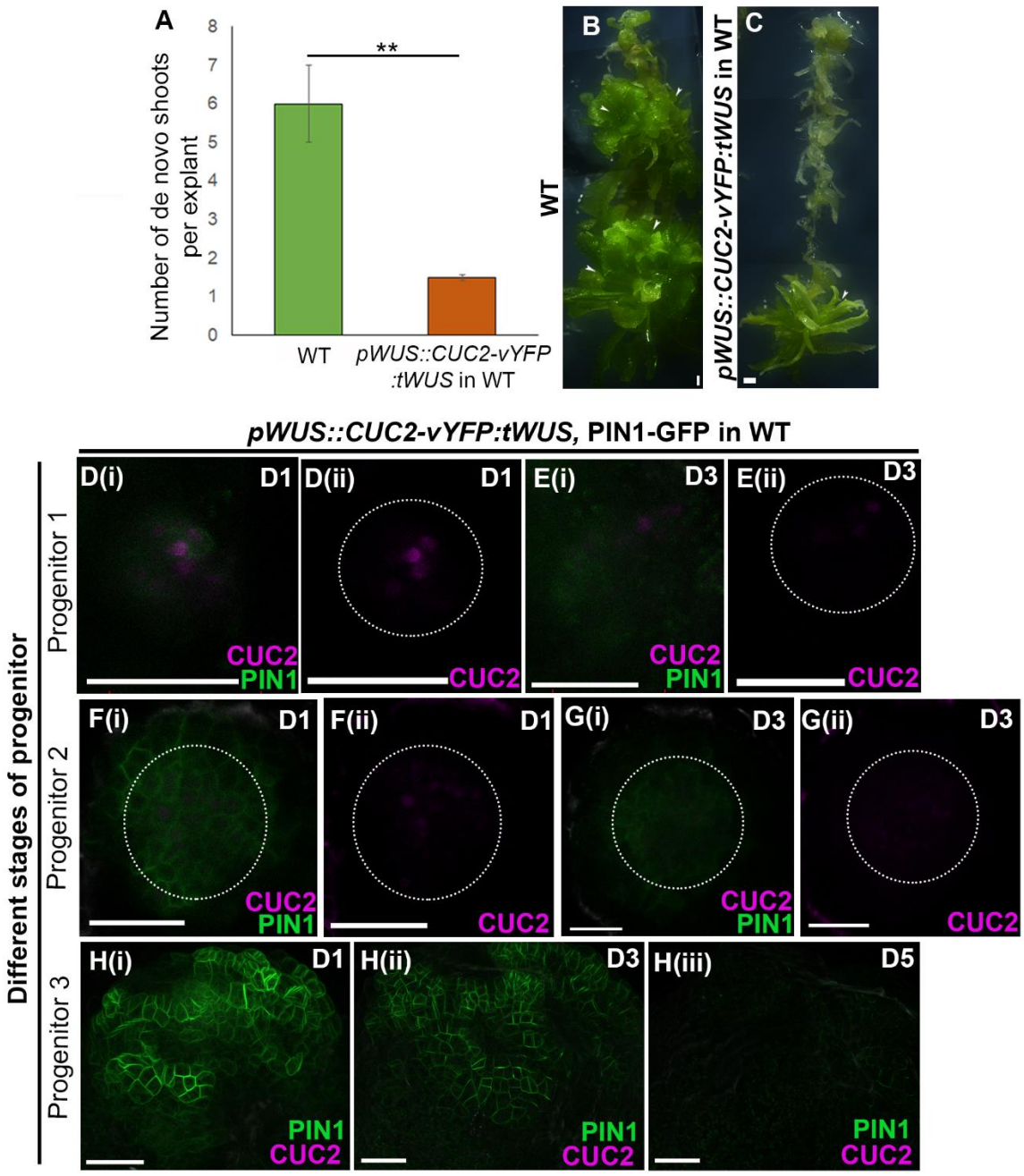

Figure 5.6: *CUC2* is essential for *de novo* shoot organogenesis and promotes the meristem formation non-cell autonomously.

(A-C) Misexpression of *CUC2* within the progenitor under the *WUS* promoter using *pWUS::CUC2-vYFP;tWUS* in WT(n=136) drastically reduced shoot regeneration (***P*=0.004244, Welch Two Sample t-test) compared to wildtype(n=69). **(D-H)** Representative real-time live images showing that ectopic expression of CUC2(magenta) within PIN1-GFP (green) marked progenitors of the 2-celled stage (n=5)(D(i)-E(ii)) or 60-celled stage (n=13) (F(ii)-G(ii)), causes delocalization and disappearance of PIN1-GFP, loss of compact packing of progenitors and abolishes progenitor progression to shoot meristem by 3rd day of progenitor spotting (D(i)-H(ii)). A White dotted circle indicates the region of CUC2 (Magenta) expression. (D(i), E(i), F(i), G(i), H(i)) shows the YFP/GFP

merge channel, and (D(ii), E(ii), F(ii), G(ii) shows the YFP channel respectively *pWUS::CUC2-vYFP;tWUS, pPIN1:gPIN1-GFP* in WT. Scale bars: 50μm (F-J), 1mm (D,E), n=sample number. Error bars represent s.e.m.

5.2.4 Modulation of CUC2 collapse the successful development of a shoot from shoot progenitor

In striking contrast, the *cuc2-3* mutant callus scarcely produced progenitors, the majority of which were non-meristem forming and resembling pseudo-progenitors, as evident from aberrant PIN1-GFP localization (Figure 5.7A,5.7B) (Anju PS, Varapparambath et al., 2022) indicating CUC2 to be crucial during *de novo* shoot regeneration. The severe reduction in shoot regeneration in the *cuc2-3* mutant (n = 70) compared to the WT (n = 68) further reflects the necessity of CUC2 in *de novo* shoot regeneration (Figure 5.7C-5.7D). Moreover, we downregulated CUC2 in an inducible fashion using pG1090:CUC2-dsRNAi in WT throughout its incubation period in SIM (30 days) (uninduced (n=114), induced (n=109)) and found a dramatic reduction in shoot regeneration (Figure 5.7F-5.7H). Corroborating these results, the inducible genome editing (IGE)-based knockout of CUC2 (*pG1090:XVE::Cas9p-tagRFP-CUC2 in pCUC2::CUC2-vYFP/WT*) (Figure 5.7I,5.7L) throughout the SIM incubation period (0-30days SIM) (n=95) or for 48Hr during the onset of progenitor formation (n=102) also led to a severe reduction in shoot regeneration compared to uninduced (n=166) (Figure 5.7O-5.7R). Note that the dead Cas9 activity did not perturb the shoot formation *de novo* (Figure 5.7J,5.7M-5.7O,5.7S-5.7U). These observations confirm the necessity and demonstrate the temporal specificity of CUC2 during shoot regeneration *de novo.*

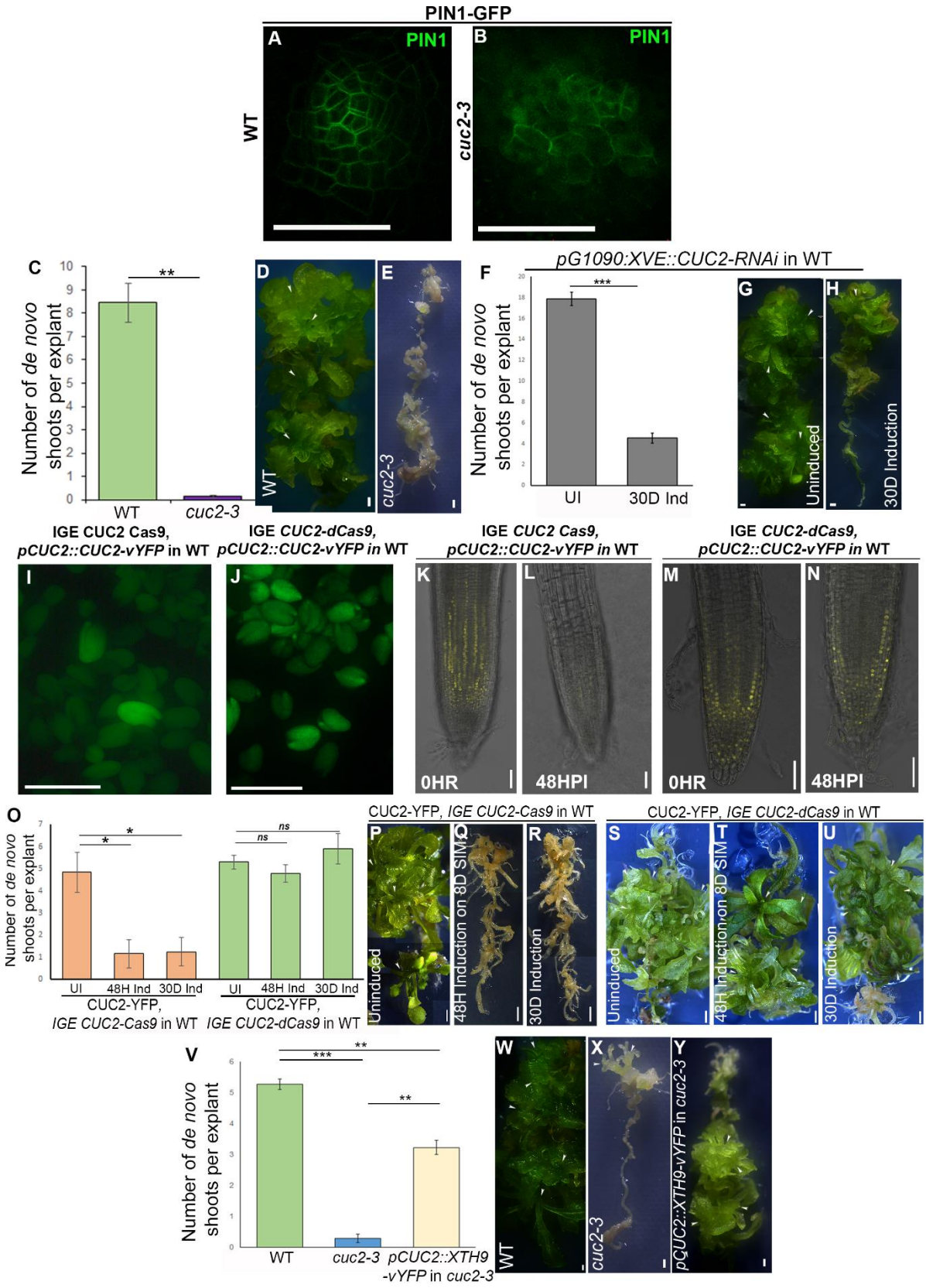

Figure 5.7: *CUC2* is essential for *de novo* shoot meristem formation.

(A-B) Representative confocal image of WT and *cuc2-3* mutant showing the PIN1polarization pattern in the progenitors. PIN1 is sharply polarized on the membrane of the progenitor in the WT (A), whereas PIN1 is delocalized and could observe in the cytoplasm in the *cuc2-3* mutant (B). **(C-E)** Shoot regeneration is severely reduced in *cuc2-3* mutant. Graph depicting severe reduction in shoot regeneration in *cuc2-3* mutant(n=70) in comparison to WT (n=68) (C). Stereo-image of WT callus (D), *cuc2-3* mutant callus (E) showing shoot regeneration. **(F-H)** Inducible downregulation of CUC2 is detrimental to shoot regeneration. Graph depicting the severe reduction in shoot regeneration upon continuous downregulation of CUC2 using *pG1090:XVE::CUC2-RNAi* in an inducible fashion throughout the incubation on SIM (0-30th day SIM)(F)(****P*=0.0006526, Welch Two Sample t-test, n=114(uninduced), 109(induced)). Stereo images show that shoot regeneration is unperturbed in uninduced calli of *pG109:;XVE::CUC2-RNAi* (G) but severely reduced in induced calli of *pG1090:XVE::CUC2-RNAi* (H). **(I-J)** Non-destructive fluorescent tagged transformed seeds containing pFG7m34GW destination vector with gOLE-GFP in *pG1090:XVE::Cas9-CUC2 sgRNA* cassettes (IGE CUC2-Cas9) in *pCUC2::gCUC2:vYFP* in WT (I) and IGE CUC2-dCAS9 in *pCUC2::gCUC2:vYFP* in WT (J) were generated for this study. **(K-L)** Confocal image showing expression of CUC2-YFP in the root tip of *pG1090:XVE::Cas9-CUC2 sgRNA* cassettes in *pCUC2::gCUC2:vYFP* in WT at 0hr induction (K). 48hr Cas9 induction using 5μM estradiol resulted in a loss of CUC2-YFP from the root tip (L). **(M-N)** But, 48hr induction using 5μM estradiol, dCas9 did not change any expression in CUC2-YFP. **(O-U)** Graph depicting that inducible gene knockout of CUC2 in *pCUC2::gCUC2::vYFP, IGE CUC2-Cas9* in WT (*pG1090:XVE::Cas9TagRFP-CUC2 sgRNA* cassettes in CUC2-YFP; WT) by transient induction for 48Hr (8th Day SIM) or by sustained induction throughout the SIM incubation (0-30 days) dramatically reduced shoot regeneration compared to uninduced(IGE CUC2-Cas9:-UI:n=166; 48HI:n=102, *P=0.03359, Welch Two Sample t-test; CI: n=95,*P=0.03986, Welch Two Sample t-test). The shoot regeneration in pCUC2::gCUC2::vYFP, IGE CUC2-dCas9 in WT (pG1090:XVE::dCas9t35S-CUC2 sgRNA cassettes in CUC2-YFP; WT) remains comparable to uninduced, even after induction of dCas9 for 48hr on 8th Day SIM or throughout the SIM incubation period (0-30 days) (O) (IGE CUC2-dCas9:-UI:n=115; 48HI:n=86, *P=0.03359, Welch Two Sample t-test; CI: n=109,*P=0.03986, Welch Two Sample t-test). Stereo-image showing shoot regeneration in an uninduced callus of IGE-CUC2-Cas9 (P) upon 48Hr induction of IGE-CUC2-Cas9 on 8th day SIM (Q), upon sustained induction of IGE-CUC2-Cas9 throughout the SIM incubation(0-30days) (R), uninduced callus of IGE-CUC2-dCas9 (S) upon 48Hr induction of IGE-CUC2-dCas9 on 8th day SIM (T), upon sustained induction of IGE-CUC2-dCas9 throughout the SIM incubation(0-30days)(U). **(V-Y)** The shoot regeneration defect in *cuc2-3* mutant with respect to WT is partially rescued by *pCUC2::XTH9-vYFP* in *cuc2-3* (WT vs *cuc2-3*:****P*=0.000142, *cuc2-3 vs pCUC2::XTH9-vYFP* in *cuc2-3*:***P*=0.001021, WT vs *pCUC2::XTH9-vYFP* in *cuc2-3* ***P*=0.009069,Welch Two Sample t-test) (*cuc2-3* (n=66), *pCUC2::XTH9-vYFP* in *cuc2-3*(n=60), WT (n=45))(U). Stereo image of WT callus (W), *cuc2-3*mutant callus (X), *pCUC2::XTH9-vYFP* in *cuc2-3* (Y) showing shoot regeneration. White arrowheads indicate regenerated shoots. Scale bars: 50μm (A,B,K-N), 1mm (D,E,G-J,P-U,W-Y), n=sample number. Error bars represent s.e.m.

We next examined the functional relevance of *CUC2*-mediated regulation of *XTH9*. If *XTH9* is indeed a downstream target of CUC2, we hypothesized that *XTH9* activity in the *CUC2* expression domain might rescue the shoot regeneration defects in the *cuc2-3* mutant callus (Figure 5.6A-5.6C). Towards this, we expressed *XTH9* under the *CUC2* promoter in the *cuc2-3* mutant (*pCUC2::XTH9-vYFP in cuc2-3).* Remarkably, *pCUC2::XTH9-*

vYFP partially rescued the shoot regeneration in *cuc2-3* (n=60), implicating that CUC2 acts through XTH9 to promote meristem formation (Figure 5.6U-5.6Y). Through all these expressions and functional studies, we demonstrate that CUC2 and CUC2-mediated XTH9 regulation confer the productive fate to regenerating progenitors by acting non-cell autonomously from the neighbouring non-progenitor cells (Figure 4.3A-4.3K, 5.3E-53L, 5.7U-5.7Y, 5.6D-5.6H). We then probed the sufficiency of CUC2 by forcing its ectopic expression under the PIN1 promoter (*pPIN1:CUC2-vYFP* in WT). It is important to note that, unlike *pPIN1:PIN1-GFP*, which recapitulates the endogenous PIN1 expression pattern, *pPIN1:CUC2-vYFP* does not follow the same expression pattern as that of PIN1-GFP. Instead, we found that the *PIN1* promoter drove *CUC2* in the endogenous *CUC2* expression domain in the root (Figure 5.8A-5.8F) and in the non-progenitor cells in the callus (Figure 5.8G-5.8I). Such ectopic expression of *CUC2* in WT callus increased the number of meristems by triggering self-organization of PIN1, indicating the sufficiency of CUC2 function in this process (Figure 5.8J-5.8L). These findings demonstrate that *CUC2* and *CUC2*-mediated *XTH9* regulation confer the productive fate to regenerating progenitors by acting non-cell autonomously from the neighbouring non-progenitor cells (Figure 54E-5.4G).

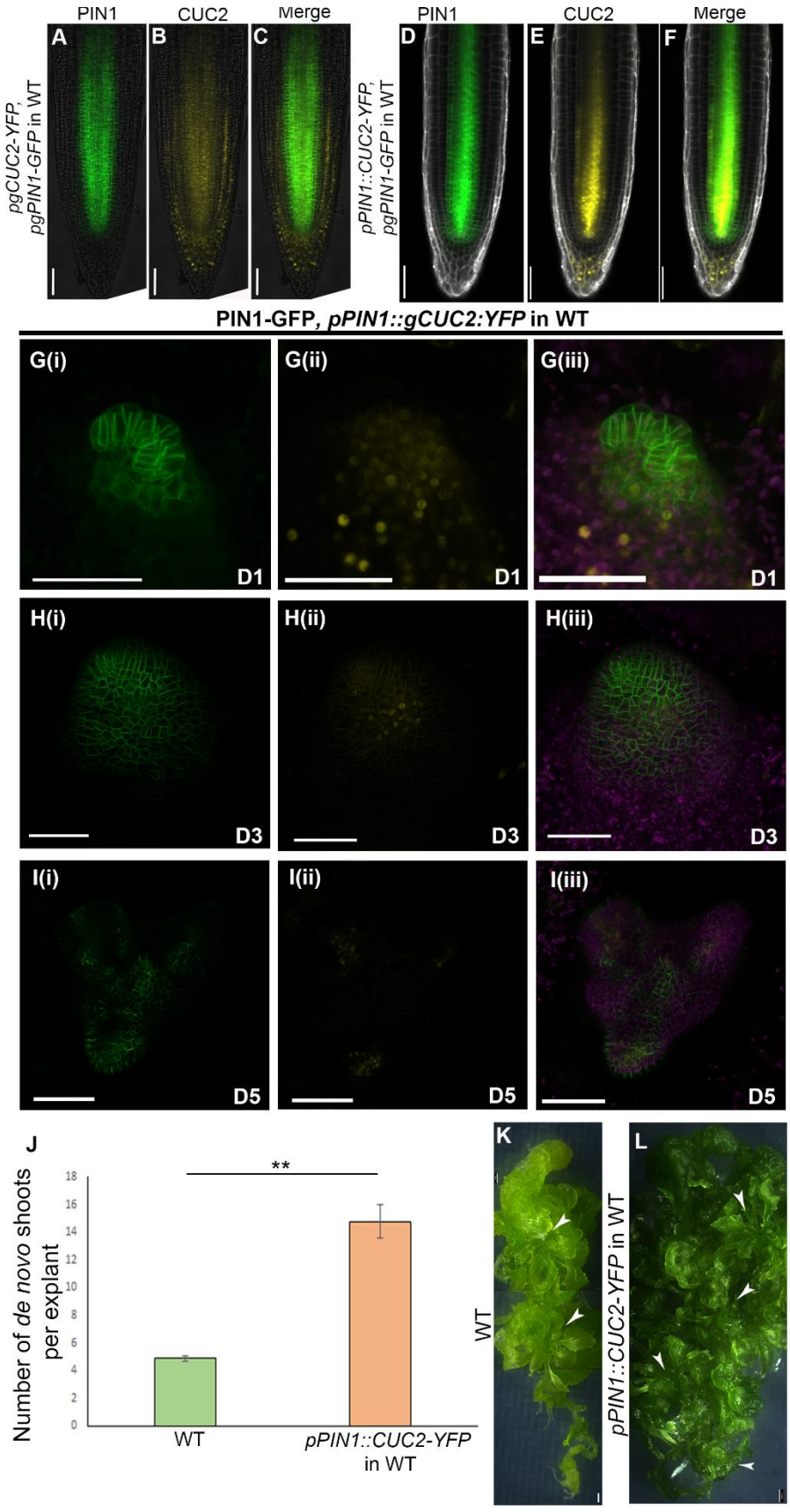
PIN1
CUC2
Merge
A
B
C
pgCUC2-YFP, pgPIN1-GFP in WT
D
E
F
pPIN1::CUC2-YFP, pgPIN1-GFP in WT
PIN1-GFP, pPIN1::gCUC2:YFP in WT
G(i)
G(ii)
G(iii)
D1
H(i)
H(ii)
H(iii)
D3
I(i)
I(ii)
I(iii)
D5
J
Number of de novo shoots per explant
**
WT
pPIN1::CUC2-YFP in WT
K
L
WT
pPIN1::CUC2-YFP in WT

Figure 5.8: Ectopic expression of CUC2 triggers self-organization of PIN1 and meristem formation indicating the sufficiency of CUC2 during shoot regeneration.

(A-C) Expression of CUC2-YFP (yellow) under its native promoter (B). **(D-F)** Expression of CUC2-YFP (yellow) under PIN1 promoter (E). PIN1 promoter alone drives the transgene in a domain other than endogenous PIN1 expression. **(G-I)** Live imaging of *pPIN1::CUC2-YFP* in WT reveals that CUC2-YFP (yellow)is excluded from the central PIN1-GFP (green) marked progenitor cells. PIN1 promoter alone drives the transgene in a domain other than endogenous PIN1 expression. **(J-L)** Ectopic CUC2 expression under the PIN1 promoter in *pPIN1::CUC2-YFP* in WT increases the shoot regeneration. Graph depicting increased shoot regeneration upon ectopic CUC2 expression (J), WT callus showing normal shoot regeneration (n=153) (K) *pPIN1::CUC2-YFP* callus (n=389) showing increased shoot regeneration (**P=0.004244, Welch Two Sample t-test). C, F, G(i), H(i), I(i), J(i)) show the YFP/GFP merge channel, A, D, G(i), H(i), I(i) shows the GFP channel and B,E, G(ii), H(ii), I(ii) show the YFP channel. Scale bars: 50µm (A-I), 1mm (K,L).

5.2.5 Cell wall modification and cell polarity in the regenerating foci act in a regulatory feedback loop to make the dome-shaped shoot meristem *de novo*.

Our functional studies on *CUC2*, *XTH9*, *PID*, and *PIN1* further corroborate the notion of coordination between the progenitor and the surrounding non-progenitor cells. We found that perturbing the shell either by downregulating *XTH9*, loss of function of *XTH9*, inducible downregulation of *CUC2*, or loss of function of *CUC2* (*cuc2-3* mutant) aborts the progenitor progression (Figure 4.5A-4.5G, 4.5Q-4.5W, 4.6A-4.6G, 5.7A-5.7F, 5.7N-5.7T). Likewise, impairing the localization pattern of PIN1-GFP using *pid,wag1,wag2* mutant, or loss of function of PIN1 activity using *pin1,pin3,pin4,pin7* mutant, resulted in downregulation of *CUC2* and *XTH9* (Figure 2.6O, 5.9A, 5.9E). We further show that disrupting the PIN1 localization pattern led to the loss of spatial specific expression of CUC2-YFP and XTH9-YFP as observed by their intrusion into the spatial domain of PIN1 marked progenitor cells in *pid,wag1,wag2* mutant (Figure 5.9B-5.9D, 5.9F-5.9G). Thus, consequences of genetic perturbations either to the progenitor or non-progenitor cells feedback on each other resulting in progenitors with disrupted PIN1 localization incapable of progressing to meristem (Figure 4.5A-4.5G, 4.5Q-4.5W, 4.6A-4.6G, 5.7A-5.7F, 5.7N-5.7T, 5.9A-5.9G). These findings reinforce the necessity of a feedback regulatory interaction between the progenitor and surrounding non-progenitor cells for making a shoot meristem.

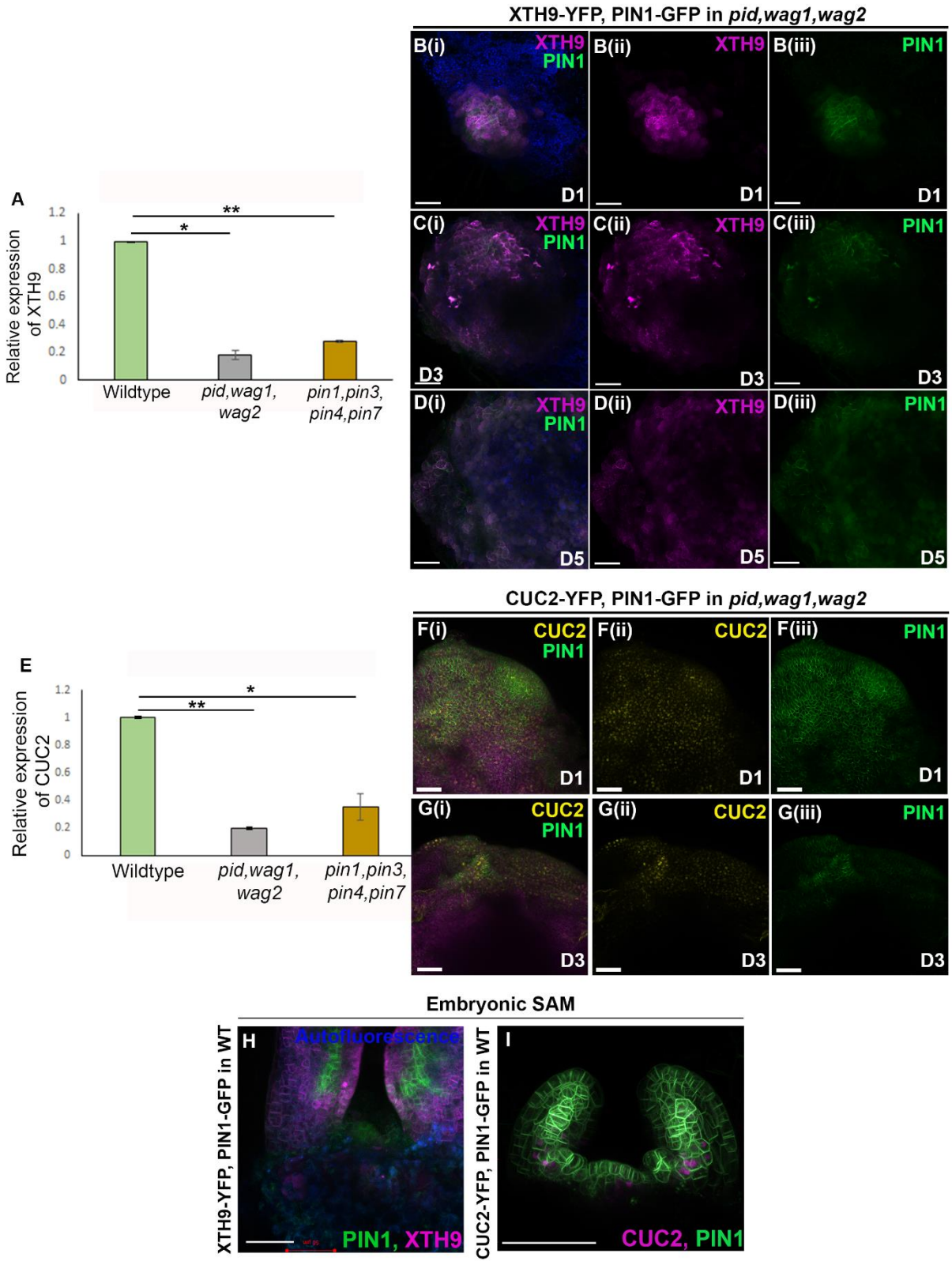
XTH9-YFP, PIN1-GFP in pid,wag1,wag2
A
Relative expression of XTH9
1.2
1
0.8
0.6
0.4
0.2
0
**
*
Wildtype
pid,wag1, wag2
pin1,pin3, pin4,pin7
B(i) XTH9 PIN1 D1
B(ii) XTH9 D1
B(iii) PIN1 D1
C(i) XTH9 PIN1 D3
C(ii) XTH9 D3
C(iii) PIN1 D3
D(i) XTH9 PIN1 D5
D(ii) XTH9 D5
D(iii) PIN1 D5
CUC2-YFP, PIN1-GFP in pid,wag1,wag2
E
Relative expression of CUC2
1.2
1
0.8
0.6
0.4
0.2
0
*
**
Wildtype
pid,wag1, wag2
pin1,pin3, pin4,pin7
F(i) CUC2 PIN1 D1
F(ii) CUC2 D1
F(iii) PIN1 D1
G(i) CUC2 PIN1 D3
G(ii) CUC2 D3
G(iii) PIN1 D3
Embryonic SAM
XTH9-YFP, PIN1-GFP in WT
H
Autofluorescence
PIN1, XTH9
CUC2-YFP, PIN1-GFP in WT
I
CUC2, PIN1

Figure 5.9: Feedback loop of *CUC2-XTH9-PIN1* module instrument the progenitor to a shoot meristem patterning.

(A) Graph depicting the downregulation of *XTH9* transcript level in *pid1,wag1,wag2* and *pin1,pin3,pin4,pin7* mutant in comparison to wildtype (WT vs *pid1,wag1,wag2*:**P*=0.02648, WT vs *pin1,pin3,pin4,pin7* ***P*= 0.006627,Welch Two Sample t-test). **(B-D)** Representative time-lapse images showing that the XTH9 expression intruded into the spatial domain of PIN1-GFP marked cells of 30-40 celled progenitor of *pid1,wag1,wag2* callus containing XTH9-YFP, PIN1-GFP(B(i)-B(iii)). Such progenitors abort their progression to shoot meristem as indicated by the disappearance of PIN1 GFP (D). (B(i),C(i),D(i))shows GFP/YFP merged channel, (B(ii), C(ii), D(ii)) shows YFP channel, and (B(iii), C(iii), D(iii)) shows GFP channel for XTH9-YFP, PIN1-GFP in *pid1,wag1,wag2* **(E)** The transcript level of *CUC2* which is a positive regulator of *XTH9* is downregulated in *pid1,wag1,wag2* and *pin1,pin3,pin4,pin7* mutants in comparison to wildtype (WT vs *pid1,wag1,wag2*: ***P*=0.002375, WT vs *pin1,pin3,pin4,pin7* **P*= 0.02357,Welch Two Sample t-test). **(F-G)** Representative time-lapse images showing that in the progenitors of *pid,wag1,wag2* callus, CUC2-YFP was found within the PIN1-GFP marked cells ((F(i), F(iii)), and such structures failed to make shoot meristem. (F(iii), G(iii)) shows GFP channel, (F(ii), G(ii)) shows YFP channel, and (F(i), G(i)) shows YFP/GFP merged channel for CUC2-YFP, PIN1-GFP in *pid1,wag1,wag2.* (H) Expression pattern of XTH9-YFP (magenta) in embryonic SAM. (I) Expression pattern of CUC2-YFP (magenta) in embryonic SAM. B(i), C(i), D(i), F(i), G(i), H,I show the YFP/GFP merge channel, . B(ii), C(ii), D(ii), F(ii), G(ii) show the YFP channel and . B(iii), C(iii), D(iii), F(iii), G(iii) show the GFP channel. Scale bars: 50µm (B-I), n=sample number. Error bars represent s.e.m.

5.2.6 Redundant activation of the *CUC* gene during *de novo* shoot regeneration

Previous studies have reported that other *CUC* genes influence *de novo* shoot regeneration (Daimon et al., 2003; Kareem et al., 2015a). As I mentioned earlier, *CUC* genes act redundantly in normal development. We examined whether such redundancy is acting during *de novo* shoot regeneration. We could observe that shoot formation is reduced in the *cuc1-5* single mutant compared to the wildtype (Figure 5.10A-5.10C). At the same time, the mutation in the *CUC2* itself (*cuc2-3*) can drastically affect the shoot regeneration and shows significant reduction compared to the *cuc1-5* single mutant (Figure 5.10A-5.10D). Next, we asked whether these two gene acts synergistically. Surprisingly, the *cuc1-5,cuc2-3* double mutant makes more shoots compared to the *cuc2-3* single mutant, but comparable to the *cuc1-5* single mutant (Figure 5.10A,5.10C-5.10E). This puzzled us, so we expected it could be the third member, *CUC3*, regulating *de novo* shoot regeneration in the absence of these two *CUC*s. To address this hypothesis, we generated an inducible knockdown of *CUC3* in the *cuc1-5,cuc2-3* double mutant (*pG1090:XVE::CUC3 dsRNAi* in *cuc1-5,cuc2-3*). We find that altering *CUC3* transcript level throughout the SIM using estradiol impaired shoot formation in the *cuc1-5,cuc2-3 compared to uninduced mutant* (Figure 5.10F-5.10H).

Suggesting that the *CUC2* gene has a significant role in *de novo* shoot regeneration compared to other redundant *CUC*. However, in the absence of *CUC1* or *CUC2*, *CUC3* can compensate for the vacancy of other *CUC*s and participate in organ regeneration.

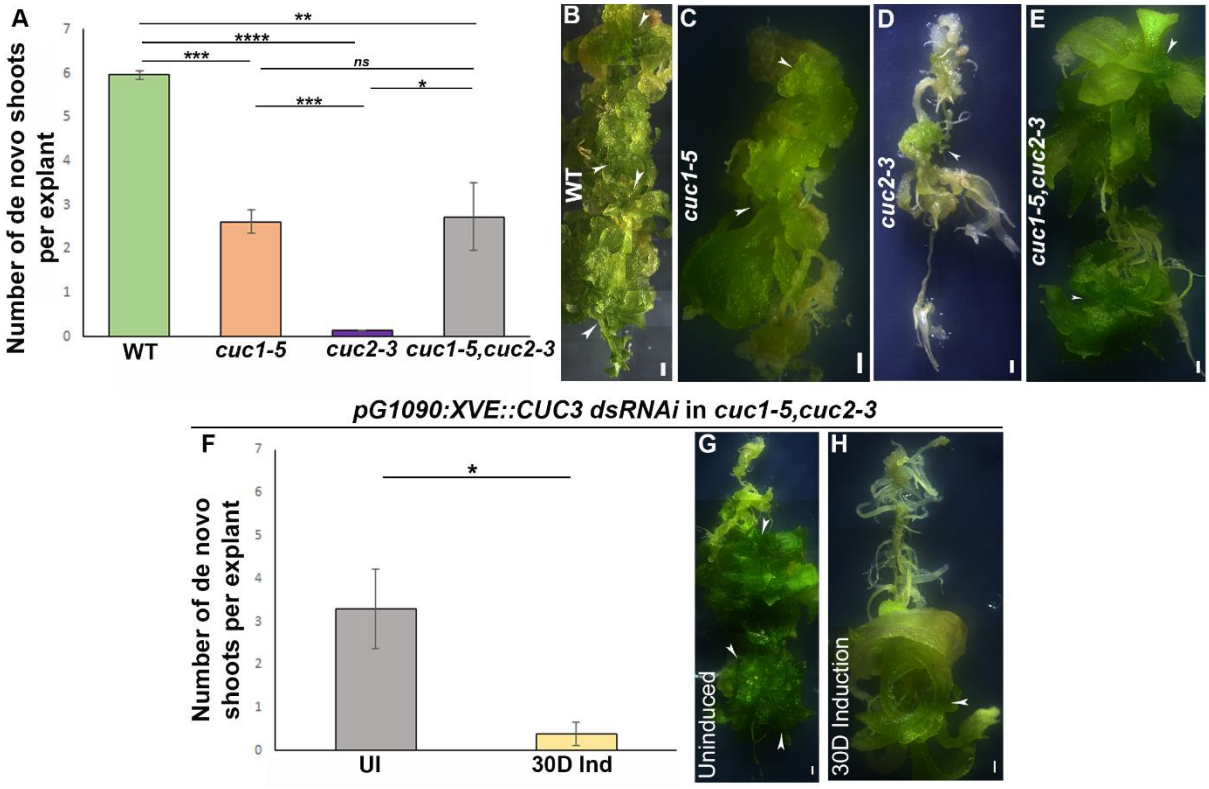

Figure 5.10: Functional redundancy of *CUC* gene in *de novo* shoot regeneration.

(A-E) Graph depicting the involvement of all *CUC* genes for shoot formation *de novo* ((wildtype:n=48, *cuc1-5*:n=66; *cuc2-3*:n=45; *cuc1-5,cuc2-3*:n=59); WT Vs. *cuc1-5* single mutant, ****P=0.0001*; WT Vs. *cuc2-3* single mutant, *****P=0.00001;* WT Vs. cuc1-5,*cuc2-3* double mutant, ***P=0.0073; cuc1-5* Vs. *cuc2-3* single mutant, ****P=0.0004*; *cuc2-3* single Vs. cuc1-5,*cuc2-3* double mutant, **P=0.0159*; *cuc1-5* single Vs. cuc1-5,*cuc2-3* double mutant, *ns=0.8634*; Unpaired t-test) (A) representative stereo-images show the shoot regeneration in WT (B), *cuc1-5* single mutant (C), *cuc2-3* single mutant (D) and cuc1-5,*cuc2-3* double mutant (E). **(F-H)** Graphical elucidation of shoot regeneration in *pG1090:XVE::CUC3 dsRNAi* in *cuc1-5,cuc2-3* shows that the shoot formation is reduced in estradiol-induced medium to downregulate *CUC3* transcript level compared to uninduced *(UI:n=23.5, I:n=18, *P=0.0109;* Unpaired t-test*) (F).* Stereo images showing the shoot formation in uninduced (G) and induced (H) of *pG1090:XVE::CUC3 dsRNAi* in *cuc1-5,cuc2-3*. Scale bars: 1mm (B-E, G,H), n=sample number. Error bars represent s.e.m.

5.3 DISCUSSION

The mechanical conflict between two types of juxtaposed cells was caused by the biochemical patterning of the *CUC2-XTH9* regulatory axis, thereby resulting in the recruitment of PIN1 on the membrane (Figure 5.7A, 5.5B). The feedback loop between the biochemical and mechanical field is necessary for shoot regeneration but dispensable for pre-patterned SAM formation during normal development (see Chapter 4). Once the *de novo* meristem is established, it behaves similarly to a pre-patterned SAM in terms of the expression of regulators tested in this study (Figure 5.8H, 5.8I). Feedback between dividing shoot progenitor and loosening surrounding cells is needed for the initial specification and self-organization of progenitors in *de novo* shoot regeneration (Figure 4.3A-4.3K). Our study demonstrates that cell polarity and cell wall mechanics are necessary for making the meristem itself *de novo*.

The process of shoot formation from a regenerating foci during shoot regeneration from calli is a complex and highly regulated process that involves the interplay of multiple factors. *CUC2*, *PIN1*, and *XTH9* have all been identified as key players in this process. Shoot-promoting factor *CUC2* plays a critical role in establishing the spatio-temporal regulation of PIN1 localization on the membrane of the shoot progenitor in a non-cell autonomous manner for the proper outgrowth of shoot progenitor (Figure 2.5A-N, 2.6A-2.6O4.5A-4.5G, 4.5Q-4.5W, 4.6A-4.6G, 5.6A-5.6F, 5.6N-5.6T, 5.8A-5.8G). In addition to this, *CUC2* directly regulates the expression of *XTH9*, a cell wall-loosening enzyme for the emergence of shoots during *de novo* shoot organogenesis (Figure 5.2A-5.2D). By creating a dynamic cell wall loosening environment, XTH9 helps to form a shell to encapsulate the PIN1 marked cells that is required to maintain the PIN1 polarization, followed by auxin efflux lay a foundation that is necessary for shoot outgrowth (Figure 4.3A-4.3F, 4.3J,4.3K). The reduced capacity of mutants of *xth9* and *cuc2* to promote meristem formation suggests a non-cell autonomous role of CUC2 and XTH9 in promoting the development of shoot progenitor labeled by PIN1 protein (4.5A-4.5C, 4.5Q-4.5W, 5.7A-5.7C,5.7N-5.7T). Also, our experimental evidence shows that CUC2 is regulated by auto-activation, and CUC2 can, in turn, activate a gene that modulates cell wall plasticity. Modulation in cell wall mechanics can clearly impinge on shoot regeneration efficiency, indicating the existence of a feedback

regulation on shoot-promoting factor *CUC2* (Figure 5.4A, 5.4B). The *de novo* shoot formation is hampered when the callus is overloaded with CUC2, indicating that CUC2 maintains its threshold level throughout *de novo* shoot regeneration.

Understanding self-organization in multicellular systems requires a detailed understanding of cell polarity, mechanics, and cell fate, which interact through regulatory feedback mechanisms. However, studying these interactions has been limited by the lack of a genetically and experimentally amenable system (E. J. Y. Kim et al., 2018). Our study overcomes this challenge by using undifferentiated, asynchronously dividing callus as a mechanistic model to test for cell polarity, mechanics, and cell fate. Moreover, the stochastic initiation of the shoot from the pluripotent callus further advocates its use as a model. Although our study did not address the mechanism of stochastic initiation of the progenitors, it is tempting to speculate that the stochastic buildup of shoot-inductive factors to threshold levels within regions of the callus can trigger the initiation of the progenitor. These findings thus far have shed valuable light on the underlying mechanisms of shoot formation and regeneration and provide a foundation for future research in this area.

Chapter 6

Conserved function of *Rice* PLT proteins in controlling developmental process and regeneration in *Arabidopsis*

6.1 INTRODUCTION

All living organisms on the planet begin their life as a single cell and share the ability to grow. In animals, their entire body plan develops during embryogenesis and shows extensive growth to maintain this plan. Unlike animals, plants make a limited structure and create a miniature form during embryogenesis, consisting of plumule, radicle, and cotyledon. Despite the development being normally associated with embryogenesis, the process of development or growth is not restricted (end) at birth. Unlike animals, plants entire body plan, such as aerial as well as underground organs, organize during their post-embryonic growth. The cells responsible for making the shoot system (consisting of true leaves, stems, and flowers) or the root system are located at the opposite poles of the plant body axis. Shoot apical meristem (SAM) controls the aerial system, and root apical meristem (RAM) controls the underground root system. Many organisms exhibit remarkable growth over an extended period of time where continuous cellular renewal and expansion continues for decades if not centuries. (Sánchez Alvarado & Yamanaka, 2014). *Azorella* plant species, the oldest living organism on earth, shows infinite growth, whereas in *Botryllus schlosseri* where their body regenerates every two weeks as a part of asexual reproduction. In the case of the model organism Planaria, if we chop its body into multiple pieces, each piece identifies the lost part and regenerates into a complete organism. Plants are remarkable in their ability to generate the entire body system from an excised mature tissue upon various external inductive tissue culturing cues. It explains the existence of stem cells positioned at various locations in these organisms. In most cases, the ability of cells to be activated or reprogramming of the cells to replace or regenerate a tissue depends on the physical assault or predator/pathogen attacks caused during their growth or by any external abiotic stimuli. However, the ability to regenerate the lost tissue or regain the organ function varies for different species (L. Liu et al., 2023). Animals, such as salamanders, can regenerate lost organs such as legs, gills, or the heart. Zebrafish can often regenerate the heart, liver, spinal cord, or fins. However, mammals can only regenerate skin, intestinal cells, bones, and liver (Aichinger et al., 2012; Chang et al., 2021; L. Liu et al., 2023; Petrie et al., 2014; Tsata et al., 2021). Plants, on the other hand, have a super-regenerative ability that allows them to create a new plant from just a few cells in order to survive. According

to the studies to date, the regeneration process can be classified into five categories: 1) Whole body regeneration, 2) Structural regeneration, 3) Organ regeneration, 4) Tissue regeneration, and 5) Cellular regeneration (Bely & Nyberg, 2010). It occurs either by rearrangement of pre-existing tissue, i.e., use of adult stem cells, or by de-differentiation and trans-differentiation of cells (Alvarado & Tsonis, 2006; Mehta & Singh, 2019).

Although animal and plant developmental research can be compared to parallel universes, one of history's most pivotal moments occurred when these parallel universes collide in concept of regeneration. Regeneration process in animals and plants; however, the differences are apparent at the same time. Animals replace the lost tissue, whereas plants can make an individual from the wounded site reason being their immobility (Birnbaum & Alvarado, 2008; Goebel, 1898; J. Sachs, 1893). Furthermore, plants regenerate similar organs, such as root from the embryo, adventitious roots from any tissue, and lateral roots from the primary root. Despite the response outcome being the same in all the conditions (the root structure is the same), the initial morphogenesis for each event differs (Sena & Birnbaum, 2010). But, what similar organizing principles are acting in plant organogenesis at different stages of development? Does regeneration employ any of these principles? What genomic toolbox is commonly used during regeneration? One possible reason could be the existence of transcription factors unique to plants, such as AP2/EREBP, WRKY families, the auxin response factors (ARFs), the trihelix DNA binding proteins, and Aux/IAA proteins that are not found in animals (Aida et al., 1997; Eulgem et al., 2000; T. Guilfoyle et al., 1998; Nagano, 2000; Riechmann et al., 2000). However, within the plant kingdom itself, regeneration capacities vary greatly. For instance, compared to higher-order plant species like the monocot, which is challenging to propagate through tissue-culture techniques, primitive plants exhibit extremely high regeneration potential (Hu et al., 2017; Liang et al., 2023). Many regeneration studies and their regulatory mechanisms are reported in *Arabidopsis*, although limited studies are known in other plant species. *PLETHORA* (*PLT*) transcription factors belong to AP2/EREBP protein category known to control a variety of regenerative responses in *Arabidopsis* (Christiaens et al., 2021; Durgaprasad et al., 2019; Efroni et al., 2016; Gordon et al., 2007; Ikeuchi et al., 2019; Kareem et al., 2015a; Radhakrishnan et al., 2020; Sabatini et al., 1999; Shanmukhan et al., 2020). Nevertheless, there is limited knowledge about the mechanism for regeneration in

other plant species. In this chapter, we will look at whether the role of PLT protein in regeneration is conserved across plant species. The purpose of this study is to determine whether the presence or absence of this specific regulatory module responsible for various regeneration processes in *Arabidopsis* correlates with the regeneration efficiency as well as regeneration ability in other plant species. Understanding how plants can create a whole new organism from a single cultivated cell through cell division and differentiation is an important topic in plant developmental biology. On the other hand, figuring out the conserved molecular factors involved in the regenerative processes of model plants, such as *Arabidopsis* and other primitive model plants, will help us to gain a better understanding of regeneration in entire plant kingdom.

6.2 RESULTS

6.2.1 *Rice* PLETHORA proteins show similarity with *Arabidopsis* PLETHORA

The *PLETHORA* genes are known to be the master regulators of regeneration in *Arabidopsis thaliana*. These transcription factors control a variety of developmental processes, such as leaf phyllotaxy and lateral root development. They are involved in multiple regenerative responses, such as *de novo* shoot regeneration, *de novo* root regeneration, and regeneration responses in aerial organs. Numerous studies have highlighted the importance of PLETHORA genes in these processes. (Durgaprasad et al., 2019; Efroni et al., 2016; Gordon et al., 2007; Hofhuis et al., 2013; Kareem et al., 2015a; Mathew & Prasad, 2021; Pinon et al., 2013; Prasad et al., 2011; Radhakrishnan et al., 2020; Shanmukhan et al., 2021). To study the *PLETHORA-LIKE* genes control regenerative responses across the plant species, we chose *Rice* as a model system representing the Monocotyledon class. *Rice* and *Arabidopsis* (Dicotyledon class) diverged 60 million years ago during the course of evolution, and they exhibit distinct and very different morphological structures compared to *Arabidopsis* and examine the functional conservation of *Rice PLT* genes in *Arabidopsis*. As a first step towards studying the functional conservation, we compared both *Arabidopsis* and *Rice* PLTs protein sequences. The level of sequence conservation can be employed as a phenotypically significant DNA variant. The variation of genes can come from different perspectives, either by variation in non-coding sequences or in coding sequences

(Dermitzakis et al., 2005; Forman et al., 2008; Groß et al., 2020; Kryukov et al., 2005; TEN ASBROEK et al., 2001). In the current study, we considered the variation in the protein sequences. We checked the identity (same amino acid) and similarity (amino acid under same group) of *Arabidopsis* AtPLT3, AtPLT5, and AtPLT7 with all *Rice* PLETHORA proteins involved in the crown root formation in *Rice* by protein sequence alignment using Emboss needle pairwise alignment tool, which gives an accurate similarity estimate. Previous studies have reported that *Arabidopsis AtPLT3, AtPLT5*, and *AtPLT7* are essential for vascular regeneration and *de novo* shoot regeneration (Kareem et al., 2015a, 2016; Radhakrishnan et al., 2018, 2020). The comparison of amino acid sequences between AtPLT3 and *Rice* PLTs revealed that OsPLT1 shared 36% identity with AtPLT3 (Table 6.1) (Figure 6.1A, 6.1B). Similarly, OsPLT2 exhibited 44.5% identity with AtPLT5 (Table 6.2) (Figure 6.2A, 6.2B), and AtPLT7 was identical to OsPLT1 with 37.7% identity (Table 6.3) (Figure 6.3A, 6.3B). Among all the alignments of *Rice* OsPLT protein sequences, OsPLT1 or OsPLT2 showed the highest similarity to these *Arabidopsis* PLTs (Table 6.1-6.3) (Figure 6.1-6.3). Next, we compared the domain-specific alignment of these two *Rice* PLTs with their corresponding *Arabidopsis* PLT to check how the domains are conserved across these two distantly related plant model systems. PLT genes belong to the AP2 family of transcription factors, which contain 2 APETALA2/ethylene response factor (AP2/ERF) domains (Gu et al., 2017). To refine the analysis, we aligned the AP2 domain 1 of *Arabidopsis* PLT with *Rice* PLT and the AP2 domain 2 of *Arabidopsis* PLT with *Rice* PLT (referred to as At_Domain1 & Os_Domain1 and At_Domain2 & Os_Domain2). As mentioned earlier, OsPLT1 showed the highest hit on AtPLT3; we found that 66.7% and 94.9% were identical between At_Domain1 & Os_Domain1 and At_Domain2 & Os_Domain2 respectively (Table 6.4) (Figure 6.1C-6.1E). Likewise, the AtPLT5-OsPLT2 combination showed 98.5% and 98.3% (Table 6.4) (Figure 6.2C-6.2E), while the AtPLT7-OsPLT1 pair showed 91% and 94.9% identical amino acids from the sequences (Table 6.4) (Figure 6.3C-6.3E). *Arabidopsis* PLT3, PLT5 or PLT7 and *Rice* PLT1or PLT2 share ~71%-100% sequence similarity, in which the AP2- domain is conserved. Suggesting that they have a common origin and may have similar functions. Although we do not rule out the possible sequence similarity with other OsPLTs; however, we selected OsPLT1 and OsPLT2 based on the highest sequence alignment percentile of full-length protein as well

as domain for further functional studies.

Table 6.1: Comparative protein sequence analysis of *Arabidopsis* AtPLT3 with all *Rice* OsPLTs.

Alignment of *Arabidopsis* AtPLT3 with *Rice*			
Rice PLT	Locus ID	Identity (%)	Similarity (%)
OsPLT1	LOC_ Os04g0653600	36	44
OsPLT9	LOC_Os03g12950	33.9	44.5
OsPLT4	LOC_Os04g42570	32.7	41.7
OsPLT2	LOC_Os06g0657500	31.2	38.2
OsPLT7	LOC_Os03g56050	27.2	35.4
OsPLT5	LOC_Os01g67410	25.9	32.6
OsPLT6	LOC_Os11g19060	24.7	29.8
OsPLT3	LOC_Os02g40070	23.8	29.8
OsPLT10	LOC_Os03g07940	21.1	26.0
OsPLT8	LOC_Os07g03250	16.1	19.5

Highlighted column represents the highest similar *Arabidopsis* AtPLT3 homology in *Rice*.

Table 6.2: Comparative protein sequence analysis of *Arabidopsis* AtPLT5 with all *Rice* OsPLTs.

Alignment of *Arabidopsis* AtPLT5 with *Rice*			
Rice PLT	Locus ID	Identity (%)	Similarity (%)
OsPLT2	LOC_Os06g0657500	44.5	55
OsPLT1	LOC_ Os04g0653600	42.6	52.6
OsPLT6	LOC_Os11g19060	39.1	50.2
OsPLT5	LOC_Os01g67410	37.0	44.8
OsPLT4	LOC_Os04g42570	36.7	44.4
OsPLT3	LOC_Os02g40070	35.8	42.7
OsPLT7	LOC_Os03g56050	34.8	46.7
OsPLT9	LOC_Os03g12950	34.1	42.3
OsPLT10	LOC_Os03g07940	30.4	36.6
OsPLT8	LOC_Os07g03250	24.6	30.8

Highlighted column represents the highest similar *Arabidopsis* AtPLT5 homology in *Rice*.

Table 6.3: Comparative protein sequence analysis of *Arabidopsis* AtPLT7 with all *Rice* OsPLTs.

Alignment of *Arabidopsis* AtPLT7 with *Rice*			
Rice PLT	Locus ID	Identity (%)	Similarity (%)
OsPLT1	LOC_ Os04g0653600	37.7	45.5
OsPLT9	LOC_Os03g12950	35.1	45.1
OsPLT6	LOC_Os11g19060	34.6	43.7
OsPLT2	LOC_Os06g0657500	32.5	38.3
OsPLT4	LOC_Os04g42570	32.3	41
OsPLT3	LOC_Os02g40070	32.1	40.8
OsPLT7	LOC_Os03g56050	30.4	39.4
OsPLT5	LOC_Os01g67410	30.4	38.9
OsPLT10	LOC_Os03g07940	27.0	34.4
OsPLT8	LOC_Os07g03250	19.8	27.2

Highlighted column represents the highest similar *Arabidopsis* AtPLT3 homology in *Rice*.

Table 6.4: Comparative AP2 domain-wise (Domain1 and Domain2) sequence analysis of *Arabidopsis* AtPLTs with corresponding *Arabidopsis* homology in *Rice*.

	AP2 domain1		AP2 domain2	
Arabidopsis PLT(D)-*Rice* PLT(D)	Identity (%)	Similarity (%)	Identity (%)	Similarity (%)
AtPLT3-OsPLT1	66.7	71.3	94.9	96.6
AtPLT5-OsPLT2	98.5	100	98.3	100
AtPLT7-OsPLT1	91	97	94.9	96.6

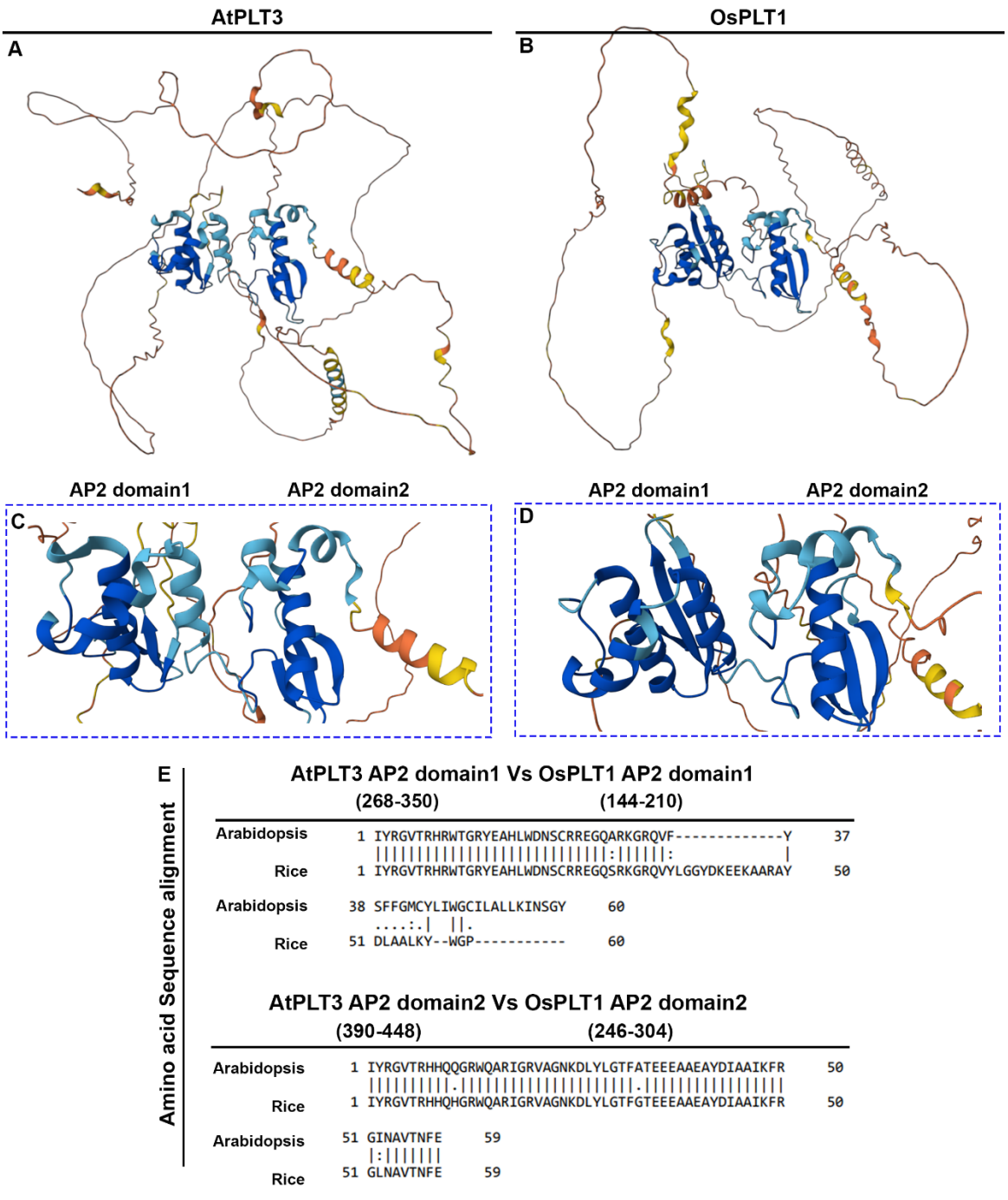

Figure 6.1: *Arabidopsis* PLT3 with its highly y similar homology *Rice* OsPLT1

(A) Protein structure of *Arabidopsis* PLT3. (B) Protein structure of *Rice* OsPLT1. (C-D) Enlarged structure of Domains (AP2 domain1 and AP2 domain2) of At PLT3 (C) and OsPLT1 (D) respectively. (E) Amino acid sequence alignment of *Arabidopsis* AP2 domain1 with *Rice* AP2 domain1 and *Arabidopsis* AP2 domain2 with *Rice* AP2 domain2 shows amino acid conservation in these two plant species.

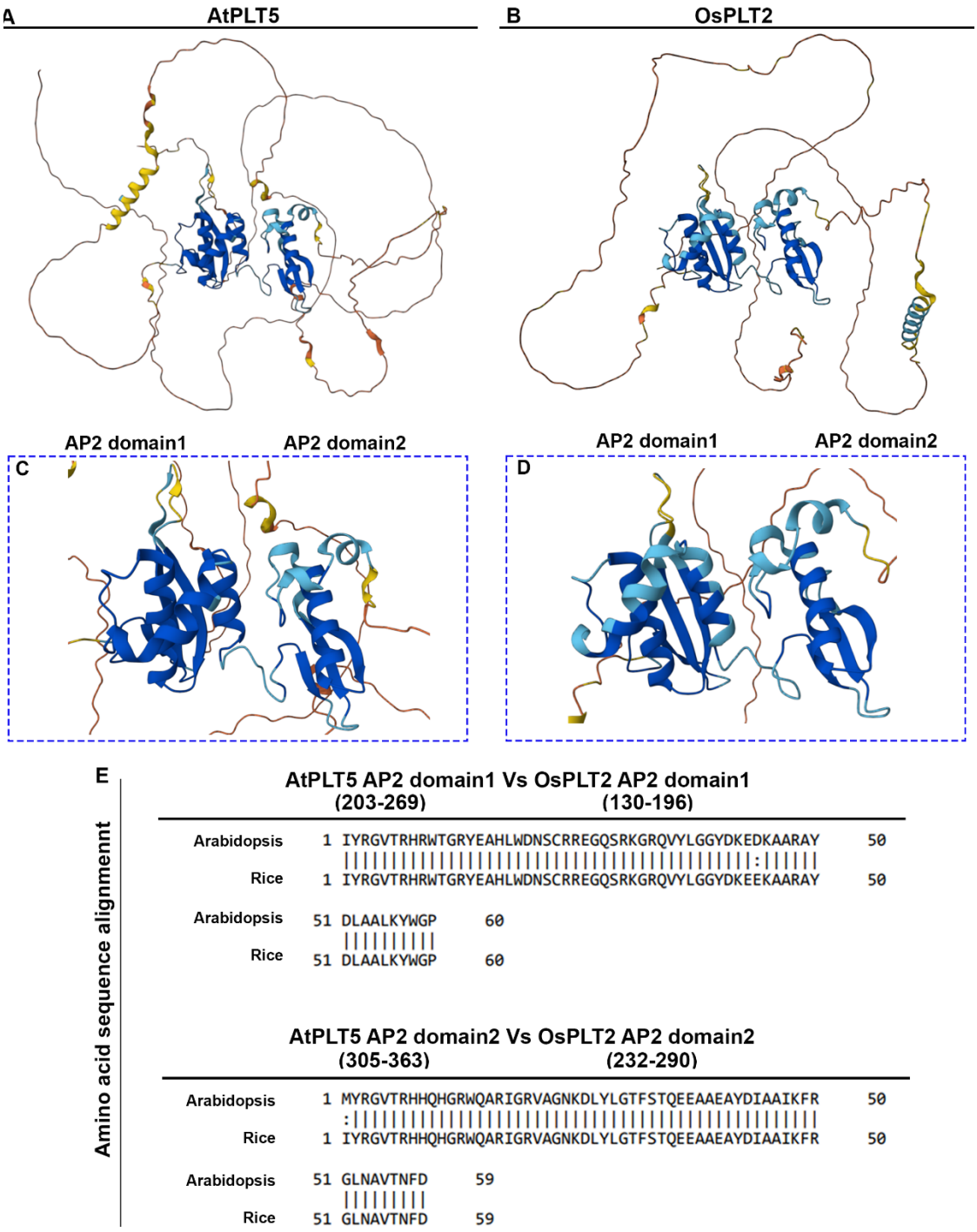

Figure 6.2: *Arabidopsis* PLT5 with its highly y similar homology *Rice* OsPLT2

(A) Protein structure of *Arabidopsis* PLT5. (B) Protein structure of *Rice* OsPLT2. **(C-D)** Enlarged structure of Domains (AP2 domain1 and AP2 domain2) of At PLT5 (C) and OsPLT2 (D), respectively. **(E)** Amino acid sequence alignment of *Arabidopsis* AP2 domain1 with *Rice* AP2 domain1 and *Arabidopsis* AP2 domain2 with *Rice* AP2 domain2 shows amino acid conservation in these two plant species.

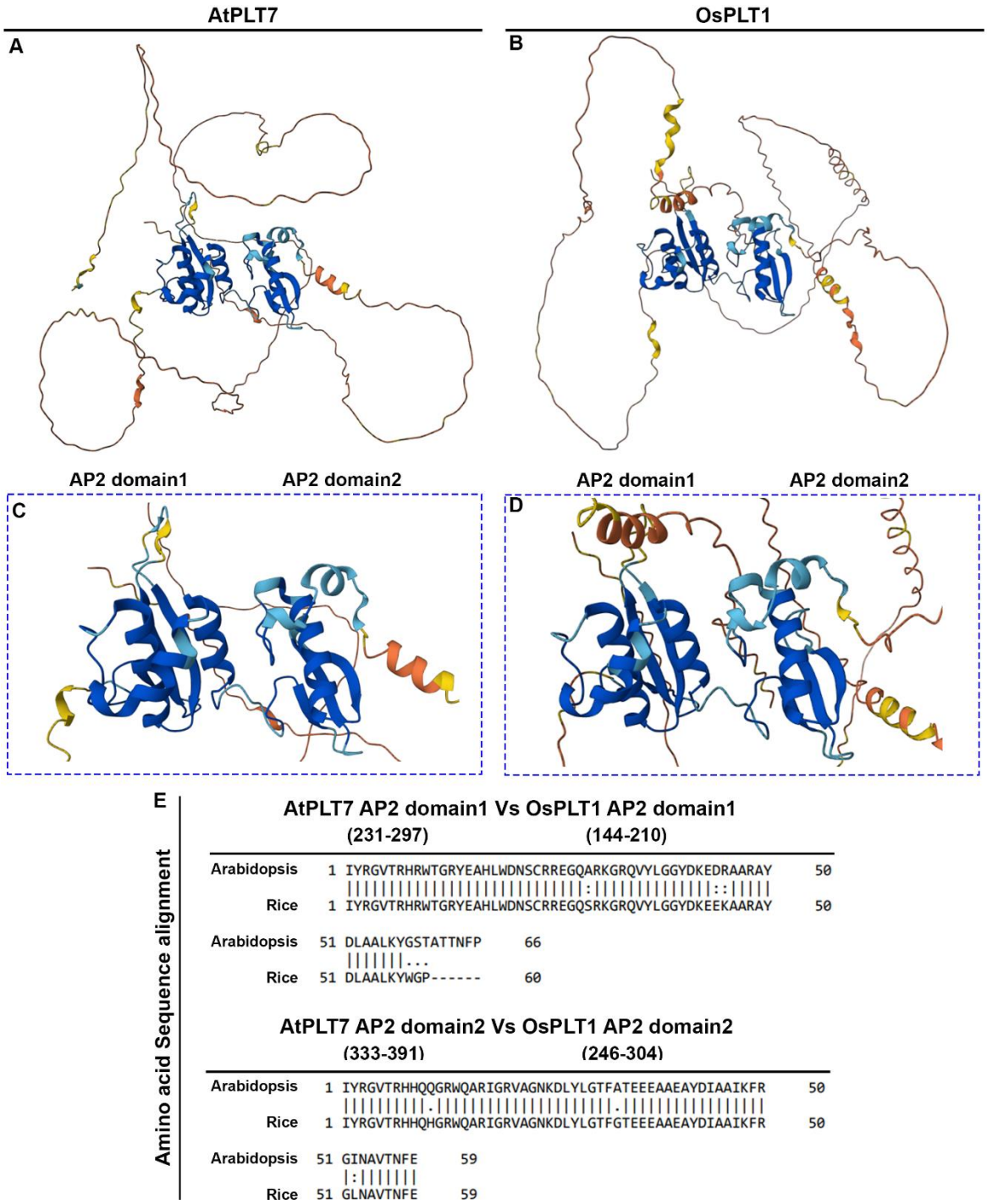

Figure 6.3: *Arabidopsis* PLT7 with its highly y similar homology *Rice* OsPLT1

(A) Protein structure of *Arabidopsis* PLT7. (B) Protein structure of *Rice* OsPLT1. **(C-D)** Enlarged structure of Domains (AP2 domain1 and AP2 domain2) of At PLT7 (C) and OsPLT1 (D) respectively. **(E)** Amino acid sequence alignment of *Arabidopsis* AP2 domain1 with *Rice* AP2 domain1 and *Arabidopsis* AP2 domain2 with *Rice* AP2 domain2 shows amino acid conservation in these two plant species.

Based on the protein sequence alignment, we cloned the

Rice PLT genes, *OsPLT1* or *OsPLT2,* under the control of *Arabidopsis AtPLT3* or *AtPLT5* promoter, respectively, with a fluorescent reporter YFP (4Xgly YFP-3AT) at the C-terminus. *Arabidopsis AtPLT3* and *AtPLT7* are originated by the gene duplication; therefore, we chose *AtPLT3* as a representative of these two *AtPLTs* for the conservation analysis (Riechmann et al., 2000). Furthermore, this construct was transformed into *Arabidopsis* in wild type (Columbia) and *plt3,plt5-2,plt7* background (homozygous triple mutant). *plt3,plt5-2,plt7* mutant shows defective in phyllotaxis and lateral root formation (Hofhuis et al., 2013; Prasad et al., 2011). We carefully analyzed the transgenic *Arabidopsis* with the *Rice* gene to determine whether it would complement the mutant phenotype.

6.2.2 Functional conservation of *Rice* PLETHORA in controlling *Arabidopsis* lateral root and shoot development

The PLETHORA family of transcription factors is involved in organ arrangement during the development. They act as a regulator of rhizotaxy and phyllotaxy in *Arabidopsis* (Hofhuis et al., 2013; Prasad et al., 2011). Lateral root outgrowth in *Arabidopsis* is regulated by a group of *PLETHORAs,* such as *PLT3, PLT5,* or *PLT7* genes (Du & Scheres, 2017; Prasad et al., 2011). To analyze if the role of *Rice PLT* gene have conserved role in controlling lateral root primordia outgrowth from root tissue across species, we expressed the *OsPLT* genes, regulating the shoot-born crown root primordia (CRP), under *Arabidopsis PLT3* or *PLT5* promoters in *plt3,plt5-2,plt7* triple mutant (Figure.7). The *Arabidopsis plt3,plt5-2,plt7* triple mutant lateral root primordia are initiated but fail to outgrow (Figure 6.4B). I expressed *Rice OsPLT1* under the *Arabidopsis* AtPLT3 promoter (*plt3,plt5-2,plt7; AtPLT3::OsPLT1-YFP*) in *plt3,plt5-2,plt7*. Strikingly, *AtPLT3::OsPLT1-YFP* rescued the lateral root outgrowth defect in the *plt3,plt5-2,plt7* triple mutant (*plt3,plt5-2,plt7; AtPLT3::OsPLT1-YFP*) (Figure 6.4A-6.4D) and expression was detected in the lateral root primordia (LRP) of *plt3,plt5-2,plt7* (Figure 6.4D). Similarly, *OsPLT2* expression under *Arabidopsis PLT5* promoter (*plt3,plt5-2,plt7; AtPLT5::OsPLT2-YFP*) also rescued lateral root outgrowth in the triple mutant (Figure 6.4E-6.4H), wherein upon reconstitution lateral root formation resembles the wildtype (Figure 6.4A,6.4E) (Columbia). The broader domain of *OsPLT2* expression near the

emerging LRP when reconstituted in the *AtPLT5* domain can be attributed to the transcriptional activity of the *AtPLT5* promoter (Fig. 7H) (Hofhuis et al., 2013). This suggests the role of *PLT* genes in controlling lateral root outgrowth is conserved across plant species.

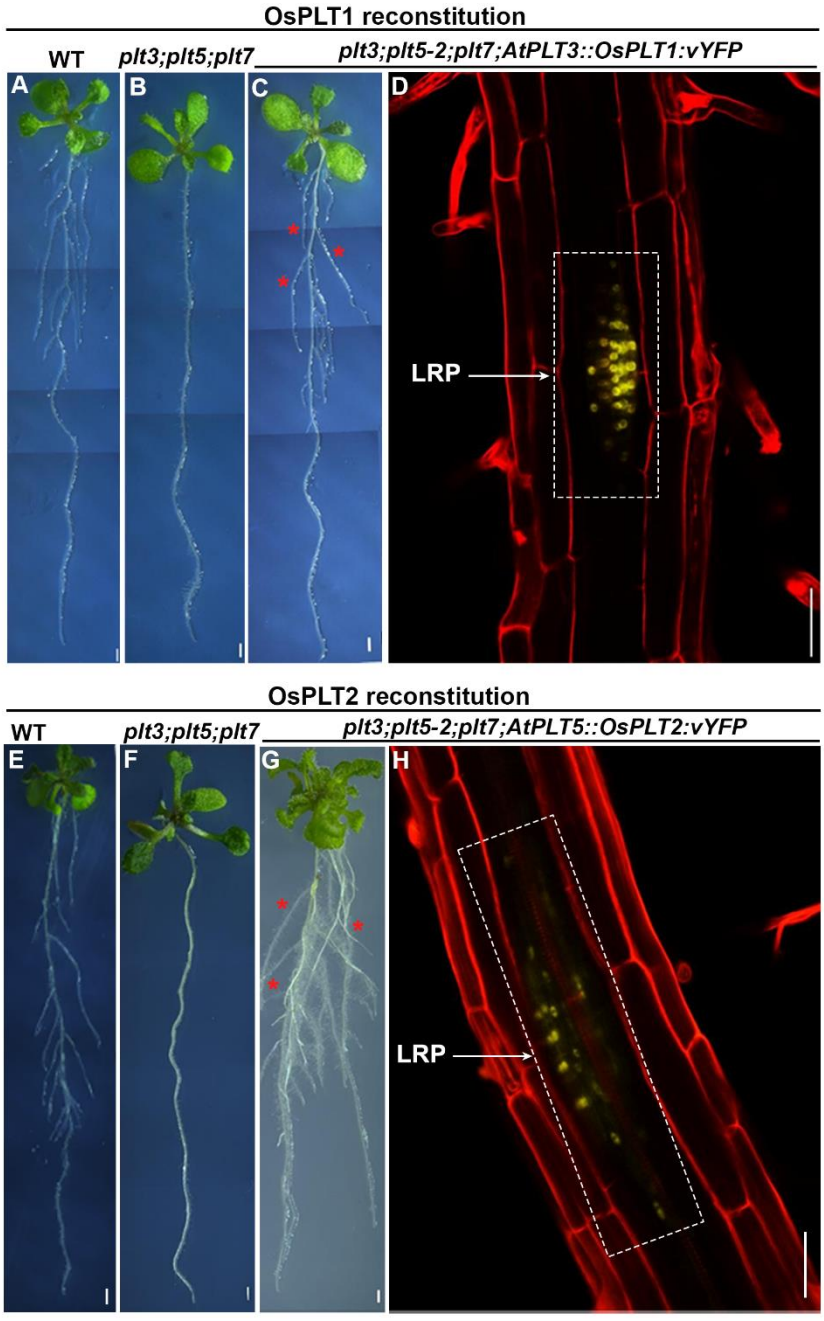

Figure 6.4:*Rice OsPLTs* are sufficient to make lateral root growth in *Arabidopsis*.

(A-C) Stereo images of 8dpg wildtype (A), plt3,plt5-2,plt7 defective in lateral root primordial outgrowth (B), and *plt3,plt5-2,plt7;AtPLT3::OsPLT1:vYFP* (C). Note the rescue of lateral root formation in *plt3;plt5-2;plt7* mutant reconstituted with

Arabidopsis PLETHORA3 promoter driving OsPLT1:vYFP (*plt3,plt5-2,plt7;AtPLT3::OsPLT1:vYFP*). **(D)** Confocal image showing expression of OsPLT1:vYFP in the lateral root primordia of *plt3,plt5-2,plt7;AtPLT3::OsPLT1:vYFP*. **(E-H)** Stereo images of wildtype (E), plt3,plt5-2,plt7 lacking lateral root (F), and *plt3,plt5-2,plt7;AtPLT5::OsPLT2:vYFP* (G). Note the rescue of lateral root formation in *plt3,plt5-2,plt7* mutant reconstituted with *Arabidopsis* PLETHORA5 promoter driving OsPLT2:vYFP (*plt3,plt52,plt7;AtPLT5::OsPLT2:vYFP*).
(H) Confocal image showing expression of OsPLT2:vYFP in the lateral root primordia of plt3,plt5-2,plt7;*AtPLT5::OsPLT2:vYFP*. Scalbars represent 1mm in (A-C,E-G) and 50µm in (D,H).

Next, we inquired about the phyllotaxis of these *OsPLT* genes carrying *plt3,plt5-2,plt7* triple mutant compared to *plt3,plt5-2,plt7*. The phyllotaxis pattern in wildtype *Arabidopsis* leaves arranged spirally on the condensed stem (Figure 6.5A), and the *plt3,plt5-2,plt7* shows rosette with opposite decussate pattern (Figure 6.5B) (Kalika 2011). We could observe that *Rice* OsPLT1 or OsPLT2 can organize the leaf pattern spirally in the *plt3,plt5-2,plt7* triple mutant, which resembled wildtype (Figure 6.5C, 6.5D). This indicates that *PLT*-like genes have evolved species-specific expression domain; perhaps, the proteins regulating the lateral root outgrowth and leaf arrangement, that is, protein function, are conserved across these species regardless of their developmental origin.

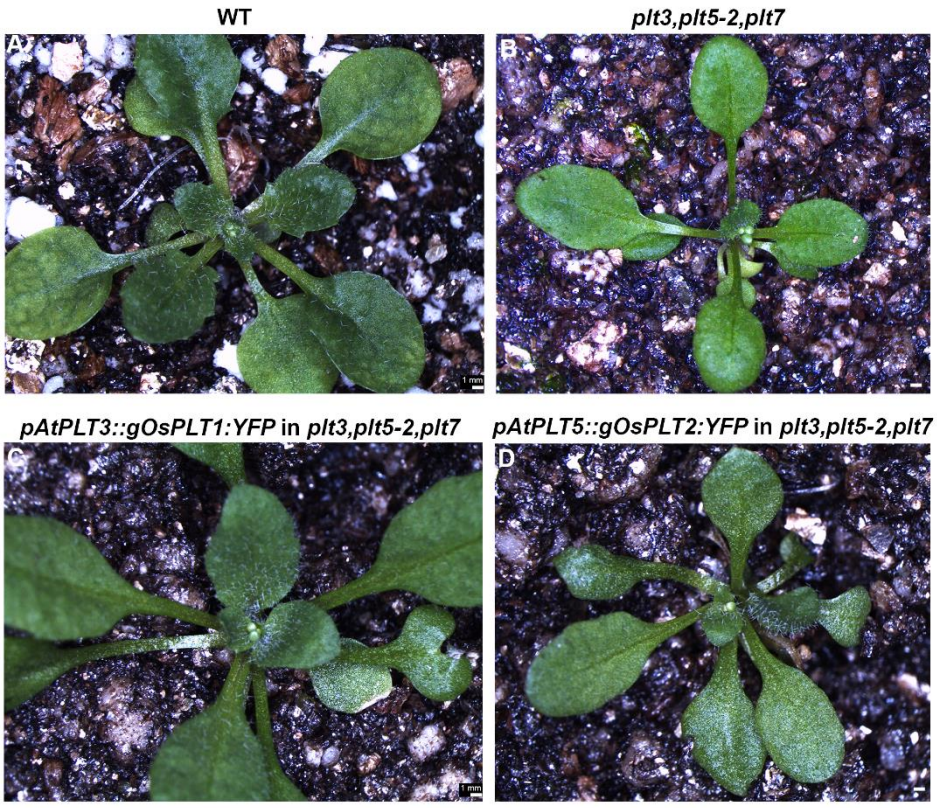

Figure 6.5: *Arabidopsis* homology in *Rice* can propel spiral phyllotaxis in *plt3,plt5-2,plt7* mutant

(A) *Arabidopsis* wildtype plant shows spiral phyllotaxis and **(B)** *plt3,plt5-2,plt7* with opposite decussate phyllotaxis. **(C)** Introduction of *Rice* OsPLT1 protein in *Arabidopsis PLT3* domain could reset the spiral phyllotaxy in *plt3,plt5-2,plt7* and in the same way *Rice* OsPLT2 under *Arabidopsis* PLT5 promoter could restore the leaf phyllotaxy (Spiral) *in plt3,plt5-2,plt7* triple mutant (decussate phyllotaxy) **(D)** which resemble wildtype.

6.2.3 ***Rice*** **PLETHORA protein can trigger vascular regeneration in the *Arabidopsis* in *plt* mutant**

Recently, the contribution of *PLT* genes in vascular tissue regeneration has been investigated and states that when mechanically disconnect the midvein of a growing leaf, the redundant transcription factors *PLT3*, *PLT5*, or *PLT7* mediate the activation of auxin biosynthesis gene *YUCC4*, followed by by an optimal hormonal environment drives the vascular restoration and the newly formed vascular tissue joined to the existing parental strand and rejoin in a D-looped shape (Radhakrishnan et al., 2020). We could observe that *Rice* OsPLT1 or OsPLT2 can rescue the phenotypic defect in the *Arabidopsis plt3,plt5-2,plt7*. So, we examined whether OsPLT-like proteins can trigger mechanical-injury-

induced regenerative responses in *Arabidopsis*. Expression of the *Rice PLT*-like gene *OsPLT2* under the *Arabidopsis PLT5* promoter in a *plt3,plt5-2,plt7* mutant (*plt3,plt5-2,plt7;AtPLT5::OsPLT2-vYFP*) promoted the wound healing in wounded *Arabidopsis plt3,plt5-2,plt7* mutant inflorescence stem by activating cell proliferation after 4-day post-abrasion (Figure 6.6A,6.6B) as evident from upregulated expression of cell cycle progression markers (Figure 6.6C,6.6D). It is important to note that *plt3,plt5-2,plt7* mutant shows residual cell proliferation in response to local abrasion of cell layers in inflorescence stem (Figure 6.6A). Further, we analyzed the vasculature regeneration in response to mid-vein injury in growing leaves. *AtPLT5::OsPLT2-vYFP* rescued leaf vascular regeneration defects in *plt3,plt5-2,plt7.* Similarly, OsPLT1 protein rescued the vein regeneration defects in *plt3,plt5-2,plt7* leaf in the form of D-loop or even through a straight connection (Figure 6.6I-6.6K). These data suggest that *OsPLT1 and OsPLT2* genes are functional homologs of *Arabidopsis PLT* genes (Figure 6.6A,6.6B,6.6E- 6.6K).

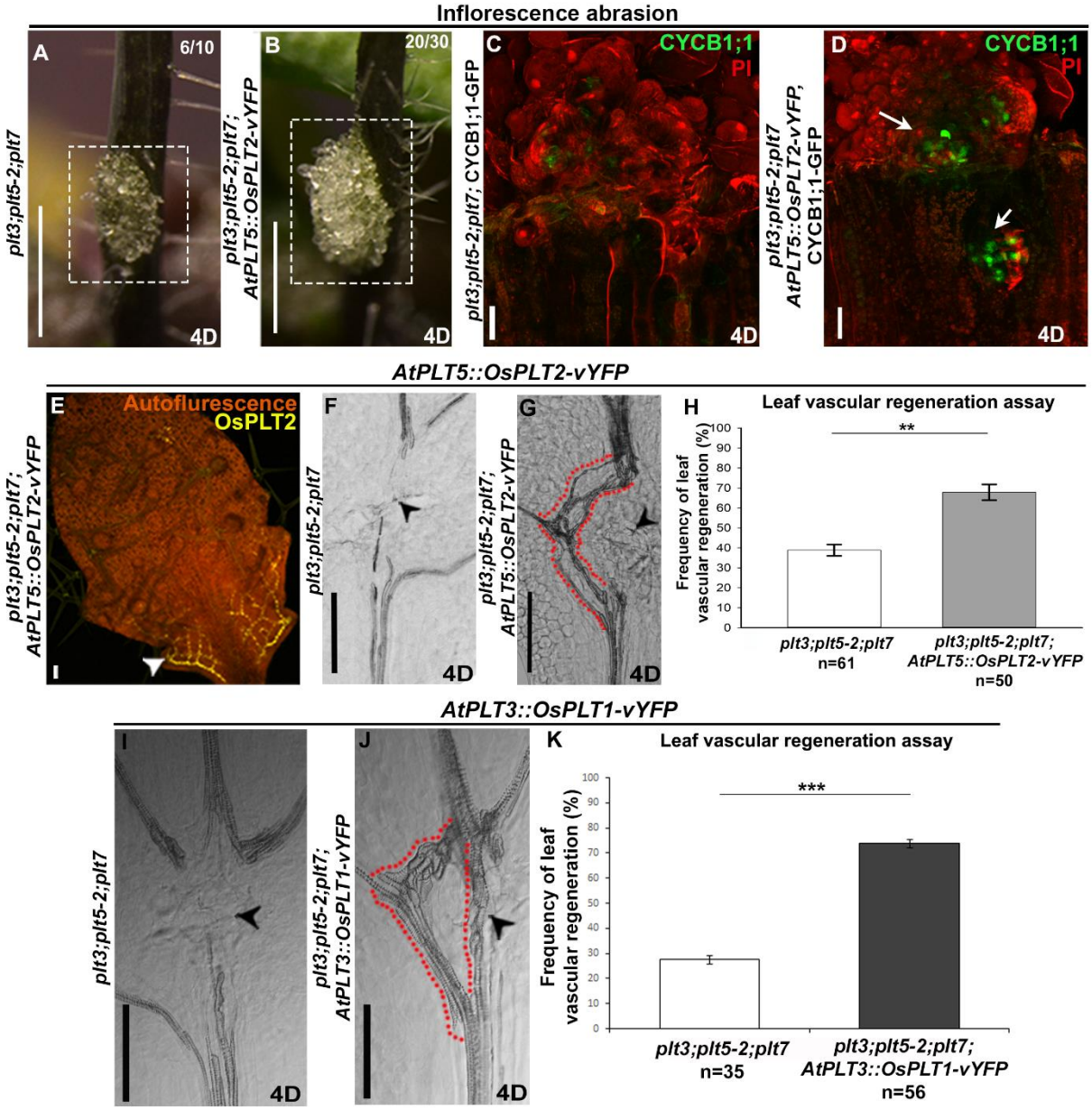

Figure 6.6: *Rice OsPLT1* introduction in *plt3,plt5-2,plt7* can restore the defect in mechanical-injury induced regenerative responses in *Arabidopsis*.

(A-B) A residual cell proliferation response is observed in *plt3,plt5-2,plt7* (A), unlike the extensive callus-like growth observed in *plt3,plt5-2,plt7;AtPLT5::OsPLT2-vYFP* (B) in response to inflorescence abrasion. The dotted rectangle indicates the area of cell proliferation. **(C-D)** Upregulated expression of CYCB1;1-GFP in the vicinity of wound where the cell proliferation occurred in response to local abrasion on the inflorescence stem (D), note that CYCB1;1 -GFP expression in the *plt3;plt5-2;plt7* is hardly visible (C). **(E)** Expression of *pAtPLT5::gOsPLT2-vYFP* in vascular tissue (white arrowhead) of a *plt3;plt5-2;plt7* leaf. **(F-H)** Rescue of vascular tissue regeneration in response to leaf incision in *plt3,plt5-2,plt7;AtPLT5::OsPLT2-vYFP* (D,E) *(**P=0.004; Pearson's χ2 test*) compared with *plt3,plt5-*

2,plt7 leaves (F), of which ~61% failed to regenerate. **(I-K)** Leaf vascular defect in the *plt3;plt5-2;plt7* is also could rescue by AtPLT3 driving *OsPLT1* gene (I, K) *(***P= 0.00072*; *Pearson's χ2 test*) compared to *plt* triple mutant (J,K). Scale bar: 1mm (A,B), 50um (C-G,I,J). Error bars represent s.e.m. Black arrowheads indicate the incision site. Red dotted lines indicate regenerated vascular strands.

6.2.4 *Rice* PLETHORA rescue *de novo* shoot regeneration defect in the *Arabidopsis plt* mutant

Finally, we examined if *OsPLTs* in *plt3,plt5-2,plt7* make shoot meristem *de novo*? As I mentioned previous chapter *plt3,plt5-2,plt7* is defective in shoot regeneration and never regenerates shoot (Kareem et al., 2015a). To test the activity of *Rice OsPLTs* in callus-mediated regeneration, we examined shoot regeneration in *plt3,plt5-2,plt7; AtPLT3::OsPLT1-YFP* and compared with *plt3,plt5-2,plt7*. Interestingly, OsPLT1 can rescue the shoot regeneration defect also in the triple mutant (*plt3,plt5-2,plt7; AtPLT3::OsPLT1-YFP; n=75,12.075±0.997*) (*plt3,plt5-2,plt7; n=152,0±0*) (Figure 6.7A-6.7D). Shoots forming efficiency of regeneration is comparable to wildtype (*n=180, 12.32±1.68*) (Figure 6.7A,6.7B). Similarly, we investigated the ability of OsPLT2 to rescue the shoot regeneration defects in *plt3,plt5-2,plt7* mutant. OSPLT2 expressed under AtPLT5 promoter (*plt3;plt5-2;plt7;AtPLT5::OsPLT2-vYFP*) triggered shoot regeneration in the triple mutant (n=50, 0±0) and established the shoot as like wild type (n=102, 17.78±0.98). These findings suggest that *Rice* PLT proteins can activate regenerative responses in *Arabidopsis* and they are likely to have conserved functions in controlling the plant regeneration.

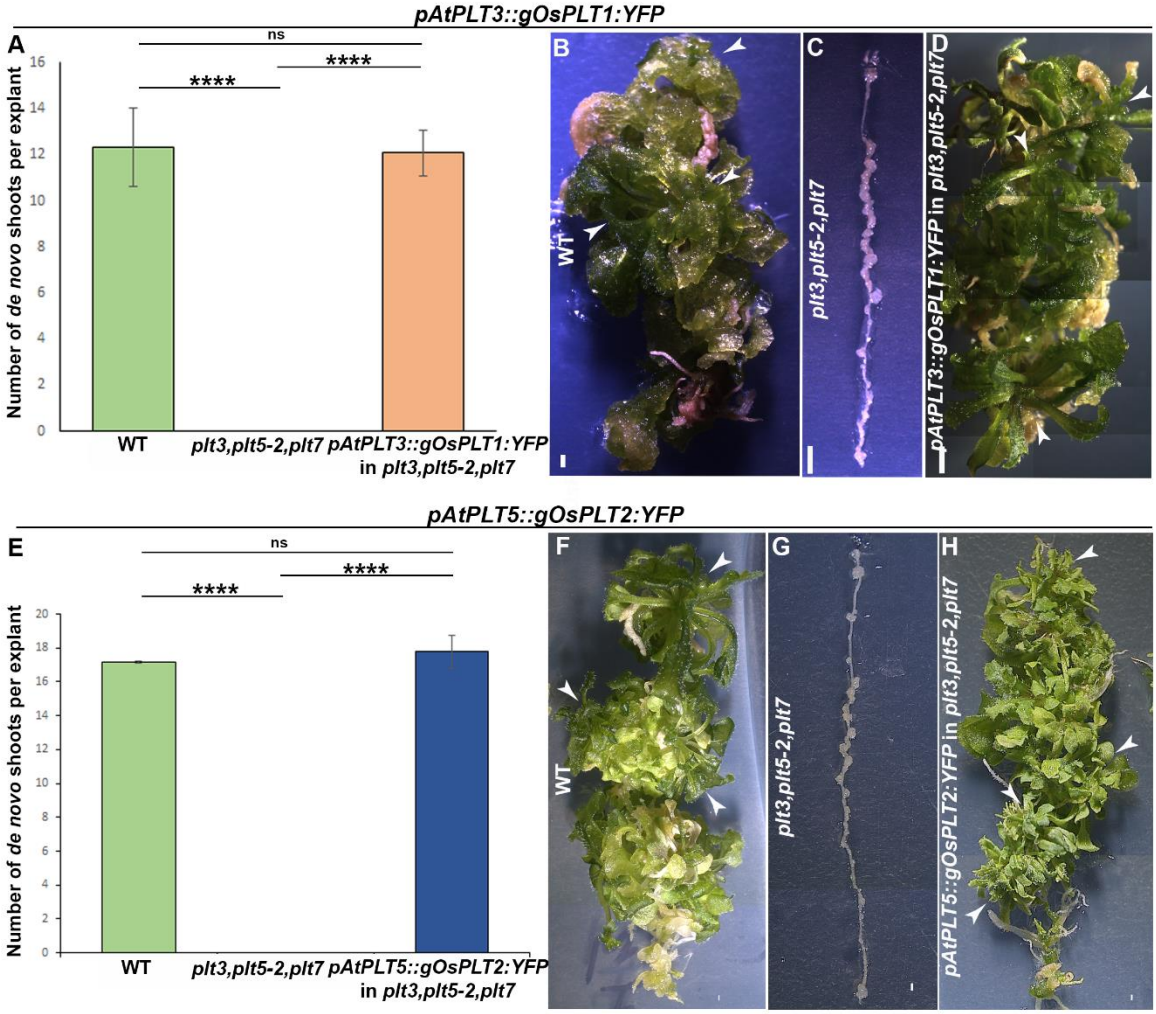

Figure 6.7: *Rice OsPLT* can make shoot meristem *de novo* in *Arabidopsis plt3,plt5-2,plt7* triple mutant.

(A) Graph depicting the rescue of shoot regeneration in *AtPLT3::OsPLT1-YFP* in *plt3;plt5-2;plt7* (WT vs. *plt3;plt5-2;plt7*:n=180,****P=0.0001; WT vs. *AtPLT3::OsPLT1-YFP* in *plt3;plt5-2;plt7*:n=75,ns=0.997; *AtPLT3::OsPLT1-YFP* in *plt3;plt5-2;plt7* vs. *plt3;plt5-2;plt7*:n=152,*****P=0.0001*, Unpaired t-test). **(B-D)** Shoot regeneration in *plt3;plt5-2;plt7*(n=152) (C) is reduced compared to WT(n=180) (B), but is rescued in *plt3;plt5-2;plt7* reconstituted with *AtPLT3::OsPLT1-YFP* (n=75) (D). **(E-H)** Rescue of *de novo* shoot regeneration in *plt3,plt5-2,plt7;AtPLT5::OsPLT2-vYFP* (E,H) (*WT vs plt3;plt5-2;plt7*:n=78,*****P=0.0001;WT vs AtPLT5::OsPLT2-YFP* in *plt3;plt5-2;plt7:n=102*,ns=*0.997; AtPLT5::OsPLT2-YFP* in *plt3;plt5-2;plt7* vs *plt3;plt5-2;plt7*:*n=50,****P=0.0001, Unpaired t-test)*. Compared with *plt3,plt5-2,plt7* mutant (E,G). Scale bar: 1mm (B-D,F-H). Error bars represent s.e.m from three independent biological replicates. White arrowheads indicate *de novo* shoot. Scale bar 1mm. n=sample number.

6.3 DISCUSSION

Functional diversity can be observed due to differences in proteins or cis-regulatory sequences driving their expression. Our studies suggest that PLETHORA proteins can activate a variety of developmental processes and regenerative responses across the plant species.

Despite variations in the gene sequences in these *PLT*s over the evolution time, their function is successfully maintained in the diverged species like *Rice* and *Arabidopsis*. Among *Rice PLT* genes, *OsPLT1* or *OsPLT2* displays the highest similarity with *Arabidopsis PLT3, PLT5*, or *PLT7*. Both, *OsPLT1* and *OsPLT2* can rescue the phenotypic defects in the *plt3,plt5-2,plt7* mutant. The action is not restricted to particular processes such as phyllotaxis or rhizotaxis; they can also promote wound repair in response to mechanical injuries and can promote tissue culture-mediated shoot regeneration. Even these *Rice PLT*s have a species-specific expression in their developmental origin, but these transcription factors can act in other species in the absence of its homology indicates the sufficiency of these *Rice* proteins in controlling developmental and the regenerative responses. Our studies provide insights into the conservation at the protein level. Future work should determine whether these PLT transcription factors have conserved cis-regulatory elements across the plant species. While *PLT* transcription regulatory modules have been characterized in *Arabidopsis*, their functions in other plant species yet need to be determined. It will be interesting to examine if these *Rice PLT* genes are essential in controlling distinct regenerative responses in *Rice*.

Chapter 7

Conclusion

7.1 Conclusion of Chapter2 - Chapter 5

7.1.1 *Mechanism of de novo* shoot regeneration – A study in model organism *Arabidopsis thaliana*

Tissue culture-mediated *de novo* organogenesis is an age-old practice that has been widely exploited for horticulture and regeneration of genetically modified crop plants. During indirect callus-mediated regeneration, an excised plant tissue is induced to form a dense mass of dividing cells called callus by external hormone supplementation. Some of the heterogenous callus cells subsequently re-specify shoot or root. Interestingly, during *de novo* shoot organogenesis, only a few initial cells known as 'progenitor' can reprogram from the callus, and among those shoot progenitors, only a few of them develop into new shoot meristem. How these initials are selected precisely and what governs their subsequent progression to a fertile organ system remain unanswered. we explored the molecular factors and biochemical cues involved in the process of shoot morphogenesis from a heterogenous callus tissue using live cell imaging and transient molecular and genetic manipulation of the shoot progenitor during *de novo* shoot regeneration.

We find that in productive progenitor, PIN1 polarizes on the membrane of the progenitor cells to create an auxin gradient between the progenitor and its surrounding non-progenitor cells. Whereas the progenitor 'termed as pseudo-progenitor' does not show polarly localized PIN1. Such progenitor experiences a high auxin level in progenitor, and neighbouring non-progenitor cells and fails to distribute the auxin during the early reprogramming stage of shoot progenitor. PIN1 polarization on the membrane of the progenitor is crucial for the differential distribution of auxin for the development of shoot meristem from a callus rich in auxin. Detailed investigation of the molecular mechanism behind the *de novo* shoot organogenesis, we identified a cell wall loosening enzyme XTH9 behind the screen that gives rationality for the PIN1-auxin combination.

The progenitor cells enriched in PIN1(polarized) are surrounded by a belt of XTH9 in the surrounding non-progenitor cells of regenerating foci. XTH9 enzymes in the surrounding cells are activated by a shoot-promoting factor *CUP-SHAPED COTYLEDON 2* (*CUC2*). An adequate biochemical environment is created by the expression of CUC2 by activating a cell-wall loosening enzyme resulting in the polar localization of PIN1 on the progenitor

that guides these cells to self-organize into a shoot meristem. Alteration of any of these factors, such as *PIN1*, auxin, *CUC2*, or *XTH9* by mutation, overexpression, or silencing through various approaches compromises the shoot regeneration *de novo*, implying a non-cell-autonomous regulation of *CUC2-XTH9* module on PIN1 marked progenitor cells.

This study led to the discovery of a new regulatory axis where a shoot-promoting factor *CUC2* activates XTH9 in the cells surrounding the progenitors, which is critical for *de novo* shoot meristem formation. Encapsulation of progenitors by a shell of cells expressing cell wall loosening enzyme serves as criteria to select the shoot progenitors from undifferentiated callus and become a productive shoot fate. *CUC2-XTH9* acts non-cell autonomously to confer the productive fate to regenerating progenitors. Interestingly cell wall modification in surrounding non-progenitor cells and cell polarity in the progenitors act in a regulatory feedback loop to make the dome-shaped shoot meristem *de novo*. Miss-expression of any factors in the regulatory loop can halt the progression of the shoot progenitor to a functional SAM fate. Therefore, each factor is considered to be the strength of a chain, i.e., the weakest link in a chain. This study provides a simple model accountable for self-organized morphogenesis in the absence of pre-pattern cues.

7.2 Conclusion of Chapter 6

7.2.1 *Rice* PLT proteins rescue the regeneration defects in *Arabidopsis plt* mutant

Regeneration studies have been going on for many decades using the model organism *Arabidopsis thaliana*. Generally, a wide variety of plants are used to propagate through tissue-culture practices are ornamental or crop plants. There are limited studies that talk about conservation biology in the field of regeneration. Here, we analyzed the molecular factors involved in the multiple regenerative responses in *Arabidopsis* with distantly related model organism *Rice*. we illustrate the presence of common genes in diverged plant species in the context of regeneration, which are acquired by vertical gene transfer during the course of evolution (from a common ancestor of dicotyledons and monocotyledons class).

A variety of regenerative processes in *Arabidopsis thaliana* are controlled by a large family of transcription factors, *PLETHORA*. They are active not only in regeneration but also involved in normal development, such as leaf patterning and root development. we interrogated the presence and the role of *PLT* genes by generating *Arabidopsis PLT* driving *Rice* PLT protein by expressing it in the *Arabidopsis plt*3,*plt5-2*,*plt7* mutant. Experimental evidences revealed the conserved function of *Rice PLETHORA* proteins in controlling both developmental processes, such as lateral root outgrowth or leaf phyllotaxy, and regenerative responses, such as regeneration of damaged tissues or complete shoot system in evolutionary diverged dicot plant species. We found that *PLETHORA* gene function is conserved in distantly related plant systems even though they have specific functionality in their origin, indicating their functional diversity. This study opens a new path to characterize ancestral genes associated with regenerative responses in other plant species.

Chapter 8

Materials and methods

Detailed methods are provided in the online version of this paper and include the following:

8.1 MATERIAL DETAILS

Table 8.1: Oligonucleotides used in this study

Oligonucleotides used for qRT-PCR	
Oligo Name	5’ to 3’
Actin 2 FP	TCGGTGGTTCCATTCTTGCT
Actin 2 RP	CTGTGAACGATTCCTGGACC
qRT-XTH9 FP	AGTGATGCCCTCACAGTAACG
qRT-XTH9 RP	TCGACGTGTGATTCAGGACAG
qRT-CUC2 FP	CGTCTTCTGCATCGACTATG
qRT-CUC2 RP	GTAGTTCCAAATACAGTCAAG
qRT-CUC2 FP (Endogenous)	GAGGTGACTTATAATTGTTCCCGTTAGGG
qRT-CUC2 RP (Endogenous)	CGAGCATAGCTTATACATATGCACGTTC
Oligonucleotides used for genotyping	
xth9 (insertion in 3’UTR) LP	GTTGGCTGATTTAAGCGTCAG
xth9 (insertion in	TGGTAGACGAAACACCGATTC

3'UTR) RP	
xth9 (insertion in 3'UTR) LBp	ATTTTGCCGATTTCGGAAC
cuc2-3 LP	GGTCACGGAGGCTAAAGAAGTACCA
cuc2-3 RP	AGCCCATTCCTCGTTTCTTT
cuc2-3 LBp	ATCTGAATTTCATAACCAATCTCGATACAC
Oligonucleotides used for cloning	
pXTH9 FP(2.3Kb)	GGGGACAACTTTGTATAGAAAAGTTGTTTGATTATGGAGATGCTGATTG
pXTH9 RP(2.3Kb)	GGGGACTGCTTTTTTGTACAAACTTGTTTTTTTTTTAACTTATCTCTCTAAATAAATC
gXTH9 FP	GGGGACAAGTTTGTACAAAAAAGCAGGCTGTATGGTCGGTATGGATTTGTTCAAATGTGT
gXTH9 RP	GGGGACCACTTTGTACAAGAAAGCTGGGTTCAAATGACGATGATGTTGGCACTCAAGAGG
pWUS FP	GGGGACAACTTTGTATAGAAAAGTTGCCTCAAGGGACGGGTAAAGAAA

pWUS RP	GGGGACTGCTTTTTTGTACAAACTTGCTGTGTTTGATTCGACTTTTGTTC
tWUS FP	GGGGACAGCTTTCTTGTACAAAGTGGCCTAGCTCTTACGCCGGTGTCG
tWUS RP	GGGGACAACTTTGTATAATAAAGTTGCGATTTCCGTTTTGCTCTCGT
pCUC2 FP	GGGGACAACTTTGTATAGAAAAGTTGTTAGATGGATCAGCATTTCCTTTGTTTTCTCC
pCUC2 RP	GGGGACTGCTTTTTTGTACAAACTTGTTAAGAAGAAAGATCTAAAGCTTTTGTTTGAG
gCUC2 FP	GGGGACAAGTTTGTACAAAAAAGCAGGCTGTATGGACATTCCGTATTACCACTACGACCATG
gCUC2 RP	GGGGACCACTTTGTACAAGAAAGCTGGGTTGTAGTTCCAAATACAGTCAAGTCCAGCATG
pCYCB1;1 FP	GGGGACAACTTTGTATAGAAAAGTTGTTAAATCGTGTCTTTTGCGTGTTCTCGAGTC
pCYCB1;1 RP	GGGGACTGCTTTTTTGTACAAACTTGTC

	TTAGTGTTCTCTTCTCTTTCTCTCAGAC
gCYCB1;1 (d BOX) FP	GGGGACAAGTTTGTACAAAAAAGCAGG CTGTATGATGACTTCTCGTTCGATTGTT CCTCAAC
gCYCB1;1 (d BOX) RP	GGGGACCACTTTGTACAAGAAAGCTGG GTTCTTCTCTCGAGCAGCAACTAAACCA AGTTC
XTH9 dsRNAi FP	AGTTCTATCTCGAGGGTTGTCTCTTGTG GTGAAGCT
XTH9 dsRNAi RP	TACATAATGGATCCCTCTGTTTCCAACT CCGTTCAC
PIN1 dsRNAi FP	AGTTCTATCTCGAGCCAACACTCTAGTC ATGGGGATA
PIN1 dsRNAi RP	TACATAATGGATCCGAAGCATTAGAAC GACGAACAGT
CUC2 dsRNAi FP	AGTTCTATCTCGAGTCCCTACTACTACT ACGGCCTTGG
CUC2 dsRNAi RP	TACATAATGGATCCCCAAATACAGTCA AGTCCAGCAT
vYFP (C'terminal-2nd box) RP	GGGGACCACTTTGTACAAGAAAGCTGG GTTTTACTTGTACAGCTCGTCCATGCC
vYFP (N'terminal 2nd box) XhoI FP	AGTTCTATCTCGAGATGGTGAGCAAGG GCGAGGAGCTGTTCAC

vYFP (N'terminal 2nd box) BamHI RP	TACATAATGGATCCGCCACCACCACCC GCCTTGTACAGCTCGTCCATGCCGAGA G
cXTH9 FP	GGGGACAAGTTTGTACAAAAAAGCAGG CTGTATGGTCGGTATGGATTTGTTCAAA TGTGT
cXTH9 RP	GGGGACCACTTTGTACAAGAAAGCTGG GTTCAAATGACGATGATGTTGGCACTC AAGAGG
gPINOID FP	GGGGACAAGTTTGTACAAAAAAGCAGG CTGTATGTTACGAGAATCAGACGGTGA GATGAG
gPINOID RP	GGGGACCACTTTGTACAAGAAAGCTGG GTTAAAGTAATCGAACGCCGCTGGTTT GTTACTAC
gYUCCA4 FP	GGGGACAAGTTTGTACAAAAAAGCAGG CTGTATGGGCACTTGTAGAGA
gYUCCA4 RP	GGGGACCACTTTGTACAAGAAAGCTGG GTTGGATTTATTGAAATGAAGATGA
pPLT5 FP	
pPLT5 RP	
gOsPLT1 FP	GGGGACAAGTTTGTACAAAAAAGCAGG CTGTATGGACATGGACACCTCGCACCA

	CTATC
gOsPLT1 RP	GGGGACCACTTTGTACAAGAAAGCTGGGTTTTCCATCCCAAAGATTGGTGTCTGAAAGGC
gOsPLT2 FP	GGGGACAAGTTTGTACAAAAAAGCAGGCTGTATGAAGTCCATGACGCGGCAGG
gOsPLT2 RP	GGGGACCACTTTGTACAAGAAAGCTGGGTTCTCCATCCCAAACAAATAGTTGTAGAAGTGGG
pLEC1 FP	GGGGACAACTTTGTATAGAAAAGTTGTTAGCGATATGATATAGTATGGGCTACTTCATACG
pLEC1 RP	GGGGACTGCTTTTTTGTACAAACTTGTTGTTTCTCTGCCGTCTTTTTTTTTTTTTGTTC
gLEC1 FP	GGGGACAAGTTTGTACAAAAAAGCAGGCTGTATGGAACGTGGAGCTCCCTTCTCTCACTATC
gLEC1 RP	GGGGACCACTTTGTACAAGAAAGCTGGGTTCTTATACTGACCATAATGGTCAAAAGCCGGCAT
CUC3 dsRNAi FP	AGTTCTATCTCGAGAATGGGTGATTTGCAGAGTGT

CUC3 dsRNAi RP	TACATAATGGATCCCAGCTGGAATCCT AAAGGACA
Oligonucleotides used for Inducible genome editing (IGE)	
U-F	CTCCGTTTTACCTGTGGAATCG
gR-R	CGGAGGAAAATTCCATCCAC
Pps-GGL	TTCAGAggtctcTctcgACTAGTATGGAATC GGCAGCAAAGG
Pgs-GG2	AGCGTGggtctcGtcagggTCCATCCACTCCA AGCTC
Pps-GG2	TTCAGAggtctcTctgacacTGGAATCGGCAG CAAAGG
Pgs-GG3	AGCGTGggtctcGtcttcacTCCATCCACTCCA AGCTC
Pps-GG3	TTCAGAggtctcTaagacttTGGAATCGGCAGC AAAGG
Pgs-GG4	AGCGTGggtctcGagtccttTCCATCCACTCCA AGCTC
Pps-GG4	TTCAGAggtctcTgactacaTGGAATCGGCAG CAAAGG
Pgs-GGR	AGCGTGggtctcGaccgACGCGTATCCATCC ACTCCAAGCTC
XTH9-TG1-gRT#+	ATGGTGTTGGTTGTCTCTTGGTTTTAGA GCTAGAAAT

XTH-9TG1-AtU3bT#-	CAAGAGACAACCAACACCATTGACCAA TGTTGCTCC
XTH9-TG2-gRT#+	CACCCTCAACAAGCTTAATCGTTTTAGA GCTAGAAAT
XTH9-TG2-AtU3dT#-	GATTAAGCTTGTTGAGGGTGTGACCAA TGGTGCTTTG
XTH9-TG3-gRT#+	AAATCGAATTCGTTGTGGTTGTTTTAGA GCTAGAAAT
XTH9-TG3-AtU6-1T#-	AACCACAACGAATTCGATTTCAATCAC TACTTCGTCT
XTH9-TG4-gRT#+	TCATTGCAAATACAGATTCAGTTTTAGA GCTAGAAAT
XTH9-TG4-AtU6-29T#-	TGAATCTGTATTTGCAATGACAATCTCT TAGTCGACT
CUC2-TG1-gRT#+	CTTCTCCGCAAAGTCCTCGAGTTTTAGA GCTAGAAAT
CUC2-TG1-AtU3bT#-	TCGAGGACTTTGCGGAGAAGTGACCAA TGTTGCTCC
CUC2-TG2-gRT#+	GTGAGCGTAAGCAGCGGTACGTTTTAG AGCTAGAAAT
CUC2-TG2-AtU3dT#-	GTACCGCTGCTTACGCTCACTGACCAAT GGTGCTTTG
CUC2-TG3-gRT#+	GGAGAAACAGGACACGTGCTGTTTTAG

	AGCTAGAAAT
CUC2-TG3-AtU6-1T#-	AGCACGTGTCCTGTTTCTCCCAATCACTACTTCGTCT
CUC2-TG4-gRT#+	GACCTTTGACTCATTCTCTTGTTTTAGAGCTAGAAAT
CUC2-TG4-AtU6-29T#-	AAGAGAATGAGTCAAAGGTCCAATCTCTTAGTCGACT

Table 8.2: Reagent or resources used for the study

REAGENT or RESOURCE SOURCE	SOURCE	IDENTIFIER
Antibodies		
Rabbit polyclonal anti-GFP	Abcam	Cat# ab290; RRID: AB_303395
Bacterial and Virus Strains		
Escherichia coli (DH5a)	N/A	N/A
Agrobacterium tumefaciens (C58)	N/A	N/A
Chemicals, Peptides, and Recombinant Proteins		
Murashige & Skoog basal salts Medium	Sigma	Cat# M5524

Plant-agar	Sigma	Cat# A7921
MES hydrate	Sigma	Cat# M2933
Gamborg's B5 basal salt mixture	Sigma	Cat# G5768
Gamborg's vitamin solution 1000X	Sigma	Cat# G1019
Sucrose	Sigma	Cat# S0389
D-Glucose	Sigma	Cat# G7021
Agarose	Sigma	Cat# A9539
2,4-Dichlorophenoxyacetic acid	Sigma	Cat# 49083
Kinetin	Sigma	Cat# K3378
Trans-zeatin	Sigma	Cat# Z0876
Biotin	Sigma	Cat# B4639
Kanamycin	Himedia	Cat# K1377
Rifampicin	Himedia	Cat# CMS1889
Spectinomycin	Himedia	Cat# TC034
Phusion High-Fidelity DNA Polymerase	New England Biolabs	Cat# M0530L
PrimeSTAR GXL DNA	Takara-Bio	Cat# R050A

Polymerase		
Agar powder, Bacteriological	Himedia	Cat# GRM026
Complete Protease Inhibitor Cocktail	Roche	Cat# 16829800
Dimethyl-sulfoxide	Sigma	Cat# D8418
NaCl	Himedia	Cat# GRM031
Propidium iodide	Sigma	Cat# P4170
b-Estradiol	Sigma	Cat# 250155
Dexamethasone	Sigma	Cat# D2915
Ampicillin	Sigma	Cat# A0166
Na2HPO4	Himedia	Cat# RM1417
NaH2PO4	Himedia	Cat# RM3964
Sodium dodecyl sulfate	Sigma	Cat# L4390
Triton X100	Sigma	Cat# X100
Glycerol	Sigma	Cat# G5516
formaldehyde	Himedia	Cat# AS017
Glycine, Molecular	SRL	Cat# 25853

Biology Grade		
Sodium deoxycholate	Sigma	Cat# D6750
Phenylmethylsulfonyl fluoride (PMSF)	Sigma	Cat# P7626
Ethylenediaminetetraacetic acid (EDTA)	Himedia	Cat# GRM678
IGEPAL	Sigma	Cat# I3021
Protein G agarose beads (Upstate)	Novex Life technologies	Cat# 10003D
LiCl	Sigma	Cat# L9650
Tris base	Himedia	Cat# TC072
40µM cell strainer	BD Falcon	Cat# 352340
2-Mercaptoetanol	Sigma	Cat# M3148
Critical Commercial Assays		
Nucleospin RNA plant extraction kit	Macherey- Nagel	Cat. # 740949
TB Green (SYBR)Premix Ex Taq II (Tli RNaseH Plus)	Takara-Bio	Cat# RR820A
Gel/PCR DNA Fragments	Macherey- Nagel	Cat#

Extraction Kit		740609
NucleoSpin Plasmid	Macherey- Nagel	Cat# 740588
Gateway BP Clonase II Enzyme Mix	Invitrogen	Cat# 11789100
Gateway LR Clonase II Plus Enzyme Mix	Invitrogen	Cat# 12538200
PrimeScript 1st strand *cDNA* synthesis kit	Takara-Bio	Cat. # 6110A
PCR purification kit	Qiagen	Cat #28106
Software and Algorithms		
ImageJ	http://rsbweb.nih.gov/ij	RRID: SCR_003070
Adobe Photoshop CS6	Adobe Acrobat	N/A
Adobe Illustrator	Adobe Acrobat	N/A
Excel	Microsoft	N/A
GraphPad Prism version 9.5.1	graphstats.net/prism	N/A
R programming	https://posit.co/download/rstudio-desktop/	N/A

bowtie version 2.2.4	(Langmead et al., 2009)	N/A
samtools version 1.2	(H. Li et al., 2009)	N/A
MACS2 (version 2.1.0)	(Y. Zhang et al., 2008)	N/A
Integrated Genome Browser	http://bioviz.org/igb/index.html	N/A
Trimmomatic	(Bolger et al., 2014)	N/A
HISAT2	(D. Kim et al., 2015)	N/A
DESeq2	(Love et al., 2014)	N/A
bedGrapghTobigwig script	(Kent et al., 2010)	N/A
Panther analysis tool	(Thomas et al., 2003)	N/A
Others		
Growth chamber	Percivial,	N/A
Leica TCS SP5 II	Leica	N/A
Zeiss LSM 880	Zeiss	N/A
Leica M205FA stereo microscope	Leica	N/A
Zeiss LSM 780	Zeiss	N/A
Branson Sonifier 250D	Marshall Scientific	N/A
QuantStudio™ 5 Real-	Applied Biosystem	N/A

Time PCR		
Zen software	Zeiss	N/A
Leica S8 APO Stereo zoom microscope	Leica	N/A
Deposited Data		
RNA sequencing	NCBI Gene Expression Omnibus	GEO: PRJNA848450
ChIP seq	NCBI Gene Expression Omnibus	GEO: PRJNA848450

Table 8.3: Experimental organisms or strains used for the study

EXPERIMENTAL MODELS: ORGANISMS/STRAINS	SOURCE	IDENTIFIER
A.thaliana: Col-0	Nottingham *Arabidopsis* Stock Centre	N/A
A.thaliana: *cuc2-3*	(Hibara et al., 2006)	N/A
A.thaliana: *cuc1-5*	(Hibara et al., 2006)	N/A

A.thaliana: *pin1-1*	(Sawchuk et al., 2013)	N/A
A.thaliana: *cuc1-5,cuc2-3*	(Hibara et al., 2006)	N/A
A.thaliana: *pid,wag1,wag2*	(Dhonukshe et al., 2015)	N/A
A.thaliana: *plt3,plt5-2,plt7*	(Prasad et al., 2011)	N/A
A.thaliana: *pin1,pin3,pin4,pin7*	(Verna et al., 2019)	N/A
A.thaliana: *plt3,plt5-2,plt7; pPLT7::cPLT1-vYFP*	(Kareem et al., 2015b)	N/A
A.thaliana: *plt3,plt5-2,plt7;pPLT7::cPLT1-vYFP;35S::CUC2:3AT*	(Kareem et al., 2015b)	N/A
A.thaliana: *Columbia;pG1090:XVE::PINOID:vYFP*	received from Dr Ari Pekka Mähönen	N/A
A.thaliana: *xth9* (insertion in 3'UTR)	(P. Xu & Cai, 2019)	N/A
A.thaliana: *Columbia;pPIN1::gPIN1:GFP*	(Gordon et al., 2007;	N/A

	Kareem et al., 2015b)	
A.thaliana: *Columbia;pG1090:XVE::axrr3-1:RFP*	Siligato et al., 2016	N/A
A.thaliana: *Columbia;35S::CUC2:GR,*	This study	N/A
A.thaliana: *Columbia;pXTH9::gXTH9:YFP, pPIN1::gPIN1:GFP*	This study	N/A
A.thaliana: *Columbia;pG1090:XVE::XTH9dsRNAi, pPIN1::gPIN1:GFP*	This study	N/A
A.thaliana: *Columbia;pG1090:XVE::CUC2dsRNAi,*	This study	N/A
A.thaliana: *Columbia;pG1090:XVE::PIN1dsRNAi,*	This study	N/A
A.thaliana: *Columbia;pG1090:XVE::Cas9p-tagRFP-XTH9 in pXTH9::XTH9-vYFP*	This study	N/A
A.thaliana: *Columbia;pG1090:XVE::dCas9p-XTH9 in pXTH9::XTH9-vYFP*	This study	N/A
A.thaliana: *xth9*(insertion in 3'UTR)*; pXTH9::XTH9-vYFP*	This study	N/A
A.thaliana: *xth9*(insertion in 3'UTR)*;*	This study	N/A

pPIN1::gPIN1:GFP		
A.thaliana: *cuc2-3;pCUC2::XTH9: vYFP, pPIN1::gPIN1:GFP*	This study	N/A
A.thaliana: *Columbia;pCUC2::gCUC2:YFP, pPIN1::gPIN1:GFP*	This study	N/A
A.thaliana: *Columbia;pWUS::CUC2-vYFP:tWUS, pPIN1::gPIN1:GFP*	This study	N/A
A.thaliana: *plt3,plt5-2,plt7;;pCYCB1;1::CYCB1;1-vYFP*	This study	N/A
A.thaliana: *Columbia;pG1090:XVE::cXTH9-vYFP, pPIN1::gPIN1:GFP*	This study	N/A
A.thaliana: *pid,wag1,wag2; pPIN1::gPIN1:GFP*	This study	N/A
A.thaliana: *pid,wag1,wag2; pCUC2::gCUC2:YFP, pPIN1::gPIN1:GFP*	This study	N/A
A.thaliana: *pid,wag1,wag2; pXTH9::gXTH9:YFP, pPIN1::gPIN1:GFP*	This study	N/A
A.thaliana:	This study	N/A

Columbia;pG1090:XVE::Cas9p-tagRFP-gCUC2 sgRNA cassettes*; pCUC2::gCUC2:YFP*		
A.thaliana: *Columbia;pG1090:XVE::dCas9p-gCUC2 sgRNA* cassettes; *pCUC2::gCUC2:YFP*	This study	N/A
A.thaliana: *cuc1-5;pPIN1::gPIN1:GFP*	This study	N/A
A.thaliana: *Columbia;pG1090:XVE::XTH9dsRNAi*	This study	N/A
A.thaliana: *cuc2-3;pPIN1::gPIN1:GFP*	This study	N/A
A.thaliana: *Columbia;pG1090:XVE::PINOID:vYFP , pPIN1::gPIN1::GFP*	This study	N/A
A.thaliana: *plt3,plt5-2,plt7; pPLT3::gOsPLT1-vYFP*	This study	N/A
A.thaliana: *plt3,plt5-2,plt7; pPLT5::gOsPLT2-vYFP*	This study	N/A
A.thaliana: *Columbia;pWUS::XTH9:tWUS*	This study	N/A
A.thaliana: *Columbia;pWUS::gYUCCA4:tWUS*	This study	N/A

A.thaliana: *Columbia;pLEC1::gLEC1:CFP, pPIN1::gPIN1:GFP*	This study	N/A
A.thaliana: *plt3,plt5-2,plt7; pPLT5::gOsPLT2-vYFP;pCYCB1;1::CYCB1;1-vYFP*	This study	N/A
A.thaliana: *cuc1-5,cuc2-3; CUC3dsRNAi,*	This study	N/A

Table 8.4: Recombinant DNA used for the study

RECOMBINANT DNA	SOURCE	IDENTIFIER
p35S::gCUC2-GR	This study	N/A
pXTH9::gXTH9-vYFP	This study	N/A
pPIN1::gPIN1-nGFP	(Kareem et al., 2015b)	N/A
pPLT7::cPLT1-vYFP	(Kareem et al., 2015b)	N/A
pG1090:XVE::PINOID:vYFP	This study	N/A
pCYCB1;1::cCYCB1;1-vYFP	This study	N/A
pG1090:XVE::cXTH9-vYFP	This study	N/A
pG1090:XVE::Cas9p-tagRFP-gXTH9 sgRNA cassettes	This study	N/A
pG1090:XVE::dCas9p-gXTH9	This study	N/A

sgRNA cassettes		
pG1090:XVE::Cas9p-tagRFP-gCUC2 sgRNA cassettes	This study	N/A
pG1090:XVE::dCas9p- gCUC2 sgRNA cassettes	This study	N/A
pG1090:XVE::XTH9dsRNAi	This study	N/A
pG1090:XVE::CUC2dsRNAi	This study	N/A
pG1090:XVE::PIN1dsRNAi	This study	N/A
pCUC2::gXTH9:vYFP	This study	N/A
pCUC2::gCUC2:vYFP	This study	N/A
pPLT3::gOsPLT1-vYFP	This study	N/A
pPLT5::gOsPLT2-vYFP	This study	N/A
pWUS::XTH9:tWUS	This study	N/A
pWUS::YUCCA4:tWUS	This study	N/A
pWUS::gCUC2-vYFP:tWUS	This study	N/A
pLEC1::gLEC1:vYFP	This study	N/A
pG1090:XVE::CUC3dsRNAi,	This study	N/A
Vectors used for the study		
p2R3a-VenusYFP-3AT	Addgene	71269
p2R3a-3AT	Addgene	71273
p221k-erTq2CFP	Addgene	71264
pYLsgRNA-AtU3b	Addgene	66198

pYLsgRNA-AtU3d	Addgene	66200
pYLsgRNA-AtU6-1	Addgene	66202
pYLsgRNA-AtU6-29	Addgene	66203
2R3z-Bsa I-ccdB-Bsa I	Addgene	118389
p221z-CAS9p-TagRFP-t35s	Addgene	118386
p221z-dCAS9p-t35s	Addgene	118387
pFG7m34GW	Addgene	133747
pIR4-pG1090:XVE	(Zuo et al., 2000)	N/A
P1R4-pPLT3	(Prasad et al., 2011)	N/A
p221-3XVENUS-NL	(Nagai et al., 2002)	N/A
pGEM-TP4P1R	(Shimotohno et al., 2018)	N/A
pGEMteasy221	(Shimotohno et al., 2018)	N/A
pGEMteasyP2RP3	(Shimotohno et al., 2018)	N/A
pCAM-Kan-R4R3	Addgene	71275
pCAM-Hyg-R4R3	Addgene	71274

Table 8.5: Gene accession number used for the study

Gene name	Locus ID	
CUC2	AT5G53950	N/A
XTH9	AT4G03210	N/A
PIN1	AT1G73590	N/A
PLT3	AT5G10510	N/A
PLT5	AT5G57390	N/A
CYCB1;1	AT4G37490	N/A
PINOID	AT2G34650	N/A
PIN3	AT1G70940	N/A
PIN4	AT2G01420	N/A
PIN7	AT1G23080	N/A
WAG1	AT1G53700	N/A
WAG2	AT3G14370	N/A
YUCCA4	AT5G11320	N/A
OsPLT1	Os04g0653600	N/A
OsPLT2	Os06g0657500	N/A

8.2 RESOURCE AVAILABILITY

Lead Contact

Further information and requests for resources should be directed to and will be fulfilled by the Lead Contact, Kalika Prasad (kalika.prasad@iiserpune.ac.in).

Materials Availability

Plasmids and transgenic plant lines generated in this study will be made available on request

to the lead contact. This study did not generate new unique reagents.

Data and Code Availability

RNA-Seq & ChIP-Seq been deposited at NCBI Gene Expression Omnibus and are publicly available as of the date of publication GEO: PRJNA848450 (http://www.ncbi.nlm.nih.gov/sra/PRJNA848450)

Raw data from main figures 1-7 & supplementary figures S1-S14 were deposited on Mendeley at https://data.mendeley.com/datasets/vxpxd3hh4p/draft?a=f5d50289-ffd9-41f3-8774-36a60bea2aee

8.3 EXPERIMENTAL MODEL AND SUBJECT DETAILS

Arabidopsis thaliana Columbia (Kareem et al., 2015b) ecotype was used as a wildtype for this study. The origin of mutants, such as single mutant *xth9* (insertion in 3'UTR)(P. Xu & Cai, 2019), *cuc2-3*(Hibara et al., 2006), *cuc1-5* (Hibara et al., 2006) and *pin1-1*(Sawchuk et al., 2013), double mutant *cuc1-5,cuc2-3* (Hibara et al., 2006), *pid,wag1,wag2* (Dhonukshe et al., 2015), and *plt3,plt5-2,plt7* triple mutant (Prasad et al., 2011); and *pin1,pin3,pin4,pin7* quadruple mutant (Verna et al., 2019) as previously described. *plt3,plt5-2,plt7; pPLT7::cPLT1-vYFP* (Kareem et al., 2015b), *plt3,plt5-2,plt7; pPLT7::cPLT1-vYFP;35S::CUC2:3AT* (Kareem et al., 2015b) *are used as previously described.* Translational fusion constructs of *G1090:XVE::PINOID:vYFP and G1090:XVE::axR3:RFP* in WT *(received from Dr Ari Pekka Mähönen), 35S::CUC2:GR, pXTH9::gXTH9:vYFP, pG1090:XVE::XTH9dsRNAi, pG1090:XVE::CUC2dsRNAi, pG1090:XVE::PIN1dsRNAi, pG1090:XVE::Cas9p-tagRFP-gXTH9;pXTH9::gXTH9-vYFP, pG1090:XVE:: dCas9p-gXTH9;pXTH9::gXTH9-vYFP, pCUC2::gXTH9:vYFP, pCLASP::vYFP-gCLASP:3AT, pCUC2::gCUC2:vYFP, pWUS::CUC2-vYFP:tWUS, pWUS::XTH9:tWUS, pWUS::YUC4:tWUS pCYCB1;1::CYCB1;1-vYFP, pG1090:XVE::cXTH9-vYFP, pPLT3::gOsPLT1-vYFP,* and *pPLT5::gOsPLT2-vYFP* in wildtype or mutant backgrounds of *Arabidopsis* by floral-dipping method(Clough & Bent, 1998) (Table 8.3-8.4).

Plant Growth Conditions

Arabidopsis thaliana seeds used for the study surface were sterilized by 70% ethanol followed by 20% sodium hypochlorite. The seeds were rinsed seven times with distilled water and stored at $4^{O}C$ for 4 days for the vernalization process. The seeds were plated on half-strength Murashige and Skoog (MS) growth medium with 0.8% plant-based agar and grown under 45 µmol/m2/s continuous white light at 22°C and 70% relative humidity.

8.4 METHOD DETAILS

8.4.1 Regeneration assay

The regeneration assay was carried out as mentioned in the previous study(Kareem et al., 2015b). The explants used for the study were root and hypocotyl collected from 7-day old plants i.e., 7 days post-germination (dpg) grown on 1/2MS (2.15g MS salt, 10g sucrose, 0.7% plant-based agar). The explants were then incubated on callus induction medium- CIM (3.2g Gamborg B5 salt mixture, 20g D-Glucose, 0.5g MES hydrate, 1ml 1000x Gamborg's vitamin solution and 0.7% plant-based agar. 0.5µg/ml 2,4-D and 0.05µg/ml kinetin used as hormones). After 8-day incubation on CIM, the explants were transferred to shoot induction medium (SIM) and incubated for 30 days (4.3g MS salt, 10g sucrose, 0.5g MES hydrate, 1ml 1000x Gamborg's vitamin solution, 1ug/ml d-Biotin and 0.7% plant-based agar (10 µM trans-zeatin used as an external hormonal inductive cue). SIM supplemented with estradiol steroid (5µM) was used for gene over-expression or silencing controlled by *G1090:XVE* artificial promoter for 24Hr or 48Hr on 8^{th} day SIM, or throughout the incubation on SIM duration (0-30^{th} day SIM) for this study. The number of shoots per explant (size of one explant taken as 2cm length) were scored after 30 days of SIM and mentioned as a graphical representation in the figures.

8.4.2 Plasmid construction and molecular cloning

Most of the gene constructs used for the study were generated in the lab (KEY RESOURCES TABLE 3). The sequence of interest was isolated from total genomic DNA prepared from the manual CTAB method. Polymerase chain reaction (PCR) was carried out

using Phusion polymerase (NEB-Biolabs). The PCR conditions were specific to each sequence and amplified using 10uM sequence-specific paired primers (see Supplementary Table:1) using BIO-RAD C1000 Touch^{TM} thermal cycler. All entry clones were propagated in DH5α strain of *E.coli* using a single gateway cloning system. To generate *pXTH9::gXTH9:vYFP* construct, 2.3Kb upstream regulatory element of *XTH9* and 1.176Kb of *XTH9* was cloned separately and incorporated yellow fluorescent protein (YFP) sequence as a reporter. To knock down the expression of *XTH9*, 337bp exon sequence was amplified from *cDNA* using region-specific primers and incorporated in the sense and antisense vector by single gateway cloning system. The sense and antisense for *XTH9* cloned under *pG1090* inducible promoter (Zuo et al., 2000) in *pCAMBIA* based *R4R3* destination vector. Similarly, the CUC2 (324bp) and PIN1 (304bp) knockdown constructs were cloned under *pG1090* inducible promoter to silence the transcript level of *CUC2* and *PIN1* respectively. *35S::CUC2:GR* was cloned by fusing *CUC2* (1.8 Kb) in-frame to rat glucocorticoid receptor- GR(Aoyama & Chua, 1997) under *35S* constitutive promoter. CYCLINB1;1, markers used for cell division in the study, d- BOX sequence (0.348Kb) amplified from cDNA and cloned under *CYCB1;1* (4.7Kb) regulatory sequence incorporated with YFP reporter. In *pWUS::gCUC2-vYFP*, the 2nd box was designed as a fusion of *CUC2-YFP* (YFP sequence at 3'end of the gene) sequence and terminator of WUS (1.6kb downstream of WUS gene) cloned in 3rd box *tWUS* to express CUC2 in the WUS domain. In the same way XTH9 and YUCCA4 genes were inserted under WUS promoter. The *CUC2-YFP* sequence amplified from *pCUC2::gCUC2:YFP* clone using 2nd box specific primers (see Supplementary Table:1). *XTH9* cDNA (341bp) was cloned under the control of *pG1090* tagged with *vYFP* to create an overexpression line for the study. To generate *pCUC2::gXTH9:vYFP, XTH9* gene was combined under *CUC2* promoter tagged with *vYFP* reporter. PLT3 promoter (7.7Kb) has used to drive *Rice* OsPLT1 tagged with vYFP to deliver the *Rice* PLETHORA in PLT3 domain. Similarly, *Rice* OsPLT2 was cloned under Arbidopsis PLT5 prmoter (5.6Kb). The sequence of g*PINOID* (1.621Kb) and *YFP* were cloned under *pG1090:XVE* to generate inducible overexpression of *PINOID.* To create a *CUC3* dsRNAi construct, ~518bp from last exon has selected and cloned under inducible *pG1090* promoter. The promoter was cloned in pGEM-TP4P1R, the gene was cloned in pGEMteasy221 and reporter or terminator were cloned in pGEMteasyP2RP3 (Shimotohno

et al., 2018). The entry clones were combined in pCAMBIA3100 based destination vector using three fragments multisite recombination gateway cloning system (Invitrogen).

8.4.3 Quantitative Real Time-PCR

*35S::gCUC2:GR;*WT explants were treated with liquid MS medium containing 20µM Dexamethasone for 8Hr or 4Hr on the 8th day of SIM incubation. The mock treatment was performed using in liquid MS medium containing 20µM Dimethyl sulfoxide (DMSO-sigma). The callus was collected separately for RNA extraction for further quantification. To determine differential expression of gene-of-interest in the *pid,wag1,wag2* (Dhonukshe et al., 2015), *pin1,pin3,pin4,pin7* (Verna et al., 2019), *cuc2-3* (Hibara et al., 2006), *plt3,plt5-2, plt7* (Prasad et al., 2011), *PLT7::PLT1:YFP; plt3,plt5-2, plt7* (Kareem et al., 2015b), *PLT7::PLT1:YFP, 35S::CUC2:3AT; plt3,plt5-2, plt7* (Kareem et al., 2015b) mutant compared to wildtype, the calli were harvested on 8th day of SIM incubation. The calli were harvested and stored at -80^{o}C for further procedures. Total RNA extracted from all the samples for the quantification using Nucleospin RNA plant extraction kit were subjected to DNase treatment according to the manual guidelines. 1µg of *cDNA* synthesis was carried out using PrimeScript 1st strand *cDNA* synthesis kit. The paired primers are designed with the NCBI Primer-Blast tool. quantitativeRT-PCR was performed in 25µl of the total volume containing 12.5µl TB Green Master mix and 100nM gene-specific primers (Supplementary Table:1) with 200ng of *cDNA* per reaction in QuantStudio^{TM} 5 Real-Time PCR. All the reactions were performed from RNA extracted from three different biological samples and each biological sample was tested with three technical replicates. -$\Delta\Delta C^{T}$ was calculated to represent the relative expression of gene in all graphical representations (Kareem et al., 2015b; Radhakrishnan et al., 2020).

8.4.4 Microscopic live imaging

Bright-field images of *de novo* shoots from the calli were captured using Leica M205FA stereo microscope. Confocal laser scanning microscopic time-lapse and time-point images were acquired using Zeiss LSM 880 and Leica TCS SP5 II confocal laser-scanning microscope as described previously (Kareem et al., 2015b; Radhakrishnan et al., 2020). The live imaging of callus was done using a 40x water dipping objective and time-point images

of the root have done using 20x (air) objective. The progenitors were located using a 10X air objective and images were captured using 40X water dipping objective. For the live imaging of the callus tissue, a small piece of green callus was pinched-off from the explant and fixed in 35 mm sterile petri-dish containing SIM or SIM with supplemented with steroid using melted agar. Droplets of slightly cooled melted agar were used to fix the sides of the callus onto the SIM media in the 35mm petri-dish. This ensured that the callus piece was not floating in the water during the live imaging using the 40X water dipping objective. The progenitors were followed till they matured into meristem. Each stage of a progenitor was captured with the same settings as that of day1 of progenitor spotting. The progenitor stage is denoted by the number of superficial progenitor cells. The imaging was performed using 50% laser power of Argon (488nm- for GFP, 514nm-for YFP and 561nm-for PI as excitation wavelength), 600-800 master gain with 50-200 range pinhole and frame size to 1, 024 by 1, 024 pixels, the line averaging adjusted to two and the digital zoom to 0.6. Master gain and the pinhole adjustment varied with samples. Z-stack images were taken in 5µM or 1µM intervals and auto-fluorescence was captured at wavelength of 633nm. Filter-sterilized 20µg/ml propidium iodide (PI) was used to stain the cell wall.

8.4.5 Treatments

8.4.5.1 Estradiol treatment to progenitors for live imaging

The progenitors located using confocal based live imaging were treated with liquid SIM supplemented with 5µM Estradiol by direct local application on the progenitors for 20minutes (short pulse). The transiently treated samples were washed with sterile milliQ post treatment and transferred onto solid SIM supplemented with 5µM estradiol for sustained induction, or solid simply SIM for further incubation.

8.4.5.2 Propidium iodide staining

To visualize the cell wall, the callus was treated with 20µg/ml Filter sterilized Propidium Iodide (PI) for 20 minutes. The progenitors were imaged using Zeiss LSM 880 and then washed with sterile milliQ to remove the stain before further growth incubation to capture live imaging in different time points (0Hr, 5Hr 30 mins, 9Hr and 24Hr).

8.4.6 Inducible CRISPR-Cas9 genome editing

The cassettes were designed as previously described (Ma et al., 2015; X. Wang et al., 2020). The *sgRNA* scaffold and promoter driving *sgRNA* cassette amplified from the vectors, *pYLsgRNA-AtU3b* (Addgene, no. 66198), *pYLsgRNA-AtU3d* (Addgene, no. 66200), *pYLsgRNA-AtU6-1* (Addgene, no. 66202) or *pYLsgRNA-AtU6-29* (Addgene, no. 66203). The PCR was performed using 10µM common primer (U-F, gR-R) and chimeric primers designed in such a way that the primer sequence of the promoter included PAM sequences (T) (AtU3/6T#- and gRT#+ (Table 8.1). To amplify the promoter, primers were designed in such a way that promoter (AtU3/6) specific at the 3'end added with target sequence at 5'end as a reverse primer and U-F as a common forward primer. Similarly, gR-R common reverse primer and chimeric forward primer, which includes sgRNA specific at 3'end and target sequence at 5'end to amplify the *sgRNA* scaffold. The purified individual amplicon of promoter and sgRNA scaffold incorporated with target sequence overlapped by the second round of PCR (overlap PCR) using Bsa I-containing primers Pps/Pgs. 4 sgRNA cassettes were combined using Golden Gate assembly. The Golden gate was performed using 120ng destination vector (*2R3z-Bsa I-ccdB-Bsa I*), 90 ng each purified *sgRNA* expression cassette, T4 DNA Ligase (20U), Bsa I-HF V2 (20U), 10X T4DNA Ligase buffer with 10 mMATP and nuclease-free water to make up to 20 µl. The reaction cocktail was incubated at 37^{O}C for 5min and 16^{O}C for 5min repeated for 30 cycles. The reaction setup was heated at 60^{O}C for 5 min before the transformation into *E.coli*. The clone that carries 4 *sgRNA* cassettes which are designed to target *gXTH9* as well as *gCUC2* were created separately in the same manner. After successive *sgRNA* expression cassettes of *gXTH9* and *gCUC2* cloned in the 3rd box cloning vector, combined with 2nd box *Cas9p-TagRFP* (Addgene, no. 118386) or *dCas9p-t35S* (Addgene, no. 118387) under *pG1090::XVE* (1st box) promoter (Zuo et al., 2000) using multisite recombination gateway cloning system (Invitrogen) in *pFG7m34GW* (Addgene, no. 133747) as a final destination vector to generate *pG1090:XVE::Cas9p-tagRFP-gXTH9 sgRNA* cassettes, *pG1090:XVE::dCas9p-gXTH9 sgRNA* cassettes, *pG1090:XVE::Cas9p-tagRFP-gCUC2 sgRNA* cassettes, and *pG1090:XVE::dCas9p- gCUC2 sgRNA* cassettes respectively. WT/*pXTH9::gXTH9: vYFP* and WT/*pCUC2::gCUC2: vYFP* plants were

infected with the C58 strain of Agrobacterium with inducible genome editing (IGE) construct respectively for developing successive transgenic lines. Positive lines of IGE were initially selected using a seed-coat tagged with fluorescence reporter (green), further selected by inducing the Cas9 activity in the WT/*pXTH9::gXTH9: vYFP* and in WT/*pCUC2::gCUC2: vYFP* translational fusion line using 5µM estradiol for 24hr or 48hr treatment respectively. These lines were further used for the experiments.

8.4.7 PIN1 polarity quantification

Multipoint and angle tools in Fiji software were used to quantify PIN1 polarity from a cell membrane region facing the wall of a cell in the productive progenitor as well as in the pseudo-progenitor, as previously described in(Nakayama et al., 2012) combined with angle measurement. Propidium iodide staining was used to identify the cell boundary and designate it as a boundary so that the centroid (white central mark inside the cell) could be calculated. To construct a connecting line between the point and the centroid, a point has been placed at the top, parallel to the centroid. A 0º angle is defined as the top point (white mark outside the cell). To measure the intensity of localized PIN1-GFP fluorescence, the Multipoint tool was used to choose pixels from the cell membrane. These three points were used to calculate the angle of multipoint (yellow cross) marked in the membrane from the 0º angle point to measure the intensity. The mean intensity gray values from each multipoint have been measured in correspondence with the angle from 0º-360º (multipoint counting may vary depending upon the area of a wall). Likewise, the intensity and corresponding angle were measured from a total of 94 cells from 6 different productive progenitors and a total of 73 cells from 6 pseudo-progenitors. The subset of Z-stack images was selected to quantify the amount of PIN1 localized on the membrane. The mean intensity grayscale value of ROI and corresponding angle were represented as a scatter plot. The angle of polarization was marked in the representative images (see the Fig1J, 1K) based on the peak values obtained from the graphical representation.

Another approach to assess the PIN1 polarity of a cell according to the arc and curvature of a cell and the localization protein on the membrane by using Blue to Yellow standard LUTs tools in ZEN2.3 SP1 black edition image processing software. Z-stack images of 1µm maximum intensity projection was used to analyse the polarity orientation in the cell and

marked the polarity of the cells in the representative figures (see the Fig1L, 1M).

8.4.8 RNA sequencing

In order to perform genome-wide transcriptome analysis, *plt3,plt5-2,plt7/pPLT7::cPLT1-vYFP*, *plt3,plt5-2,plt7/pPLT7:cPLT1-vYFP,35S::CUC2-3AT* and WT/35S::CUC2:GR explants were prepared as mentioned above and incubated till 8day on SIM. WT/*35S::CUC2:GR* calli were treated with 20µM DEX in liquid MS medium for 8Hr before collecting the samples, the DMSO (20 µM) was used as a mock treatment. The callus harbouring regeneration foci were dissected from 20 explants and pooled together for each biological replicate and used to extract total RNA using Nucleospin RNA plant extraction kit. 150bp single-end, as well as paired-end Illumina Hiseq 2500 and library construction, were performed by Fasteris, Life Science Genesupport SA is in Plan-Les-Ouates (GE), Switzerland.

Two independent biological replicates were filtered before the data analysis to obtain good quality reads for downstream analysis. The evaluation of RNA-Seq raw reads was done using FastQC quality control tool (http://www.bioinformatics.babraham.ac.uk/projects/fastqc/) and the reads were filtered using Trimmomatic software (https://github.com/usadellab/Trimmomatic) (Bolger et al., 2014) to remove the adapter sequences and trim the base with the cut off Q30. The reference genome (gff file) of *Arabidopsis thaliana* (TAIR10) has been downloaded (https://www.arabidopsis.org/download/indexauto.jsp?dir=%2Fdownload_files%2FGenes%2FTAIR10_genome_release%2FTAIR10_gff3) and converted into gtf format using gffread (https://anaconda.org/bioconda/gffread)(G. Pertea & Pertea, 2020). Further, the clean reads were mapped to the reference genome using HISAT2 (http://daehwankimlab.github.io/hisat2/) (D. Kim et al., 2015) followed by StringTie (https://ccb.jhu.edu/software/stringtie/)(M. Pertea et al., 2016) to generate potential transcripts. The quantification of the mapped reads has been done using featureCounts (http://subread.sourceforge.net/)(Liao et al., 2014), and quantified data (FPKM) was subjected to DESeq2 (https://bioconductor.org/packages/release/bioc/html/DESeq2.html) (Love et al., 2014) for differential gene expression. The genes exhibiting more than a 1.24-fold change in gene expression (0.3 ratios of Log2 value) and P-Value < 0.05 were considered differentially expressed genes for gene ontology. The gene ontology has been

done using the Panther analysis tool (http://www.pantherdb.org/) (Thomas et al., 2003), with *Arabidopsis thaliana* (TAIR10) genome ontology as the background.

8.4.9 ChIP followed by Next-Generation Sequencing

To identify the direct targets of CUC2 protein, we performed Chromatin immunoprecipitation (ChIP) followed by next-generation sequencing as described previously (Salvi et al., 2020; Yamaguchi et al., 2014). The callus of *pCUC2::gCUC2:YFP* in Col-0 incubated on SIM and dissected from the 100 explants harbouring the shoot progenitor at the onset of progenitor formation (8-10 day on SIM) and pooled together. It was used as a sample for the experiment. The callus tissue was fixed in 1.8% formaldehyde in 1X PBS and vacuum infiltrated for 20 min at room temperature to cross-link the plant tissue. Washed off the solution and cold 0.125 M glycine solution (in 1X PBS) was added followed by vacuum infiltration for 5 min to quench the reaction. The solution was filtered away and removed wet using Kin-wipes. Tissue was frozen in Liquid Nitrogen. The frozen tissue was powdered in the Liquid Nitrogen, resuspended in Nuclei extraction buffer (50mM Tris-HCl pH 7.5, 150mM NaCl, 1% Triton X-100, 0.1% Na deoxycholate, 2.5mM EDTA, 10% glycerol, supplemented with 1X protease inhibitor cocktail (Roche,) and 1mM PMSF (Sigma) and filtered the solution using 40µM cell strainer (BD Falcon). Centrifuge the content at $4^{O}C$ to pellet the nuclei. Resuspend the pellet in ice-cold Nuclei lysis buffer (50mM Tris-HCl pH 8, 5mM EDTA pH 8, 0.5% SDS). The solution was sonicated for 8 cycles of 10 seconds with 15sec gap at 35% amplitude (Branson Sonifier, Marshall Scientific). 1.1%triton was added to the sonicated sample and centrifugated to isolate the supernatant. Preclearing of the sample has done by adding 20µl of Dynabeads protein G (Novex Life technologies, cat. no. 10003D) and incubated at 4˚C for 2hr. An aliquot of the sample is stored as Input for the experiment. The sample was treated with rabbit polyclonal antibody to GFP (ab290; Abcam) overnight and Dynabeads protein was added to immunoprecipitate the DNA fragment for 5 hr. Sequential washes were performed in the beads using cold low salt wash buffer (150 mM NaCl, 0.2% SDS, 0.5% Triton X-100, 2 mM EDTA pH 8, 20 mM Tris-HCl pH 8), cold high salt wash buffer (500 mM NaCl,.2% SDS, 0.5% Triton X-100, 2 mM EDTA pH 8, 20 mM Tris-HCl pH 8), cold 250mM LiCl wash buffer (0.25 M LiCl, 0.5% IGEPAL, 0.5% sodium deoxycholate, 1 mM EDTA pH 8,

10 mM Tris-HCl pH 8) and 0.5X TE. Repeated the step one more time. Collected the magnetic beads and resuspended in TES (25mM Tris-HCl pH 8, 5mM EDTA pH 8, 0.5% SDS). 5M NaCl was added to the sample and input control to reverse the cross-links overnight at 65˚C. DNA fragments were purified using a PCR purification kit (Cat #28106,Qiagen). 150bp paired-end Illumina NovaSeq 6000 and library construction were performed and Libraries were validated using Qubit and Agilent TapeStation by AgriGenome Labs Pvt Ltd –Kochi, India.

The reads from both Input and ChIP libraries were aligned to the *Arabidopsis* genome, TAIR10 by Bowtie version 2.2.4 (Langmead et al., 2009) with the following settings ‘‘-k 1 –local -no-unal –sam’’. Duplicated reads, reads with low mapping quality, mitochondrial and plastid reads were identified and removed with Samtools version 1.2 (H. Li et al., 2009). Enriched intervals between IP sample and its relative Input were identified by MACS2 (version 2.0.10) program (Y. Zhang et al., 2008) with following settings ‘‘BAMPE, -g 1.35e8, and -q 0.05’’ (Anderson et al., 2018; Ezer et al., 2017; Gallego-Bartolomé et al., 2019; Wei et al., 2021). The generated BedGraph file were converted into bigWig file using bedGrapghTobigwig script (Kent et al., 2010). BigWig and BedGraph files were visualized with the Integrated Genome Browser (https://bioviz.org) to observe the protein binding on the chromatin. MEME

8.4.10 Statistical analysis

Statistical analysis was performed for all the experiment and quantification data. Welch’s Two Sample t-test and unpaired & paired t-test was used for regeneration assay, quantitative RT-PCR microtubule quantification. Statistical analysis for auxin quantification and growth differential quantification was performed by using Mann-Whitney U test. Length to breadth ratio statistically tested using Two sample paired t test. R programming was used for all the statistical analysis of quantitative RT-PCR, length to breadth ratio, microtubule and auxin quantification. Kruskal-Wallis one-way ANOVA was used to analyze the quantification of PIN1 and analysed using Origin programing. TAIR10 by bowtie version 2.2.4, MACS2 and Integrated Genome Browser (IGB) used to analyse the data of ChIP-sequencing. Genome-wide transcriptome analysis was performed using tools such as FastQC, Trimmomatic software, HISAT2 and DESeq2.

Chapter 9

Reference

Aichinger, E., Kornet, N., Friedrich, T., & Laux, T. (2012). Plant Stem Cell Niches. *Annual Review of Plant Biology*, *63*(1), 615–636. https://doi.org/10.1146/annurev-arplant-042811-105555

Aida, M., Beis, D., Heidstra, R., Willemsen, V., Blilou, I., Galinha, C., Nussaume, L., Noh, Y.-S., Amasino, R., & Scheres, B. (2004). The PLETHORA Genes Mediate Patterning of the Arabidopsis Root Stem Cell Niche. *Cell*, *119*(1), 109–120. https://doi.org/10.1016/j.cell.2004.09.018

Aida, M., Beis, D., Heidstra, R., Willemsen, V., Blilou, I., Galinha, C., Nussaume, L., Noh, Y., Amasino, R., Scheres, B., Univ-me, U. M. R. C. C. E. A., & Paul, F.- Saint. (2004). of the Arabidopsis Root Stem Cell Niche. *Cell*, *119*, 109–120.

Aida, M., Ishida, T., Fukaki, H., Fujisawa, H., & Tasaka, M. (1997). Genes involved in organ separation in Arabidopsis: An analysis of the cup-shaped cotyledon mutant. *Plant Cell*, *9*(6), 841–857. https://doi.org/10.1105/tpc.9.6.841

Aida, M., Ishida, T., & Tasaka, M. (1999). Shoot apical meristem and cotyledon formation during Arabidopsis embryogenesis: Interaction among the CUP-SHAPED COTYLEDON and SHOOT MERISTEMLESS genes. *Development*, *126*(8), 1563–1570.

Aida, M., & Tasaka, M. (2006). Genetic control of shoot organ boundaries. *Current Opinion in Plant Biology*, *9*(1), 72–77. https://doi.org/10.1016/j.pbi.2005.11.011

Aida, M., Vernoux, T., Furutani, M., Traas, J., & Tasaka, M. (2002). Roles of *PIN-FORMED1* and *MONOPTEROS* in pattern formation of the apical region of the *Arabidopsis* embryo. *Development*, *129*(17), 3965–3974. https://doi.org/10.1242/dev.129.17.3965

Akama, K., Shiraishi, H., Ohta, S., Nakamura, K., Okada, K., & Shimura, Y. (1992). Efficient transformation of Arabidopsis thaliana: comparison of the efficiencies with various organs, plant ecotypes and Agrobacterium strains. *Plant Cell Reports*, *12*(1). https://doi.org/10.1007/BF00232413

Ali, S., Khan, N., & Xie, L. (2020). Molecular and hormonal regulation of leaf morphogenesis in arabidopsis. *International Journal of Molecular Sciences*, *21*(14), 1–31. https://doi.org/10.3390/ijms21145132

Alvarado, A. S., & Tsonis, P. A. (2006). Bridging the regeneration gap: genetic insights from diverse animal models. *Nature Reviews Genetics*, *7*(11), 873–884. https://doi.org/10.1038/nrg1923

Amano, R., Momoi, R., Omata, E., Nakahara, T., Kaminoyama, K., Kojima, M., Takebayashi, Y., Ikematsu, S., Okegawa, Y., Sakamoto, T., Kasahara, H., Sakakibara, H., Motohashi, K., & Kimura, S. (2020). Molecular and Biochemical Differences in Leaf Explants and the Implication for Regeneration Ability in Rorippa aquatica (Brassicaceae). *Plants*, *9*(10), 1372. https://doi.org/10.3390/plants9101372

Amano, R., Nakayama, H., Momoi, R., Omata, E., Gunji, S., Takebayashi, Y., Kojima, M., Ikematsu, S., Ikeuchi, M., Iwase, A., Sakamoto, T., Kasahara, H., Sakakibara, H., Ferjani, A., & Kimura, S. (2019). Molecular Basis for Natural Vegetative Propagation via Regeneration in North American Lake Cress, Rorippa aquatica (Brassicaceae). *Plant and Cell Physiology*, *61*(2), 353–369. https://doi.org/10.1093/pcp/pcz202

Anderson, S. J., Kramer, M. C., Gosai, S. J., Yu, X., Vandivier, L. E., Nelson, A. D. L., Anderson, Z. D., Beilstein, M. A., Fray, R. G., Lyons, E., & Gregory, B. D. (2018). N6-Methyladenosine Inhibits Local Ribonucleolytic Cleavage to Stabilize mRNAs in Arabidopsis. *Cell Reports*, *25*(5), 1146-1157.e3. https://doi.org/10.1016/j.celrep.2018.10.020

Aoyama, T., & Chua, N. H. (1997). A glucocorticoid-mediated transcriptional induction system in transgenic plants. *Plant Journal*, *11*(3), 605–612.

https://doi.org/10.1046/j.1365-313X.1997.11030605.x

Asahina, M., Azuma, K., Pitaksaringkarn, W., Yamazaki, T., Mitsuda, N., Ohme-Takagi, M., Yamaguchi, S., Kamiya, Y., Okada, K., Nishimura, T., Koshiba, T., Yokota, T., Kamada, H., & Satoh, S. (2011). Spatially selective hormonal control of RAP2.6L and ANAC071 transcription factors involved in tissue reunion in *Arabidopsis*. *Proceedings of the National Academy of Sciences*, *108*(38), 16128–16132. https://doi.org/10.1073/pnas.1110443108

Asnacios, A., & Hamant, O. (2012). The mechanics behind cell polarity. *Trends in Cell Biology*, *22*(11), 584–591. https://doi.org/https://doi.org/10.1016/j.tcb.2012.08.005

Atta, R., Laurens, L., Boucheron-Dubuisson, E., Guivarc'h, A., Carnero, E., Giraudat-Pautot, V., Rech, P., & Chriqui, D. (2009). Pluripotency of Arabidopsis xylem pericycle underlies shoot regeneration from root and hypocotyl explants grown *in vitro*. *The Plant Journal*, *57*(4), 626–644. https://doi.org/10.1111/j.1365-313X.2008.03715.x

Baker, C. C., Sieber, P., Wellmer, F., & Meyerowitz, E. M. (2005). The early extra petals1 Mutant Uncovers a Role for MicroRNA miR164c in Regulating Petal Number in Arabidopsis. *Current Biology*, *15*(4), 303–315. https://doi.org/10.1016/j.cub.2005.02.017

Bandurski, R. S., Cohen, J. D., Slovin, J. P., & Reinecke, D. M. (1995). Auxin biosynthesis and metabolism. *Plant Hormones: Physiology, Biochemistry and Molecular Biology*, 39–65.

Bargmann, B. O. R., & Estelle, M. (2014). Auxin perception: in the IAA of the beholder. *Physiologia Plantarum*, *151*(1), 52–61. https://doi.org/10.1111/ppl.12135

Bartel, B. (1997). Auxin biosynthesis. *Annual Review of Plant Biology*, *48*, 51–66. https://doi.org/10.1146/annurev.arplant.48.1.51

Bartel, B., & Fink, G. R. (1995). ILR1, an Amidohydrolase That Releases Active Indole-3-Acetic Acid from Conjugates. *Science*, *268*(5218), 1745–1748. https://doi.org/10.1126/science.7792599

Barton, M. K., & Poethig, R. S. (1993). Formation of the shoot apical meristem in *Arabidopsis thaliana* : an analysis of development in the wild type and in the *shoot meristemless* mutant. *Development*, *119*(3), 823–831.

https://doi.org/10.1242/dev.119.3.823

Bely, A. E., & Nyberg, K. G. (2010). Evolution of animal regeneration: re-emergence of a field. *Trends in Ecology & Evolution*, *25*(3), 161–170. https://doi.org/10.1016/j.tree.2009.08.005

Benjamins, R., Quint, A., Weijers, D., Hooykaas, P., & Offringa, R. (2001). The PINOID protein kinase regulates organ development in *Arabidopsis* by enhancing polar auxin transport. *Development*, *128*(20), 4057–4067. https://doi.org/10.1242/dev.128.20.4057

Benková, E., & Hejátko, J. (2009). Hormone interactions at the root apical meristem. *Plant Molecular Biology*, *69*(4), 383–396. https://doi.org/10.1007/s11103-008-9393-6

Benková, E., Michniewicz, M., Sauer, M., Teichmann, T., Seifertová, D., Jürgens, G., & Friml, J. (2003). Local, Efflux-Dependent Auxin Gradients as a Common Module for Plant Organ Formation. *Cell*, *115*(5), 591–602. https://doi.org/10.1016/S0092-8674(03)00924-3

Bidhendi, A. J., CHEBLI, Y., & GEITMANN, A. (2020). Fluorescence visualization of cellulose and pectin in the primary plant cell wall. *Journal of Microscopy*, *278*(3), 164–181. https://doi.org/10.1111/jmi.12895

Bilsborough, G. D., Runions, A., Barkoulas, M., Jenkins, H. W., Hasson, A., Galinha, C., Laufs, P., Hay, A., Prusinkiewicz, P., & Tsiantis, M. (2011). Model for the regulation of Arabidopsis thaliana leaf margin development. *Proceedings of the National Academy of Sciences of the United States of America*, *108*(8), 3424–3429. https://doi.org/10.1073/pnas.1015162108

Birnbaum, K. D., & Alvarado, A. S. (2008). Slicing across Kingdoms: Regeneration in Plants and Animals. *Cell*, *132*(4), 697–710. https://doi.org/10.1016/j.cell.2008.01.040

Blakeslee, J. J., Peer, W. A., & Murphy, A. S. (2005). Auxin transport. *Current Opinion in Plant Biology*, *8*(5), 494–500. https://doi.org/10.1016/j.pbi.2005.07.014

Blilou, I., Xu, J., Wildwater, M., Willemsen, V., Paponov, I., Friml, J., Heidstra, R., Aida, M., Palme, K., Scheres, B., Billou, I., Xu, J., Wildwater, M., Willemsen, V., Paponov, I., Frimi, J., Heldstra, R., Aida, M., Palme, K., & Scheres, B. (2005). The PIN auxin efflux facilitator network controls growth and patterning in Arabidopsis roots. *Nature*, *433*(7021), 39–44. https://doi.org/10.1038/nature03184

Bolger, A. M., Lohse, M., & Usadel, B. (2014). Trimmomatic: A flexible trimmer for Illumina sequence data. *Bioinformatics*, *30*(15), 2114–2120. https://doi.org/10.1093/bioinformatics/btu170

Borghi, L., Gutzat, R., Fütterer, J., Laizet, Y., Hennig, L., & Gruissem, W. (2010). *Arabidopsis* RETINOBLASTOMA-RELATED Is Required for Stem Cell Maintenance, Cell Differentiation, and Lateral Organ Production . *The Plant Cell*, *22*(6), 1792–1811. https://doi.org/10.1105/tpc.110.074591

Boutté, Y., Crosnier, M.-T., Carraro, N., Traas, J., & Satiat-Jeunemaitre, B. (2006). The plasma membrane recycling pathway and cell polarity in plants: studies on PIN proteins. *Journal of Cell Science*, *119*(7), 1255–1265. https://doi.org/10.1242/jcs.02847

Bowman, J. L., & Floyd, S. K. (2008). Patterning and Polarity in Seed Plant Shoots. *Annual Review of Plant Biology*, *59*(1), 67–88. https://doi.org/10.1146/annurev.arplant.57.032905.105356

Braidwood, L., Breuer, C., & Sugimoto, K. (2014). My body is a cage: Mechanisms and modulation of plant cell growth. *New Phytologist*, *201*(2), 388–402. https://doi.org/10.1111/nph.12473

Brett, C. T., & Waldron, K. W. (1996). *Physiology and biochemistry of plant cell walls* (Vol. 2). Springer Science & Business Media.

Bünning, E. (1952). Morphogenesis in plants. In *Survey of biological progress* (Vol. 2, pp. 105–140). Elsevier.

Bustillo-Avendaño, E., Ibáñez, S., Sanz, O., Sousa Barros, J. A., Gude, I., Perianez-Rodriguez, J., Micol, J. L., Del Pozo, J. C., Moreno-Risueno, M. A., & Pérez-Pérez, J. M. (2017). Regulation of Hormonal Control, Cell Reprogramming, and Patterning during De Novo Root Organogenesis. *Plant Physiology*, *176*(2), 1709–1727. https://doi.org/10.1104/pp.17.00980

Campanale, J. P., Sun, T. Y., & Montell, D. J. (2017). Development and dynamics of cell polarity at a glance. *Journal of Cell Science*, *130*(7), 1201–1207. https://doi.org/10.1242/jcs.188599

Carpita, N. C., & Gibeaut, D. M. (1993). Structural models of primary cell walls in flowering plants: consistency of molecular structure with the physical properties of

the walls during growth. *The Plant Journal*, *3*(1), 1–30. https://doi.org/10.1111/j.1365-313X.1993.tb00007.x

Carpita, N., Tierney, M., & Campbell, M. (2001). *Molecular biology of the plant cell wall: searching for the genes that define structure, architecture and dynamics*. Springer.

Celenza, J. L., Grisafi, P. L., & Fink, G. R. (1995). A pathway for lateral root formation in Arabidopsis thaliana. *Genes & Development*, *9*(17), 2131–2142. https://doi.org/10.1101/gad.9.17.2131

Chang, W., Pedroni, A., Bertuzzi, M., Kizil, C., Simon, A., & Ampatzis, K. (2021). Locomotion dependent neuron-glia interactions control neurogenesis and regeneration in the adult zebrafish spinal cord. *Nature Communications*, *12*(1), 4857. https://doi.org/10.1038/s41467-021-25052-1

Chatfield, S. P., Capron, R., Severino, A., Penttila, P.-A., Alfred, S., Nahal, H., & Provart, N. J. (2013). Incipient stem cell niche conversion in tissue culture: using a systems approach to probe early events in *WUSCHEL* -dependent conversion of lateral root primordia into shoot meristems. *The Plant Journal*, *73*(5), 798–813. https://doi.org/10.1111/tpj.12085

Che, P., Lall, S., & Howell, S. H. (2007). Developmental steps in acquiring competence for shoot development in Arabidopsis tissue culture. *Planta*, *226*(5), 1183–1194. https://doi.org/10.1007/s00425-007-0565-4

Che, P., Lall, S., Nettleton, D., & Howell, S. H. (2006). Gene Expression Programs during Shoot, Root, and Callus Development in Arabidopsis Tissue Culture. *Plant Physiology*, *141*(2), 620–637. https://doi.org/10.1104/pp.106.081240

Chen, X., & Engert, F. (2014). Navigational strategies underlying phototaxis in larval zebrafish. *Frontiers in Systems Neuroscience*, *8*(March), 39. https://doi.org/10.3389/fnsys.2014.00039

Chen, X., Qu, Y., Sheng, L., Liu, J., Huang, H., & Xu, L. (2014). A simple method suitable to study de novo root organogenesis. *Frontiers in Plant Science*, *5*. https://doi.org/10.3389/fpls.2014.00208

Christensen, S. K., Dagenais, N., Chory, J., & Weigel, D. (2000). Regulation of auxin response by the protein kinase PINOID. *Cell*, *100*(4), 469–478. https://doi.org/10.1016/s0092-8674(00)80682-0

Christiaens, F., Canher, B., Lanssens, F., Bisht, A., Stael, S., De Veylder, L., & Heyman, J. (2021). Pars Pro Toto: Every Single Cell Matters. *Frontiers in Plant Science*, *12*. https://doi.org/10.3389/fpls.2021.656825

Clark, L. J., Whalley, W. R., & Barraclough, P. B. (2003). How do roots penetrate strong soil? *Roots: The Dynamic Interface between Plants and the Earth: The 6th Symposium of the International Society of Root Research, 11–15 November 2001, Nagoya, Japan*, 93–104.

Clough, S. J., & Bent, A. F. (1998). Floral dip: a simplified method for Agrobacterium-mediated transformation of Arabidopsis thaliana. *The Plant Journal*, *16*(6), 735–743.

Cooke, T. J., Poli, D., & Cohen, J. D. (2004). Did auxin play a crucial role in the evolution of novel body plans during the Late Silurian-Early Devonian radiation of land plants? In *The Evolution of Plant Physiology* (pp. 85–107). Elsevier. https://doi.org/10.1016/B978-012339552-8/50006-8

Cooke, T. J., Poli, D., Sztein, A. E., & Cohen, J. D. (2002). Evolutionary patterns in auxin action. *Auxin Molecular Biology*, 319–338.

Cooper, J. B., Chen, J. A., Gerrit-Jan, van H., & Varner, J. E. (1987). Hydroxyproline-rich glycoproteins of plant cell walls. *Trends in Biochemical Sciences*, *12*, 24–27. https://doi.org/10.1016/0968-0004(87)90012-0

Cosgrove, D. J. (1999). Enzymes and other agents that enhance cell wall extensibility. *Annual Review of Plant Biology*, *50*(1), 391–417. https://doi.org/10.1146/annurev.arplant.50.1.391

Cosgrove, D. J. (2005). Growth of the plant cell wall. *Nature Reviews Molecular Cell Biology*, *6*(11), 850–861. https://doi.org/10.1038/nrm1746

Cosgrove, D. J. (2016). Plant cell wall extensibility: Connecting plant cell growth with cell wall structure, mechanics, and the action of wall-modifying enzymes. *Journal of Experimental Botany*, *67*(2), 463–476. https://doi.org/10.1093/jxb/erv511

Cosgrove, D. J., & Jarvis, M. C. (2012). Comparative structure and biomechanics of plant primary and secondary cell walls. *Frontiers in Plant Science*, *3*(AUG), 1–6. https://doi.org/10.3389/fpls.2012.00204

Crews, S. T., & Pearson, J. C. (2009). Transcriptional autoregulation in development. *Current Biology*, *19*(6), R241–R246. https://doi.org/10.1016/j.cub.2009.01.015

Crowell, E. F., Gonneau, M., Vernhettes, S., & Höfte, H. (2010). Regulation of anisotropic cell expansion in higher plants. *Comptes Rendus Biologies*, *333*(4), 320–324. https://doi.org/10.1016/j.crvi.2010.01.007

Cruz-Ramírez, A., Díaz-Triviño, S., Blilou, I., Grieneisen, V. A., Sozzani, R., Zamioudis, C., Miskolczi, P., Nieuwland, J., Benjamins, R., Dhonukshe, P., Caballero-Pérez, J., Horvath, B., Long, Y., Mähönen, A. P., Zhang, H., Xu, J., Murray, J. A. H., Benfey, P. N., Bako, L., … Scheres, B. (2012). A Bistable Circuit Involving SCARECROW-RETINOBLASTOMA Integrates Cues to Inform Asymmetric Stem Cell Division. *Cell*, *150*(5), 1002–1015. https://doi.org/10.1016/j.cell.2012.07.017

Cruz-Ramírez, A., Díaz-Triviño, S., Wachsman, G., Du, Y., Arteága-Vázquez, M., Zhang, H., Benjamins, R., Blilou, I., Neef, A. B., Chandler, V., & Scheres, B. (2013). A SCARECROW-RETINOBLASTOMA Protein Network Controls Protective Quiescence in the Arabidopsis Root Stem Cell Organizer. *PLoS Biology*, *11*(11), e1001724. https://doi.org/10.1371/journal.pbio.1001724

Daimon, Y., Takabe, K., & Tasaka, M. (2003). The CUP-SHAPED COTYLEDON genes promote adventitious shoot formation on calli. *Plant and Cell Physiology*, *44*(2), 113–121. https://doi.org/10.1093/pcp/pcg038

De Smet, I., Lau, S., Mayer, U., & Jürgens, G. (2010). Embryogenesis - the humble beginnings of plant life. *The Plant Journal*, *61*(6), 959–970. https://doi.org/10.1111/j.1365-313X.2010.04143.x

Deepak, S., Shailasree, S., Kini, R. K., Muck, A., Mithöfer, A., & Shetty, S. H. (2010). Hydroxyproline-rich Glycoproteins and Plant Defence. *Journal of Phytopathology*. https://doi.org/10.1111/j.1439-0434.2010.01669.x

Dermitzakis, E. T., Reymond, A., & Antonarakis, S. E. (2005). Conserved non-genic sequences — an unexpected feature of mammalian genomes. *Nature Reviews Genetics*, *6*(2), 151–157. https://doi.org/10.1038/nrg1527

Dhonukshe, P., Huang, F., Galvan-Ampudia, C. S., Mähönen, A. P., Kleinevehn, J., Xu, J., Quint, A., Prasad, K., Friml, J., Scheres, B., & Offringa, R. (2015). Plasma membrane-bound AGC3 kinases phosphorylate PIN auxin carriers at TPRXS(N/S) motifs to direct apical PIN recycling. *Development (Cambridge)*, *142*(13), 2386–2387. https://doi.org/10.1242/dev.127415

Dong, J., MacAlister, C. A., & Bergmann, D. C. (2009). BASL Controls Asymmetric Cell Division in Arabidopsis. *Cell*, *137*(7), 1320–1330. https://doi.org/10.1016/j.cell.2009.04.018

Drubin, D. G., & Nelson, W. J. (1996). Origins of cell polarity. *Cell*, *84*(3), 335–344.

Du, Y., & Scheres, B. (2017). PLETHORA transcription factors orchestrate de novo organ patterning during *Arabidopsis* lateral root outgrowth. *Proceedings of the National Academy of Sciences*, *114*(44), 11709–11714. https://doi.org/10.1073/pnas.1714410114

Duclercq, J., Sangwan-Norreel, B., Catterou, M., & Sangwan, R. S. (2011). De novo shoot organogenesis: From art to science. *Trends in Plant Science*, *16*(11), 597–606. https://doi.org/10.1016/j.tplants.2011.08.004

Dumais, J., & Kwiatkowska, D. (2002). Analysis of surface growth in shoot apices. *The Plant Journal*, *31*(2), 229–241. https://doi.org/10.1046/j.1365-313X.2001.01350.x

Durgaprasad, K., Roy, M. V., Venugopal M., A., Kareem, A., Raj, K., Willemsen, V., Mähönen, A. P., Scheres, B., & Prasad, K. (2019). Gradient Expression of Transcription Factor Imposes a Boundary on Organ Regeneration Potential in Plants. *Cell Reports*, *29*(1), 162. https://doi.org/10.1016/j.celrep.2019.08.099

Duval, M., Hsieh, T.-F., Kim, S. Y., & Thomas, T. L. (2002). Molecular characterization of AtNAM: a member of the Arabidopsis NAC domain superfamily. In *Plant Molecular Biology* (Vol. 50).

Efroni, I., & Birnbaum, K. D. (2016). The potential of single-cell profiling in plants. *Genome Biology*, *17*(1), 1–8. https://doi.org/10.1186/s13059-016-0931-2

Efroni, I., Mello, A., Nawy, T., Ip, P.-L. L., Rahni, R., Delrose, N., Powers, A., Satija, R., & Birnbaum, K. D. (2016). Root Regeneration Triggers an Embryo-like Sequence Guided by Hormonal Interactions. *Cell*, *165*(7), 1721–1733. https://doi.org/10.1016/j.cell.2016.04.046

Eulgem, T., Rushton, P. J., Robatzek, S., & Somssich, I. E. (2000). The WRKY superfamily of plant transcription factors. *Trends in Plant Science*, *5*(5), 199–206. https://doi.org/10.1016/S1360-1385(00)01600-9

Evans, M. L. (1984). Functions of Hormones at the Cellular Level of Organization. In *Hormonal Regulation of Development II* (pp. 23–79). Springer Berlin Heidelberg.

https://doi.org/10.1007/978-3-642-67731-1_3

Ezer, D., Jung, J. H., Lan, H., Biswas, S., Gregoire, L., Box, M. S., Charoensawan, V., Cortijo, S., Lai, X., Stöckle, D., Zubieta, C., Jaeger, K. E., & Wigge, P. A. (2017). The evening complex coordinates environmental and endogenous signals in Arabidopsis. *Nature Plants*, *3*(June). https://doi.org/10.1038/nplants.2017.87

Fan, M., Xu, C., Xu, K., & Hu, Y. (2012). LATERAL ORGAN BOUNDARIES DOMAIN transcription factors direct callus formation in Arabidopsis regeneration. *Cell Research*, *22*(7), 1169–1180. https://doi.org/10.1038/cr.2012.63

Feldman, L. J. (1976). The de novo origin of the quiescent center regenerating root apices of Zea mays. *Planta*, *128*(3), 207–212. https://doi.org/10.1007/BF00393230

Feldman, L. J. (1985). Root gravitropism. *Physiologia Plantarum*, *65*(3), 341–344. https://doi.org/10.1111/j.1399-3054.1985.tb02405.x

Feraru, E., Feraru, M. I., Kleine-Vehn, J., Martinière, A., Mouille, G., Vanneste, S., Vernhettes, S., Runions, J., & Friml, J. (2011). PIN polarity maintenance by the cell wall in Arabidopsis. *Current Biology*, *21*(4), 338–343. https://doi.org/10.1016/j.cub.2011.01.036

Finet, C., & Jaillais, Y. (2012). AUXOLOGY: When auxin meets plant evo-devo. *Developmental Biology*, *369*(1), 19–31. https://doi.org/10.1016/j.ydbio.2012.05.039

Forman, J. J., Legesse-Miller, A., & Coller, H. A. (2008). A search for conserved sequences in coding regions reveals that the *let-7* microRNA targets Dicer within its coding sequence. *Proceedings of the National Academy of Sciences*, *105*(39), 14879–14884. https://doi.org/10.1073/pnas.0803230105

Friml, J., Benková, E., Blilou, I., Wisniewska, J., Hamann, T., Ljung, K., Woody, S., Sandberg, G., Scheres, B., Jürgens, G., & Palme, K. (2002). AtPIN4 Mediates Sink-Driven Auxin Gradients and Root Patterning in Arabidopsis. *Cell*, *108*(5), 661–673. https://doi.org/10.1016/S0092-8674(02)00656-6

Friml, J., Vieten, A., Sauer, M., Weijers, D., Schwarz, H., Hamann, T., Offringa, R., & Jürgens, G. (2003). Efflux-dependent auxin gradients establish the apical–basal axis of Arabidopsis. *Nature*, *426*(6963), 147–153. https://doi.org/10.1038/nature02085

Friml, J., Yang, X., Michniewicz, M., Weijers, D., Quint, A., Tietz, O., Benjamins, R., Ouwerkerk, P. B. F., Ljung, K., Sandberg, G., Hooykaas, P. J. J., Palme, K., &

Offringa, R. (2004). A PINOID-dependent binary switch in apical-basal PIN polar targeting directs auxin efflux. *Science (New York, N.Y.)*, *306*(5697), 862–865. https://doi.org/10.1126/science.1100618

Fry, S. C. (1989). Cellulases, hemicelluloses and auxin-stimulated growth: a possible relationship. *Physiologia Plantarum*, *75*(4), 532–536. https://doi.org/10.1111/j.1399-3054.1989.tb05620.x

Fry, S. C. (1995). Polysaccharide-Modifying Enzymes in the Plant Cell Wall. *Annual Review of Plant Physiology and Plant Molecular Biology*, *46*(1), 497–520. https://doi.org/10.1146/annurev.pp.46.060195.002433

Fry, S. C., Smith, R. C., Renwick, K. F., Martin, D. J., Hodge, S. K., & Matthews, K. J. (1992). Xyloglucan endotransglycosylase, a new wall-loosening enzyme activity from plants. *Biochemical Journal*, *282*(3), 821–828. https://doi.org/10.1042/bj2820821

Fukaki, H., & Tasaka, M. (2009). Hormone interactions during lateral root formation. *Plant Molecular Biology*, *69*(4), 437–449. https://doi.org/10.1007/s11103-008-9417-2

Fulcher, N., & Sablowski, R. (2009). Hypersensitivity to DNA damage in plant stem cell niches. *Proceedings of the National Academy of Sciences*, *106*(49), 20984–20988. https://doi.org/10.1073/pnas.0909218106

Furutani, M., Vernoux, T., Traas, J., Kato, T., Tasaka, M., & Aida, M. (2004a). PIN-FORMED1 and PINOID regulate boundary formation and cotyledon development in Arabidopsis embryogenesis. *Development*, *131*(20), 5021–5030. https://doi.org/10.1242/dev.01388

Furutani, M., Vernoux, T., Traas, J., Kato, T., Tasaka, M., & Aida, M. (2004b). *PIN-FORMED1* and *PINOID* regulate boundary formation and cotyledon development in *Arabidopsis* embryogenesis. *Development*, *131*(20), 5021–5030. https://doi.org/10.1242/dev.01388

Gainvors, A., Frézier, V., Lemaresquier, H., Lequart, C., Aigle, M., & Belarbi, A. (1994). Detection of polygalacturonase, pectin-lyase and pectin-esterase activities in aSaccharomyces cerevisiae strain. *Yeast*, *10*(10), 1311–1319. https://doi.org/10.1002/yea.320101008

Galinha, C., Hofhuis, H., Luijten, M., Willemsen, V., Blilou, I., Heidstra, R., & Scheres, B. (2007). PLETHORA proteins as dose-dependent master regulators of Arabidopsis

root development. *Nature*, *449*(7165), 1053–1057. https://doi.org/10.1038/nature06206

Gallavotti, A. (2013). The role of auxin in shaping shoot architecture. *Journal of Experimental Botany*, *64*(9), 2593–2608. https://doi.org/10.1093/jxb/ert141

Gallego-Bartolomé, J., Liu, W., Kuo, P. H., Feng, S., Ghoshal, B., Gardiner, J., Zhao, J. M. C., Park, S. Y., Chory, J., & Jacobsen, S. E. (2019). Co-targeting RNA Polymerases IV and V Promotes Efficient De Novo DNA Methylation in Arabidopsis. *Cell*, *176*(5), 1068-1082.e19. https://doi.org/10.1016/j.cell.2019.01.029

Gallois, J.-L., Nora, F. R., Mizukami, Y., & Sablowski, R. (2004). WUSCHEL induces shoot stem cell activity and developmental plasticity in the root meristem. *Genes & Development*, *18*(4), 375–380. https://doi.org/10.1101/gad.291204

Gälweiler, L., Guan, C., Müller, A., Wisman, E., Mendgen, K., Yephremov, A., & Palme, K. (1998). Regulation of Polar Auxin Transport by AtPIN1 in *Arabidopsis* Vascular Tissue. *Science*, *282*(5397), 2226–2230. https://doi.org/10.1126/science.282.5397.2226

Gee, M. A., Hagen, G., & Guilfoyle, T. J. (1991). Tissue-specific and organ-specific expression of soybean auxin-responsive transcripts GH3 and SAURs. *The Plant Cell*, *3*(4), 419–430. https://doi.org/10.1105/tpc.3.4.419

Gerber, T., Murawala, P., Knapp, D., Masselink, W., Schuez, M., Hermann, S., Gac-Santel, M., Nowoshilow, S., Kageyama, J., Khattak, S., Currie, J. D., Camp, J. G., Tanaka, E. M., & Treutlein, B. (2018). Single-cell analysis uncovers convergence of cell identities during axolotl limb regeneration. *Science*, *362*(6413). https://doi.org/10.1126/science.aaq0681

Goebel, K. (1898). *Organographie der Pflanzen, insbesondere der Archegoniaten und Samenpflanzen*. G. Fischer,. https://doi.org/10.5962/bhl.title.20547

Gonçalves, B., Hasson, A., Belcram, K., Cortizo, M., Morin, H., Nikovics, K., Vialette-Guiraud, A., Takeda, S., Aida, M., Laufs, P., & Arnaud, N. (2015). A conserved role for *CUP-SHAPED COTYLEDON* genes during ovule development. *The Plant Journal*, *83*(4), 732–742. https://doi.org/10.1111/tpj.12923

Gordon, S. P., Heisler, M. G., Reddy, G. V, Ohno, C., Das, P., & Meyerowitz, E. M. (2007). Pattern formation during de novo assembly of the Arabidopsis shoot meristem.

Development, *134*(19), 3539–3548. https://doi.org/10.1242/dev.010298

Grieneisen, V. A., Xu, J., Marée, A. F. M., Hogeweg, P., & Scheres, B. (2007). Auxin transport is sufficient to generate a maximum and gradient guiding root growth. *Nature*, *449*(7165), 1008–1013. https://doi.org/10.1038/nature06215

Groß, C., Bortoluzzi, C., de Ridder, D., Megens, H.-J., Groenen, M. A. M., Reinders, M., & Bosse, M. (2020). Prioritizing sequence variants in conserved non-coding elements in the chicken genome using chCADD. *PLOS Genetics*, *16*(9), e1009027. https://doi.org/10.1371/journal.pgen.1009027

Gu, C., Guo, Z.-H., Hao, P.-P., Wang, G.-M., Jin, Z.-M., & Zhang, S.-L. (2017). Multiple regulatory roles of AP2/ERF transcription factor in angiosperm. *Botanical Studies*, *58*(1), 6. https://doi.org/10.1186/s40529-016-0159-1

Guilfoyle, T., Hagen, G., Ulmasov, T., & Murfett, J. (1998). How Does Auxin Turn On Genes? *Plant Physiology*, *118*(2), 341–347. https://doi.org/10.1104/pp.118.2.341

Guilfoyle, T. J. (2015). The PB1 Domain in Auxin Response Factor and Aux/IAA Proteins: A Versatile Protein Interaction Module in the Auxin Response. *The Plant Cell*, *27*(1), 33–43. https://doi.org/10.1105/tpc.114.132753

Guo, J., Wei, J., Xu, J., & Sun, M.-X. (2014). Inducible knock-down of GNOM during root formation reveals tissue-specific response to auxin transport and its modulation of local auxin biosynthesis. *Journal of Experimental Botany*, *65*(4), 1165–1179. https://doi.org/10.1093/jxb/ert475

Haberlandt, G. (1902). Experiments on the culture of isolated plant cells. *The Botanical Review*, *35*(1), 68–88. https://doi.org/10.1007/BF02859889

Harada, J. J. (2001). Role of Arabidopsis LEAFY COTYLEDON genes in seed development. *Journal of Plant Physiology*, *158*(4), 405–409. https://doi.org/10.1078/0176-1617-00351

Hardtke, C. S., & Berleth, T. (1998). *The Arabidopsis gene MONOPTEROS encodes a transcription factor mediating embryo axis formation and vascular development*. *17*(5), 1405–1411. https://doi.org/10.1093/emboj/17.5.1405

Hasson, A., Plessis, A., Blein, T., Adroher, B., Grigg, S., Tsiantis, M., Boudaoud, A., Damerval, C., & Laufs, P. (2011). Evolution and Diverse Roles of the *CUP-SHAPED COTYLEDON* Genes in *Arabidopsis* Leaf Development . *The Plant Cell*, *23*(1), 54–

68. https://doi.org/10.1105/tpc.110.081448

Hayashi, T. (1989). Xyloglucans in the Primary Cell Wall. *Annual Review of Plant Physiology and Plant Molecular Biology*, *40*(1), 139–168. https://doi.org/10.1146/annurev.pp.40.060189.001035

Hazak, O., Bloch, D., Poraty, L., Sternberg, H., Zhang, J., Friml, J., & Yalovsky, S. (2010). A Rho Scaffold Integrates the Secretory System with Feedback Mechanisms in Regulation of Auxin Distribution. *PLoS Biology*, *8*(1), e1000282. https://doi.org/10.1371/journal.pbio.1000282

Heisler, M. G., Hamant, O., Krupinski, P., Uyttewaal, M., Ohno, C., Jönsson, H., Traas, J., & Meyerowitz, E. M. (2010). Alignment between PIN1 Polarity and Microtubule Orientation in the Shoot Apical Meristem Reveals a Tight Coupling between Morphogenesis and Auxin Transport. *PLoS Biology*, *8*(10), e1000516. https://doi.org/10.1371/journal.pbio.1000516

Heisler, M. G., Ohno, C., Das, P., Sieber, P., Reddy, G. V., Long, J. A., & Meyerowitz, E. M. (2005). Patterns of Auxin Transport and Gene Expression during Primordium Development Revealed by Live Imaging of the Arabidopsis Inflorescence Meristem. *Current Biology*, *15*(21), 1899–1911. https://doi.org/10.1016/j.cub.2005.09.052

Hervieux, N., Tsugawa, S., Fruleux, A., Dumond, M., Routier-Kierzkowska, A.-L., Komatsuzaki, T., Boudaoud, A., Larkin, J. C., Smith, R. S., Li, C.-B., & Hamant, O. (2017). Mechanical Shielding of Rapidly Growing Cells Buffers Growth Heterogeneity and Contributes to Organ Shape Reproducibility. *Current Biology*, *27*(22), 3468-3479.e4. https://doi.org/10.1016/j.cub.2017.10.033

Heyman, J., Cools, T., Canher, B., Shavialenka, S., Traas, J., Vercauteren, I., Van den Daele, H., Persiau, G., De Jaeger, G., Sugimoto, K., & De Veylder, L. (2016). The heterodimeric transcription factor complex ERF115–PAT1 grants regeneration competence. *Nature Plants*, *2*(11), 16165. https://doi.org/10.1038/nplants.2016.165

Hibara, K. I., Karim, M. R., Takada, S., Taoka, K. I., Furutani, M., Aida, M., & Tasaka, M. (2006). Arabidopsis CUP-SHAPED COTYLEDON3 regulates postembryonic shoot meristem and organ boundary formation. *Plant Cell*, *18*(11), 2946–2957. https://doi.org/10.1105/tpc.106.045716

Hibara, K. I., Takada, S., & Tasaka, M. (2003). CUC1 gene activates the expression of

SAM-related genes to induce adventitious shoot formation. *Plant Journal*, *36*(5), 687–696. https://doi.org/10.1046/j.1365-313X.2003.01911.x

Hofhuis, H., Laskowski, M., Du, Y., Prasad, K., Grigg, S., Pinon, V., & Scheres, B. (2013). Phyllotaxis and rhizotaxis in Arabidopsis are modified by three plethora transcription factors. *Current Biology*, *23*(11), 956–962. https://doi.org/10.1016/j.cub.2013.04.048

Hong, J. H., Savina, M., Du, J., Devendran, A., Kannivadi Ramakanth, K., Tian, X., Sim, W. S., Mironova, V. V., & Xu, J. (2017). A Sacrifice-for-Survival Mechanism Protects Root Stem Cell Niche from Chilling Stress. *Cell*, *170*(1), 102-113.e14. https://doi.org/10.1016/j.cell.2017.06.002

Horstman, A., Willemsen, V., Boutilier, K., & Heidstra, R. (2014). AINTEGUMENTA-LIKE proteins: hubs in a plethora of networks. *Trends in Plant Science*, *19*(3), 146–157. https://doi.org/10.1016/j.tplants.2013.10.010

Hu, B., Zhang, G., Liu, W., Shi, J., Wang, H., Qi, M., Li, J., Qin, P., Ruan, Y., Huang, H., Zhang, Y., & Xu, L. (2017). Divergent regeneration-competent cells adopt a common mechanism for callus initiation in angiosperms. *Regeneration*, *4*(3), 132–139. https://doi.org/10.1002/reg2.82

Huang, B., & Yeoman, M. M. (1995). Somatic embryogenesis in Arabidopsis thaliana L. *Somatic Embryogenesis and Synthetic Seed II*, 371–384.

Hyodo, H., Yamakawa, S., Takeda, Y., Tsuduki, M., Yokota, A., Nishitani, K., & Kohchi, T. (2003). Active gene expression of a xyloglucan endotransglucosylase/hydrolase gene, XTH9, in inflorescence apices is related to cell elongation in Arabidopsis thaliana. *Plant Molecular Biology*. https://doi.org/10.1023/A:1023904217641

Ikeda-Iwai, M. (2002). Establishment of a reproducible tissue culture system for the induction of Arabidopsis somatic embryos. *Journal of Experimental Botany*, *53*(374), 1575–1580. https://doi.org/10.1093/jxb/erf006

Ikeuchi, M., Favero, D. S., Sakamoto, Y., Iwase, A., Coleman, D., Rymen, B., & Sugimoto, K. (2019). Molecular Mechanisms of Plant Regeneration. *Annual Review of Plant Biology*, *70*(1), 377–406. https://doi.org/10.1146/annurev-arplant-050718-100434

Plant regeneration: Cellular origins and molecular mechanisms, 143 Development (Cambridge) 1442 (2016). https://doi.org/10.1242/dev.134668

Ikeuchi, M., Sugimoto, K., & Iwase, A. (2013). Plant Callus: Mechanisms of Induction and

Repression. *The Plant Cell*, *25*(9), 3159–3173. https://doi.org/10.1105/tpc.113.116053

Ishida, T., Aida, M., Takada, S., & Tasaka, M. (2000). Involvement of CUP-SHAPED COTYLEDON Genes in Gynoecium and Ovule Development in Arabidopsis thaliana. *Plant and Cell Physiology*, *41*(1), 60–67. https://doi.org/10.1093/pcp/41.1.60

Iwase, A., Mitsuda, N., Koyama, T., Hiratsu, K., Kojima, M., Arai, T., Inoue, Y., Seki, M., Sakakibara, H., Sugimoto, K., & Ohme-Takagi, M. (2011). The AP2/ERF transcription factor WIND1 controls cell dedifferentiation in arabidopsis. *Current Biology*, *21*(6), 508–514. https://doi.org/10.1016/j.cub.2011.02.020

Jönsson, H., Heisler, M. G., Shapiro, B. E., Meyerowitz, E. M., & Mjolsness, E. (2006). An auxin-driven polarized transport model for phyllotaxis. *Proceedings of the National Academy of Sciences*, *103*(5), 1633–1638. https://doi.org/10.1073/pnas.0509839103

Kareem, A., Durgaprasad, K., Sugimoto, K., Du, Y., Pulianmackal, A. J., Trivedi, Z. B., Abhayadev, P. V., Pinon, V., Meyerowitz, E. M., Scheres, B., & Prasad, K. (2015a). PLETHORA Genes Control Regeneration by a Two-Step Mechanism. *Current Biology*, *25*(8), 1017–1030. https://doi.org/10.1016/j.cub.2015.02.022

Kareem, A., Durgaprasad, K., Sugimoto, K., Du, Y., Pulianmackal, A. J., Trivedi, Z. B., Abhayadev, P. V, Pinon, V., Meyerowitz, E. M., Scheres, B., & Prasad, K. (2015b). PLETHORA Genes Control Regeneration by a Two-Step Mechanism. *Curr Biol*, *25*(8), 1017–1030. https://doi.org/10.1016/j.cub.2015.02.022

Kareem, A., Radhakrishnan, D., Sondhi, Y., Aiyaz, M., Roy, M. V., Sugimoto, K., & Prasad, K. (2016). De novo assembly of plant body plan: a step ahead of Deadpool. *Regeneration*, *3*(4), 182–197. https://doi.org/10.1002/reg2.68

Kawamura, E., Horiguchi, G., & Tsukaya, H. (2010). Mechanisms of leaf tooth formation in Arabidopsis. *The Plant Journal*, *62*(3), 429–441. https://doi.org/10.1111/j.1365-313X.2010.04156.x

Kent, W. J., Zweig, A. S., Barber, G., Hinrichs, A. S., & Karolchik, D. (2010). BigWig and BigBed: Enabling browsing of large distributed datasets. *Bioinformatics*, *26*(17), 2204–2207. https://doi.org/10.1093/bioinformatics/btq351

Kim, D., Langmead, B., & Salzberg, S. L. (2015). HISAT: A fast spliced aligner with low

memory requirements. *Nature Methods*, *12*(4), 357–360. https://doi.org/10.1038/nmeth.3317

Kim, E. J. Y., Korotkevich, E., & Hiiragi, T. (2018). Coordination of Cell Polarity, Mechanics and Fate in Tissue Self-organization. *Trends in Cell Biology*, *28*(7), 541–550. https://doi.org/10.1016/j.tcb.2018.02.008

King, P. (1988). Plant hormone mutants. *Trends in Genetics*, *4*(6), 157–162. https://doi.org/10.1016/0168-9525(88)90021-2

Kleine-Vehn, J., & Friml, J. (2008). Polar targeting and endocytic recycling in auxin-dependent plant development. *Annual Review of Cell and Developmental Biology*, *24*, 447–473. https://doi.org/10.1146/annurev.cellbio.24.110707.175254

Kryukov, G. V, Schmidt, S., & Sunyaev, S. (2005). Small fitness effect of mutations in highly conserved non-coding regions. *Human Molecular Genetics*, *14*(15), 2221–2229. https://doi.org/10.1093/hmg/ddi226

Kuchen, E. E., Fox, S., De Reuille, P. B., Kennaway, R., Bensmihen, S., Avondo, J., Calder, G. M., Southam, P., Bangham, A., & Coen, E. (2012). Generation of leaf shape through early patterns of growth and tissue polarity. *Science*. https://doi.org/10.1126/science.1214678

Kwiatkowska, D. (2004). Surface growth at the reproductive shoot apex of Arabidopsis thaliana pin-formed 1 and wild type. *Journal of Experimental Botany*, *55*(399), 1021–1032. https://doi.org/10.1093/jxb/erh109

Kwon, C. S., Chen, C., & Wagner, D. (2005). *WUSCHEL* is a primary target for transcriptional regulation by SPLAYED in dynamic control of stem cell fate in *Arabidopsis*. *Genes & Development*, *19*(8), 992–1003. https://doi.org/10.1101/gad.1276305

Lamport, D. T. (1963). Oxygen fixation into hydroxyproline of plant cell wall protein. *The Journal of Biological Chemistry*, *238*, 1438–1440.

Landrein, B., Kiss, A., Sassi, M., Chauvet, A., Das, P., Cortizo, M., Laufs, P., Takeda, S., Aida, M., Traas, J., Vernoux, T., Boudaoud, A., & Hamant, O. (2015). Mechanical stress contributes to the expression of the STM homeobox gene in Arabidopsis shoot meristems. *ELife*, *4*. https://doi.org/10.7554/eLife.07811

Langmead, B., Trapnell, C., Pop, M., & Salzberg, S. L. (2009). Ultrafast and memory-

efficient alignment of short DNA sequences to the human genome. *Genome Biology*, *10*(3). https://doi.org/10.1186/gb-2009-10-3-r25

Laskowski, M., Grieneisen, V. A., Hofhuis, H., Ten Hove, C. A., Hogeweg, P., Marée, A. F. M., & Scheres, B. (2008). Root system architecture from coupling cell shape to auxin transport. *PLoS Biology*, *6*(12), 2721–2735. https://doi.org/10.1371/journal.pbio.0060307

Laufs, P., Peaucelle, A., Morin, H., & Traas, J. (2004). MicroRNA regulation of the CUC genes is required for boundary size control in *Arabidopsis* meristems. *Development*, *131*(17), 4311–4322. https://doi.org/10.1242/dev.01320

Lavenus, J., Goh, T., Roberts, I., Guyomarc'h, S., Lucas, M., De Smet, I., Fukaki, H., Beeckman, T., Bennett, M., & Laplaze, L. (2013). Lateral root development in Arabidopsis: fifty shades of auxin. *Trends in Plant Science*, *18*(8), 450–458. https://doi.org/10.1016/j.tplants.2013.04.006

Lee, H. W., Kim, N. Y., Lee, D. J., & Kim, J. (2009). *LBD18/ASL20* Regulates Lateral Root Formation in Combination with *LBD16/ASL18* Downstream of *ARF7* and *ARF19* in Arabidopsis. *Plant Physiology*, *151*(3), 1377–1389. https://doi.org/10.1104/pp.109.143685

Leibfried, A., To, J. P. C., Busch, W., Stehling, S., Kehle, A., Demar, M., Kieber, J. J., & Lohmann, J. U. (2005). WUSCHEL controls meristem function by direct regulation of cytokinin-inducible response regulators. *Nature*, *438*(7071), 1172–1175. https://doi.org/10.1038/nature04270

Leyser, H. M. O., Pickett, F. B., Dharmasiri, S., & Estelle, M. (1996). Mutations in the AXR3 gene of Arabidopsis result in altered auxin response including ectopic expression from the SAUR-AC1 promoter. *The Plant Journal*, *10*(3), 403–413. https://doi.org/10.1046/j.1365-313x.1996.10030403.x

Leyser, O. (2005). Auxin distribution and plant pattern formation: how many angels can dance on the point of PIN? *Cell*, *121*(6), 819–822. https://doi.org/10.1016/j.cell.2005.06.005

Leyser, O. (2018). Auxin Signaling. *Plant Physiology*, *176*(1), 465–479. https://doi.org/10.1104/pp.17.00765

Li, H., Handsaker, B., Wysoker, A., Fennell, T., Ruan, J., Homer, N., Marth, G., Abecasis,

G., & Durbin, R. (2009). The Sequence Alignment/Map format and SAMtools. *Bioinformatics*, *25*(16), 2078–2079. https://doi.org/10.1093/bioinformatics/btp352

Li, R., Li, J., Li, S., Qin, G., Novák, O., Pěnčík, A., Ljung, K., Aoyama, T., Liu, J., Murphy, A., Gu, H., Tsuge, T., & Qu, L.-J. (2014). ADP1 Affects Plant Architecture by Regulating Local Auxin Biosynthesis. *PLoS Genetics*, *10*(1), e1003954. https://doi.org/10.1371/journal.pgen.1003954

Li, W., Liu, H., Cheng, Z. J., Su, Y. H., Han, H. N., Zhang, Y., & Zhang, X. S. (2011). DNA Methylation and Histone Modifications Regulate De Novo Shoot Regeneration in Arabidopsis by Modulating WUSCHEL Expression and Auxin Signaling. *PLoS Genetics*, *7*(8), e1002243. https://doi.org/10.1371/journal.pgen.1002243

Liang, Y., Heyman, J., Lu, R., & De Veylder, L. (2023). Evolution of wound-activated regeneration pathways in the plant kingdom. *European Journal of Cell Biology*, *102*(2), 151291. https://doi.org/10.1016/j.ejcb.2023.151291

Liao, Y., Smyth, G. K., & Shi, W. (2014). FeatureCounts: An efficient general purpose program for assigning sequence reads to genomic features. *Bioinformatics*, *30*(7), 923–930. https://doi.org/10.1093/bioinformatics/btt656

Lin, Y., Wang, Y., Zhu, J. K., & Yang, Z. (1996). Localization of a Rho GTPase Implies a Role in Tip Growth and Movement of the Generative Cell in Pollen Tubes. *The Plant Cell*, 293–303. https://doi.org/10.1105/tpc.8.2.293

Liu, J., Sheng, L., Xu, Y., Li, J., Yang, Z., Huang, H., & Xu, L. (2014). *WOX11* and *12* Are Involved in the First-Step Cell Fate Transition during de Novo Root Organogenesis in *Arabidopsis*. *The Plant Cell*, *26*(3), 1081–1093. https://doi.org/10.1105/tpc.114.122887

Liu, L., Qiu, L., Zhu, Y., Luo, L., Han, X., Man, M., Li, F., Ren, M., & Xing, Y. (2023). Comparisons between Plant and Animal Stem Cells Regarding Regeneration Potential and Application. *International Journal of Molecular Sciences*, *24*(5). https://doi.org/10.3390/ijms24054392

Liu, Z., Li, J., Wang, L., Li, Q., Lu, Q., Yu, Y., Li, S., Bai, M., Hu, Y., & Xiang, F. (2016). Repression of callus initiation by the miRNA-directed interaction of auxin-cytokinin in *Arabidopsis thaliana*. *The Plant Journal*, *87*(4), 391–402. https://doi.org/10.1111/tpj.13211

Ljung, K., Bhalerao, R. P., & Sandberg, G. (2002). Sites and homeostatic control of auxin biosynthesis in Arabidopsis during vegetative growth. *The Plant Journal*, *28*(4), 465–474. https://doi.org/10.1046/j.1365-313X.2001.01173.x

Love, M. I., Huber, W., & Anders, S. (2014). Moderated estimation of fold change and dispersion for RNA-seq data with DESeq2. *Genome Biology*, *15*(12), 1–21. https://doi.org/10.1186/s13059-014-0550-8

Ludwig-Müller, J. (2011). Auxin conjugates: their role for plant development and in the evolution of land plants. *Journal of Experimental Botany*, *62*(6), 1757–1773. https://doi.org/10.1093/jxb/erq412

Ma, X., Zhang, Q., Zhu, Q., Liu, W., Chen, Y. Y., Qiu, R., Wang, B., Yang, Z., Li, H., Lin, Y., Xie, Y., Shen, R., Chen, S., Wang, Z., Chen, Y. Y., Guo, J., Chen, L., Zhao, X., Dong, Z., & Liu, Y.-G. G. (2015). A Robust CRISPR/Cas9 System for Convenient, High-Efficiency Multiplex Genome Editing in Monocot and Dicot Plants. *Molecular Plant*, *8*(8), 1274–1284. https://doi.org/10.1016/j.molp.2015.04.007

Mähönen, A. P., Tusscher, K. ten, Siligato, R., Smetana, O., Díaz-Triviño, S., Salojärvi, J., Wachsman, G., Prasad, K., Heidstra, R., & Scheres, B. (2014). PLETHORA gradient formation mechanism separates auxin responses. *Nature*, *515*(7525), 125–129. https://doi.org/10.1038/nature13663

Malamy, J. E., & Benfey, P. N. (1997). Organization and cell differentiation in lateral roots of Arabidopsis thaliana. *Development*, *124*(1), 33–44.

Mallory, A. C., Dugas, D. V, Bartel, D. P., & Bartel, B. (2004). MicroRNA Regulation of NAC-Domain Targets Is Required for Proper Formation and Separation of Adjacent Embryonic, Vegetative, and Floral Organs. *Current Biology*, *14*(12), 1035–1046. https://doi.org/10.1016/j.cub.2004.06.022

Mansfield, S. G., & Briarty, L. G. (1991). Early embryogenesis in *Arabidopsis thaliana* . II. The developing embryo. *Canadian Journal of Botany*, *69*(3), 461–476. https://doi.org/10.1139/b91-063

Marhava, P., Hoermayer, L., Yoshida, S., Marhavý, P., Benková, E., & Friml, J. (2019). Re-activation of Stem Cell Pathways for Pattern Restoration in Plant Wound Healing. *Cell*, *177*(4), 957-969.e13. https://doi.org/10.1016/j.cell.2019.04.015

Mathew, M. M., & Prasad, K. (2021). Model systems for regeneration: Arabidopsis.

Development (Cambridge), *148*(6). https://doi.org/10.1242/dev.195347

Matosevich, R., Cohen, I., Gil-Yarom, N., Modrego, A., Verna, C., Scarpella, E., & Efroni, I. (2019). A dynamic pattern of local auxin sources is required for root regeneration. *BioRxiv*, 783480.

Mayer, K. F. ., Schoof, H., Haecker, A., Lenhard, M., Jürgens, G., & Laux, T. (1998). Role of WUSCHEL in Regulating Stem Cell Fate in the Arabidopsis Shoot Meristem. *Cell*, *95*(6), 805–815. https://doi.org/10.1016/S0092-8674(00)81703-1

Mayer, U., Ruiz, R. A. T., Berleth, T., Miséra, S., & Jürgens, G. (1991). Mutations affecting body organization in the Arabidopsis embryo. *Nature*, *353*(6343), 402–407. https://doi.org/10.1038/353402a0

Mazur, E., Benková, E., & Friml, J. (2016). Vascular cambium regeneration and vessel formation in wounded inflorescence stems of Arabidopsis. *Scientific Reports*, *6*(1), 33754. https://doi.org/10.1038/srep33754

McNeil, M., Darvill, A. G., Fry, S. C., & Albersheim, P. (1984). STRUCTURE AND FUNCTION OF THE PRIMARY CELL WALLS OF PLANTS. *Annual Review of Biochemistry*, *53*(1), 625–663. https://doi.org/10.1146/annurev.bi.53.070184.003205

Meents, M. J., Watanabe, Y., & Samuels, A. L. (2018). The cell biology of secondary cell wall biosynthesis. *Annals of Botany*, *121*(6), 1107–1125. https://doi.org/10.1093/aob/mcy005

Mehta, A. S., & Singh, A. (2019). Insights into regeneration tool box: An animal model approach. *Developmental Biology*, *453*(2), 111–129. https://doi.org/10.1016/j.ydbio.2019.04.006

Meyerowitz, E. M. (2002). Plants Compared to Animals: The Broadest Comparative Study of Development. *Science*, *295*(5559), 1482–1485. https://doi.org/10.1126/science.1066609

Michniewicz, M., Zago, M. K., Abas, L., Weijers, D., Schweighofer, A., Meskiene, I., Heisler, M. G., Ohno, C., Zhang, J., Huang, F., Schwab, R., Weigel, D., Meyerowitz, E. M., Luschnig, C., Offringa, R., & Friml, J. (2007). Antagonistic Regulation of PIN Phosphorylation by PP2A and PINOID Directs Auxin Flux. *Cell*, *130*(6), 1044–1056. https://doi.org/10.1016/j.cell.2007.07.033

Miehe, H. (1905). *Wachstum, Regeneration und Polarität isolierter Zellen*.

Mitchison GJ, & Brenner S. (1980). A model for vein formation in higher plants. *Proceedings of the Royal Society of London. Series B. Biological Sciences*, *207*(1166), 79–109. https://doi.org/10.1098/rspb.1980.0015

Molendijk, A. J. (2001). Arabidopsis thaliana Rop GTPases are localized to tips of root hairs and control polar growth. *The EMBO Journal*, *20*(11), 2779–2788. https://doi.org/10.1093/emboj/20.11.2779

Moller, B., & Weijers, D. (2009). Auxin Control of Embryo Patterning. *Cold Spring Harbor Perspectives in Biology*, *1*(5), a001545–a001545. https://doi.org/10.1101/cshperspect.a001545

Moo-Young, M. (2019). *Comprehensive biotechnology*. Elsevier.

Murdoch, J. N. (2003). Disruption of scribble (Scrb1) causes severe neural tube defects in the circletail mouse. *Human Molecular Genetics*, *12*(2), 87–98. https://doi.org/10.1093/hmg/ddg014

Muroyama, A., & Bergmann, D. (2019). Plant Cell Polarity: Creating Diversity from Inside the Box. *Annual Review of Cell and Developmental Biology*, *35*(1), 309–336. https://doi.org/10.1146/annurev-cellbio-100818-125211

Nagai, T., Ibata, K., Park, E. S., Kubota, M., Mikoshiba, K., & Miyawaki, A. (2002). A variant of yellow fluorescent protein with fast and efficient maturation for cell-biological applications. *Nature Biotechnology*, *20*(1), 87–90.

Nagano, Y. (2000). Several Features of the GT-Factor Trihelix Domain Resemble Those of the Myb DNA-Binding Domain. *Plant Physiology*, *124*(2), 491–494. https://doi.org/10.1104/pp.124.2.491

Nakayama, N., Smith, R. S., Mandel, T., Robinson, S., Kimura, S., Boudaoud, A., & Kuhlemeier, C. (2012). Mechanical regulation of auxin-mediated growth. *Current Biology*, *22*(16), 1468–1476.

Nance, J., & Zallen, J. A. (2011). Elaborating polarity: PAR proteins and the cytoskeleton. *Development*, *138*(5), 799–809. https://doi.org/10.1242/dev.053538

Nikovics, K., Blein, T., Peaucelle, A., Ishida, T., Morin, H., Aida, M., & Laufs, P. (2006). The Balance between the *MIR164A* and *CUC2* Genes Controls Leaf Margin Serration in *Arabidopsis*. *The Plant Cell*, *18*(11), 2929–2945. https://doi.org/10.1105/tpc.106.045617

Nishitani, K. (1995). Endo-Xyloglucan Transferase, a New Class of Transferase Involved in Cell Wall Construction. In *Journal of Plant Research* (Vol. 108).

Nishitani, K. (1997). *The Role of Endoxyloglucan Transferase in the Organization of Plant Cell Walls* (pp. 157–206). https://doi.org/10.1016/S0074-7696(08)62477-8

Nishitani, K., & Vissenberg, K. (2006). Roles of the XTH protein family in the expanding cell. In *The expanding cell* (pp. 89–116). Springer.

Nole-Wilson, S., Tranby, T. L., & Krizek, B. A. (2005). AINTEGUMENTA-like (AIL) genes are expressed in young tissues and may specify meristematic or division-competent states. *Plant Molecular Biology*, *57*(5), 613–628. https://doi.org/10.1007/s11103-005-0955-6

Nowak, K., & Gaj, M. D. (2016). Stress-related function of bHLH109 in somatic embryo induction in Arabidopsis. *Journal of Plant Physiology*, *193*, 119–126. https://doi.org/10.1016/j.jplph.2016.02.012

Okada, K., Ueda, J., Komaki, M. K., Bell, C. J., & Shimura, Y. (1991). Requirement of the Auxin Polar Transport System in Early Stages of Arabidopsis Floral Bud Formation. *The Plant Cell*, 677–684. https://doi.org/10.1105/tpc.3.7.677

Okushima, Y., Fukaki, H., Onoda, M., Theologis, A., & Tasaka, M. (2007). ARF7 and ARF19 Regulate Lateral Root Formation via Direct Activation of *LBD/ASL* Genes in *Arabidopsis*. *The Plant Cell*, *19*(1), 118–130. https://doi.org/10.1105/tpc.106.047761

Ouellet, F., Overvoorde, P. J., & Theologis, A. (2001). IAA17/AXR3: Biochemical Insight into an Auxin Mutant Phenotype. *The Plant Cell*, *13*(4), 829–841. https://doi.org/10.1105/tpc.13.4.829

Overvoorde, P., Fukaki, H., & Beeckman, T. (2010). Auxin control of root development. *Cold Spring Harbor Perspectives in Biology*, *2*(6), a001537–a001537. https://doi.org/10.1101/cshperspect.a001537

Pagnussat, G. C., Alandete-Saez, M., Bowman, J. L., & Sundaresan, V. (2009). Auxin-Dependent Patterning and Gamete Specification in the *Arabidopsis* Female Gametophyte. *Science*, *324*(5935), 1684–1689. https://doi.org/10.1126/science.1167324

Paque, S., & Weijers, D. (2016). Q&A: Auxin: the plant molecule that influences almost anything. *BMC Biology*, *14*(1), 67. https://doi.org/10.1186/s12915-016-0291-

0

Passioura, J., & Fry, S. (1992). Turgor and Cell Expansion: Beyond the Lockhart Equation. *Functional Plant Biology*, *19*(5), 565. https://doi.org/10.1071/PP9920565

Peaucelle, A., Braybrook, S. A. A., Le Guillou, L., Bron, E., Kuhlemeier, C., Höfte, H., Le Guillou, L., Bron, E., Kuhlemeier, C., & Höfte, H. (2011). Pectin-induced changes in cell wall mechanics underlie organ initiation in Arabidopsis. *Current Biology*, *21*(20), 1720–1726. https://doi.org/10.1016/j.cub.2011.08.057

Pertea, G., & Pertea, M. (2020). GFF Utilities: GffRead and GffCompare. *F1000Research*, *9*, ISCB Comm J-304. https://doi.org/10.12688/f1000research.23297.2

Pertea, M., Kim, D., Pertea, G. M., Leek, J. T., & Salzberg, S. L. (2016). Transcript-level expression analysis of RNA-seq experiments with HISAT, StringTie and Ballgown. *Nature Protocols*, *11*(9), 1650–1667.

Petrášek, J., & Friml, J. (2009). Auxin transport routes in plant development. *Development*, *136*(16), 2675–2688. https://doi.org/10.1242/dev.030353

Petrie, T. A., Strand, N. S., Tsung-Yang, C., Rabinowitz, J. S., & Moon, R. T. (2014). Macrophages modulate adult zebrafish tail fin regeneration. *Development*, *141*(13), 2581–2591. https://doi.org/10.1242/dev.098459

Pinon, V., Prasad, K., Grigg, S. P., Sanchez-Perez, G. F., & Scheres, B. (2013). Local auxin biosynthesis regulation by PLETHORA transcription factors controls phyllotaxis in Arabidopsis. *Proceedings of the National Academy of Sciences of the United States of America*, *110*(3), 1107–1112. https://doi.org/10.1073/pnas.1213497110

Prasad, K., Grigg, S. P., Barkoulas, M., Yadav, R. K., Sanchez-Perez, G. F., Pinon, V., Blilou, I., Hofhuis, H., Dhonukshe, P., Galinha, C., Mähönen, A. P., Muller, W. H., Raman, S., Verkleij, A. J., Snel, B., Reddy, G. V., Tsiantis, M., & Scheres, B. (2011). Arabidopsis PLETHORA transcription factors control phyllotaxis. *Current Biology*, *21*(13), 1123–1128. https://doi.org/10.1016/j.cub.2011.05.009

Pulianmackal, A. J., Kareem, A. V. K., Durgaprasad, K., Trivedi, Z. B., & Prasad, K. (2014). Competence and regulatory interactions during regeneration in plants. *Frontiers in Plant Science*, *5*(APR), 1–16. https://doi.org/10.3389/fpls.2014.00142

Quatrano, R. S. (1978). Development of Cell Polarity. *Annual Review of Plant Physiology*, *29*(1), 487–510. https://doi.org/10.1146/annurev.pp.29.060178.002415

Radhakrishnan, D., Kareem, A., Durgaprasad, K., Sreeraj, E., Sugimoto, K., & Prasad, K. (2018). Shoot regeneration: a journey from acquisition of competence to completion. *Current Opinion in Plant Biology*, *41*(Cim), 23–31. https://doi.org/10.1016/j.pbi.2017.08.001

Radhakrishnan, D., Shanmukhan, A. P., Kareem, A., Aiyaz, M., Varapparambathu, V., Toms, A., Kerstens, M., Valsakumar, D., Landge, A. N., Shaji, A., Mathew, M. K., Sawchuk, M. G., Scarpella, E., Krizek, B. A., Efroni, I., Mähönen, A. P., Willemsen, V., Scheres, B., & Prasad, K. (2020). A coherent feed-forward loop drives vascular regeneration in damaged aerial organs of plants growing in a normal developmental context. *Development (Cambridge, England)*, *147*(6), 1–10. https://doi.org/10.1242/dev.185710

Rayle, D. L., & Cleland, R. E. (1992). The Acid Growth Theory of auxin-induced cell elongation is alive and well. *Plant Physiology*, *99*(4), 1271–1274. https://doi.org/10.1104/pp.99.4.1271

Reinhardt, D., Mandel, T., & Kuhlemeier, C. (2000). Auxin Regulates the Initiation and Radial Position of Plant Lateral Organs. *The Plant Cell*, *12*(4), 507–518. https://doi.org/10.1105/tpc.12.4.507

Reinhardt, D., Pesce, E.-R., Stieger, P., Mandel, T., Baltensperger, K., Bennett, M., Traas, J., Friml, J., & Kuhlemeier, C. (2003). Regulation of phyllotaxis by polar auxin transport. *Nature*, *426*(6964), 255–260. https://doi.org/10.1038/nature02081

Riechmann, J. L., Heard, J., Martin, G., Reuber, L., Jiang, C.-Z. Z., Keddie, J., Adam, L., Pineda, O., Ratcliffe, O. J., Samaha, R. R., Creelman, R., Pilgrim, M., Broun, P., Zhang, J. Z., Ghandehari, D., Sherman, B. K., -L. Yu, G., & Yu, G. L. (2000). Arabidopsis transcription factors: Genome-wide comparative analysis among eukaryotes. *Science*, *290*(5499), 2105–2110. https://doi.org/10.1126/science.290.5499.2105

Ringli, C. (2010). The hydroxyproline-rich glycoprotein domain of the Arabidopsis LRX1 requires Tyr for function but not for insolubilization in the cell wall. *The Plant Journal*, *63*(4), 662–669. https://doi.org/10.1111/j.1365-313X.2010.04270.x

Ritter, D. I., Dong, Z., Guo, S., & Chuang, J. H. (2012). Transcriptional Enhancers in Protein-Coding Exons of Vertebrate Developmental Genes. *PLoS ONE*, *7*(5), e35202.

https://doi.org/10.1371/journal.pone.0035202

Rose, J. K. C., Braam, J., Fry, S. C., & Nishitani, K. (2002). The XTH Family of Enzymes Involved in Xyloglucan Endotransglucosylation and Endohydrolysis: Current Perspectives and a New Unifying Nomenclature. *Plant and Cell Physiology*, *43*(12), 1421–1435. https://doi.org/10.1093/pcp/pcf171

Rosspopoff, O., Chelysheva, L., Saffar, J., Lecorgne, L., Gey, D., Caillieux, E., Colot, V., Roudier, F., Hilson, P., Berthomé, R., Da Costa, M., & Rech, P. (2017). Direct conversion of root primordium into shoot meristem relies on timing of stem cell niche development. *Development*. https://doi.org/10.1242/dev.142570

Ruiz Rosquete, M., Barbez, E., & Kleine-Vehn, J. (2012). Cellular Auxin Homeostasis: Gatekeeping Is Housekeeping. *Molecular Plant*, *5*(4), 772–786. https://doi.org/10.1093/mp/ssr109

Sabatini, S., Beis, D., Wolkenfelt, H., Murfett, J., Guilfoyle, T., Malamy, J., Benfey, P., Leyser, O., Bechtold, N., Weisbeek, P., & Scheres, B. (1999). An Auxin-Dependent Distal Organizer of Pattern and Polarity in the Arabidopsis Root. *Cell*, *99*(5), 463–472. https://doi.org/10.1016/S0092-8674(00)81535-4

Sachs, J. (1893). Physiologische Notizen. *Flora*, *75*, 1–3.

Sachs, T. (1968). On the Determination of the Pattern of Vascular Tissue in Peas. *Annals of Botany*, *32*(4), 781–790. https://doi.org/10.1093/oxfordjournals.aob.a084249

Sachs, T. (1969). Polarity and the Induction of Organized Vascular Tissues. *Annals of Botany*, *33*(2), 263–275. https://doi.org/10.1093/oxfordjournals.aob.a084281

Sachs, T. (1981). *The Control of the Patterned Differentiation of Vascular Tissues* (pp. 151–262). https://doi.org/10.1016/S0065-2296(08)60351-1

Sachs, T. (1991). Cell polarity and tissue patterning in plants. *Development*, *113*(Supplement 1).

Salvi, E., Rutten, J. P., Di Mambro, R., Polverari, L., Licursi, V., Negri, R., Dello Ioio, R., Sabatini, S., & Ten Tusscher, K. (2020). A Self-Organized PLT/Auxin/ARR-B Network Controls the Dynamics of Root Zonation Development in Arabidopsis thaliana. *Developmental Cell*, *53*(4), 431-443.e23. https://doi.org/10.1016/j.devcel.2020.04.004

Sánchez Alvarado, A., & Yamanaka, S. (2014). Rethinking differentiation: Stem cells,

regeneration, and plasticity. *Cell*, *157*(1), 110–119. https://doi.org/10.1016/j.cell.2014.02.041

Santuari, L., Sanchez-Perez, G. F., Luijten, M., Rutjens, B., Terpstra, I., Berke, L., Gorte, M., Prasad, K., Bao, D., Timmermans-Hereijgers, J. L. P. M. P. M., Maeo, K., Nakamura, K., Shimotohno, A., Pencik, A., Novak, O., Ljung, K., van Heesch, S., de Bruijn, E., Cuppen, E., … Heidstra, R. (2016). The PLETHORA Gene Regulatory Network Guides Growth and Cell Differentiation in Arabidopsis Roots. *The Plant Cell*, *28*(12), 2937–2951. https://doi.org/10.1105/tpc.16.00656

Sassi, M., Ali, O., Boudon, F., Cloarec, G., Abad, U., Cellier, C., Chen, X., Gilles, B., Milani, P., Friml, J., Vernoux, T., Godin, C., Hamant, O., & Traas, J. (2014). An Auxin-Mediated Shift toward Growth Isotropy Promotes Organ Formation at the Shoot Meristem in Arabidopsis. *Current Biology*, *24*(19), 2335–2342. https://doi.org/10.1016/j.cub.2014.08.036

Sawchuk, M. G., Edgar, A., & Scarpella, E. (2013). Patterning of leaf vein networks by convergent auxin transport pathways. *PLoS Genetics*, *9*(2), e1003294.

Schechter, V. (1935). THE EFFECT OF CENTRIFUGING ON THE POLARITY OF AN ALGA, GRIFFITHSIA BORNETIANA. *The Biological Bulletin*, *68*(2), 172–179. https://doi.org/10.2307/1537261

Scheres, B., van den Berg, C., Willemsen, V., Hendriks, G., & Weisbeek, P. (1997). Short-range control of cell differentiation in the *Arabidopsis* root meristem. *Nature*, *390*(6657), 287–289. https://doi.org/10.1038/36856

Schiavone, F. M., & Racusen, R. H. (1991). Regeneration of the root pole in surgically transected carrot embryos occurs by position-dependent, proximodistal replacement of missing tissues. *Development*, *113*(4), 1305–1313. https://doi.org/10.1242/dev.113.4.1305

Schmitz, G., & Theres, K. (2005). Shoot and inflorescence branching. *Current Opinion in Plant Biology*, *8*(5), 506–511. https://doi.org/10.1016/j.pbi.2005.07.010

Schoof, H., Lenhard, M., Haecker, A., Mayer, K. F. ., Jürgens, G., & Laux, T. (2000). The Stem Cell Population of Arabidopsis Shoot Meristems Is Maintained by a Regulatory Loop between the CLAVATA and WUSCHEL Genes. *Cell*, *100*(6), 635–644. https://doi.org/10.1016/S0092-8674(00)80700-X

Sena, G., & Birnbaum, K. D. (2010). Built to rebuild: in search of organizing principles in plant regeneration. *Current Opinion in Genetics & Development*, *20*(4), 460–465. https://doi.org/10.1016/j.gde.2010.04.011

Sena, G., Wang, X., Liu, H.-Y., Hofhuis, H., & Birnbaum, K. D. (2009). Organ regeneration does not require a functional stem cell niche in plants. *Nature*, *457*(7233), 1150–1153. https://doi.org/10.1038/nature07597

Serra, L., & Perrot-Rechenmann, C. (2020). Spatiotemporal control of cell growth by CUC3 shapes leaf margins. *Development (Cambridge)*, *147*(6), 1–10. https://doi.org/10.1242/dev.183277

Serrano-Mislata, A., Fernández-Nohales, P., Doménech, M. J., Hanzawa, Y., Bradley, D., & Madueño, F. (2016). Separate elements of the *TERMINAL FLOWER 1* cis-regulatory region integrate pathways to control flowering time and shoot meristem identity. *Development*. https://doi.org/10.1242/dev.135269

Shang, B., Xu, C., Zhang, X., Cao, H., Xin, W., & Hu, Y. (2016). Very-long-chain fatty acids restrict regeneration capacity by confining pericycle competence for callus formation in *Arabidopsis*. *Proceedings of the National Academy of Sciences*, *113*(18), 5101–5106. https://doi.org/10.1073/pnas.1522466113

Shanmukhan, A. P., Mathew, M. M., Aiyaz, M., Kareem, A., Radhakrishnan, D., & Prasad, K. (2020). Regulation of touch dependant de novo root regeneration in Arabidopsis. *BioRxiv*, 2020.11.04.367714. https://doi.org/10.1101/2020.11.04.367714

Shanmukhan, A. P., Mathew, M. M., Aiyaz, M., Varaparambathu, V., Kareem, A., Radhakrishnan, D., & Prasad, K. (2021). Regulation of touch-stimulated de novo root regeneration from Arabidopsis leaves. *Plant Physiology*, *187*(1), 52–58. https://doi.org/10.1093/plphys/kiab286

Shao, W., & Dong, J. (2016). Polarity in plant asymmetric cell division: Division orientation and cell fate differentiation. *Developmental Biology*, *419*(1), 121–131. https://doi.org/10.1016/j.ydbio.2016.07.020

Shemer, O., Landau, U., Candela, H., Zemach, A., & Eshed Williams, L. (2015). Competency for shoot regeneration from Arabidopsis root explants is regulated by DNA methylation. *Plant Science*, *238*, 251–261. https://doi.org/10.1016/j.plantsci.2015.06.015

Shimotohno, A., Heidstra, R., Blilou, I., & Scheres, B. (2018). Root stem cell niche organizer specification by molecular convergence of PLETHORA and SCARECROW transcription factor modules. *Genes and Development*, *32*(15–16), 1085–1100. https://doi.org/10.1101/gad.314096.118

Shuai, B., Reynaga-Peña, C. G., & Springer, P. S. (2002). The *Lateral Organ Boundaries* Gene Defines a Novel, Plant-Specific Gene Family. *Plant Physiology*, *129*(2), 747–761. https://doi.org/10.1104/pp.010926

Siligato, R., Wang, X., Yadav, S. R., Lehesranta, S., Ma, G., Ursache, R., Sevilem, I., Zhang, J., Gorte, M., Prasad, K., Wrzaczek, M., Heidstra, R., Murphy, A., Scheres, B., & Mähönen, A. P. (2016). MultiSite Gateway-Compatible Cell Type-Specific Gene-Inducible System for Plants. *Plant Physiology*, *170*(2), 627 LP – 641. https://doi.org/10.1104/pp.15.01246

Skoog, F., & Miller, C. O. (1957). Chemical regulation of growth and organ formation in plant tissues cultured in vitro. *Symposia of the Society for Experimental Biology*, *11*, 118–130.

Smith, R. S., Guyomarc'h, S., Mandel, T., Reinhardt, D., Kuhlemeier, C., Prusinkiewicz, P., Guyomarc'h, S., Mandel, T., Reinhardt, D., Kuhlemeier, C., & Prusinkiewicz, P. (2006). A plausible model of phyllotaxis. *Proceedings of the National Academy of Sciences*, *103*(5), 1301 LP – 1306. https://doi.org/10.1073/pnas.0510457103

Smith, R. S., Guyomarc'h, S., Mandel, T., Reinhardt, D., Kuhlemeier, C., & Prusinkiewicz, P. (2006). A plausible model of phyllotaxis. *Proceedings of the National Academy of Sciences*, *103*(5), 1301 LP – 1306. https://doi.org/10.1073/pnas.0510457103

Sorefan, K., Girin, T., Liljegren, S. J., Ljung, K., Robles, P., Galván-Ampudia, C. S., Offringa, R., Friml, J., Yanofsky, M. F., & Østergaard, L. (2009). A regulated auxin minimum is required for seed dispersal in Arabidopsis. *Nature*, *459*(7246), 583–586. https://doi.org/10.1038/nature07875

St Johnston, D., & Ahringer, J. (2010). Cell Polarity in Eggs and Epithelia: Parallels and Diversity. *Cell*, *141*(5), 757–774. https://doi.org/10.1016/j.cell.2010.05.011

Stepanova, A. N., Yun, J., Robles, L. M., Novak, O., He, W., Guo, H., Ljung, K., & Alonso,

J. M. (2011). The *Arabidopsis* YUCCA1 Flavin Monooxygenase Functions in the Indole-3-Pyruvic Acid Branch of Auxin Biosynthesis. *The Plant Cell*, *23*(11), 3961–3973. https://doi.org/10.1105/tpc.111.088047

Stewart, J. L., & Nemhauser, J. L. (2010). Do Trees Grow on Money? Auxin as the Currency of the Cellular Economy. *Cold Spring Harbor Perspectives in Biology*, *2*(2), a001420–a001420. https://doi.org/10.1101/cshperspect.a001420

Stone, S. L., Braybrook, S. A., Paula, S. L., Kwong, L. W., Meuser, J., Pelletier, J., Hsieh, T.-F., Fischer, R. L., Goldberg, R. B., & Harada, J. J. (2008). *Arabidopsis* LEAFY COTYLEDON2 induces maturation traits and auxin activity: Implications for somatic embryogenesis. *Proceedings of the National Academy of Sciences*, *105*(8), 3151–3156. https://doi.org/10.1073/pnas.0712364105

Su, Y. H., Zhao, X. Y., Liu, Y. B., Zhang, C. L., O'Neill, S. D., & Zhang, X. S. (2009). Auxin-induced *WUS* expression is essential for embryonic stem cell renewal during somatic embryogenesis in Arabidopsis. *The Plant Journal*, *59*(3), 448–460. https://doi.org/10.1111/j.1365-313X.2009.03880.x

Sugimoto, K., Gordon, S. P., & Meyerowitz, E. M. (2011). Regeneration in plants and animals: dedifferentiation, transdifferentiation, or just differentiation? *Trends in Cell Biology*, *21*(4), 212–218. https://doi.org/10.1016/j.tcb.2010.12.004

Sugimoto, K., Jiao, Y., & Meyerowitz, E. M. (2010). Arabidopsis Regeneration from Multiple Tissues Occurs via a Root Development Pathway. *Developmental Cell*, *18*(3), 463–471. https://doi.org/10.1016/j.devcel.2010.02.004

Sugimoto, K., & Meyerowitz, E. M. (2013). *Regeneration in Arabidopsis Tissue Culture* (pp. 265–275). https://doi.org/10.1007/978-1-62703-221-6_18

Takada, S., Hibara, K. I., Ishida, T., & Tasaka, M. (2001). The CUP-SHAPED COTYLEDON1 gene of Arabidopsis regulates shoot apical meristem formation. *Development*. https://doi.org/10.1242/dev.128.7.1127

Takahashi, K., & Yamanaka, S. (2006). Induction of Pluripotent Stem Cells from Mouse Embryonic and Adult Fibroblast Cultures by Defined Factors. *Cell*, *126*(4), 663–676. https://doi.org/10.1016/j.cell.2006.07.024

Taoka, K., Yanagimoto, Y., Daimon, Y., Hibara, K., Aida, M., & Tasaka, M. (2004). The NAC domain mediates functional specificity of CUP-SHAPED COTYLEDON

proteins. *The Plant Journal*, *40*(4), 462–473. https://doi.org/10.1111/j.1365-313X.2004.02238.x

TEN ASBROEK, A. L. M. A., OLSEN, J., HOUSMAN, D., BAAS, F., & STANTON, V. (2001). Genetic variation in mRNA coding sequences of highly conserved genes. *Physiological Genomics*, *5*(3), 113–118. https://doi.org/10.1152/physiolgenomics.2001.5.3.113

Thomas, P. D., Campbell, M. J., Kejariwal, A., Mi, H., Karlak, B., Daverman, R., Diemer, K., Muruganujan, A., & Narechania, A. (2003). PANTHER: A library of protein families and subfamilies indexed by function. *Genome Research*, *13*(9), 2129–2141. https://doi.org/10.1101/gr.772403

Thompson, B. J. (2013). Cell polarity: models and mechanisms from yeast, worms and flies. *Development*, *140*(1), 13–21. https://doi.org/10.1242/dev.083634

Thompson, J. E., & Fry, S. C. (2001). Restructuring of wall-bound xyloglucan by transglycosylation in living plant cells. *The Plant Journal*, *26*(1), 23–34. https://doi.org/10.1046/j.1365-313x.2001.01005.x

Thorpe, T. A., & Stasolla, C. (2001). Somatic embryogenesis. *Current Trends in the Embryology of Angiosperms*, 279–336.

Treml, B. S., Winderl, S., Radykewicz, R., Herz, M., Schweizer, G., Hutzler, P., Glawischnig, E., & Ruiz, R. A. T. (2005). The gene *ENHANCER OF PINOID* controls cotyledon development in the *Arabidopsis* embryo. *Development*, *132*(18), 4063–4074. https://doi.org/10.1242/dev.01969

Tsata, V., Möllmert, S., Schweitzer, C., Kolb, J., Möckel, C., Böhm, B., Rosso, G., Lange, C., Lesche, M., Hammer, J., Kesavan, G., Beis, D., Guck, J., Brand, M., & Wehner, D. (2021). A switch in pdgfrb cell-derived ECM composition prevents inhibitory scarring and promotes axon regeneration in the zebrafish spinal cord. *Developmental Cell*, *56*(4), 509-524.e9. https://doi.org/10.1016/j.devcel.2020.12.009

Turing, A. M., & Brooker, R. (1952). Programmers' handbook for the manchester electronic computer mark ii. *University of Manchester*.

Uggla, C., Moritz, T., Sandberg, G., & Sundberg, B. (1996). Auxin as a positional signal in pattern formation in plants. *Proceedings of the National Academy of Sciences*, *93*(17), 9282–9286. https://doi.org/10.1073/pnas.93.17.9282

Vaahtera, L., Schulz, J., & Hamann, T. (2019). Cell wall integrity maintenance during plant development and interaction with the environment. *Nature Plants*, *5*(9), 924–932. https://doi.org/10.1038/s41477-019-0502-0

Valvekens, D., Montagu, M. Van, & Lijsebettens, M. Van. (1988). *Agrobacterium tumefaciens* -mediated transformation of *Arabidopsis thaliana* root explants by using kanamycin selection. *Proceedings of the National Academy of Sciences*, *85*(15), 5536–5540. https://doi.org/10.1073/pnas.85.15.5536

van den Berg, C., Willemsen, V., Hage, W., Weisbeek, P., & Scheres, B. (1995). Cell fate in the Arabidopsis root meristem determined by directional signalling. *Nature*, *378*(6552), 62–65. https://doi.org/10.1038/378062a0

van den Berg, C., Willemsen, V., Hendriks, G., Weisbeek, P., & Scheres, B. (1997). Short-range control of cell differentiation in the Arabidopsis root meristem. *Nature*, *390*(6657), 287–289. https://doi.org/10.1038/36856

Van Sandt, V. S. T. T., Suslov, D., Verbelen, J.-P. P., & Vissenberg, K. (2007). Xyloglucan endotransglucosylase activity loosens a plant cell wall. *Annals of Botany*, *100*(7), 1467–1473. https://doi.org/10.1093/aob/mcm248

Vanneste, S., & Friml, J. (2009). Auxin: A Trigger for Change in Plant Development. *Cell*, *136*(6), 1005–1016. https://doi.org/10.1016/j.cell.2009.03.001

Varapparambath, V., Mathew, M. M., Shanmukhan, A. P., Radhakrishnan, D., Kareem, A., Verma, S., Ramalho, J. J., Manoj, B., Vellandath, A. R., Aiyaz, M., Radha, R. K., Landge, A. N., Mähönen, A. P., Heisler, M. G., Weijers, D., & Prasad, K. (2022). Mechanical conflict caused by a cell-wall-loosening enzyme activates de novo shoot regeneration. *Developmental Cell*, *57*(17), 2063-2080.e10. https://doi.org/10.1016/j.devcel.2022.07.017

Verna, C., Ravichandran, S. J., Sawchuk, M. G., Linh, N. M., & Scarpella, E. (2019). Coordination of tissue cell polarity by auxin transport and signaling. *ELife*, *8*, 1–30. https://doi.org/10.7554/eLife.51061

Vernoux, T., Kronenberger, J., Grandjean, O., Laufs, P., & Traas, J. (2000). PIN-FORMED 1 regulates cell fate at the periphery of the shoot apical meristem. *Development*, *127*(23), 5157–5165. https://doi.org/10.1242/dev.127.23.5157

Virchow, R. (1859). Pigment und diffuse Melanose der Arachnoides. *Archiv Für*

Pathologische Anatomie Und Physiologie Und Für Klinische Medicin, *16*(1–2), 180–182.

Vroemen, C. W., Mordhorst, A. P., Albrecht, C., Kwaaitaal, M. A. C. J. C. J., & De Vries, S. C. (2003). The CUP-SHAPED COTYLEDON3 gene is required for boundary and shoot meristem formation in Arabidopsis. *Plant Cell*, *15*(7), 1563–1577. https://doi.org/10.1105/tpc.012203

Waaland, S. D. (1975). Evidence for a species-specific cell fusion hormone in red algae. *Protoplasma*, *86*(1–3), 253–261. https://doi.org/10.1007/BF01275635

Waaland, S. D., & Cleland, R. (1972). Development in the red alga, Griffithsia pacifica: Control by internal and external factors. *Planta*, *105*(3), 196–204. https://doi.org/10.1007/BF00385391

Wachsman, G., Zhang, J., Moreno-Risueno, M. A., Anderson, C. T., & Benfey, P. N. (2020). Cell wall remodeling and vesicle trafficking mediate the root clock in Arabidopsis. *Science*, *370*(6518), 819–823. https://doi.org/10.1126/science.abb7250

Wang, Q., Hasson, A., Rossmann, S., & Theres, K. (2016). *Divide et impera* : boundaries shape the plant body and initiate new meristems. *New Phytologist*, *209*(2), 485–498. https://doi.org/10.1111/nph.13641

Wang, Q., Kohlen, W., Rossmann, S., Vernoux, T., & Theres, K. (2014). Auxin Depletion from the Leaf Axil Conditions Competence for Axillary Meristem Formation in *Arabidopsis* and Tomato. *The Plant Cell*, *26*(5), 2068–2079. https://doi.org/10.1105/tpc.114.123059

Wang, X., Ye, L., Lyu, M., Ursache, R., Löytynoja, A., & Mähönen, A. P. (2020). An inducible genome editing system for plants. *Nature Plants*, *6*(7), 766–772. https://doi.org/10.1038/s41477-020-0695-2

Wang, Y., & Jiao, Y. (2018). Auxin and above-ground meristems. *Journal of Experimental Botany*, *69*(2), 147–154. https://doi.org/10.1093/jxb/erx299

Wang, Y., Wang, J., Shi, B., Yu, T., Qi, J., Meyerowitz, E. M., & Jiao, Y. (2014). The Stem Cell Niche in Leaf Axils Is Established by Auxin and Cytokinin in *Arabidopsis*. *The Plant Cell*, *26*(5), 2055–2067. https://doi.org/10.1105/tpc.114.123083

Wei, H., Cheng, Y., Sun, Y., Zhang, X., He, H., & Liu, J. (2021). Genome-Wide Identification of the ARF Gene Family and ARF3 Target Genes Regulating Ovary

Initiation in Hazel via ChIP Sequencing. *Frontiers in Plant Science*, *12*(August), 1–16. https://doi.org/10.3389/fpls.2021.715820

Weir, I., Lu, J., Cook, H., Causier, B., Schwarz-Sommer, Z., & Davies, B. (2004). *CUPULIFORMIS* establishes lateral organ boundaries in *Antirrhinum*. *Development*, *131*(4), 915–922. https://doi.org/10.1242/dev.00993

West, M., & Harada, J. J. (1993). Embryogenesis in Higher Plants: An Overview. *The Plant Cell*, 1361–1369. https://doi.org/10.1105/tpc.5.10.1361

West, M., Yee, K. M., Danao, J., Zimmerman, J. L., Fischer, R. L., Goldberg, R. B., & Harada, J. J. (1994). LEAFY COTYLEDON1 Is an Essential Regulator of Late Embryogenesis and Cotyledon Identity in Arabidopsis. *The Plant Cell*, 1731–1745. https://doi.org/10.1105/tpc.6.12.1731

Whitney, S. E. C., Gothard, M. G. E., Mitchell, J. T., & Gidley, M. J. (1999). Roles of Cellulose and Xyloglucan in Determining the Mechanical Properties of Primary Plant Cell Walls. *Plant Physiology*, *121*(2), 657–664. https://doi.org/10.1104/pp.121.2.657

Wiśniewska, J., Xu, J., Seifertová, D., Brewer, P. B., Růžička, K., Blilou, I., Rouquié, D., Benková, E., Scheres, B., & Friml, J. (2006). Polar PIN Localization Directs Auxin Flow in Plants. *Science*, *312*(5775), 883–883. https://doi.org/10.1126/science.1121356

Wodarz, A. (2002). Establishing cell polarity in development. *Nature Cell Biology*, *4*(2), E39–E44. https://doi.org/10.1038/ncb0202-e39

Won, C., Shen, X., Mashiguchi, K., Zheng, Z., Dai, X., Cheng, Y., Kasahara, H., Kamiya, Y., Chory, J., & Zhao, Y. (2011). Conversion of tryptophan to indole-3-acetic acid by TRYPTOPHAN AMINOTRANSFERASES OF *ARABIDOPSIS* and YUCCAs in *Arabidopsis*. *Proceedings of the National Academy of Sciences*, *108*(45), 18518–18523. https://doi.org/10.1073/pnas.1108436108

Woodward, A. W. (2005). Auxin: Regulation, Action, and Interaction. *Annals of Botany*, *95*(5), 707–735. https://doi.org/10.1093/aob/mci083

Xie, Q., Frugis, G., Colgan, D., & Chua, N.-H. (2000). *Arabidopsis* NAC1 transduces auxin signal downstream of TIR1 to promote lateral root development. *Genes & Development*, *14*(23), 3024–3036. https://doi.org/10.1101/gad.852200

Xu, J., Hofhuis, H., Heidstra, R., Sauer, M., Friml, J., & Scheres, B. (2006). A Molecular

Framework for Plant Regeneration. *Science*, *311*(5759), 385–388. https://doi.org/10.1126/science.1121790

Xu, P., & Cai, W. (2019). Nitrate-responsive OBP4-XTH9 regulatory module controls lateral root development in Arabidopsis thaliana. *PLoS Genetics*, *15*(10), e1008465. https://doi.org/10.1371/journal.pgen.1008465

Yamaguchi, N., Winter, C. M., Wu, M.-F., Kwon, C. S., William, D. A., & Wagner, D. (2014). PROTOCOL: Chromatin Immunoprecipitation from Arabidopsis Tissues. *The Arabidopsis Book*, *12*, e0170. https://doi.org/10.1199/tab.0170

Yang, M., & Jiao, Y. (2016). Regulation of Axillary Meristem Initiation by Transcription Factors and Plant Hormones. *Frontiers in Plant Science*, *7*. https://doi.org/10.3389/fpls.2016.00183

Yang, T., Law, D. M., & Davies, P. J. (1993). Magnitude and Kinetics of Stem Elongation Induced by Exogenous Indole-3-Acetic Acid in Intact Light-Grown Pea Seedlings. *Plant Physiology*, *102*(3), 717–724. https://doi.org/10.1104/pp.102.3.717

Yang, Z. (2008). Cell polarity signaling in Arabidopsis. *Annual Review of Cell and Developmental Biology*, *24*, 551–575. https://doi.org/10.1146/annurev.cellbio.23.090506.123233

Yokoyama, R., & Nishitani, K. (2001). A Comprehensive Expression Analysis of all Members of a Gene Family Encoding Cell-Wall Enzymes Allowed us to Predict cis-Regulatory Regions Involved in Cell-Wall Construction in Specific Organs of Arabidopsis. *Plant and Cell Physiology*, *42*(10), 1025–1033. https://doi.org/10.1093/pcp/pce154

Zhai, N., & Xu, L. (2021). Pluripotency acquisition in the middle cell layer of callus is required for organ regeneration. *Nature Plants*, *7*(11), 1453–1460. https://doi.org/10.1038/s41477-021-01015-8

Zhang, G., Zhao, F., Chen, L., Pan, Y., Sun, L., Bao, N., Zhang, T., Cui, C.-X., Qiu, Z., Zhang, Y., Yang, L., & Xu, L. (2019). Jasmonate-mediated wound signalling promotes plant regeneration. *Nature Plants*, *5*(5), 491–497. https://doi.org/10.1038/s41477-019-0408-x

Zhang, T.-Q., Lian, H., Tang, H., Dolezal, K., Zhou, C.-M., Yu, S., Chen, J.-H., Chen, Q., Liu, H., Ljung, K., & Wang, J.-W. (2015). An Intrinsic MicroRNA Timer Regulates

Progressive Decline in Shoot Regenerative Capacity in Plants. *The Plant Cell*, *27*(2), 349–360. https://doi.org/10.1105/tpc.114.135186

Zhang, T.-Q., Lian, H., Zhou, C.-M., Xu, L., Jiao, Y., & Wang, J.-W. (2017). A two-step model for de novo activation of WUSCHEL during plant shoot regeneration. *The Plant Cell*, *29*(5), 1073–1087.

Zhang, Y., & Dong, J. (2018). Cell polarity: compassing cell division and differentiation in plants. *Current Opinion in Plant Biology*, *45*, 127–135. https://doi.org/10.1016/j.pbi.2018.06.003

Zhang, Y., Liu, T., Meyer, C. A., Eeckhoute, J., Johnson, D. S., Bernstein, B. E., Nussbaum, C., Myers, R. M., Brown, M., Li, W., & Shirley, X. S. (2008). Model-based analysis of ChIP-Seq (MACS). *Genome Biology*, *9*(9). https://doi.org/10.1186/gb-2008-9-9-r137

Zhang, Y., Zheng, L., Hong, J. H., Gong, X., Zhou, C., Pérez-Pérez, J. M., & Xu, J. (2016). No Title. *Plant Physiology*, *171*(1), 483–493. https://doi.org/10.1104/pp.15.01754

Zhao, Y., Christensen, S. K., Fankhauser, C., Cashman, J. R., Cohen, J. D., Weigel, D., & Chory, J. (2001). A Role for Flavin Monooxygenase-Like Enzymes in Auxin Biosynthesis. *Science*, *291*(5502), 306–309. https://doi.org/10.1126/science.291.5502.306

Zhou, W., Lozano-Torres, J. L., Blilou, I., Zhang, X., Zhai, Q., Smant, G., Li, C., & Scheres, B. (2019). A Jasmonate Signaling Network Activates Root Stem Cells and Promotes Regeneration. *Cell*, *177*(4), 942-956.e14. https://doi.org/10.1016/j.cell.2019.03.006

Zimmerman, J. L. (1993). Somatic Embryogenesis: A Model for Early Development in Higher Plants. *The Plant Cell*, 1411–1423. https://doi.org/10.1105/tpc.5.10.1411

Zuo, J., Niu, Q., & Chua, N. (2000). An estrogen receptor-based transactivator XVE mediates highly inducible gene expression in transgenic plants. *The Plant Journal*, *24*(2), 265–273.